Proceedings of the Fourth International Workshop on Measurement and Computation of Turbulent Nonpremixed Flames

Darmstadt, Germany

June 27th – 29th, 1999

Fourth International Workshop on Measurement and Computation of Turbulent Nonpremixed Flames

Darmstadt, Germany
June 27 – 29, 1999

Contents

SUMMARY AND COLLECTED COMMENTS ON THE FOURTH INTERNATIONAL WORKSHOP ON MEASUREMENT AND COMPUTATION OF TURBULENT NONPREMIXED FLAMES

27-29 June 1999
Darmstadt, Germany

Edited by R. Barlow with contributions by
R. Bilger, J.-Y. Chen, E. Hassel, A. Hinz, J. Janicka, A. Masri, D. Roekaerts
Summary revision date: 20 October 1999

INTRODUCTION:

The Fourth International Workshop on Measurement and Computation of Turbulent Nonpremixed Flames (TNF4) was hosted by the Darmstadt University of Technology and was attended by 87 researchers from 10 countries. The main topics of discussion included:

- results for the piloted CH_4/air jet flames D, E, and F
- progress on calculations of bluff-body stabilized flames
- progress on LES for combustion
- experimental progress on flames of interest to the workshop
- priorities for TNF-related research
- organization of TNF5

This summary provides comments on the main discussion topics as reflected by the notes of some of the organizers and participants. These comments do not necessarily represent a consensus of opinion, and they are not intended to be a complete record of TNF4 discussions. This summary and the complete TNF4 Proceedings are available on the Web at http://www.ca.sandia.gov/tdf/Workshop.html. The Proceedings include the agenda, list of attendees, plotted comparisons of measured and modeled results for the target flames (piloted CH_4/air jet flames), poster abstracts, and materials (vugraph copies) on some of the discussion topics.

Background, Scope, and Objectives

The TNF Workshop series is intended to facilitate collaboration and information exchange among experimental and computational researchers in the field of turbulent nonpremixed combustion, with an emphasis on fundamental issues of turbulence-chemistry interactions. Our overall objectives are: i) to provide an effective framework for comparison of different combustion modeling approaches, ii) to identify and correct inconsistencies or gaps in the experimental data sets, and iii) to establish a series of benchmark experiments and calculations that cover a progression in geometric and chemical kinetic complexity. We emphasize that this is not a competition among models, but rather a means of identifying areas for potential improvements in a variety of modeling approaches. This collaborative process benefits from contributions by participants having different areas of expertise, including velocity measurements, scalar measurements, turbulence modeling, chemical kinetics, reduced mechanisms, mixing models, radiation, and combustion theory. The process also benefits from the rapid time scale of communication that is afforded by the internet.

Recommended Restrictions on Use of TNF Proceedings

Results in this and other TNF Workshop proceedings are contributed in the spirit of open collaboration to facilitate information exchange among active research projects. Some results represent completed work, while others are from work in progress. Readers should keep this in mind when reviewing these materials. It would be inappropriate to quote or reference specific results from these proceedings without first checking with the individual authors for permission and for their latest information on results and references.

PILOTED FLAMES D, E, AND F:

The piloted CH_4/air flames were the only target flames for which multiple simulation results were submitted for comparison with experiments. Comparisons were plotted and presented by Rob Barlow (update on flame D) and Alex Hinz (E and F results and D, E, F progression). Major points from the presenters' observations and from the discussion sessions are listed below.

Flame D:

1. **Velocity Field** – Ten new calculations of Flame D were submitted in addition to the seven from TNF3. These new calculations showed a wider spread in the results for the overall flow field as represented by the axial and radial profiles of mean velocity and velocity fluctuations. The reasons for this are not clear, but it is generally true that models were not tuned to match the flow field. Some participants expressed the opinion that more complete guidelines or requirements for calculations of target flames be used in the future in order to minimize ambiguity in the comparison of turbulence/chemistry submodels. Part of this job would be to provide updated and more complete velocity boundary conditions for the piloted flames, including recent LDV measurements from Darmstadt and perhaps a recommended exit profile of the turbulent energy dissipation. It may also be useful to provide a reference calculation for flame D. However, the main focus of the TNF workshop remains on fundamental issues of turbulence/chemistry interactions, rather than refinement of RANS models. The approach adopted in Naples that allows for tuning (and reporting) of model constants to match the overall flow/mixing field is still considered to be appropriate for the TNF Workshop purposes.

2. **Mixture Fraction Field** – Most of the calculations of flame D are in reasonable agreement with the axial profiles of the Favre means and rms fluctuations of mixture fraction and temperature. This is not to say that the calculations fall mainly within the experimental error bars. However, the level of agreement for most of the calculations is believed to be close enough to allow meaningful comparison of turbulence/chemistry results in mixture fraction coordinates.

3. **Some Anomalies** – Conditional means reveal problems with a few of the calculations. First, the ILDM results for CO and H_2 are unrealistic outside the near-stoichiometric region. As discussed by Maas in Boulder, this implementation of ILDM uses two progress variables (CO_2 and H_2O), and the manifold is only defined for a limited interval in mixture fraction. The unrealistic results for CO and H_2 are due to unrealistic assumptions that are applied outside this interval. ILDM is, however, able to predict localized extinction. Second, the two calculations based on 4-step reduced chemistry yield unrealistic values for H_2. This may result from the implementation of the 4-step mechanism rather than a fundamental problem with the 4-step representation of the chemistry. Third, the conditional means from the LES calculation are inconsistent with other measured and computed results. However, it was made clear that these LES calculations should be viewed only as works in progress.

4. **Rich-Side Problems** – The majority of calculations of flame D yield good agreement with measured conditional means of all scalars for fuel-lean conditions and for mixture fractions up to about f=0.4. In fuel-rich samples the calculated results tend to diverge, with ODT, CMC, and steady flamelet methods predicting higher mass fractions of CO and H_2 and lower mass fractions of CH_4 than are measured. The two steady flamelet (Le=1) calculations by Chen and Coelho give very similar results, even though different chemical mechanisms were used.

5. **Unresolved Question** – Related to the above, an important question from TNF3 has yet to be resolved. Why do the different methods (flamelet, CMC, PDF) predict significantly different results for fuel-rich mixtures when the calculations are run using the same mechanism. J-Y Chen presented results of a parametric set of PDF calculations that showed

a dependence of the CO mass fraction on the localness (in mixture fraction space) of the mixing model. Plots are included in the section on Additional Contributions in the TNF4 Proceedings. Bob Bilger expressed the opinion that the chemical mechanism may be a primary issue, and that GRI Mech may be predicting too rapid a rate of methane consumption at fuel-rich conditions in these partially premixed flames. Resolution of these issues is one of the highest priorities for the TNF Workshop.

6. **Pdf Results** – With the exception of problems noted in 3, the various pdf calculations gave similar results for conditional means. The Lindstedt calculation yields somewhat higher peak values for CO and H_2. A comparison presented at TNF3 by J-Y Chen of pdf calculations of flame D using several different mechanisms showed relatively small differences between CO and H_2 predictions using the GRI 1.2 and Warnatz (1998) mechanisms. This comparison is also included under the Additional Contributions in the TNF4 Proceedings. Expanding this comparison to include the mechanisms from Lindstedt, Williams, and Peters would be interesting. Flame D results suggest there are not great differences between the Chen 12-step, Lindstedt 16-step, and Peters mechanisms, as far as major species and CO are concerned. PDF/EMST/ISAT calculations of flames D and F by Xu & Pope were not available in time for inclusion in the overall comparison plots. However, vugraphs on these rather impressive results were presented separately and are included in the TNF4 Proceedings under Additional Contributions.

7. **Validation of Chemical Mechanisms** – The need for validation of chemical mechanisms against detailed measurements of laminar, opposed-flow, partially-premixed flames was discussed at some length. Experimental data on such flames is limited. Li and Williams (C&F 118:399-414) report measurements in flames with equivalence ratios of 1.5 and 2.5 on the fuel side. Peter Lindstedt and J-Y Chen plan to run laminar flame calculations to compare with these measurements. Laser measurements in laminar opposed-flow flames with the same fuel composition (equivalence ratio 3.17) as the piloted flames are planned by the Darmstadt group and later at Sandia. Some results may be available before TNF5.

8. **NO Prediction** – There are now several calculations of NO mass fractions in flame D. Some of these are in good agreement with the measurements. It is not clear, however, that this agreement is achieved for the right reasons. Accurate prediction of NO in these flames (right answer for the right reasons) requires accurate prediction of the overall flow/mixing field and radiation losses, as well as the various chemical pathways for NO formation and destruction. Questions were raised at TNF3 regarding the accuracy of the measured radiant fraction and the appropriateness of the optically-thin assumption for the piloted flames. Checks on these have yet to be done. It was suggested that future calculations report the total radiant fraction. Regarding chemistry, the comment was made that the rate of prompt NO formation from GRI Mech may be off by a factor of two due to problems with CH. Comparison of NO results based on different chemical mechanisms used within the same turbulent flame code would be interesting. Comparisons of the relative importance of prompt, thermal, and reburn chemistry in these calculations would also be interesting.

Flames E and F:

9. **Overview** – Five calculations were submitted for flame E (including PDF, CMC, and ODT methods), and seven calculations were submitted for flame F (including PDF, ODT, and LES methods). Again, the LES calculations of flames D and F are considered works in progress, and they are not included in the following comments.

10. **Favre Averages** – While each of the models shows good agreement with some aspects of the measured Favre average velocity and mixture fraction profiles, none of the models gives good overall agreement with the experiment. For example, the Hinz PDF-ILDM calculation gives relatively good agreement with the measured radial profiles of mean and rms velocity, but does less well on mixture fraction. The reverse can be said of the Chen calculations. The more rapid decay of the axial profile of mixture fraction in the extinction region of flame F as compared to flame D is not reproduced by the calculations.

This may be due to the under prediction of extinction by the models. Generally, the Favre average profiles of mixture fraction and temperature are most useful in comparing different models. Results on species are best compared in mixture fraction coordinates.

11. **Conditional Means** – Conditional means show differences among rich-side predictions that are similar to those noted for flame D. Flame E has a slightly longer stoichiometric length than D, so that measured conditional means at x/d=45 extend to higher mixture fraction values. This reveals relatively good agreement between the experiment and some of the models for most scalars up to f=0.5 (or higher) at this streamwise location where the flame is fully re-ignited.

12. **Degree of Extinction** – The scatter plots for measured temperature at x/d=15 and 30 in flame F show greater effects of local extinction than most of the predictions, especially for fuel-rich conditions. The Xu & Pope comparisons do not include scatter plots, but their conditional pdf's for flame F indicate that extinction and reignition are captured relatively well. ODT does not predict any extinction in these flames. CMC would need a higher order closure to capture local extinction. Scatter plots show that the IEM mixing model generates deterministic patterns of highly-strained or extinguished samples.

13. **Extinction as Target Problem** – Predicting the probability of localized extinction in these piloted flames is expected to be a difficult problem. It is observed experimentally that flames with significant local extinction are extremely sensitive to small changes in boundary conditions. Furthermore, small asymmetries in the burner or inlet flows can cause large asymmetries in the flame. Therefore, it seems unreasonable to expect close agreement between measured and modeled results for any one such flame. The prediction of trends observed in the series of piloted flames may be more reasonable near-term goal. Comparison of scatter plots, conditional means, and conditional pdf's can be useful in this regard. However, the limited number of samples in most of the PDF calculations limits the usefulness of the cpdf comparison plots. Definition of convenient measure of reactedness or convenient criteria for local extinction would be useful for quantitative comparisons of trends in extinction and re-ignition.

14. **Conditional Pdf's** – Only the ODT calculation and the PDF calculations by Lindstedt and Xu & Pope include a large enough sample size to allow clear interpretation of the conditional pdfs. The complete set of cpdf's from the Lindstedt calculations was not available for inclusion in the notebook. Comparisons of the Xu & Pope results with measured cpdf's for flames D and F are included in the TNF4 Proceedings under Additional Contributions. This calculation yields more extinction than the other PDF calculations, and the resulting cpdf's are in relatively good agreement with measurements, given the limitations mentioned above. Other PDF calculations show a trend of increasing extinction with increasing jet velocity. However, the cpdf's are generally too noisy for detailed comparisons. Inclusion of more particles per cell in future PDF calculations would be useful, though cost is an issue. One of the places where a measured trend is clearly seen in a calculation is in the burning part of the cpdf's of OH at x/d=15 from the ODT calculation. There is a shift to higher OH mass fractions as the jet velocity increases.

15. **Proper Normalization of Conditional Pdf's** – Conditional pdf's in the TNF4 Proceedings are not properly normalized (divided by bin width) to yield unity area under the pdf. This follows an error in presenting the measured cpdf's (Barlow and Frank, 27th Combustion Symposium). Any future TNF Workshop comparisons of pdf's should use proper normalization.

16. **Flame Stabilization** – Some calculations required special treatment of the near field in order to obtain a stable burning solution (e.g., Chen PDF-MC) while others did not. (e.g., Lindstedt and Xu & Pope). The reasons for this are not clear and may involve several aspects of the calculations. One particular question to resolve is whether the number of particles per cell affects the stability of a PDF calculation. There may also be effects of turbulence model, mixing model, boundary conditions, chemical mechanism, grid

resolution, numerics, and the interactions of these. Some further investigations on what parts of the calculations influence flame stability would be useful, particularly in the context of the E and F flames, where significant local extinction is measured at 15 diameters from the nozzle.

PROBLEMS AND NUMERICAL ISSUES IN COMPUTING THE BLUFF-BODY FLOWS:

One of the original objectives for TNF4 was to encourage modelers to apply "advanced" methods to the bluff body problem. Only one new calculation of the Sydney CH_4/H_2 bluff-body flame was submitted for comparison with measurements, and it became clear that one year was not sufficient time for major progress in this area. Consequently, Assaad Masri organized the session as a discussion opportunity with contributions from four groups that have been working on these flows (Imperial College, Fluent, TU Delft, and Cornell). The first two groups are using LES, while the latter two are using PDF methods. The objectives of the session were to exchange ideas and to promote collaboration on this difficult problem. Some of the information presented is in the poster abstracts. A few points from the discussions are: i) 3D is essential for LES of the bluff-body geometry, ii) grid-independent solutions are difficult to achieve but may be easier to achieve in combination with more refined (low Re) treatment of the near-wall region, iii) both LES and PDF calculations are sensitive to boundary conditions and need to be started upstream of the bluff-body surface.

Obtaining good predictions for the flow and mixing fields is essential before attempting any serious calculations of the composition field. In the previous workshop (TNF3), calculations using standard turbulence modeling approaches such as k-e and RS were attempted and compared with experimental data. In order to get the correct flow and mixing fields some adjustment of the model constants was done. This, if necessary, seems to be an acceptable strategy. At the conclusion of TNF4, it was seen as useful to use the standard modeling approaches (as well as advanced ones) with detailed chemistry to compute the compositional structure in these flames and especially in the reaction zone with a special focus on NO. Four or five research groups have expressed interest in attempting such computations for TNF5.

PROSPECTIVE TARGET FLAMES AND OTHER EXPERIMENTAL PROGRESS:

A stated objective of the TNF Workshop series is to develop a library of a few well-documented flames that are appropriate for investigations of fundamental issues in turbulent combustion and for collaborative testing of various models. The data library includes flames with increasing complexity in terms of flow geometry and chemical complexity. As a practical matter, the workshop has selected target flames based on the level of interest among the modelers, and not all flames in the library are expected to be used as formal targets. Participants in the TNF Workshops have interests that range from fundamental to applied. Therefore, as progress is made on the "simpler" flames, we can expect the TNF to look toward more complicated flames.

The planning of experiments must normally be done at least a year ahead of the time when the TNF Workshop might take up a flame as a target for calculations. Discussions between experimentalists and modelers during the planning stages are extremely valuable, and this is considered to be a major function of the workshop. New experiments on flames that have already been targets can also be valuable, particularly in the context of LES model validation. We can expect that the addition of new flames and the improvement of data sets already in the library will proceed in parallel.

Several prospective target flames were discussed at TNF4:

17. **Sydney Swirl Flame** – Assaad Masri presented information on a swirl burner under investigation at U Sydney. The geometry is similar to that of the Sydney bluff-body flame,

but with the addition of an annular flow of swirling air. This flame is intended as a simpler alternative to the Tecflam swirl flame. One point of discussion involved the possibility of obtaining velocity measurements inside the air annulus.

18. **Tecflam Swirl Flame** – Several groups in Germany have been working on this flame for a number of years. Wolfgang Leuckel presented an overview of experimental work. This is a relatively complicated burner to operate and to calculate. However, the fact that it is closer to practical applications is a significant motivating factor for several participants. Before this flame can serve as a TNF target, it will be necessary for the data to be consolidated, checked for consistency, documented, and made available on the internet.

19. **Berkeley Jet in Products** – As presented by Bob Dibble, this is essentially a jet flame burning in a coflow of lean products of combustion. The intent is to investigate the same chemistry as in a recirculation zone, while avoiding the fluid-dynamic complications of a recirculating flow with wall interactions.

20. **Turbulent Opposed Jet Flows and Flames** – Several TNF participants plan to investigate the opposed jet geometry as a test case for fundamental research on turbulence models (including LES) and mixing models. Nondas Mastorakos presented an overview of past work on opposed jet flames. His annotated bibliography on this topic is under Additional Contributions in the TNF4 Proceedings. Dirk Geyer introduced the burner design that has been developed at Darmstadt. This burner was also demonstrated during the laboratory tour.

21. **O_2 Coflow Jet Flame** – Jim Driscoll presented imaging results on a CH_4/N_2 jet burning in a coflow of pure O_2. In the context of the TNF data library the interesting features of this flame are: simple jet flame geometry, no partial premixing with air, minimal differential diffusion of fuel components, low levels of soot precursors that interfere with laser diagnostics. The diagnostic technique identifies the stoichiometric surface in 2D, and results may be useful for comparison with LES.

In addition, results were outlined from some recent experiments on flames that are already in the TNF library.

22. **DLR $CH_4/H_2/N_2$ Flames** – Wolfgang Meier presented results of scalar measurements in the two jet flames (Re=15,200 and Re=22,800) that were measured using the Raman/Rayleigh/LIF system in the TDF Lab at Sandia. These new measurements add OH and NO to the data set, as well as improved measurements of CO.

23. **Delft Piloted Flames** – Theo Van der Meer presented favorable comparisons of CARS temperature measurements in the Delft III flame with previous Rayleigh/Raman measurements. Multi-shot OH PLIF images have been obtained recently in these flames through a collaboration with the Alden group at Lund University.

PROGRESS ON LES FOR COMBUSTION:

This session included brief work-in-progress presentations from several groups. Poster abstracts include additional information on these contributions. The increasing level of LES activity among active workshop participants makes it clear that LES for combustion will be an important topic of future TNF Workshops. This will include greater attention to experiments that are relevant to LES.

Contributions regarding LES during TNF4

24. **ODT of Jet Flames** – Tarek Echekki and John Hewson presented an overview of recent work on the one-dimensional turbulence (ODT) model. The model resolves the full range of scalars in a single dimension, providing exact treatment of chemical reaction and

molecular mixing at Reynolds and Damkohler numbers not accessible to DNS. ODT results for flames D, E, and F (Echekki) are included in the comparisons outlined above. The calculation was carried out on a 1D-domain transverse to the mean flow by evolving the time series of 1D Lagrangian fields and ensemble averaging the results. A 12-step chemistry model and mixture-averaged transport using the CHEMKIN library were implemented. ODT results for $CO/H_2/N_2$ flames were presented by John Hewson. Both ODT calculations cast the problem as a planar jet, which means that spatial profiles cannot be compared directly.

25. **LES of H_2 Flame** – In the contribution of Forkel and Janicka a time integration procedure for LES of incompressible, reacting flows was presented. The method was applied to the simulation of a turbulent hydrogen diffusion flame and good agreement with measurements was achieved. The numerical procedure is based on the pressure correction scheme that is well known for LES of constant density flows. The local chemical composition of the fluid is described by solving a transport equation for the Favre-filtered mixture fraction. Density, temperature and species mass fractions are evaluated applying a laminar flamelet model with zero scalar-dissipation-rate. A β-function is assumed for the sub-grid PDF, the variance of the mixture fraction is calculated from the resolved fluctuations.

26. **LES of Flame D** – DiMare and Jones carried out a LES calculation of the piloted methane diffusion flames (Sandia Flame D). They applied the Smagorinsky SGS model and a steady flamelet with zero scalar dissipation. Comparisons between predictions and measurements are shown up to x/D=10. Pitsch and Steiner also presented a LES of the flame D. The species mass fractions as functions of mixture fraction are obtained using the unsteady flamelet model. The pdf is presumed to follow a β-function, whose shape is determined by the mean and the subgrid-scale variance of the mixture fraction. The mixture fraction variance and the Smagorinsky constant are determined by a dynamic procedure. The spatial filtered scalar dissipation rate is expressed in terms of the eddy diffusivity and the gradient of the resolved mixture fraction.

Conclusions and Future Work on LES

The discussion can be summarized as follows:

27. **Future of Combustion LES** – LES appears to be a promising tool for the prediction of turbulent combustion processes. The principle weakness of this method with respect to the simulation of near-wall behavior is less critical for combustion processes compared to, e.g., aerodynamic applications because the combustion takes place mainly in the large-scale dominated region far away from walls inside a combustor.

28. **Combustion Submodels** – Up to now only state of the art RANS-combustion models have been employed for LES combustion simulation. Application range, advantages, and disadvantages of these models are not known for the time being and will be subjects of future research.

29. **Sensitivity to BC's** – The precise description of flow- and scalar fields via LES requires the precise knowledge of boundary conditions. LES models are more sensitive to boundary conditions than RANS models. Obviously, physically correct conditions in a LES environment are more difficult to generate.

30. **Scalar Transport** – First LES calculation of the bluff-body flames yield a reasonable prediction of the flow field combined with unsatisfactory results for the scalar field. Scalar-transport models based on an eddy-viscosity approach with constant Schmidt-number may account for this observation. More sophisticated scalar transport models are needed for the future.

31. **Experimental Needs** – Additional experimental information are required for the validation of LES. Because LES reveals detailed spatial structures, suitable experiments like line-Raman are needed to meet this requirement. The sensitivity of LES to boundary conditions places additional demands on experiments. These considerations accentuate the need for collaboration among modelers and experimentalists in the design of experiments that will support LES model validation.

PRIORITIES FOR TNF-RELATED RESEARCH:

The final session included discussion of the priorities for research related to the TNF workshop. Listed below are some specific items that were identified as important for further progress on the piloted and bluff-body flames. Work was initiated on some topics in the weeks after TNF4, and it is hoped that results can be reported for some items well before TNF5.

32. **Compare and Validate Methane Mechanisms** – Comparisons of chemical mechanisms should be expanded to include all the major methane mechanisms used by various groups involved in the TNF Workshop. It would be useful to have comparisons for turbulent flames and for laminar flames over a range of strain rates. Methane mechanisms also need to be validated for laminar partially premixed flames. Experimental data on such flames are limited, and there is a clear need for detailed measurements of laminar opposed-jet flames with partial premixing. If possible, comparisons and data should include NO.

33. **Compare Mixing Models** – Further work is needed to understand the influence of mixing models on the rich-side predictions for the piloted flames. Can chemical mechanism and mixing model be considered as independent submodels?

34. **Update Boundary Conditions for Piloted and BB Flames** – Updated and more complete velocity boundary conditions for the piloted flames should be assembled and made available as soon as possible. Tests of the sensitivity of calculations to details of the boundary conditions would be useful in this context. Data on the bluff-body surface temperature for the CH_4/H_2 cases are needed.

35. **Resolve Radiation Questions** – Accuracy of the measurements of radiant fraction needs to be evaluated. The validity of the optically thin radiation model for the various target flames should be assessed. These are both important for any comparison of measured and predicted NO levels. Modelers should plan to calculate and report radiant fraction for all calculations that include NO.

36. **Particles per Cell** – The influence (if any) of the number of particles per cell on the stable burner of the piloted flames should be resolved.

37. **Tecflam Consolidation** – Four groups expressed interest in calculating the Tecflam swirl burner. Data from the various sources should be consolidated, evaluated for consistency and completeness, and made available on the internet.

ORGANIZATION OF TNF5:

38. **Location and Dates** – The Fifth TNF Workshop will be hosted by Dirk Roekaerts at the Delft University of Technology. Tentative dates are 26-28 July 2000, just before the 28th Combustion Symposium.

39. **Target Problems –** Several groups expressed interest in pursuing work on the following three tentative target problems. Primary contacts for each flame are listed:

(a) Piloted CH_4/air flames with emphasis on resolution of issues outlined above and on detailed consideration of NO. Additional measurements and guidance on the radiation problem will be needed. (Rob Barlow)

(b) Bluff-body CH_4/H_2 flame with emphasis on prediction of NO in the recirculation zone. Guidance on boundary conditions and grid resolution maybe useful. Additional information on bluff-body surface temperature is needed. (Assaad Masri)

(c) Tecflam burner. Four groups intend to calculate it. Data and boundary conditions need to be consolidated and documented. (Egon Hassel)

In addition, there is ongoing experimental work on several prospective target flames, ongoing work on submodel development, and ongoing modeling work by individuals on the DLR $CH_4/H_2/N_2$ flames and the Sandia $CO/H_2/N_2$. We can expect to hear about progress in some of these areas. Parametric studies that isolate the sensitivity of results to changes in a single submodel or parameter are encouraged.

40. **Avoiding Conflicts** – The TNF organizers are in agreement that the workshop activities should complement the Combustion Symposium, rather than conflict with it. As a general guideline, TNF participants will be asked to avoid presenting results at the workshop that are included in a Symposium paper.

41. **Initial Poster Session –** It is likely that we will begin TNF5 with an afternoon/evening poster session and reception on Wednesday July 26th. This will allow more time for participants to view and discuss posters without cutting into the main discussion sessions. An effort will be made to have target-flame comparison presented on posters, so participants can review results before the regular sessions. This arrangement is preferred over a proposed alternative of scheduling 3-minute presentations on each poster. We will try to schedule more time for informal discussions in the poster room.

42. **Limited Attendance** – Attendance will be limited at TNF5. This is considered by the organizers as a necessary step to maintain the productive atmosphere of a small workshop. Based on past experience, attendance between 60 and 75 is sensible. Final numbers will depend on the level of interest and the available facilities. Preference will be given to those groups most directly involved in research related to the TNF Workshop topics.

43. **TNF Emphasis** – The Workshop organizers will continue to promote an emphasis on open discussion rather than formal presentation, cooperation rather than competition in addressing research problems, and exchange of information on what does not work as well as what does work. A primary objective of the TNF Workshop series is to promote collaboration among experimental and computational researchers. Several groups have active and continuous collaborations, and all TNF participants are encouraged to maintain a steady exchange of questions, results, and ideas throughout the year.

Fourth International Workshop on Measurement and Computation of Turbulent Nonpremixed Flames

Darmstadt, Germany
June 27 – 29, 1999

Agenda

Sunday Evening Session -- Welcome

18.00	Welcome and Early Bird Registration Hotel Weinmichel Taverne

Monday Morning Session -- Registration, Results on Target Flames – Piloted Flames

08.00	Registration Georg-Christoph-Lichtenberg-Haus
09.00	Welcome, Introduction (Janicka, Hassel)
09.15	Summary of Previous Workshops (Hassel)
	Results on Target Flames – Piloted Flames Chair: J.-Y. Chen
09.30	Comparison for Piloted Flames D, E, F (Barlow, Hinz)
10.45	*Coffee, Poster Session*
11.15	Comparisons for Piloted Flames D, E, F (cont.) (Barlow, Hinz)
12.45	*Lunch, Poster Session*

Monday Afternoon Session -- More Target Flame Results, Future Swirling Target Flames

	More Target Flame Results, Chair: R.W. Dibble
14.00	Bluff Body Flame from Sydney (Masri, N.N.)
	Future Swirling Target Flames
15.45	Confined Swirling Flame (TECFLAM) (Leuckel)
16.15	Swirl Flame from Sydney (Masri)
16.30	*Coffee, Poster Session*

Monday Evening Session -- Special Event

19.30 *Lab-Party and Poster Session at the Institute Energie- und Kraftwerkstechnik, TU-Lichtwiese*
(Bus L)

Tuesday Morning Session -- Combustion Models and Target Flames, Perspectives on Combustion LES

Combustion Models and Target Flames
Chair: W.P. Jones

09.00 Effects of a Slow Chemical Reaction on the Integral Time Scale and the Turbulent Diffusity
(H. Wenzel, N. Peters)

09.30 More (prospective) Target Flames
Counter Flow Diff. Flame, Delft Flame, CH_4-H_2-DLR-Flame
(Meier, Mastorakos, Geyer, Peeters, N.N.)

10.45 *Coffee, Poster Session*

Perspectives on Combustion LES
Chair: J. Janicka

11.15 LES Prediction in Combustion Systems
(Echekki, Hewson, W.P. Jones, Forkel, N.N.)

12.30 *Lunch, Poster Session*

Tuesday Afternoon Session -- Final Discussion

Final Discussion
Chair: R.W. Bilger

14.00 Objectives for the next Workshop, Future Research Priorities with Respect to Models and Experiments, Publications, Funding

16.00 *Coffee, Poster Session*

16.30 End

Fourth International Workshop on Measurement and Computation of Turbulent Nonpremixed Flames

Darmstadt, Germany, June 27th - 29th

Preface

The main objective of this series of International Workshops on Measurement and Computation of Turbulent Nonpremixed Flames is to optimize the collaboration between experimentalists and modelers in the field of non-premixed turbulent combustion. A main issues hereby is to enhance the understanding of the turbulence-chemistry interaction by careful analysis of various comparisons between many calculations with different sub-models with reliable experimental data. Contrary to conference style with more formal presentation of well done work and ideal results, the workshops focus on problems, non-solved issues, discussions, repeated measurements and calculations of the same object, emphasize of deviations and unexpected showings and detail of experiments, models and numerics.

The procedure for the whole workshop venture so far is:

- Selection of well documented flames, keeping in mind simplicity and provision of boundary conditions
- Collecting complete data sets, including boundary conditions, velocity field, concentration of major and minor species, temperature, repeatedly with different techniques at different places, eliminate any problems, make data available for community via internet www
- Make many well documented simulations with different sub-models and compare them to the data. Emphasize deviations and look where they come from. Improve models
- Go to next step regarding complexity of target object, e.g. from hydrogen to hydrocarbon, or from open to confined

The main results of the first workshop in Naples, Italy (1996), was a selection and definition of so called target flames with the task to provide complete and reliable data bases and make first calculations. The basic ground rules for future collaboration were established. On the second workshop in Heppenheim, Germany (1997), focus was on hydrogen flames, including NO. First results were shown and first conclusions drawn. Simple hydrogen flames were pretty much finished at this stage. The quest was for 'real' fuel. The third workshop, Boulder, Colorado (1998), focused on four target flames with methane and natural gas as fuel. An excellent proceeding was compiled and is available at the www-address shown below. Because hydrocarbon fuel flames are much harder to tackle, work is still in progress on this field and will be continued on the Darmstadt Fourth Workshop in 1999. The scope for the Fourth Workshop is mainly:

- Results from piloted methane flames from about 27 different calculations.
- Progress on bluff body and swirl flames: simulation comparisons.
- Report on new target flames.
- Perspectives on combustion models, especially LES

The number of participants of the previous workshops was between 50 and 80, this time we expect about 85 people including the organizer team. This booklet contains the material which was send to the organizers until one week prior to the workshop. This is mainly abstracts of presentations and posters.

Acknowledgment: Organization was done by Chr. Schneider, TU Darmstadt, and his team of PhD students. The workshop was partly sponsored by Spindler & Hoyer, Fluent Deutschland GmbH, LaVision 2D-Messtechnik GmbH and DANTEC/invent Measurement Technology GmbH. The scientific input, contribution and collaboration of many volunteers is gratefully appreciated.

For more workshop information: www.ca.sandia.gov/tdf/Workshop.html

Organizing committee: R. Barlow, J.-Y. Chen, R. Bilger, E. Hassel, J. Janicka, A. Masri, T. Peeters, N. Peters, S. Pope

We wish you a pleasant, successful and sunny stay in Darmstadt, E. Hassel and J. Janicka

Name	Firstname	Position	Company	Address	Zipcode	City	Country	email
Aigner	Manfred	Prof.	DLR Stuttgart	Phys. Chemie der Verbrennung Pfaffenwaldring 38-40	70569	Stuttgart	Germany	manfred.aigner@dlr.de
Bajaj	Pankaz		ETH Zürich	Inst. of Energy Technology, ETH Zentrum	8092	Zürich	Switzerland	Bajaj@ltnt.iet.mavt.ethz.ch
Barlow	Robert	Prof.	Sandia National Laboratories	MS 9051, PO Box 969	94551	Livermore, CA	USA	barlow@ca.sandia.gov
Beck	John		University of California Berkeley	6163 Etcheverry Hall Dept. of M.E.UC	94720	Berkeley, CA	USA	
Bender	Roland		ITV Institut Uni Stuttgart	Pfaffenwaldring 12	70569	Stuttgart	Germany	bender@itv.uni-stuttgart.de
Bilger	Robert W.	Prof.	University of Sidney	Department of Mechanical Engineering	2006	Sidney	Australia	bilger@tiny.me.su.oz.au
Binninger	B.	Dr.	RWTH Aachen Institut für Technische Mechanik	Templergraben 64	52056	Aachen	Germany	
Blasenbrey	Tilmann		ITV Institut Uni Stuttgart	Pfaffenwaldring 12	70569	Stuttgart	Germany	blasenbrey@itv.uni-stuttgart.de
Böckle	Stefan		Uni Heidelberg, PCI Institut	Im Neuenheimer Feld 253	69120	Heidelberg		hv5@ix.urz.uni-heidelberg.de
Branley	Niall	Dr.	Imperal College, Chem. Eng. & Chem. Tech.	Prince Consort Rd	SW7 2BY	London	United Kingdom	m.branley@ic.ac.uk
Cabra	Ricardo		University of California Berkeley	6163 Etcheverry Hall Dept. of M.E.UC	94720	Berkeley, CA	USA	ricardo@newton.me.berkeley.edu

Name	Firstname	Position	Company	Address	Zipcode	City	Country	email
Chen	Jyh-Yuan	Prof.	University of California Berkeley	6163 Etcheverry Hall Dept. of M.E.UC	94720	Berkeley, CA	USA	jychen@pyrolab.me.berkeley.edu
Chen	Ming		RWTH Aachen Institut für Technische Mechanik	Templergraben 64	52056	Aachen	Germany	
Coelho	Pedro	Prof.	RWTH Aachen Institut für Technische Mechanik	Templergraben 64	52056	Aachen	Germany	p.coelho@itm.rwth-aachen.de
Di Mare	Francesca		Imperal College, Chem. Eng. & Chem. Tech.	Prince Consort Rd	SW7 2BY	London	United Kingdom	f.di.mare@ic.ac.uk
Dibble	Robert	Prof.	University of California Berkeley	6163 Etcheverry Hall Dept. of M.E.UC	94720	Berkeley, CA	USA	dibble@newton.me.berkeley.edu
Ding	Tieying		TU Delft	Dept. Applied Physics, P.O. Box 5046	2600	Delft, GA	The Netherlands	tieying@wt.tn.tudelft.nl
Dreizler	Andreas	Dr.rer. nat.	ITV Institut, Uni Stuttgart	Pfaffenwaldring 12	70569	Stuttgart	Germany	dreizler@itv.uni-stuttgart.de
Driscoll	James F.	Prof.	University of Michigan	2422 Meadowridge Ct.	48105	Ann Arbor, MI	USA	Jamesfd@umich.edu
Echekki	Tarek	Dr.	Sandia National Laboratories	MS 9051, 7011 East Ave., PO Box	94551 - 0969	Livermore, CA	USA	techekk@ca.sandia.gov
Ferreira	Jorge C.	Dr.	AEA Technology	Staudenweg 12	83624	Otterfing	Germany	if@ascg.de

Name	Firstname	Position	Company	Address	Zipcode	City	Country	email
Forkel	Hendrik		TU Darmstadt Institute of Energy- and Powerplant Technology	Petersenstr. 30	64287	Darmstadt	Germany	forkel@krabat.ekt.maschinenbau.tu-darmstadt.de
Gass	Jürg	Dr.	ETHZ Inst. für Energietechnik	ETH Zentrum LOW	8092	Zürich	Switzerland	gass@ltnt.iet.mavt.ethz.ch
Geiß	Stefan		TU Darmstadt Institute of Energy- and Powerplant Technology	Petersenstr. 30	64287	Darmstadt	Germany	sgeiss@hrz2.hrz.tu-darmstadt.de
Geyer	Dirk		TU Darmstadt Institute of Energy- and Powerplant Technology	Petersenstr. 30	64287	Darmstadt	Germany	geyer@hrz2.hrz.tu-darmstadt.de
Gill	Albrecht	Dr.	Fluent GmbH	Hindenburgstrasse 36	64295	Darmstadt	Germany	Ag@fluent.de
Girard	James W.		University of California Berkeley	6163 Etcheverry Hall Dept. of M.E.UC	94720	Berkeley, CA	USA	jwgirard@firebug.me.berkeley.edu
Goldin	Graham	Dr.	Fluent Inc.	10 Cavendish Ct.	03766	NH	Lebanon	gmg@fluent.com
Gutheil	Eva	Prof.	IWR Universität Heidelberg	Im Neuenheimer Feld 368	69120	Heidelberg	Germany	gutheil@iwr.uni-heidelberg.de
Habisreuther	Peter		Engler-Bunte-Institiut	Richard Willstaetter-Allee 5	76128	Karlsruhe	Germany	Peter.Habisreuther@ciw.uni-karlsruhe.de
Hassel	Egon	Dr.	TU Darmstadt Institute of Energy- and Powerplant Technology	Petersenstr. 30	64287	Darmstadt	Germany	hassel@hrz1.hrz.tu-darmstadt.de

Name	Firstname	Position	Company	Address	Zipcode	City	Country	email
Hewson	John C.	Dr.	Sandia National Laboratories	MS 9051, 7011 East Ave., PO Box	94551 - 0969	Livermore, CA	USA	jhewson@honoh.ca.sandia.gov
Hinz	Alexander		TU Darmstadt Institute of Energy- and Powerplant Technology	Petersenstr. 30	64287	Darmstadt	Germany	ahinz@hrzpub.tu-darmstadt.de
Huebner	Werner		TU Delft	Dept. Applied Physics, P.O. Box 5046	2600	Delft, GA	The Netherlands	werner@wt.tn.tudelft.nl
Ikeda	Yuji	Prof.	Kobe-University, Dept. of Mech. Eng.	Rokko, Nada		Kobe	Japan	kojima@mech.kobe-u.ac.jp
Janicka	Johannes	Prof.	TU Darmstadt Institute of Energy- and Powerplant Technology	Petersenstr. 30	64287	Darmstadt	Germany	janicka@hrz1.hrz.tu-darmstadt.de
Jenny	Patrick	Dr.	Cornell University	258 Upson Hall	14850	Ithaca, NY	USA	jenny@mae.cornell.edu
Jones	William P.	Prof.	Imperal College, Chem. Eng. & Chem. Tech.	Prince Consort Rd	SW7 2BY	London	United Kingdom	w.jones@ic.ac.uk
Kazenwadel	Jan		Universität Heidelberg, PCI Institut	Im Neuenheimer Feld 253	69120	Heidelberg	Germany	f79@ix.urz.uni-heidelberg.de
Keck	Olaf		DLR	Pfaffenwaldring 38	70569	Stuttgart	Germany	olaf.keck.@drl.de

Name	Firstname	Position	Company	Address	Zipcode	City	Country	email
Klein	Markus		TU Darmstadt Institute of Energy- and Powerplant Technology	Petersenstr. 30	64287	Darmstadt	Germany	kleinm@hrzpub.tu-darmstadt.de
Kojima	Jun		Kobe-University, Dept. of Mech. Eng.	Rokko, Nada		Kobe	Japan	kojima@ms-5.mech.kobe-u.ac.jp
Krieger	Guenther	Dr.	Universidade de Sâo Paulo	Departamento den Engenharia Mecânica	05508-900	Sâo Paulo	Brazil	Guenther@usp.br
Kronenburg	Andreas	Dr.	Daimler Chryler AG	HPC:B209 Abt.:M/EBB	70546	Stuttgart	Germany	andreas.kronenburg@str.daimler-benz.com
Kunz	Oliver	Dr.	DLR	Pfaffenwaldring 38	70569	Stuttgart	Germany	Oliver.kunz@dlr.de
Kunzelmann	Thomas		Uni Heidelberg, PCI Institut	Im Neuenheimer Feld 253	69120	Heidelberg	Germany	
Landenfeld	Tilo	Dr.	TU Darmstadt Institute of Energy- and Powerplant Technology	Petersenstr. 30	64287	Darmstadt	Germany	tlandenf@hrz1.hrz.tu-darmstadt.de
Leuckel	Wolfgang	Prof.	Engler Bunte Institut	Engler-Bunte-Feuerungstechnik Kaiserstr. 12	76128	Karlsruhe	Germany	Wolfgang.Leuckel@ciw.uni-karlsruhe.de
Lindstedt	R.P.	Dr.	Imperial College / MED	Exhibition Road	SW 72 BX	London	United Kingdom	p.Lindstedt@ic.ac.uk
Linow	Sven		TU Darmstadt Institute of Energy- and Powerplant Technology	Petersenstr. 30	64287	Darmstadt	Germany	slinow@hrzpub.tu-darmstadt.de

Name	Firstname	Position	Company	Address	Zipcode	City	Country	email
Long	Marshall	Prof.	Yale University	Dept. of M.E., P.O. Box 208284	6520	New Haven, CT	USA	Marshall.long@yale.edu
Louloudi	Sofia		Imperial College / MED	Exhibition Road	SW 72 BX	London	United Kingdom	s.louloudi@ic.ac.uk
Masri	Assaad R.	Dr.	Dept. of M. and Mechatronic Engr.	University of Sydney	2006	Sidney	Australia	masri@mech.eng.usyd.edu.au
Mastorakos	Epaminon-das		Foundation for Research and Technology-Hellas	PO BOX 1414	26500	Patras	Greece	mastorak@iceht.forth.gr
Mbiock	Aristide	Dr.	Delft University	Lorentzweg 1	2600	Ga Delft	The Netherlands	
Meier	Wolfgang	Dr.	DLR	Pfaffenwaldring 38	70569	Stuttgart	Germany	wolfgang.meier@dlr.de
Mengler	Christian		TU Darmstadt Institute of Energy- and Powerplant Technology	Petersenstr. 30	64287	Darmstadt	Germany	cmengler@hrz2.hrz.tu-darmstadt.de
Muradoglu	Metin		Cornell University	258 Upson Hall	14850	Ithaca, NY	USA	metinom@mae.cornell.edu
Neumann	Mike		TU Dresden, IF Thermodynamik und TGA	Helmholtzstraße 14	01069	Dresden	Germany	Siehe Zschunke
Niemann	Holger		IWR Universität Heidelberg	Im Neuenheimer Feld 368	69120	Heidelberg	Germany	niemann@iwr.uni-heidelberg.de
Obieglo	Andreas			Inst. of Energy Technology, ETH Zentrum	8092	Zürich	Switzerland	Obieglo@ltnt.iet.mavt.ethz.ch

Name	Firstname	Position	Company	Address	Zipcode	City	Country	email
Paczko	Günther		RWTH Aachen Institut für Technische Mechanik	Templergraben 64	52056	Aachen	Germany	g.paczko@itm.rwth-aachen.de
Peeters	Tim	Dr.	Delft University	Lorentzweg 1	2600	Ga Delft	The Netherlands	tim@wt.tn.tudelft.nl
Peters	Norbert	Prof.	RWTH Aachen Institut für Technische Mechanik	Templergraben 64	52056	Aachen	Germany	n.peters@itm.rwth-aachen.de
Pfitzner	Michael	Dr.	BMW Rolls-Royce GmbH	Eschenweg 11	15827	Dahlewitz	Germany	michael.pfitzner@brr.de
Pitsch	Heinz		Stanford University	Center for Integrated Turbulence Simulations	CA 94305-3030	Stanford	USA	h.pitsch@stanford.edu
Prasetyo	Yudi		Imperal College, Chem. Eng. & Chem. Tech	Prince Consort Rd	SW7 2BY	London	United Kingdom	y.prasetyo@ic.ac.uk
Repp	Stefan		TU Darmstadt Institute of Energy- and Powerplant Technology	Petersenstr. 30	64287	Darmstadt	Germany	srepp@hrzpub.tu-darmstadt.de
Riesmeier	Elmar		RWTH Aachen Institut für Technische Mechanik	Templergraben 64	52056	Aachen	Germany	e.riesmeier@itm.rwth-aachen.de
Roekaerts	Dirk J. E. M.	Prof.	Delft University	Lorentzweg 1	2600	Ga Delft	The Netherlands	dirkr@duttwta.wt.tn.tudelft.nl

Name	Firstname	Position	Company	Address	Zipcode	City	Country	email
Roth	Bertram		TU Darmstadt Institute of Energy- and Powerplant Technology	Petersenstr. 30	64287	Darmstadt	Germany	broth@hrzpub.tu-darmstadt.de
Rüdiger	Frank	Dr.	Schott GmbH	Göschwitzer Str.20		Jena	Germany	ruedg@ml.schott.de
Sadiki	Amsini	Dr.	TU Darmstadt Institute of Energy- and Powerplant Technology	Petersenstr. 30	64287	Darmstadt	Germany	sadiki@hrz2.hrz.tu-darmstadt.de
Schäfer	Olaf		ITS, Uni-Karlsruhe			Karlsruhe	Germany	Olaf.schaefer@its.uni-karlsruhe.de
Schmidt	Dietmar	Dr.	ITV Institut Uni Stuttgart	Pfaffenwaldring 12	70569	Stuttgart	Germany	schmidt@itv.uni-stuttgart.de
Schmittel	Peter		Engler Bunte Institut	Richard-Willstätter Allee 5	76128	Karlsruhe	Germany	pesc@ebifsol6.ciw.uni-karlsruhe.de
Schneider	Christoph		TU Darmstadt Institute of Energy- and Powerplant Technology	Petersenstr. 30	64287	Darmstadt	Germany	cschneid@hrz2.hrz.tu-darmstadt.de
Schramm	Berthold		IWR Universität Heidelberg	Im Neuenheimer Feld 368	69120	Heidelberg	Germany	Schramm@iwr.uni-heidelberg.de
Schroth	Günther		TU Darmstadt Institute of Energy- and Powerplant Technology	Petersenstr. 30	64287	Darmstadt	Germany	schroth@hrzpub.tu-darmstadt.de
Steiner	Boris		ITV Institut Uni Stuttgart	Pfaffenwaldring 12	70569	Stuttgart	Germany	steiner@itv.uni-stuttgart.de

Name	Firstname	Position	Company	Address	Zipcode	City	Country	email
Strauß	Silvio		TU Dresden, IF Thermodynamik und TGA	Helmholtzstraße 14	01069	Dresden	Germany	Siehe Zschunke
Theisen	Peter		DLR Köln	Linder Höhe	51147	Köln	Germany	Peter.theisen@dlr.de
Thévenin	Dominique	Dr.	EM2C Lab Ecole Centrale Paris			Paris	France	Thevenin@em2c.ecp.fr
Turpin	Guillaume		Matra Bae Dynamics	20/22 rue Grange Dame Rose B.P. 150	78141	Vélizy-Villacoublay cedex	France	turpin@onera.fr
Ukai	Osamu		Mitsubishi Heavy Industries, Ltd.	1-8-1 Sachiura, Kanazawa-ku	236-0003	Yokohama	Japan	Ukai@atrc.mhi.co.jp
Van der Meer	Theo H.	Dr.	TU Delft	Dept. Applied Physics, P.O. Box 5046	2600	Delft, GA	The Netherlands	theo@wt.tn.tudelft.nl
Van Slooten	Paul R.	Dr.	United Techn. Research Center	Mail Stor 129-16 411 Silver Lane	CT 06108	East Hartford	USA	vanslopr@utrc.utc.com
Warnatz	Jürgen	Prof.	IWR Universität Heidelberg	Im Neuenheimer Feld 368	69120	Heidelberg	Germany	warnatz@iwr.uni-heidelberg.de
Wenzel	Holger		RWTH Aachen Institut für Technische Mechanik	Templergraben 64	52056	Aachen	Germany	H.Wenzel@itm.rwth-aachen.de
Xiao	Kejian		ITV Institut Uni Stuttgart	Pfaffenwaldring 12	70569	Stuttgart	Germany	xiao@itv.uni-stuttgart.de
Xu	Jun		Cornell University	258 Upson Hall	14850	Ithaca, NY	USA	xujun@mae.cornell.edu
Yuasa	Atsushi		University of California Berkeley	6163 Etcheverry Hall Dept. of M.E.UC	94720	Berkeley, CA	USA	Yuasa@firebug.ma.berkeley.edu

Name	Firstname	Position	Company	Address	Zipcode	City	Country	email
Zschunke	Tobias	Dr.	TU Dresden, IF Thermodynamik und TGA	Helmholtzstraße 14	01069	Dresden	Germany	zschunke@MTTNV01.mw.TU-Dresden.de

SECTION 1

Piloted CH_4/Air Jet Flames

Fourth International Workshop on Measurements and Computations of Turbulent Nonpremixed Flames at Darmstadt, June 27 - 29, 1999

Piloted Methane / Air Jet Flames (Flame D, E, F) Comparisons

Coordinators: Robert Barlow, Alexander Hinz

Flame Description:
The Flame D, E and F represent a series of piloted jet flames operated using Sydney University piloted burner geometry [1,2]. This burner has a nozzle of $d = 7.2$ mm and a premixed pilot that extends to a diameter of $D = 18.2$ mm. The main jet composition is 25 % CH_4 and 75 % air, selected to reduce the level of flourescence interference from soot precursors. The pilot fuel gas is composed using C_2H_2, H_2, air, CO_2, and N_2. This premixture has the same nominal enthalpy and equilibrium composition as methane/air at this equivalence ratio and therefore the system can be described by one mixture fraction. The stoichiometric value of the mixture fraction is 0.351, and the stoichiometric flame length is $\sim 47d$.

The complete series of six flames spans the jet Reynolds numbers of 1,100 (Flame A) to 44,800 (Flame F). Flame D has a jet Reynolds number of 22,400 and has only a small probability of localized extinction. Flame E has a jet Reynolds number of 33,400 and Flame F of 44,800. In particular the Flame F shows a significant amount of local extinction.

Experimental Overview:
The data base on Flame D, E, and F includes simultaneous point measurements of T, N_2, O_2, CH_4, CO_2, H_2O, and H_2 by Rayleigh/Raman scattering and of OH, NO, and CO by laser-induced flourescence [1,2]. Two component LDV data were measured during this and the past year at TU Darmstadt. The burner and the set of calibrated flow controllers were loaned from Sandia in order to insure equivalence of flow conditions.

Contributed Calculations:
Results of 27 calculations of flames D, E, and F were submitted for comparison with the experiment. This includes the 7 calculations of flame D from the TNF3 Workshop in Boulder. The following tables give a brief overview of the of the calculations for each flame. More detailed information on can be found in the one-page summaries from each group.

Flame D / TNF3:

GROUP	*METHOD*	*CHEMISTRY*
Chen, UC Berkeley	Monte Carlo PDF - Mod. Curl	GRI-Mech 1.2
Chen, UC Berkeley	Monte Carlo PDF - Mod. Curl	Flamelet, Le=1
Chen, UC Berkeley	Monte Carlo PDF - Mod. Curl	Flamelet, diff-diff
Hinz, Janicka, TU Darmstadt	Monte Carlo PDF - Mod. Curl	ILDM
Roomina, Bilger, U Sydney	CMC	GRI-Mech 2.1
Roomina, Bilger, U Sydney	CMC	GRI-Mech 2.1 w/ radiation
Paul, Sivathanu, Gore, U Purdue	LFSR	GRI-Mech 2.11

Flame D / TNF4:

GROUP	*METHOD*	*CHEMISTRY*
Chen, UC Berkeley	Monte Carlo PDF - IEM	Reduced 12-step
Chen, UC Berkeley	Monte Carlo PDF - Mod. Curl	Reduced 12-step
Coelho, Peters, RWTH Aachen	Finite Volume	Steady Flamelet
Coelho, Peters, RWTH Aachen	Finite Volume	Unsteady Flamelet
di Mare, Jones, IC London	LES	Flamelet
Echekki, Sandia Labs	ODT	Reduced 12-step
Hinz, Janicka, TU Darmstadt	Monte Carlo PDF - Mod. Curl	ILDM
Hinz, Janicka, TU Darmstadt	Monte Carlo PDF - Mod. Curl	Reduced 4-step
Lindstedt, IC London	Monte Carlo PDF - Mod. Curl	Reduced 16-step
Obieglo, Gass, ETH Zürich	Monte Carlo PDF - IEM	Reduced 4-step

Flame E:

GROUP	*METHOD*	*CHEMISTRY*
Chen, UC Berkeley	Monte Carlo PDF - IEM	Reduced 12-step
Chen, UC Berkeley	Monte Carlo PDF - Mod. Curl	Reduced 12-step
Echekki, Sandia Labs	ODT	Reduced 12-step
Hinz, Janicka, TU Darmstadt	Monte Carlo PDF - Mod. Curl	ILDM
Roomina, Bilger, U Sydney	CMC	GRI-Mech 2.11

Flame F:

GROUP	*METHOD*	*CHEMISTRY*
Chen, UC Berkeley	Monte Carlo PDF - IEM	Reduced 12-step
Chen, UC Berkeley	Monte Carlo PDF - Mod. Curl	Reduced 12-step
di Mare, Jones, IC London	LES	Flamelet
Echekki, Sandia Labs	ODT	Reduced 12-step
Hinz, Janicka, TU Darmstadt	Monte Carlo PDF - Mod. Curl	ILDM
Hinz, Janicka, TU Darmstadt	Monte Carlo PDF - Mod. Curl	Reduced 4-step
Lindstedt, IC London	Monte Carlo PDF - Mod. Curl	Reduced 16-step

Contents of this Section

After the one-page abstracts of all calculations the results of Flame D, E, and F are given successively. For Flame D, each page of results is followed by the respective TNF3-results as reference except for the scatter plots. Also the summaries of Flame D calculations turned in to the TNF3 workshop are added as reference after the current summaries. For a better orientation the page numbers are indicated where the results of the respective flame can be found.

- Summaries of calculation methods
- Axial profiles of velocity, mixture fraction, temperature and Favre-average species mass fractions
- Radial profiles of $\tilde{u}$, $\sqrt{\widetilde{u''^2}}$, and $\widetilde{u''v''}$ at $x/d = 15, 45$

- Radial profiles of Favre-averages of f, $\sqrt{\widetilde{f''^2}}$, T, Y_{CO}, Y_{H_2}, and Y_{OH} at $x/d = 15, 30, 45$
- Conditional means of T, Y_{CO_2}, Y_{H_2O}, and Y_{CH_4}, Y_{O_2}, Y_{CO}, Y_{H_2}, and Y_{OH} at $x/d = 15, 30, 45$
- Scatter plots of T, Y_{CO_2}, Y_{CO}, Y_{H_2O}, Y_{H_2}, Y_{OH} at $x/d = 15, 30$
- Conditional PDF of T, Y_{H_2O}, Y_{CO_2}, Y_{OH}, Y_{CO}, and Y_{H_2} at $x/d = 15, 30, 45$

Remarks

- For Flame D the Favre- and conditionally averaged results from TNF3 are plotted separately. Scatter plots from the TNF3 calculations are not included here and may be found in the TNF3 Proceedings on the web.
- The legends below the graphs contain all contributors although the particular data have not always been available or not evaluated.
- The scatter plots contain a flamelet solution as reference using $a = 100s^{-1}$ and equal diffusivity. Each graph shows in the order of 10,000 samples.
- The experimental data are plotted with estimated error bars. This is to give an orientation on the accuracy of the data set. The estimated errors are given in the following table.

Quantity	*Error*	*Quantity*	*Error*	*Quantity*	*Error*
U	$\pm$2.5%, rel.	$\sqrt{\widetilde{u''^2}}$	$\pm$3.5%, rel.	$\widetilde{u''v''}$	$\pm$3.5%, rel.
F	$\pm$3.0%, rel.	$\sqrt{\widetilde{f''^2}}$	–	T	$\pm$3.0%, rel.
$\sqrt{\widetilde{T''^2}}$	$\pm$50 [K], abs.	Y_{O_2}	$\pm$0.006, abs.	Y_{CH_4}	$\pm$0.004, abs.
Y_{CO_2}	$\pm$4.0%, rel.	Y_{H_2O}	$\pm$4.0%, rel.	Y_{CO}	$\pm$10.0%, rel.
Y_{OH}	$\pm$10.0%, rel.	Y_{H_2}	$\pm$10.0%, rel.	Y_{NO}	$\pm$15.0%, rel.

Note on Experimental Error Bars (R. Barlow):
The plots of Favre- and conditional averages include error bars on the experimental data. The basis for the uncertainty estimates that are represented by these error bars is described in Ref. [1]. In most cases, uncertainty intervals are plotted as a fixed percentage of the local value, which is a simplification. The estimated uncertainties are representative of the high-temperature region (roughly 0.25 to 0.55 in mixture fraction). Uncertainties for CO, H_2, OH, and NO are greater outside this high temperature range than is indicated by the graphs. Consequently, the error bars for these scalars underestimate the actual uncertainties at locations away from the peak mass fractions. Uncertainties in the conditional means of CH_4 and O_2 are plotted as fixed values in mass fraction, which is also a simplification. Uncertainty in the mixture fraction fluctuations, $\sqrt{\widetilde{f''^2}}$, cannot be represented simply and is not plotted on some graphs. The error bars in the $\sqrt{\widetilde{f''^2}}$ plots for the TNF4 calculations of Flame D should be taken as representative of uncertainties in all three flames.
The plotted error bars may not fully account for the effect of fluorescence interferences on the Raman measurements. We have applied the same interference correction procedures to all locations in all flame. However, it is expected that the details of the interference spectra depend on the local

composition of the *hydrocarbon soup* that is produced in fuel-rich samples. This composition is expected to depend on residence time and the mixing conditions of each flame. In particular, there is some suspicion that the H_2 and CO_2 measurements in the richest samples at $x/d = 45$ in flame D may be affected by fluorescence interferences, and caution is advised when interpreting these particular results.

Preliminary Observations

A major strength of the this data set is in the measurements of combustion intermediates and minor species. Accordingly, the comparisons included here emphasize issues of chemistry more than the details of flow/mixing fields.

Flame D (R. Barlow)

Results of 17 calculations of Flame D are included, 7 from TNF3 and 10 new calculations. Many different modeling approaches are represented. A few observations are listed that may prompt further discussion.

1. There is a wider spread among the new results for the overall flow and fixing fields, as represented by the axial and radial profiles of velocity and mixture fraction, than there was in the TNF3 round of calculations. Axial profiles of $\tilde{u}_c$ and $\sqrt{\widetilde{u''^2}}$, in particular, are less consistent in the TNF4 plots, and it appears that some aspects of the turbulence models may have been changed by the groups that submitted calculations to both workshops. Some discussion on the convergence of turbulence models for these jet flames might be useful.

2. Most calculations are in reasonably good agreement with the measured axial profiles of $\tilde{f}$, $\sqrt{\widetilde{f''^2}}$, $\tilde{T}$, and $\sqrt{\widetilde{T''^2}}$. This is not to say that the calculations fall mainly within the experimental error bars.

3. Radial profiles of $\tilde{u}$, $\sqrt{\widetilde{u''^2}}$, and $\widetilde{u''v''}$ at $x/d = 45$ show mixed results. Most of the calculations under predict the measured turbulent fluctuations of velocity.

4. The majority of the models yield broader radial profiles of F than are measured at $x/d = 15$, 30, and 45. The majority of models predict the magnitude of F'' reasonably well.

5. Radial profiles of temperature and mass fraction at the downstream locations in Flame D are tied directly to the $\tilde{f}$ and $\sqrt{\widetilde{f''^2}}$ results and to the chemistry predictions (conditional means). Therefore, it is more useful to compare species results in terms of conditional means and scatter plots, rather than radial profiles.

6. The conditional means show some anomalies. First, the ILDM results for CO and H_2 are unrealistic outside the near-stoichiometric region. As discussed by Maas in Boulder, this implementation of ILDM uses two progress variables (CO_2 and H_2O), and the manifold is only defined for a limited interval in mixture fraction. The unrealistic results for CO and H_2 result from assumptions made regarding these species outside this interval. ILDM is, however, able to predict localized extinction. Second, the two calculations based on reduced 4-step mechanisms yield unrealistic results for H_2 on the lean side. Third, the conditional means from the LES calculation are inconsistent with the other measured and computed results.

7. The majority of calculations yield good agreement with measured conditional means of all scalar for fuel-lean conditions and for mixture fractions up to roughly 0.4. In fuel-rich samples the results tend to diverge, with the flamelet, CMC, and ODT methods predicting significantly higher mass fractions of CO and H_2 than are measured. The two steady flamelet calculations (Chen and Coelho) yield very similar results for fuel-rich conditions. Some of the pdf calculations also predict higher CO and H_2, but here the comparison is complicated by considerations of localized extinction.

8. Related to the above, an important question from TNF3 has yet to be resolved. Why do the different methods (flamelet, CMC, pdf) predict significantly different results for rich-side chemistry when the calculations are run using the same chemistry.

9. There are now several calculations of NO, some of which are in close agreement with measurements. Can we determine whether these calculations getting the right answers for the right reasons?

Flame D, E, F (A. Hinz)

The comments above also hold for Flame E and F. An interesting characteristic of this flame series is the increasing amount of localized extinction.

1. The drop in the axial mixture fraction profile observed in Flame F is not reproduced by the simulations. Local extinction effects to this large extent are not captured by the simulations turned in to this workshop.

2. The trend of an increase of local extinction can be observed in scatter plots and also conditional PDFs for most of the calculations, in particular the scatter plots of the simulation using a 16-step mechanism (Lindstedt) show a large amount of local extinction. Since flame stability problems occurred for the 4-step mechanism (Hinz) the mixing rate is increased and, hence, local extinction effects suppressed.

3. The conditional mean of temperature for Flame F at $x/d < 15, 30$ show a significant drop on the rich-fuel side ($f > 0.4$). Is local extinction a rich-fuel region phenomena due to the slow time scales of rich-fuel chemistry?

4. The ODT model (Echekki) does not show a clear trend of local extinction in the conditional PDFs of temperature and major species. But for the conditional PDFs of minor species (H_2, OH, CO) there is good agreement between experiments and ODT.

5. Extra treatment to insure a stably burning flame is necessary for the 4-step mechanism (Hinz; ILDM chemistry for $x/d < 7.5$, increased scalar mixing) and the 12-step mechanism (Chen; flamelet solution for $x/d < 7.5$) but not for ILDM (Hinz) and 16-step mechanism (Lindstedt).

References:

[1] Barlow, R., Frank, J.H. (1998), 27^{th} *Symp (Int.) Comb.*, pp. 1087-1095.

[2] http://www.ca.sandia.gov/tdf/Workshop.html

Model Summaries (TNF4)

J.-Y. Chen University of California at Berkeley: Flames D, E, F

-Turbulence model: Reynolds stress model with parabolic code

-Chemistry Model and Kinetic Mechanism :Reduced Chemistry 12-step with NO_x developed from GRI2.11[2]

-Mixing Model and Number of PDF Particles (if appropriate): Modified Curl's mixing model & IEM model.

-Coupling Model: Joint scalar PDF (Probability Density Function)[1]

-Solution Domain (xmin, xmax, ymin, ymax) and Grid Structure

50 girds across half of the jet with the assumption of axisymmetric flows.
(xmin= x/D=0; xmax: x/D=90; ymin=0 centerline; ymax= expands as air is entrained into the jet)

-Boundary Conditions (state any difference from those in the documentation file)

Inlet velocity and scalar specified according to the information in the workshop web

-Location Start of Computation: x/D=0

-Convergence Criteria or Length of Calculation: Marching algorithm with implicit scheme up to x/D=90

-Machine used and approx. CPU Time required

PC Pentium II 450 Linux about 5 days per run.

-Radiation Model

Optical thin limit model with absoption coefficients of H_2O, CO_2, CO, and CH_4 as recommended by the TNF workshop web page.

-Comments on Modeling Issues

Special near field treatment: use flamelet model (a=100/s) from x/D=0-7.5 without NO
Note: without this special treatment flame blows out at downstream around x/D~10-15

-References

1. Pope, S.B. Prog. Energy Combust. Sci 11:119 (1985)
2. Frenklach, M., Wang, H., Yu, C.-L., Goldenberg, M., Bowman, C. T., Hanson, R. K., Davidson, D. F., Chang, E. J., Smith, G. P., Golden, D. M., Gardiner, W. C., and Lissianski, V., http://www.me.berkeley.edu/gri_mech/.

Numerical Simulation of a Turbulent Piloted Methane/Air Jet Flame Using a Laminar Flamelet Model

P.J. Coelho (*) and N. Peters (**)

* Instituto Superior Técnico, Technical University of Lisbon, Av. Rovisco Pais, 1049-001 Lisboa, Portugal
e-mail: coelho@vangogh.ist.utl.pt
(work performed during a sabbatical leave at RWTH Aachen)
** Institut fur Technische Mechanik, RWTH Aachen, Templergraben 64, 52062 Aachen, Germany
e-mail: N.Peters@itm.rwth-aachen.de

Turbulence Model:

The Reynolds stress model implemented in version 4.8 of Fluent is used. The diffusive transport term is described by the gradient transport approximation (1). The pressure/strain is approximated following (2). The dissipation term is modelled using an isotropic dissipation rate. Version 4.8 of FLUENT does not contain terms that account for variable density effects and no effort was undertaken to improve this. Standard values are used for the constants of the model. The ϵ equation is modified according to (3) in order to improve the prediction of the spreading rate of the fuel jet.

Chemistry model and kinetic mechanism:

A steady flamelet library is generated using RIF, an ITM-RWTH in-house code based on the solution of the flamelet equations. Flamelets are computed for scalar dissipation rates of 0.1, 0.2, 0.5, 1, 2, 5, 10, 20, 50, 100 and 200 (1/s) assuming Le=1 for all species. The chemical mechanism, also developed at ITM-RWTH, comprises 49 species and 547 reactions, including those of the NO mechanism. The temperature calculated from flamelet equations is not used, since it does not consider the radiation. Instead, an enthalpy equation with a radiative source term is solved in the CFD code, and the temperature is obtained from the defintion of enthalpy and using the species mass fractions. A presumed beta pdf is used to compute mean (Favre averaged) quantities. Unsteady flamelet calculations are performed in a post-processing stage using marker particle transport equations with 6 flamelets initialized on the rich side of the contour of mean stoichiometric mixture (4).

Solution domain:

The grid is axisymmetric with 200x100 grid nodes mapping the domain from x/d=0 to xd/=100, and from r/d=0 to r/d=20. Twelve grid nodes in radial direction are placed inside the fuel jet, and 18 grid nodes are inside the pilot fuel flame.

Boundary conditions:

Temperature and mixture fraction at the inlet are prescribed according to the data. The experimental mean and fluctuating velocity are fitted by cubic splines and interpolated to the grid nodes. It is assumed that the inlet normal stresses in the radial and tangential directions are equal to one half of the axial normal stress, and that the shear stress is zero.

Location of start of computations:

An elliptic solver was used.

Convergence criteria or length of calculation:

The sum of the absolute residuals extended over all the grid nodes is requested to decrease below a specified tolerance. This is taken as 10^{-3} for mass and velocities, $5*10^{-3}$ for normal and shear stresses and $5*10^{-6}$ for the enthalpy and mixture fraction.

Machine used and approximate CPU time required:

A HP workstation is used. The steady calculations are performed in three steps: first isothermal, then with combustion and k-ϵ model, and finally with Reynolds stress model. The overall number of iterations is about 5000, and the calculations with the full model take about 1 minute per iteration. The unsteady calculations take about 1.5 hours per flamelet.

Radiation model:

The optically thin approximation is used with absorption coefficients oh H2O, CO2, CO and CH4 taken from the fit to the RADCAL calculations, as reported in the web documentation.

Comments on modelling issues:

The modification of the ϵ equation described in (3) improves the prediction of the spreading rate of the fuel jet. The unsteady flamelet calculations yield an improvement of the predicted CO and H2 profiles. The NO profile is also significantly improved by the unsteady calculations, although the NO levels are still overestimated.

References:

1 - Launder, B.E., Reece, G.J. and Rodi, W., J. Fluid Mechanics, Vol. 68, Pt. 3, pp. 537-566, 1975.
2 - Launder, B.E., Int. J. Heat Fluid Flow, Vol. 10, No. 4, pp. 282-300, 1989.
3 - Pope, S.B., AIAA J., Vol 16, No. 3, pp. 279-281, 1978.
4 - Barths, H., Peters, N., Brehm, N., Mack, A., Pfitzner, M. and Smiljanovski, V., 27th Symposium (Int.) on Combustion, 1998.

Large-Eddy-Simulation of Partially Premixed CH_4/Air Turbulent Flames - Flame D

F di Mare and W. P. Jones
Department of Chemical Engineering and Chemical Technology
Imperial College of Science, Technology and Medicine
London SW7 2BY
United Kingdom

Modeling Procedures
The spatially-filtered continuity and momentum equations are solved along with a transport equation for the mixture fraction. Closure is provided with the standard Smagorinsky Sub-Grid model, with $C_s = 0.15$. A presumed-shape pdf (β-pdf) approach, coupled with a flamelet assumption [1], is applied to solve the compositional field.

Solution Method
The method [2] chosen for this computation utilises a fully implicit formulation and an approximate factorisation technique is adopted to determine the pressure. Spatial derivatives are evaluated using second order accurate central differences. For time derivatives a second order accurate three point backward difference scheme is used.

Solution Domain
The solution domain extends for 47 jet diameters in the streamwise direction (L_z) and for 41 jet diameters in the normal and spanwise directions (L_x,L_y). A stretched orthogonal grid has been used accounting for $147 \times 147 \times 61$ cells in the three coordinate directions.

Boundary and Initial Conditions
Inlet conditions for velocity and mixture fraction have been prescribed according to the experimental data (web) At the outlet convective outflow boundary conditions have been applied, while in the normal and spanwise directions free-slip conditions have been enforced. The calculation has been impulsively started.

Duration of the Calculation
About 9 flow-through times ($U_{cl,0}/L_z$) have been calculated. The maximum value for CFL was 0.4 and the average time step was 10^{-7}.

Computer Facility
The present computation was started on a Cray T3D at the University of Edinburgh, UK, on 128 processors, and then transferred to an SGI Origin r10000 at Imperial College. Only 16 processors could be used on this machine. The CPU time required for this computation was 34000 hs (266 hs per processor) on the Cray T3D and 1010 hs (63 hs per processor) on the SGI r10000.

References

[1] W.P. Jones. *Turbulence modelling and numerical solution methods for variable density and combusting flows*, chapter 6, pages 309–374. Academic Press, London, 1987.

[2] W.P. Jones. *BOFFIN: a computer program for flow and combustion in complex geometries*, 1991.

Large-Eddy-Simulation of Partially Premixed CH_4/Air Turbulent Flames - Flame F

F di Mare and W. P. Jones
Department of Chemical Engineering and Chemical Technology
Imperial College of Science, Technology and Medicine
London SW7 2BY
United Kingdom

Modeling Procedures
The spatially-filtered continuity and momentum equations are solved along with a transport equation for the mixture fraction. Closure is provided with the standard Smagorinsky Sub-Grid model. The model constant is set equal to 0.15. A presumed-shape pdf (β-pdf) approach, coupled with a flamelet assumption [1], is applied to solve the compositional field.

Solution Method
The method [2] chosen for this computation utilises a fully implicit formulation and an approximate factorisation technique is adopted to determine the pressure. Spatial derivatives are evaluated using second order accurate central differences. For time derivatives a second order accurate three point backward difference scheme is used.

Solution Domain
The solution domain extends for 47 jet diameters in the streamwise direction (L_z) and for 41 jet diameters in the normal and spanwise directions (L_x,L_y). A stretched orthogonal grid has been used accounting for $147 \times 147 \times 61$ cells in the three coordinate directions.

Boundary and Initial Conditions
Inlet profiles for velocity and mixture fraction have been prescribed according to the experimental data (web) At the outlet convective outflow boundary conditions have been applied, while in the normal and spanwise directions free-slip conditions have been enforced. The calculation has been impulsively started.

Duration of the Calculation
About 7 flow-through times ($U_{cl,0}/L_z$) have been calculated. The maximum value for CFL was 0.4 and the average time step was 10^{-7}.

Computer Facility
The present computation was carried out on a Cray T3D at the University of Edinburgh, UK, on 128 processors. The CPU time required for this computation was 60637 hs (474 hs per processor).

References

[1] W.P. Jones. *Turbulence modelling and numerical solution methods for variable density and combusting flows*, chapter 6, pages 309–374. Academic Press, London, 1987.

[2] W.P. Jones. *BOFFIN: a computer program for flow and combustion in complex geometries*, 1991.

'One-Dimensional Turbulence' Simulation of Piloted Methane-Air Jet Diffusion Flames

Tarek Echekki, Alan R. Kerstein
Combustion Research Facility, MS 9051
Sandia National Laboratories
Livermore, CA 94551-0969

and J.Y. Chen
Department of Mechanical Engineering, UC Berkeley
Berkeley, CA 94720-1740

phone: (+1) 925 294 2793 – fax: (+1) 925 2595 – e-mail: techekk@ca.sandia.gov

Turbulence Model:
The 'One-Dimensional Turbulence' (ODT) model (1) is used. The ODT model formulation is based on a deterministic integration of unsteady reaction-diffusion equations (for species, temperature and the streamwise velocity) and stochastic implementation of turbulent advection through stirring events ('triplet maps') (2) applied to the streamwise velocity and thermochemical scalar profiles on a 1D domain. The 1D domain corresponds to a radial direction (transverse to the mean flow). The temporal evolution of these 1D profiles is interpreted as a downstream evolution using a bulk velocity based on the jet momentum. The rate distribution of stirring events is governed by the local strain (i.e. the resolved streamwise velocity on the 1D domain). The model has two parameters, which govern the rate distribution of stirring events and the evolution of the large scales. The parameters are adopted from recent validations of hydrogen-air simulations with experiment.

Chemistry Model and Kinetic Mechanism:
Sixteen species are included in the methane-air simulations. They are: H_2, H, O_2, OH, H_2O, HO_2, H_2O_2, CH_4, CO, CO_2, CH_2O, C_2H_2, C_2H_4, C_2H_6 and N_2. The chemistry is based on a twelve-step reduced mechanism for methane-air chemistry (3).

Mixing and Coupling Models:
Mixing and coupling models in ODT are self-contained in the ODT formulation outlined above.

Solution Domain
The temporal evolution of the 1D profiles for the transported scalars is converted to a downstream evolution. A typical realization spans a range of x/d from 0 to 80 and y/d (the 1D domain) between -25 to 25.

Initial Conditions:
Top-hat profiles are imposed for velocity, species and temperature at the inlet (initial conditions) of the fuel, pilot and oxidizer streams. Therefore, centerline streamwise velocity in the ODT simulation represents the bulk velocity instead of the published developed flow velocity and are expected to be lower than the measured centerline values. The pilot, fuel and oxidizer streams have the same composition and temperature as outlined in the TNF web site.

Boundary Conditions:
Boundaries are maintained at free stream conditions and outside the 'turbulent zone.'

Machine Used and Approximate CPU time required:
Silicon Graphics Octane^{TM} 175MHz IP30 processor. Approximate time per realization is 1 hour.

Comments:
· Two hundred realizations, representing different histories of the stochastic implementation of turbulent advection, were simulated to obtain ensemble-averaged statistics reported here · to match the ratios of the fuel to pilot mass fluxes between the planar simulations and the experiment, the initial width of the pilot jet was increased.

References:

1. Kerstein, A.R., One-Dimensional Turbulence: Model Formulation and Application to Homogeneous Turbulence, Shear Flows, and Buoyant Stratified Flows, in press *J. Fluid Mech.* (1999).
2. Kerstein, A.R., *J. Fluid Mech.* **231**: 361–394 (1991).
3. http://www.princeton/~cklaw/kinetics/12-step.

Finite-Volume - Monte-Carlo-PDF Code

Alexander Hinz, Egon P. Hassel, Johannes Janicka
FG Energie– u. Kraftwerkstechnik, Technische Universität Darmstadt,
Petersenstr. 30, 64287 Darmstadt, Germany
phone: +49-6151/16 2502, fax: +49-6151/16 6555, e-mail: ekt@hrzpub.tu-darmstadt.de

Turbulence model: Reynolds stress model based on Jones and Musonge [5] in its revised version [4]. Turbulent viscosity in PDF diffusion term $\nu_t = C_\mu/\sigma_f \cdot \tilde{k}^2/\tilde{\varepsilon}$ with $\sigma_f = 0.83$.

Chemistry model and kinetic mechanism: ILDM table parameterized with mixture fraction f and reaction progress variables Y_{CO_2} and Y_{H_2O} [6].

Mixing model, number of PDF particles: Modified Curl's model [3] for scalar mixing with 100 particles in each cell.

Coupling Model: Eulerian composition PDF solved via fractional step method in coupling with a CFD code (2D elliptic finite-volume code, staggered grid, SIMPLE method, TDMA-ADI solver) (Hybrid method) [2,7].

Solution domain: Assuming axis-symmetry; grid: $N_x \times N_y = 80 \times 70$ nodes, condensed near the centerline and the burner, $L_x \times L_y = 140D \times 70D$.

Boundary conditions: At inlet boundary, scalars assigned according to documentation with all particles having the same values in a particular cell (Dirac-PDF). Velocities and turbulent quantities according to measurements for $r \leq 10.43$ mm and to estimations in documentation for $r > 10.43$ mm, linearly interpolated onto the grid. Dissipation rate is estimated from $P = -\widetilde{u_i''u_j''}\partial\tilde{u}_i/\partial x_j = \tilde{\varepsilon}$ to yield $\tilde{\varepsilon} = \sqrt{C_\mu}\tilde{k}\sqrt{(\partial\tilde{u}/\partial r)^2 + (\partial\tilde{w}/\partial r - \tilde{w}/r)^2}$. Entrainment is allowed to occur. Outlet conditions are non-reflecting.

Location of start of computation: Computation starts at $x/D = 0$.

Convergence criteria or length of calculation: PDF procedure takes about 30 000 steps with a time step $dt = 10^{-5}$ s which corresponds to more than 0.3 s real time ($L_x/U_{bulk,D} = 1$ m$/49.8$ m/s ≈ 0.02 s).

Machine used and approximate CPU time required: About 100 h on an ALPHA lx533, including process of evolving stably burning flame.

Comments: The start profile is a block profile extended axially in the domain according to the inlet conditions. Time scales become large far downstream, thus the evolution of a converged solution takes comparatively long and larger scattering can be observed in the profiles. The evolution from the initial state is accelerated by a larger mixing rate.

References:

[1] Barlow, R., Frank, J.H. (1998), 27^{th} *Symp (Int.) Comb.*, pp. 1087-1095.

[2] Correa, S.M. and Pope, S.B. (1992), 27^{th} *Symp (Int.) Comb.*, pp. 279-285.

[3] Janicka, J., Kolbe, W., Kollmann, W. (1979), *J. Non-Equil. Thermodyn.*, 4, pp. 47-66.

[4] Jones, W.P. (1994), In P. A. Libby and F. A. Williams, editors, *Turbulent Reacting Flows*, pages 309–374. Academic Press, London, San Diego, New York.

[5] Jones, W.P. and Musonge, P. (1988), *Journal of Non-Equilibrium Thermodynamics*, 4:47–66, 1979.

[6] Maas, U., Pope, S.B. (1992), *Comb. Flame*,88 (3), pp. 239-264.

[7] Pope, S.B. (1981), *Combust. Sci. Technol.*, 25, pp. 159-174.

4^{th} International Workshop on Measurement and Computation of Turbulent Non-Premixed Flames

R.P.Lindstedt, S.A.Louloudi and E.M.Vaos

e-mail:p.lindstedt@ic.ac.uk

Imperial College of Science,Technology and Medicine
Mechanical Engineering Department
London SW7 2BX, U.K.

- **Turbulence Model:** The velocity field is modelled using the SSG [1] second moment closure. The $C_{\epsilon 2}$ constant in the dissipation rate equation is adjusted from 1.92 to 1.8 in order to improve the predicted spreading rate.
- **Chemistry Model and Kinetic Mechanism:** The chemistry [2] is based on the work of Lindstedt and co-workers [3,4]. The systematically reduced form used in the present work includes comprehensive NO_x chemistry and features 48 species of which 16 are treated as independent scalars.
- **Mixing Model and Number of PDF Particles:** Joint Scalar *pdf* with modified Curl's Model [5] for scalar mixing. Average of 600 and 800 moving Lagrangian particles (e.g. [6]) per cell for flames D and F respectively.
- **Solution Domain:** Implicit parabolic axisymmetric formulation with 70 cross stream nodes.
- **Boundary Conditions:** Inlet conditions (x/D=0) according to WWW page.
- **Length of Calculation:** Computations performed up to x/D=80.
- **Machine Used and Approximate CPU Time:** About 2 weeks with 800 particles/cell on a SGI Power Indigo^2 with a 195 MHz R10000 processor running IRIX 6.2. The time is reduced to 2 days with 100 particles/cell.
- **Comment on Modelling issues:** No special treatment of stabilisation region required. The computations assume adiabatic flow conditions.

References

1. Speziale, C.G., Sarkar, S. and Gatski, T.B., *JFM* 227:245-272 (1991).
2. Leung, K.M. and Lindstedt, R.P., *Brite Euram Contract 95-0056* April 1999.
3. Sick, V., Hildenbrand, F. and Lindstedt, R.P., *27^{th} Symposium (Int.) on Combustion*, pp.1401-1409 (1998).
4. Juchmann, W., Latzel, H., Shin, D.I., Peiter, G., Dreier, T., Volpp, H.R., Wolfrum, J., Lindstedt, R.P. and Leung, K.M., *27^{th} Symposium (Int.) on Combustion*, pp. 469-476 (1998).
5. Janicka, J. and Kollmann, W., *J. Non-equilib. Thermodyn.* 4:47 (1978).
6. Hulek, T. and Lindstedt, R.P., *Combust. Sci. Tech.* 136:303-331 (1998).

Numerical Simulation of a Piloted Methane/Air Flame (Flame D) using a Finite-Volume - Monte Carlo-PDF Code

A. Obieglo, J. Gass
Institute of Energy Technology, ETH Zurich
Laboratory of Thermodynamics in Emerging Technologies
LOW C2, ETH-Zentrum, Switzerland
phone: +41-1-6323645, fax: +41-1-6321023, e-mail: obieglo@ltnt.iet.mavt.ethz.ch

Turbulence Model:

Modified $k-\varepsilon$ model with constants according to Launder [Launder74]. Turbulent viscosity $\nu_t = C_\mu/\sigma_f * \tilde{k}^2/\tilde{\varepsilon}$ with $\sigma_f = 0.8$ and *Pope*-correction [Pope78] used.

Chemistry model and kinetic mechanism

Reduced 4-Step-mechanism [Rogg91] with eight species. Description of the system in tables with mixture fraction and mass concentrations of $n_{\mathrm{CH_4}}, n_{\mathrm{CO}}, n_{tot}$ and n_{H} [Chen89].

Mixing Model and number of pdf particles

LMSE model [Dopazo75] with 64 particles/cell.

Coupling model

Eulerian composition PDF with fractional step [Pope85, Laxander96], coupling with finite volume code for flow field solution (CFX-TASCflow).

Solution Domain

Axisymmetric grid, 120x90 grid nodes, 0-80 diameters in axial direction, 0-20 diameters in radial direction. Grid refinement around centre axis and nozzle exit.

Boundary Condition

Boundary Conditions according to documentation; all particles have the same values in each cell (Dirac-PDF). Velocities and turbulent quantities linearly interpolated to the grid.

Location of start of computation:

x=0

Convergence criteria or length of calculation

Computation of the reacting flow field at the beginning with a simple combustion model (EDM) until field reached steady state - after that PDF calculation with about 6000 steps (each step $10^{-4}s$).

Machine used and approximate CPU time required

About 190 h total computational time on a HP J282 workstation.

Comments

Problems arise within the flow field on the centreline. Tuning of the model constant σ_f to get the velocity profile at x/d = 45.

References

Barlow,R.,Frank,J.H.(1998),*27th Symp. (Int.) Comb.*
Dopazo,C. (1975), *Physics of Fluids*, 18(4), pp. 397-404
Launder,B.E.,Spalding,D.B. (1974), *Comput. Methods Appl. Mech. Engrg.*, 3, pp. 269-289
Laxander,A. (1996), *PhD thesis*, TU Stuttgart
Pope,S.B.(1978), *AIAA Journal*,16, pp. 279-281
Pope,S.B.(1981), *Combust. Sci. and Techn.*, 25, pp. 159-174
Rogg,B. (1991),*Lecture Notes in Physics*, 384, pp. 159-192
Chen,J.Y.,Kollmann,W.,Dibble,R.W. (1989) *Combust. Sci. and Techn.*, 64, pp. 315-346

Conditional Moment Closure Modelling of Piloted Flame E: Summary Page

M.R. Roomina and R.W. Bilger
Department of Mechanical and Mechatronic Engineering
The University of Sydney, NSW 2006, Australia
Roomina@cances.atp.com.au; Bilger@mech.eng.usyd.edu.au

- Turbulence model, including values of model constants:
  The governing equations for the flow and mixing field are expressed by the Favre-averaged equations in axisymmetric boundary-layer form for continuity, momentum, turbulence kinetic energy, turbulent kinetic dissipation rate and the mean and variance of the mixture fraction. The closure used here for the turbulence is the *k-e-g* model of Launder et al. (1972).

Turbulence coefficients for *k-e-g* model											
C_m	C_r	C_{e1}	C_{e2}	C_{e3}	C_{g1}	C_{g2}	s_k	s_e	s_g	s_x	
0.09- 0.04f	*0.5*	*1.43*	*1.92-0.0667f*	0.72	*2.7*	*1.79*	*1.0*	*1.3*	*0.7*	*0.7*	$f \equiv \left\lvert \frac{R_m}{1.6u_0}\left(\frac{du_c}{dx} - \left\lvert\frac{du_c}{dx}\right\rvert\right)\right\rvert^{0.2}$

  Subscript c denotes centreline value, u_0 is the jet exit velocity and R_m represents the radial width of mixing region.

- Chemistry model and kinetic mechanism
  GRI-Mech 2.11, 49species, 279 reactions.
- Mixing model and number of pdf particles (if appropriate)

Clipped Gaussian pdf

- Coupling model

Conditional Moment Closure

- Solution domain (xmin,xmax,ymin,ymax) and grid structure

x/D=0 to x/D=80 and y/D=0 to y/D=15.

- Boundary conditions (state any differences from those in the documentation file)
  The coflow velocity is taken 1.0 m/s
  The fuel and air temperatures are assumed 300K instead of 294K.
  It is also assumed that the pilot is a stoichiometric mixture of the main fuel.
- Location of start of computations

Adiabatic equilibrium compositions are employed for the reactive scalars down to five jet diameters (x/D=5), in order to assure the ignition of the flame in the near-field region due to high mixing rates.

- Convergence criteria or length of calculation

The calculations are carried out down to *x/D*=80.

Currently absolute tolerance levels of 10^{-8} for major species, 10^{-12} for minor species and 10^{-4} for enthalpy are employed. The relative tolerance level is taken as 10^{-4}.

- Machine used and approximate CPU time required

DEC 3000/400 ALPHA work station. Approximate CPU time is 120 hrs.

- Comments on modeling issues
  Check on the adequacy of number of grid points in the cross-stream direction. When the starting profiles are not smooth, the truncation error in the CFD solver may seriously affect the solution if convection is large. This check can be done by examination of flow and mixing field results, in particular radial profiles of velocity and mixture fraction along with conservation of mass and momentum. Additional grid points can be introduced to smooth up the radial profiles.
  Check on the unity of integral of pdf over mixture fraction space at various axial locations. Significant deficiency in magnitude of pdf may lead to inaccurate conditional mean scalar dissipation and consequently conditional and unconditional species mass fractions.
  Check on initial profiles of species concentration where equilibrium initialisation is employed. High equilibrium concentration levels are inappropriate for some of minor species in particular NO and NO_2. Correct NO and NO_2 levels can be predicted if concentration of these species are suppressed in the initial profiles.
- Reference
  Launder, B. E., Morse, A., Rodi, W. and Spalding, D. B.(1972). The prediction of free shear flows—A comparison of six turbulence models. *NASA Free Shear Flows Conference*, Virginia, NASA Report Number SP-311.

Model Summaries (TNF3)

Joint Scalar PDF Simulation of Turbulent Reacting Flows with Detailed Chemistry on a Parallel Cluster

J.-Y. Chen
Department of Mechanical Engineering
University of California at Berkeley
Berkeley, California 94720
phone: (510)-642-3286 Fax: (510) 642-6163
e-mail: jychen@euler.me.berkeley.edu

C. Yam*, and R. Armstrong
Sandia National Laboratories
* postdoctoral researcher, currently with Aerojet.

Turbulence Model:

K-ε model with $C_{\varepsilon 2}$=1.8 (Standard value=1.94). Turbulent viscosity in the joint scalar pdf $\nu_t=C_\mu/\sigma_f$, where σ_f =0.8.

Chemistry model and kinetic mechanism:

Detailed GRI 1.2 mechanism.

Mixing model and number of pdf particles:

Modified Curl's model with 50 particles/cell.

Coupling model:

Eulerian composition PDF with fractional step. 2-D elliptic time dependent flow solver with projection method. Second-order accuracy in space and time for flow field. The scalar PDF is first order accurate in time.

Solution domain:

Axisymmetric grids of 50x70 nodes clustered around the jet centerline and near field.
Physical domain: 0-70 diameters in axial direction, 0-18 diameters from jet centerline to outer stream.

Boundary conditions (state any differences from those in the documentation file):

Scalar field is prescribed according to experimental data (web). Mean velocity is prescribed to give the same mean values. The exact form differs from the experimentally suggested shape due to difficulty in treating the sharp changes in the boundary layer (noted below).

Location of start of computations:

x=0.

Convergence criteria or length of calculation:

Computations were performed using well-mixed reactor until mean flow field reached steady state (30,000 steps roughly). Finite rate mixing was turned on and the computation proceeded up to 2,000 steps. Time step=1.4E-5 second with CFL=0.2.

Machine used and approximate CPU time required:

Pentium Pro. 200MZ, 256MB, 4 CPU (max. equipped). Operating System: LINUX.
Total number of CPU used: 32 (load balancing is not applied for this run).
Total run time is about 7 days for 2,000 steps with direct stiff solver DVODE.

Comments on modeling issues:

When the inlet velocity is prescribed with sharp boundary layers for the fuel jet and the pilot, the k-ε model blows up, even with a very small CFL number (say, 0.05). Instead of a sharp boundary layer, a smooth profile was used, and the k-e model was run with $C_{\varepsilon 2}$=1.8. If the standard value $C_{\varepsilon 2}$=1.94 is used, the velocity decays too fast in the near field compared to the experimental data.

Steady State Flamelet Modeling of Turbulent Reacting Flows based on Monte Carlo Joint Scalar PDF

J.-Y. Chen
Department of Mechanical Engineering
University of California at Berkeley
Berkeley, California 94720
phone: (510)-642-3286 Fax: (510) 642-6163
e-mail: jychen@euler.me.berkeley.edu

Turbulence Model:

Reynolds stress modeling with C_{cor}=0.025 (details are given in Ref. 1)

Chemistry model and kinetic mechanism:

Steady state flamelets generated with detailed GRI 2.11 mechanism using Sandia's opposed Tsuji burner code. Flamelets computed for multi-component diffusion a=5, 10,25,50,100,200,300,400,600,700 (1/s); for equal diffusivity (setting diffusivity = thermal diffusivity) a=5, 10,25,50,100,200,300,400,600,800,1000 (1/s).
Library generated using mixture fraction and scalar dissipation rate (f,X_f) as two parameters. NO is computed by splitting source into positive and negative parts using a sink time scale, i.e., W_{NO}= SNO- [NO]/τ_{NO} (Ref. 2).

Mixing model and number of pdf particles:

Modified Curl's model with 800 particles/cell. A lognormal distribution is assumed for the scalar dissipation rate. The particle properties are computed from flamelet library (f,X_f) where X_f is sampled from the lognormal distribution with its mean value estimated based scalar fluctuation and mean turbulence time scale (Ref. 2).

Coupling model:

Eulerian composition PDF with parabolic marching downstream code using von Miss transformation.

Solution domain:

Axisymmetric grids of 50 across half of the jet. About 1400 steps to reach x/D=90 with variable step size.

Boundary conditions (state any differences from those in the documentation file):

Scalar field is prescribed according to experimental data (web). Mean velocity and turbulence statistics are prescribed according to experimental data (or estimated) in the Sandia's Workshop Web for Flame D.

Location of start of computations:

x=0.

Convergence criteria or length of calculation:

Up to 90 diameters.

Machine used and approximate CPU time required:

Pentium Pro. 200MZ, 256MB, 90 minutes (1 and 1/2 hours). Operating System: LINUX.

Radiation Model:

Only H_2O and CO_2 are included with absorption coefficients recommended by the workshop. Only SNO is modified with an exponenetial ratio described in Ref. 2.

Comments on modeling issues:

The source splitting is used to compute NO in order to include 'reburning' of NO in rich parts of flame.

Reference:

1) Chen, J.-Y. and Kollmann, W. "Comparison of prediction and measurement in nonpremixed turbulent flames," Chapter 5 in *Turbulent Reactive Flows*, Edited by P. Libby and F.A. Williams, Academic Press, Ltd., 1994.
2) Chen, J.-Y. and Chang, W.-C., *Twenty-Sixth Symposium (International) on Combustion*, The Combustion Institute, 1996, pp. 2207-2214.

Conditional Moment Closure Modeling of Piloted Flame D: Summary Page

M. R. Roomina and R. W. Bilber
Department of Mechanical and Mechatronic Engineering
The University of Sydney, NSW 2006, AUSTRALIA
roomina@mech.eng.usyd.edu.au; biger@mech.

Turbulence model, including values of model constants:

The governing equations for the flow and mixing field are expressed by the Favre-averaged equations in axisymmetric boundary-layer form for continuity, momentum, turbulence kinetic energy, turbulent kinetic dissipation rate and the mean and variance of the mixture fraction. The closure used here for the turbulence is the *k*-ε-*g* model of Launder et al. (1972).

Turbulence coefficients for *k*-ε-*g* model											
C_μ	C_ρ	$C_{\varepsilon 1}$	$C_{\varepsilon 2}$	$C_{\varepsilon 3}$	C_{g1}	C_{g2}	σ_k	σ_ε	σ_g	σ_ξ	
0.09- 0.04f	*0.5*	*1.43*	*1.92-0.0667f*	0.72	*2.7*	*1.79*	*1.0*	*1.3*	*0.7*	*0.7*	$f \equiv \left\lvert \frac{R_\mu}{1.6u_0}\left(\frac{du_c}{dx} - \left\lvert\frac{du_c}{dx}\right\rvert\right)\right\rvert^{0.2}$

Subscript c denotes centreline value, u_0 is the jet exit velocity and R_μ represents the radial width of mixing region.

Chemistry model and kinetic mechanism:

GRI-Mech 2.11, 49species, 279 reactions.

Mixing model and number of pdf particles (if appropriate):

Clipped Gaussian pdf

Coupling model:

Conditional Moment Closure

Solution domain (xmin,xmax,ymin,ymax) and grid structure:

x/D=0 to x/D=100 and y/D=0 to y/D=15.

Boundary conditions (state any differences from those in the documentation file):

The coflow velocity is taken 1.0 m/s

The fuel and air temperatures are assumed 300°K instead of 294°K.

It is also assumed that the pilot is a stoichiometric mixture of the main fuel.

Location of start of computations:

Adiabatic equilibrium compositions are employed for the reactive scalars down to five jet diameters (x/D=5), in order to assure the ignition of the flame in the near-field region due to high mixing rates.

Convergence criteria or length of calculation:

The calculations are carried out down to *x/D*=100.

Currently absolute tolerance levels of 10^{-8} for major species, 10^{-12} for minor species and 10^{-4} for enthalpy are employed. The relative tolerance level is taken as 10^{-4}.

Machine used and approximate CPU time required:

DEC 3000/400 ALPHA work station. Approximate CPU time is 120 hrs.

Comments on modeling issues:

Check on the adequacy of number of grid points in the cross-stream direction. When the starting profiles are not smooth, the truncation error in the CFD solver may seriously affect the solution if convection is large. This check can be done by examination of flow and mixing field results, in particular radial profiles of velocity and mixture fraction along with conservation of mass and momentum. Additional grid points can be introduced to smooth up the radial profiles.

Check on the unity of integral of pdf over mixture fraction space at various axial locations. Significant deficiency in magnitude of pdf may lead to inaccurate conditional mean scalar dissipation and consequently conditional and unconditional species mass fractions.

Check on initial profiles of species concentration where equilibrium initialisation is employed. High equilibrium concentration levels are inappropriate for some of minor species in particular NO and NO_2. Correct NO and NO_2 levels can be predicted if concentration of these species are suppressed in the initial profiles.

Reference:

Launder, B. E., Morse, A., Rodi, W. and Spalding, D. B.(1972). The prediction of free shear flows—A comparison of six turbulence models. *NASA Free Shear Flows Conference*, Virginia, NASA Report Number SP-311.

Numerical Simulation of a Turbulent Piloted Methane / Air Jet Flame (Flame D) using a Finite-Volume - Monte-Carlo-PDF Code: Models and Boundary Conditions

Alexander Hinz, Egon P. Hassel, Johannes Janicka
FG Energie– u. Kraftwerkstechnik, Technische Universität Darmstadt,
Petersenstr. 30, 64287 Darmstadt, Germany
phone: +49-6151/16 2502, fax: +49-6151/16 6555, e-mail: ekt@hrzpub.tu-darmstadt.de

Overview about models, boundary and initial conditions, and comments on the simulation.

Turbulence Model:

Modified $k-\varepsilon$ model with constants C_μ and $C_{\varepsilon 2}$ according to [Launder72]. Turbulent viscosity in PDF diffusion term $\nu_t = C_\mu/\sigma_f \cdot \tilde{k}^2/\tilde{\varepsilon}$ with $\sigma_f = 0.83$.

Chemistry Model and Kinetic Mechanism:

ILDM table parameterized with mixture fraction and two reaction progress variables x_{CO_2} and x_{H_2O} [Maas90].

Mixing Model, Number of PDF Particles:

Modified Curl's model [Janicka79] for scalar mixing with 100 particles in each cell.

Coupling Model:

Eulerian composition PDF solved via fractional step method in coupling with a CFD code (2D elliptic finite-volume code, staggered grid, SIMPLE method, TDMA-ADI solver) (Hybrid method) [Pope81, Chen96].

Solution Domain:

Assuming axis-symmetry; grid: 120×80 nodes, condensed near the centerline and the inlet boundary, $L_x = 1000$ mm, $L_r = 677$ mm with 11 nodes inside the jet radius, $r(12) = 3.6$ mm, 12 nodes inside the pilot, $r(25) = 9.1$ mm, 55 nodes in the coflow. The expansion factors are $\alpha_x = 1.04$, $\alpha_r = 1.05$ for $r \leq 9.1$ mm and $\alpha_r = 1.09$ for $r > 9.1$ mm.

Boundary Conditions:

At inlet boundary, scalars assigned according to documentation with all particles having the same values in a particular cell (Dirac-PDF). Velocities and turbulent quantities according to measurements for $r \leq 10.43$ mm and to estimations in documentation for $r > 10.43$ mm, linearly interpolated onto the grid. Dissipation according to [Masri90], reduced to get $\partial\tilde{k}/\partial x = 0$ at the nozzle.

Location of Start of Computation:

Computation starts at $x = 0.0$ mm.

Convergence Criteria or Length of Calculation:

PDF procedure takes about 30 000 steps (including fine-tuning of constants) with a time step $dt = 1 \cdot 10^{-5}$ s which corresponds to more than 0.3 s real time ($L_x/U_{bulk} = 1$ m$/49.8$ m/s ≈ 0.02 s).

Machine used and Approx. CPU Time:

About 140 h on an ALPHA lx533, including process of evolving stably burning flame.

Comments:

Problems arise with the IEM model to get the flame stably burning. Evolution of a burning flame is partly successful with increase of decay rate ($C_\phi = 8$) for $x/d < 5$. The standard $k-\varepsilon$ model yields too steep centerline decay. The start profile is a block profile extended axially in the domain according to the inlet conditions. Time scales become large far downstream, thus the evolution of a converged solution takes comparatively long and larger scattering can be observed in the profiles.

References:

Barlow, R., Frank, J.H. (1998), 27^{th} *Symp (Int.) Comb.*, accepted

Chen, J.-Y., Chang, W.-C. (1996), 26^{th} *Symp (Int.) Comb.*, pp. 2207-2214

Janicka, J., Kolbe, W., Kollmann, W. (1979), *J. Non-Equil. Thermodyn.*, 4, pp. 2292-2307

Launder, B.E., Morse, A., Rodi, W., Spalding, D.B. (1972), *Tech. Report, NASA SP-311*

Maas, U., Pope, S.B. (1992), *Comb. Flame*,88 (3), pp. 239-264

Masri, A.R., Pope, S.B. (1990), *Comb. Flame*,81, pp. 13-29

Pope, S.B. (1981), *Combust. Sci. Technol.*, 25, pp. 159-174

Laminar Flamelet State Relationships based calculation for Sandia piloted CH_4-Air Flame D

R. N. Paul, Y. R. Sivathanu and J. P. Gore
Thermal Sciences and Propulsion Center
Purdue University
West Lafayette, IN-47907

Favre averaged mean and RMS (root mean square) of temperature and species mole fractions are calculated using the laminar flamelet concept. Predictions of Favre averaged mean and RMS temperature, N_2, O_2, H_2O, H_2, CH_4, CO, CO_2, OH and NO are compared with the measurements. The laminar flamelet state relationships (LFSR) for density, temperature and species are constructed using the Sandia one-dimensional code OPPDIF in conjunction with the GRI kinetic mechanism, version 2.11. For the LFSR calculations, the fuel is premixed with limited amount of air to yield a stream whose composition is identical to the jet fluid used in Flame D. The opposed oxidizer stream is air. The fuel stream and air stream velocities are varied between 5 – 50 cm/s to parametrically consider the effects of stretch rate. Equal velocities for fuel and air with a separation distance of 2 cm are used for LFSR calculations. Radiation effects are studied using the optically thin emission approximation and the Planck mean absorption coefficients summarized at the TNF web site.

OPPDIF calculations to generate LFSR took most of the computer time for the present calculations. The calculations are performed on IBM 370 UNIX based workstation. The first solution takes around 10 hours of CPU time starting with an initial guess corresponding to the equilibrium composition. However, if a good initial guess is available, state relationships can be obtained in typically half an hour of CPU time. A mixture fraction is calculated from the OPPDIF solutions by adding the local carbon and hydrogen mass and multiplying it by the ratio of the total mass to the mass of carbon and hydrogen in the fuel stream.

Given the state relationships, the Favre averaged mean and RMS of scalar flow properties are found using a clipped Gaussian, Favre averaged probability function (PDF) of mixture fraction. The parameters of the mixture fraction PDF are obtained from the Favre mean and RMS of the mixture fractions from the experimental data provided at the TNF Workshop web site. Calculations of Favre averaged scalars are performed individually for each locations where measurements are available.

A comparison between mean and RMS values of temperatures and major species concentrations shows that the laminar flamelet concept is applicable for the operating conditions of Sandia flame D. The temperature and major species mole fractions predictions based on the state relationships involving an order of magnitude variation in stretch rates are in agreement with each other and with the data within the experimental uncertainty. For CO, H_2, and NO mole fractions, consideration of radiative heat loss improves the agreement between measurements and predictions significantly. However, for these species, the effects of higher stretch rates and those of radiative heat loss are qualitatively similar. Therefore, in spite of the encouraging agreement between measurements and predictions for major species concentrations, laminar flamelet state relationships with radiation heat loss and stretch-rate as parameters appear necessary, for minor species predictions.

Comparison Plots: Flame D

TNF4 Piloted Flame D: Axial Profiles of U, F, and T

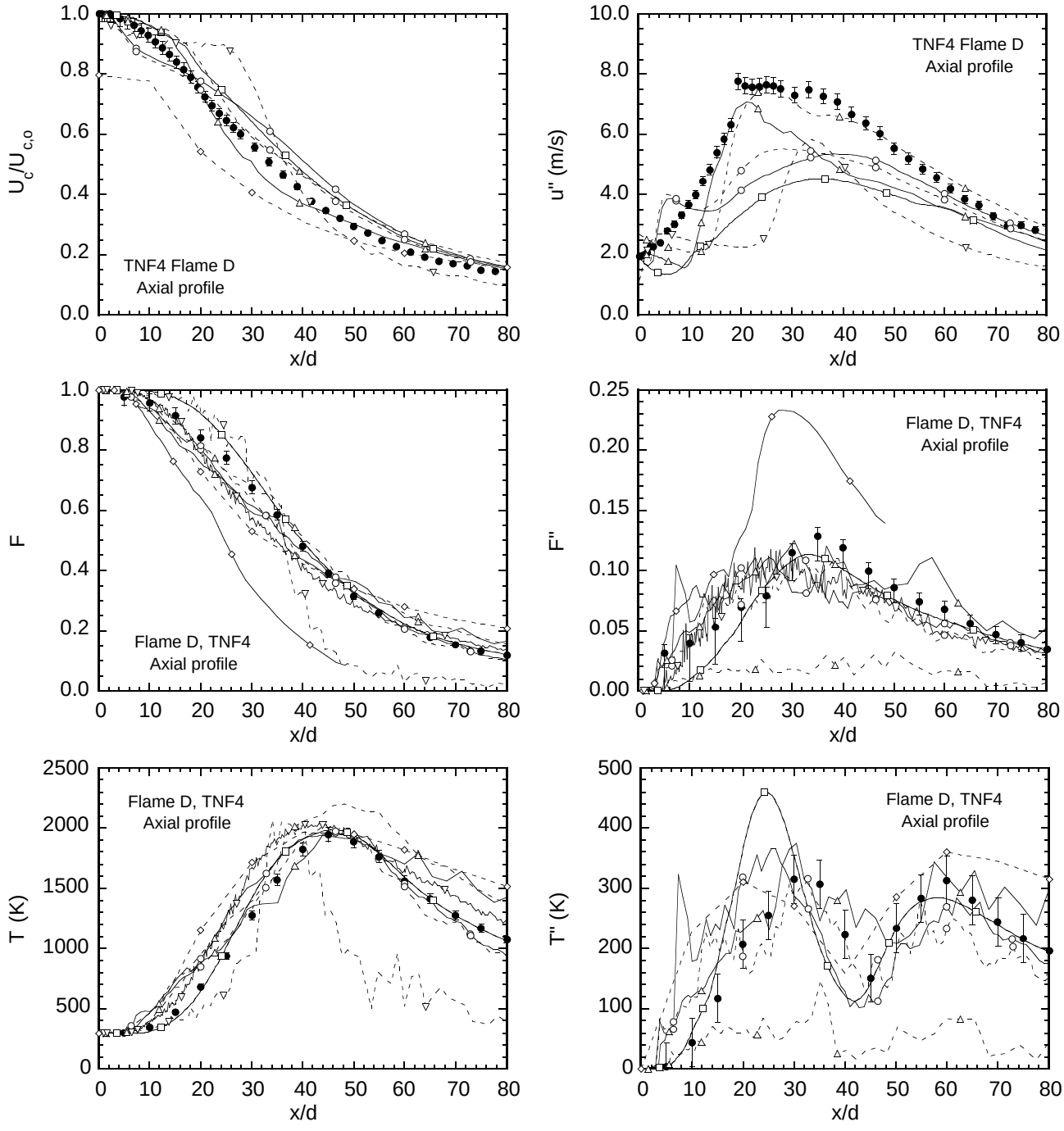

TNF3 Piloted Flame D: Axial Profiles of U, F, and T

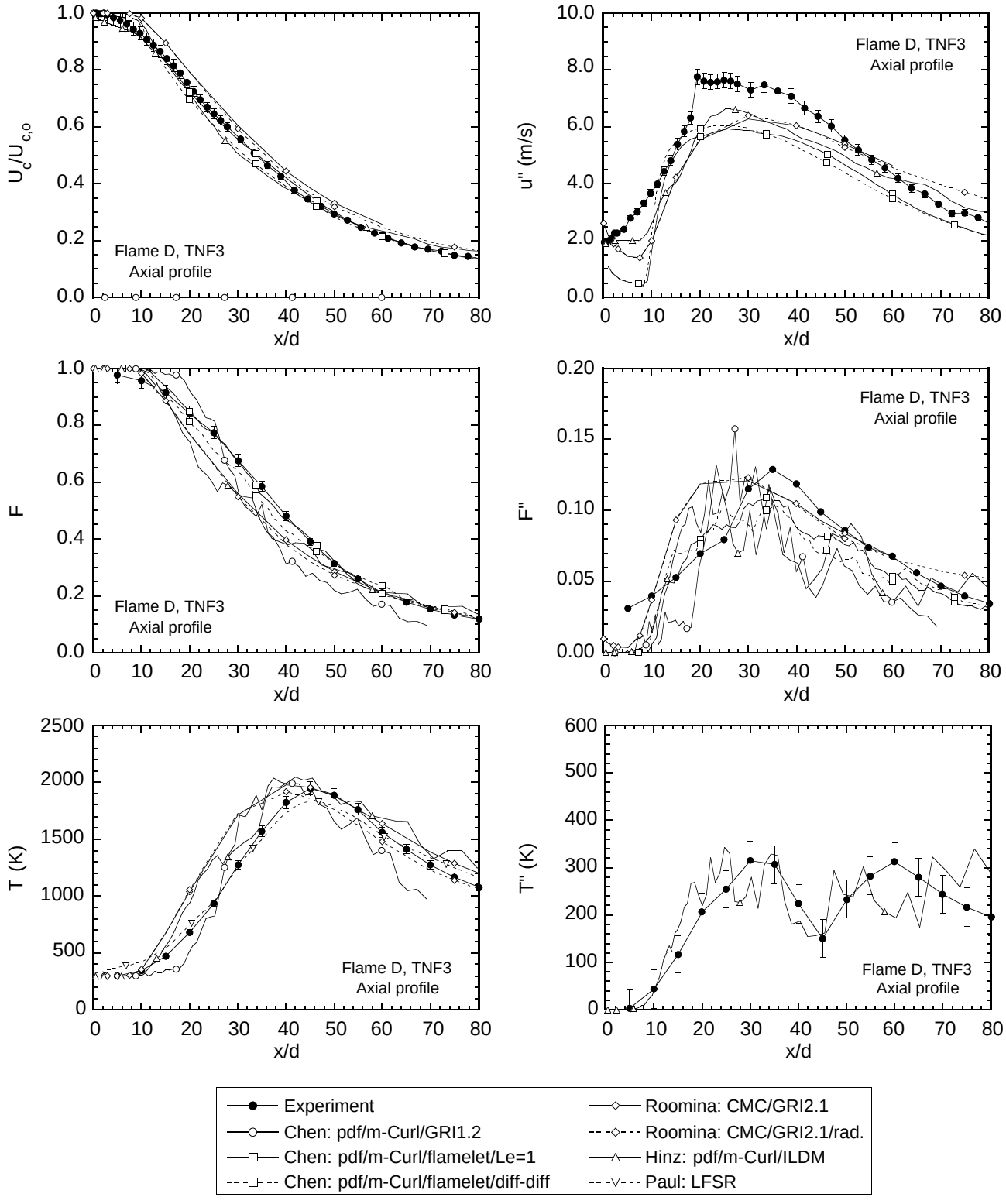

TNF4 Piloted Flame D: Axial Profiles of Species Mass Fractions

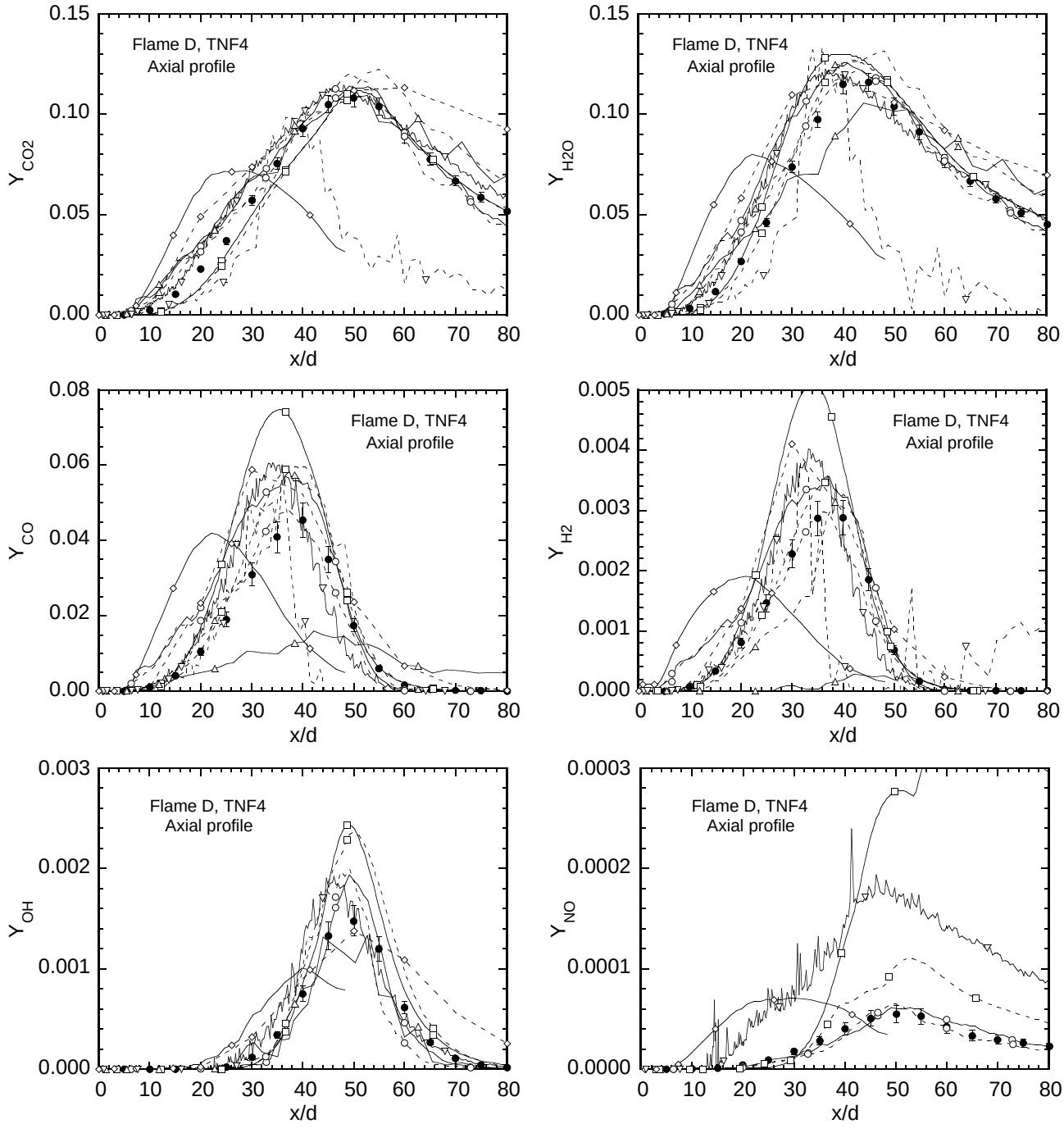

TNF3 Piloted Flame D: Axial Profiles Species Mass Fractions

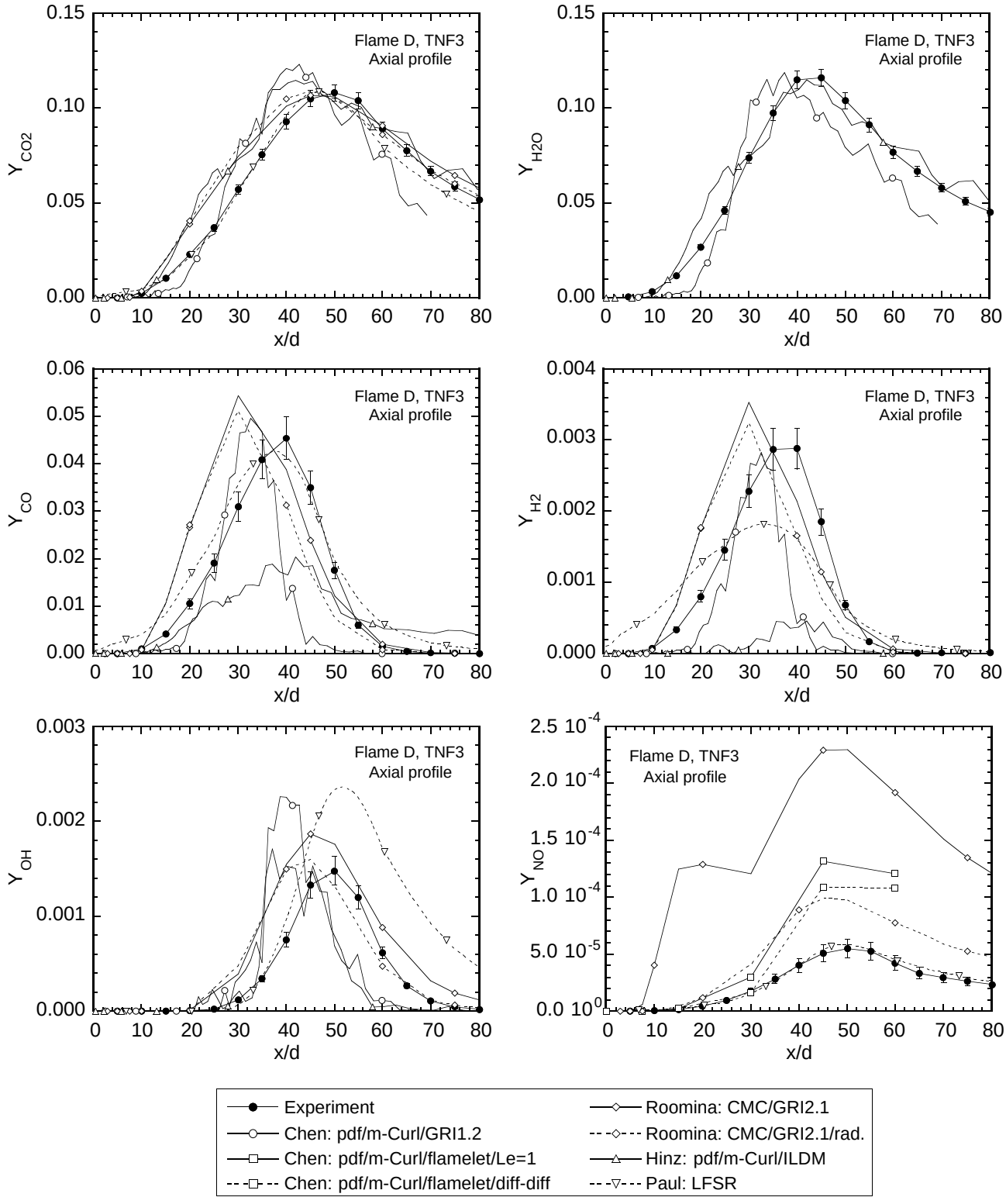

Combined Results for NO from TNF3 and TNF4

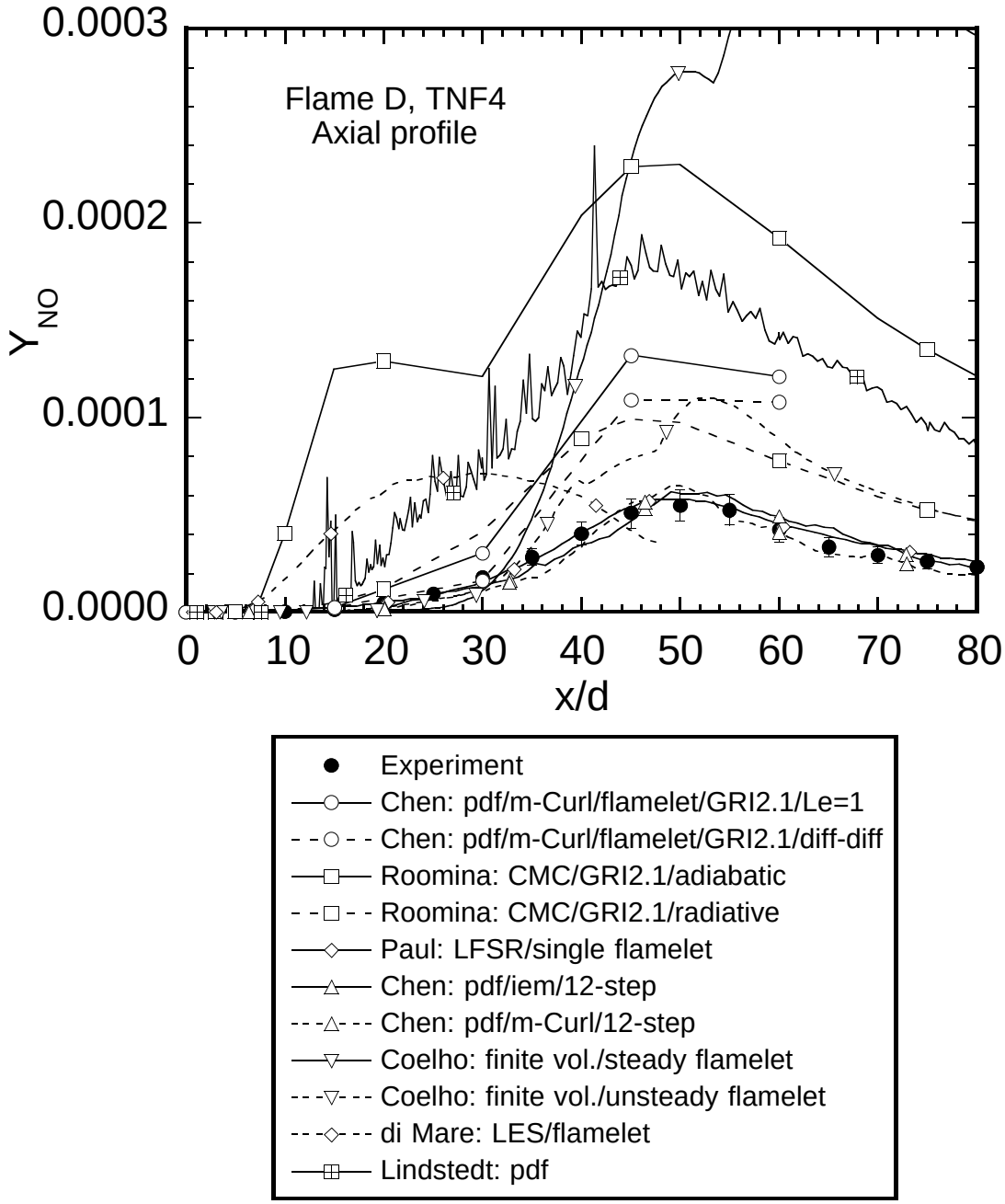

TNF4 Piloted Flame D: Radial Profiles of U, u'', u''v'' at x/d=45

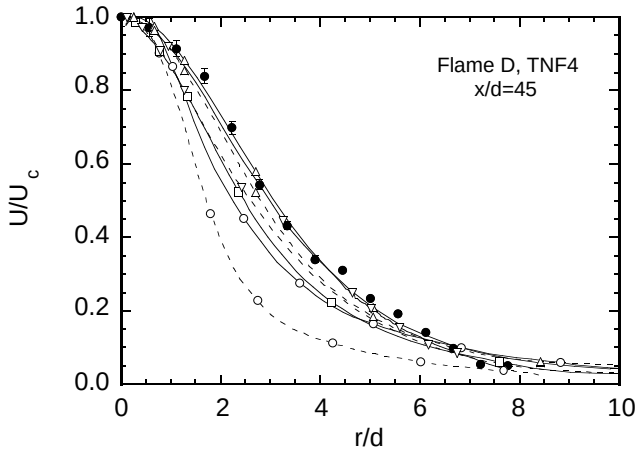

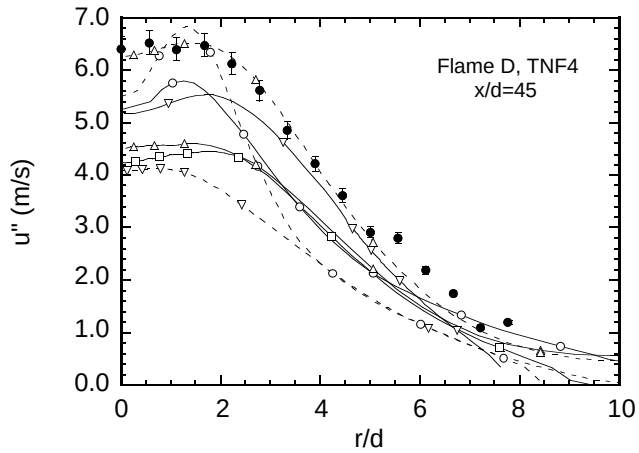

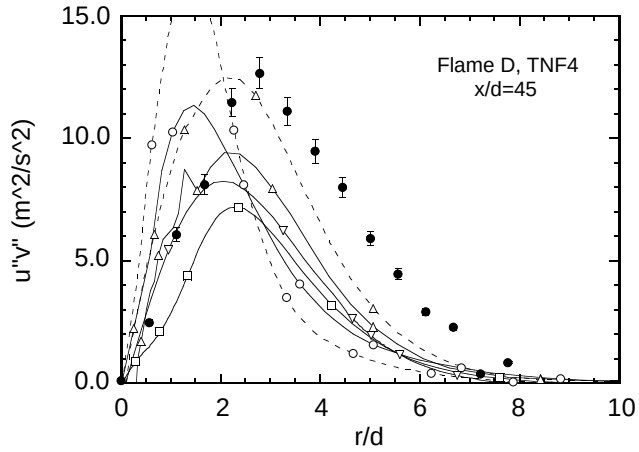

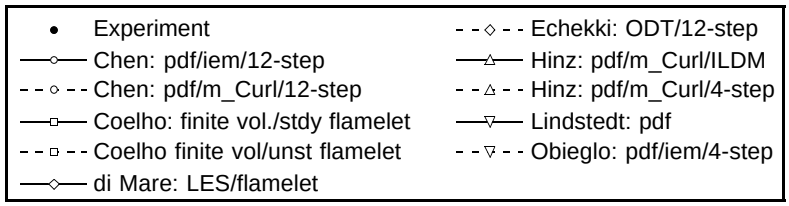

TNF3 Piloted Flame D: Radial Profiles of U, u", u"v" at x/d=45

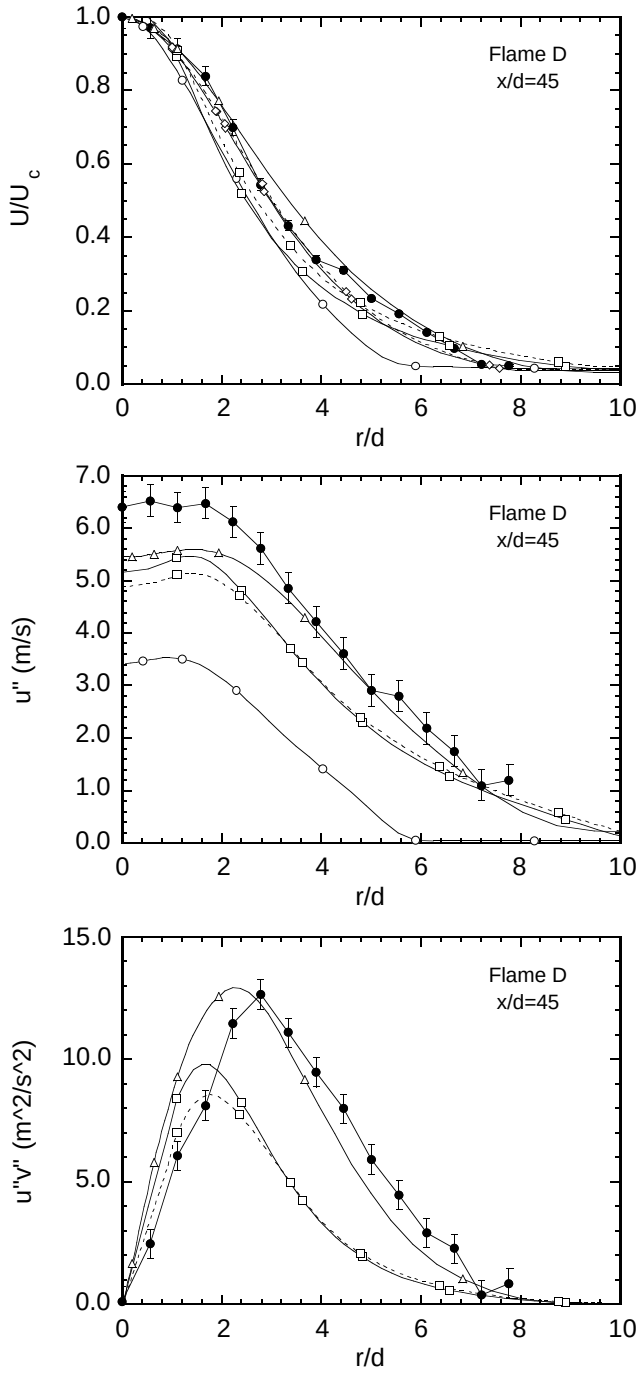

Experiment
Chen: pdf/m-Curl/GRI1.2
Chen: pdf/m-Curl/flamelet/Le=1
Chen: pdf/m-Curl/flamelet/diff-diff
Roomina: CMC/GRI2.1
Roomina: CMC/GRI2.1/rad.
Hinz: pdf/m-Curl/ILDM
Paul: LFSR

TNF4 Piloted Flame D: Radial Profiles at x/d=15

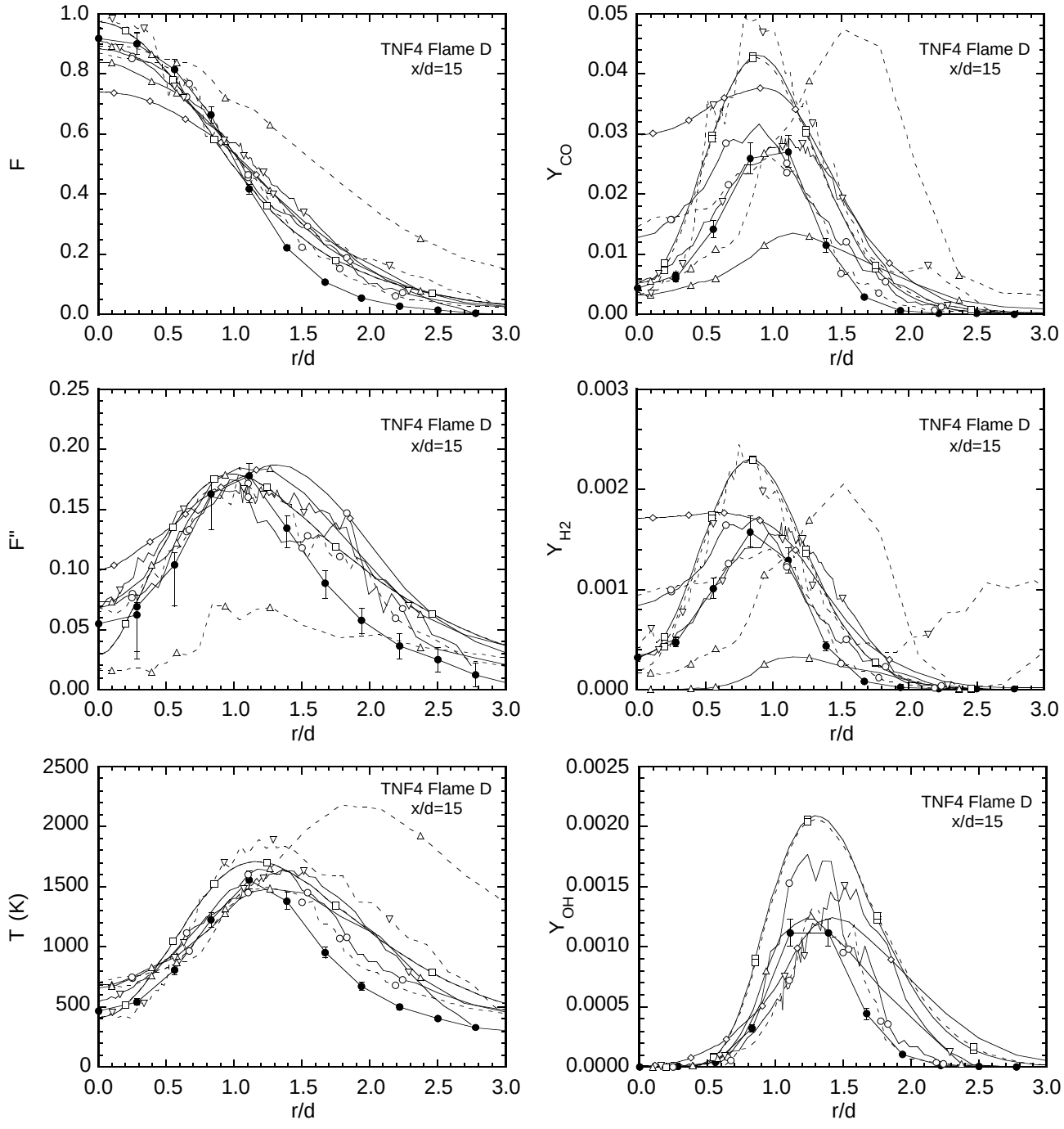

TNF3 Piloted Flame D: Radial Profiles at x/d=15

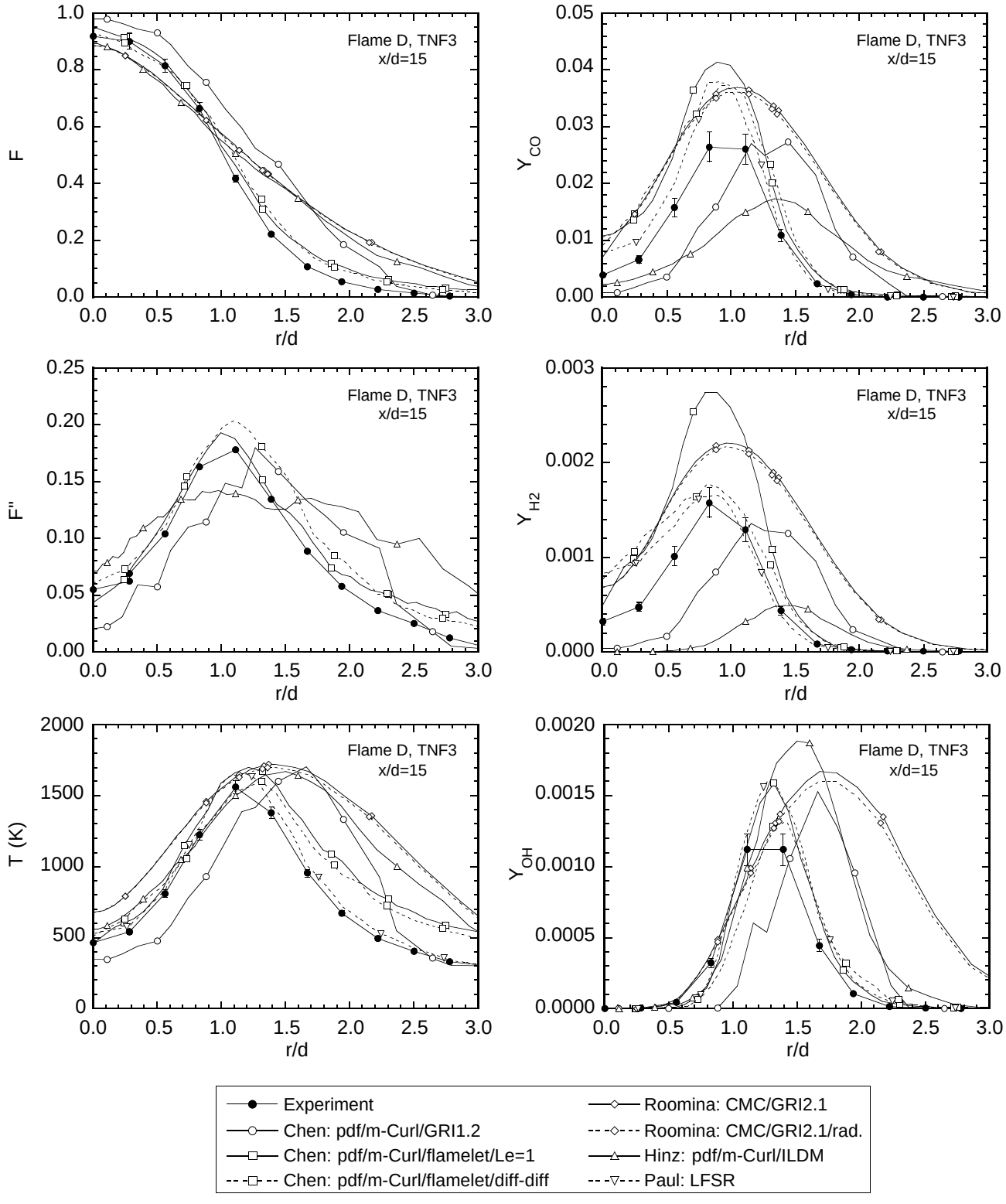

TNF4 Piloted Flame D: Radial Profiles at x/d=30

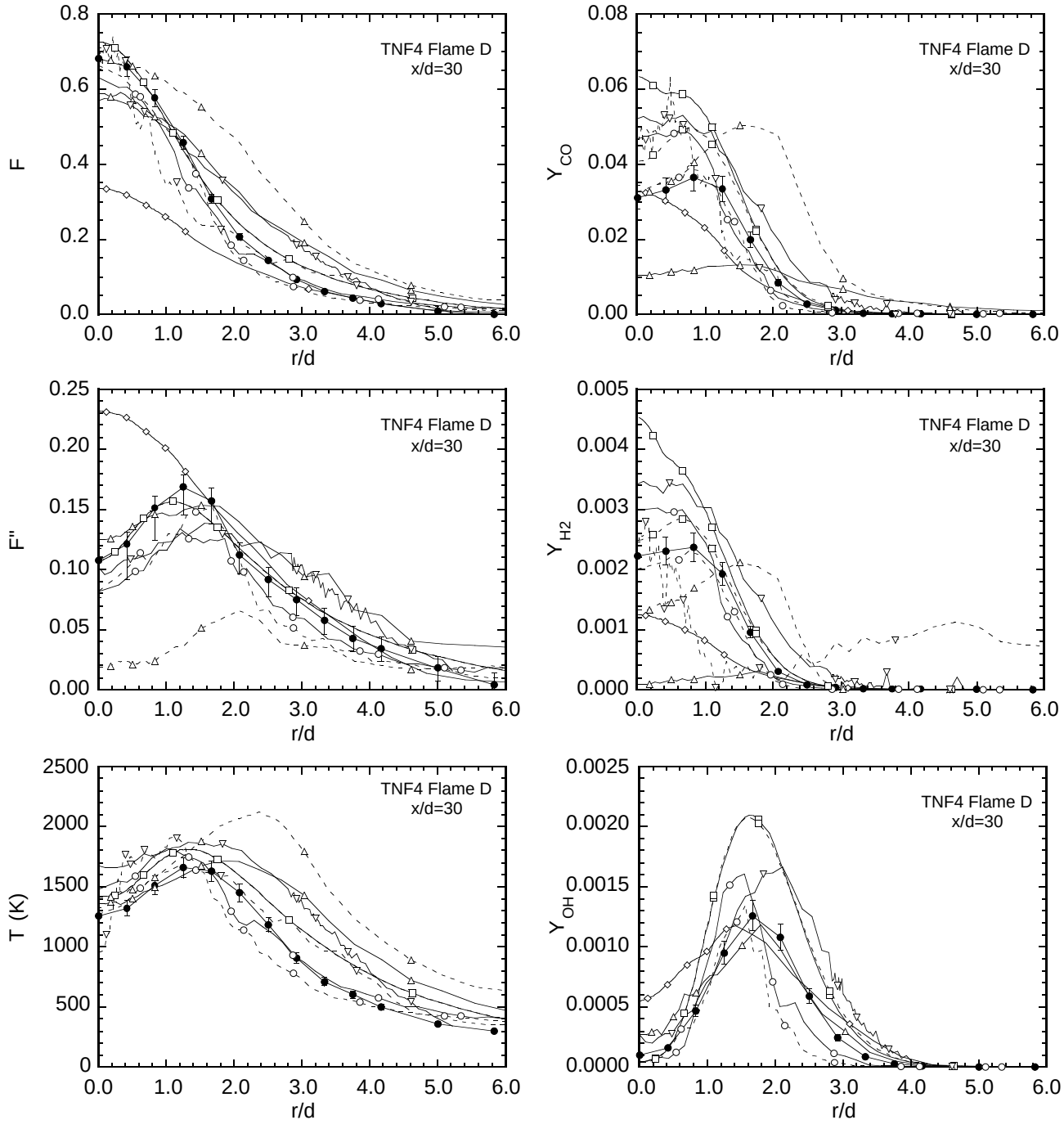

TNF3 Piloted Flame D: Radial Profiles at x/d=30

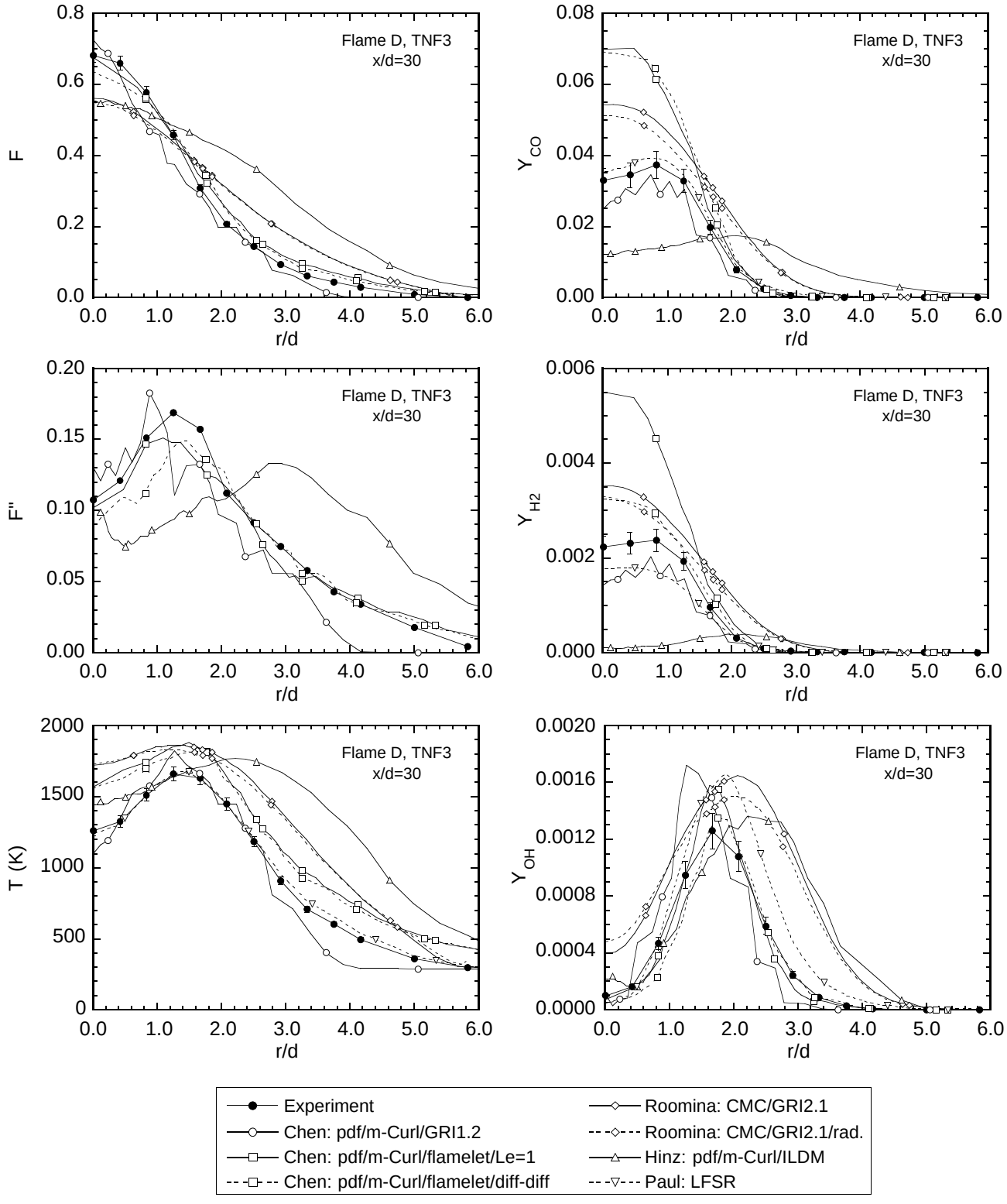

TNF4 Piloted Flame D: Radial Profiles at x/d=45

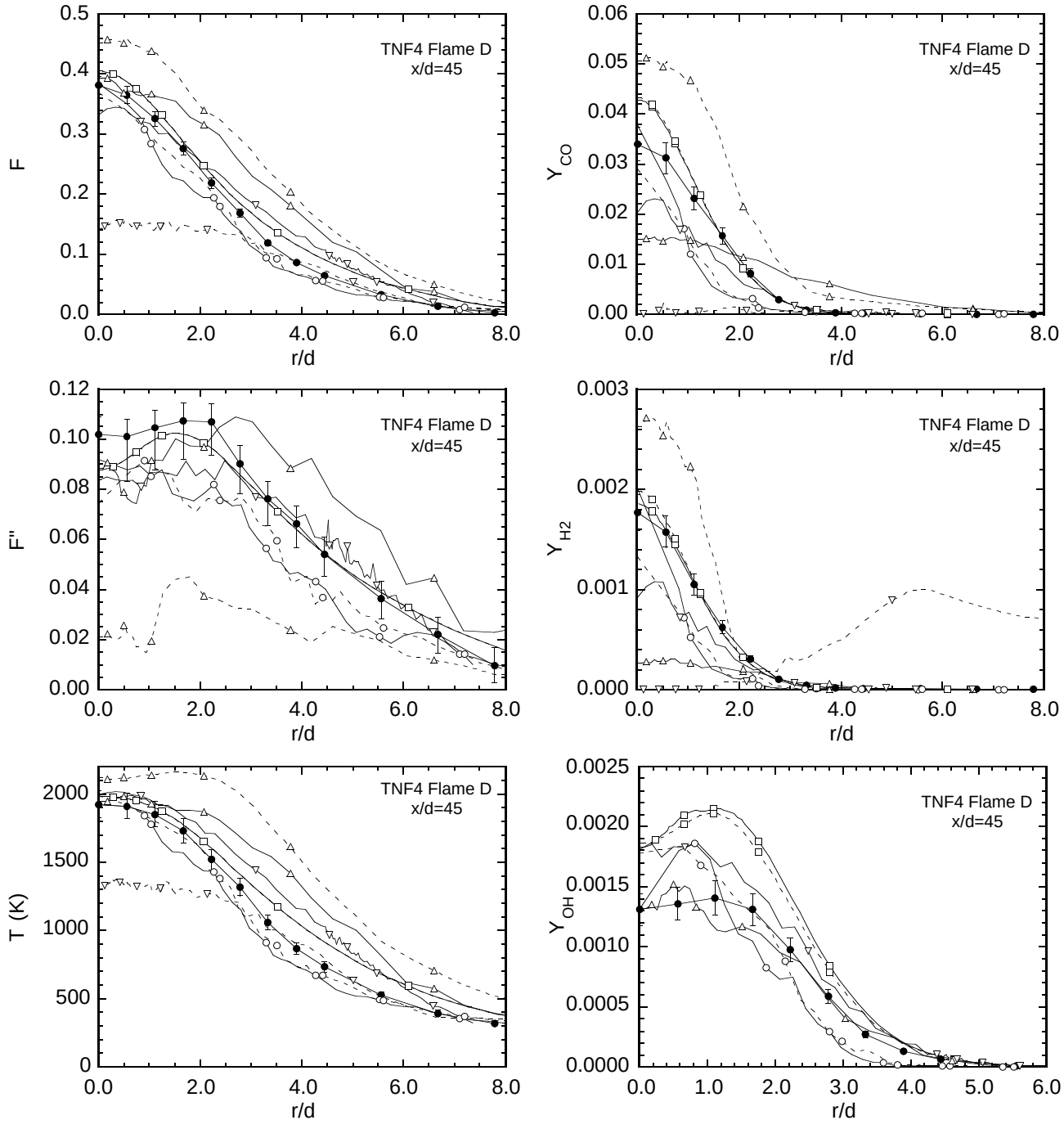

TNF3 Piloted Flame D: Radial Profiles at x/d=45

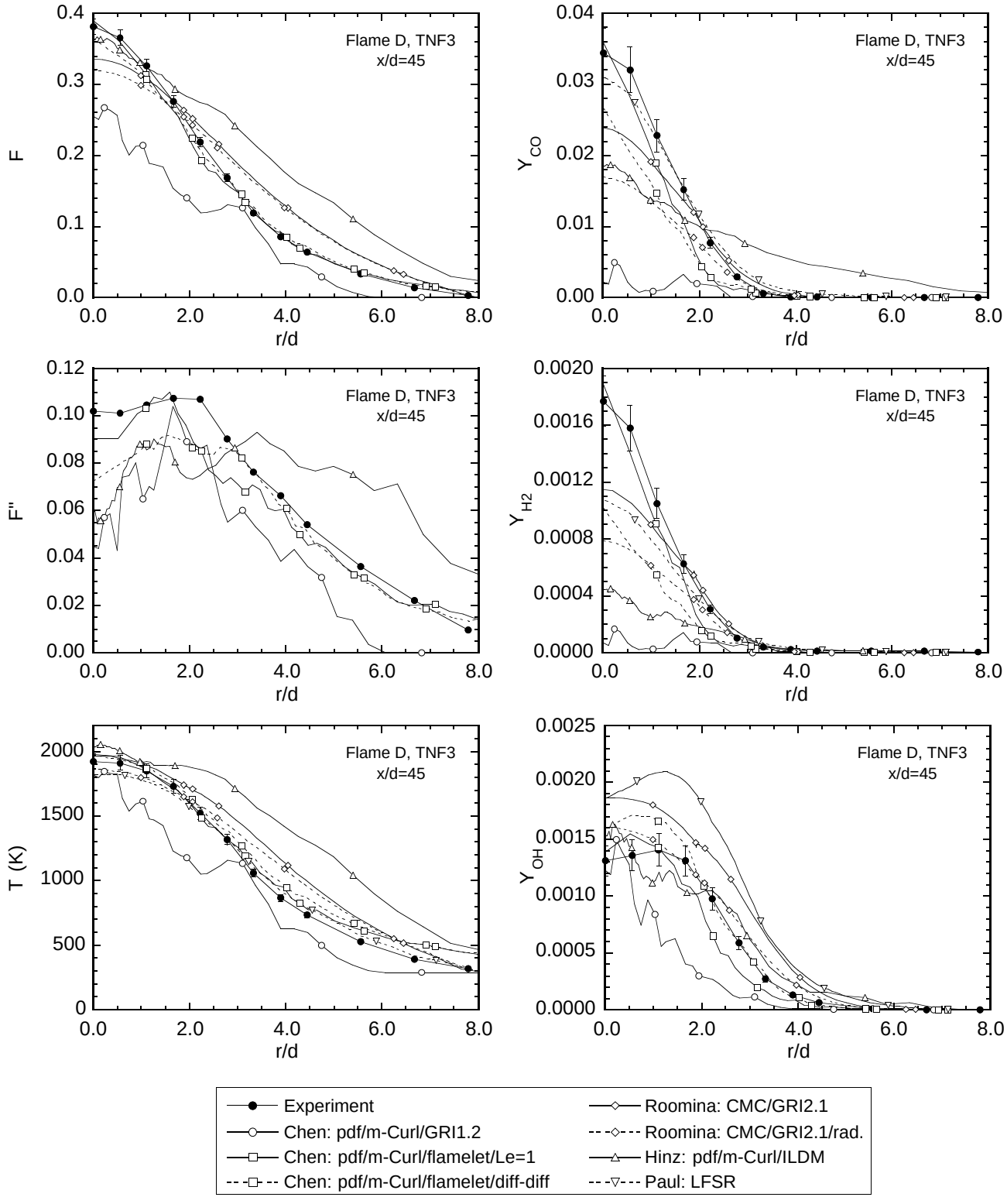

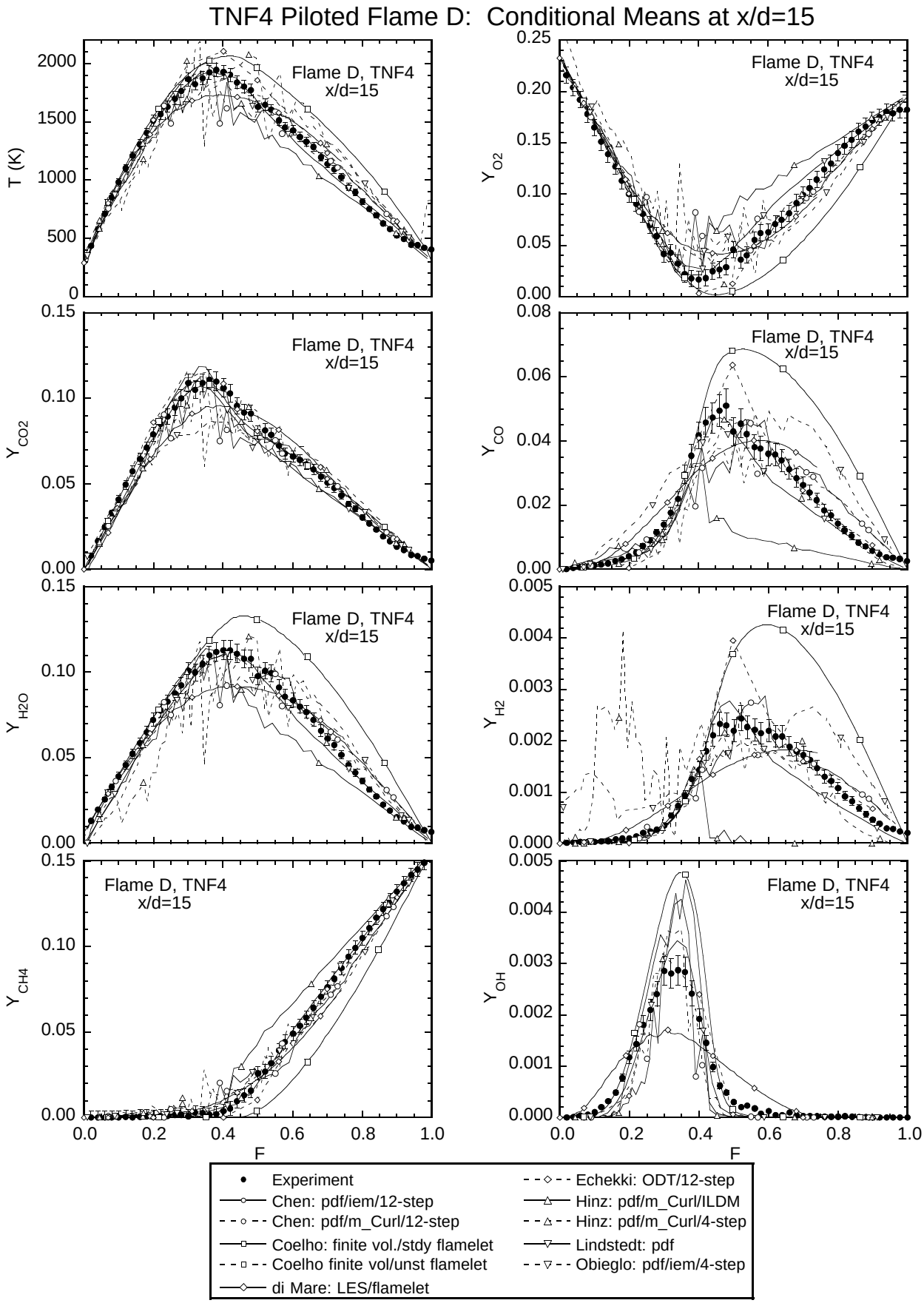
TNF4 Piloted Flame D: Conditional Means at x/d=15
Flame D, TNF4
x/d=15
T (K)
Y_{O2}
Y_{CO2}
Y_{CO}
Y_{H2O}
Y_{H2}
Y_{CH4}
Y_{OH}
F
Experiment
Chen: pdf/iem/12-step
Chen: pdf/m_Curl/12-step
Coelho: finite vol./stdy flamelet
Coelho finite vol/unst flamelet
di Mare: LES/flamelet
Echekki: ODT/12-step
Hinz: pdf/m_Curl/ILDM
Hinz: pdf/m_Curl/4-step
Lindstedt: pdf
Obieglo: pdf/iem/4-step

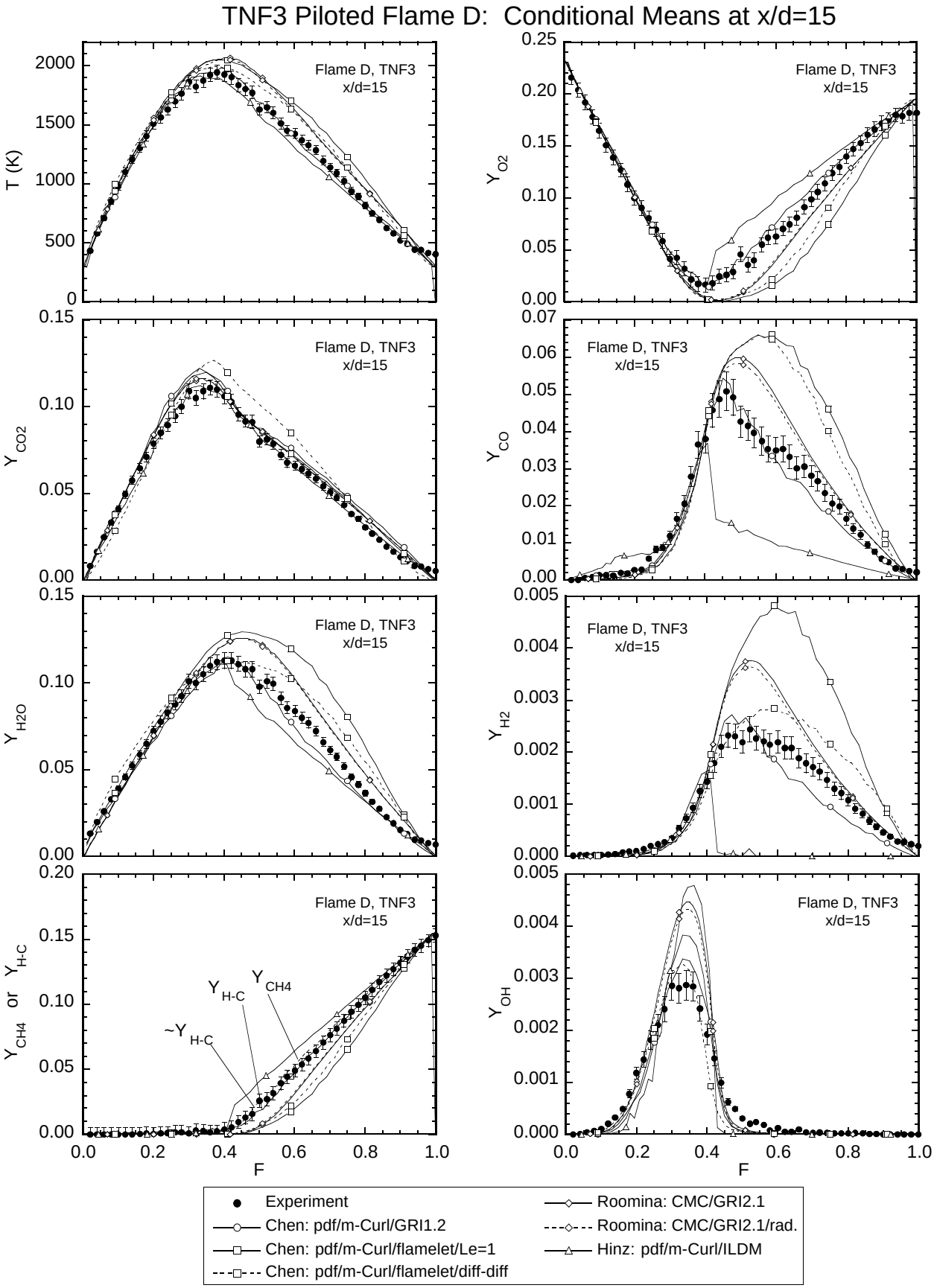
TNF3 Piloted Flame D: Conditional Means at x/d=15
Flame D, TNF3
x/d=15
T (K)
Y_{O2}
Y_{CO2}
Y_{CO}
Y_{H2O}
Y_{H2}
Y_{CH4} or Y_{H-C}
Y_{OH}
Y_{H-C}
Y_{CH4}
$\sim Y_{H-C}$
F
Experiment
Chen: pdf/m-Curl/GRI1.2
Chen: pdf/m-Curl/flamelet/Le=1
Chen: pdf/m-Curl/flamelet/diff-diff
Roomina: CMC/GRI2.1
Roomina: CMC/GRI2.1/rad.
Hinz: pdf/m-Curl/ILDM

TNF4 Piloted Flame D: Conditional Means at x/d=30

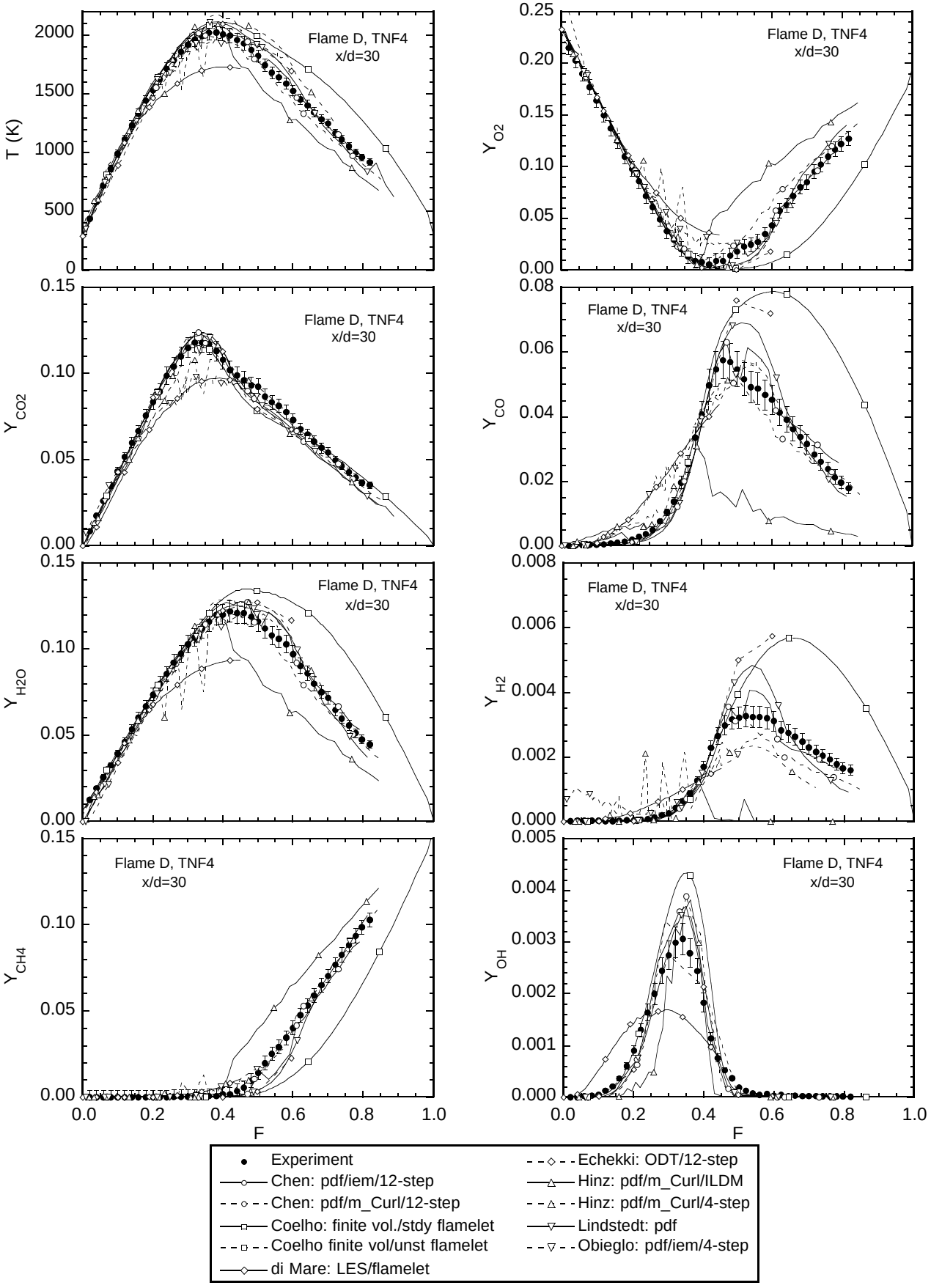

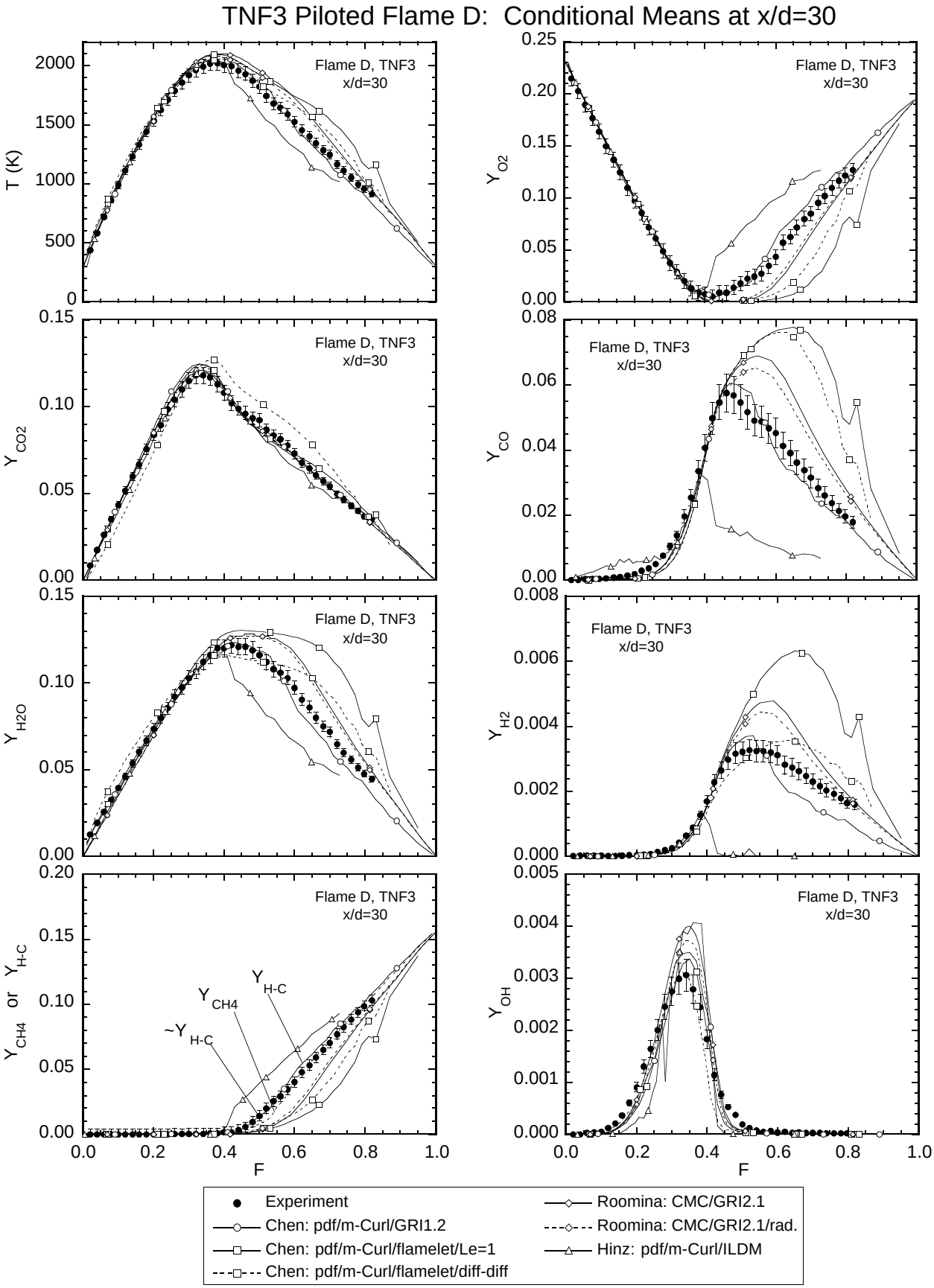
TNF3 Piloted Flame D: Conditional Means at x/d=30
Flame D, TNF3
x/d=30
T (K)
Y_{O2}
Y_{CO2}
Y_{CO}
Y_{H2O}
Y_{H2}
Y_{CH4} or Y_{H-C}
Y_{OH}
Y_{H-C}
Y_{CH4}
$\sim Y_{H-C}$
F
Experiment
Chen: pdf/m-Curl/GRI1.2
Chen: pdf/m-Curl/flamelet/Le=1
Chen: pdf/m-Curl/flamelet/diff-diff
Roomina: CMC/GRI2.1
Roomina: CMC/GRI2.1/rad.
Hinz: pdf/m-Curl/ILDM

TNF4 Piloted Flame D: Conditional Means at x/d=45

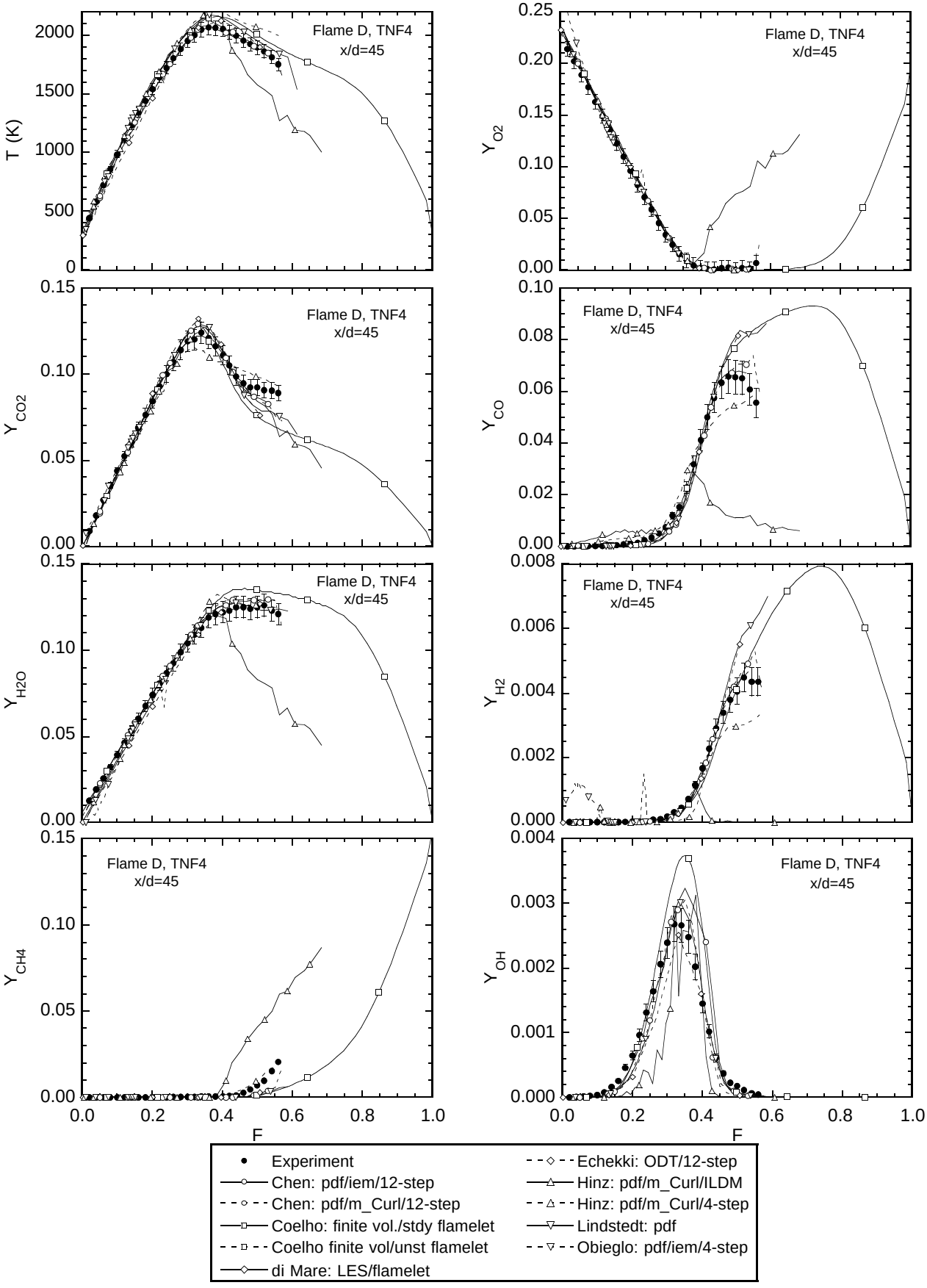

TNF3 Piloted Flame D: Conditional Means at x/d=45

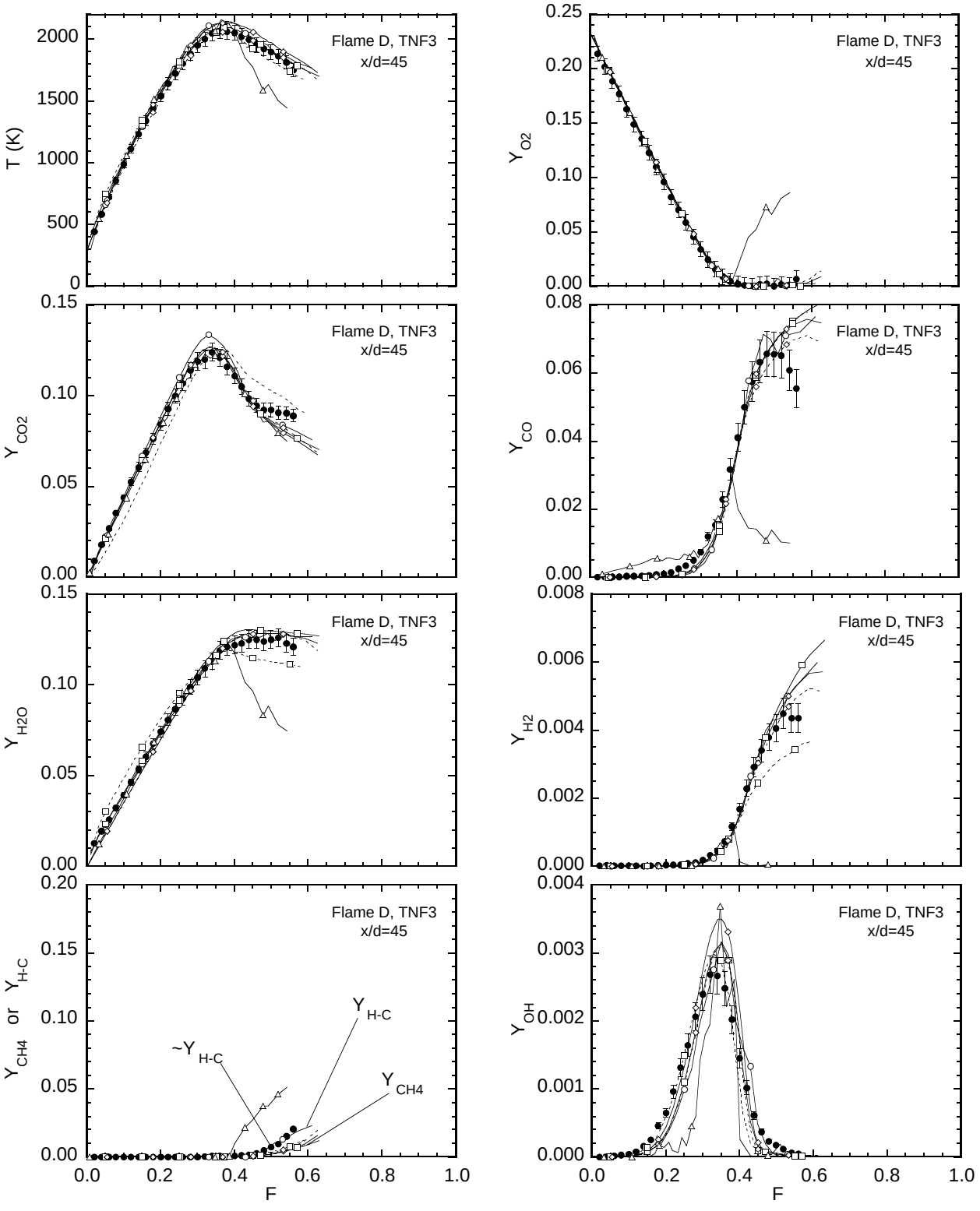

TNF4 Piloted Flame D: Temperature Scatter Plots at x/d=15

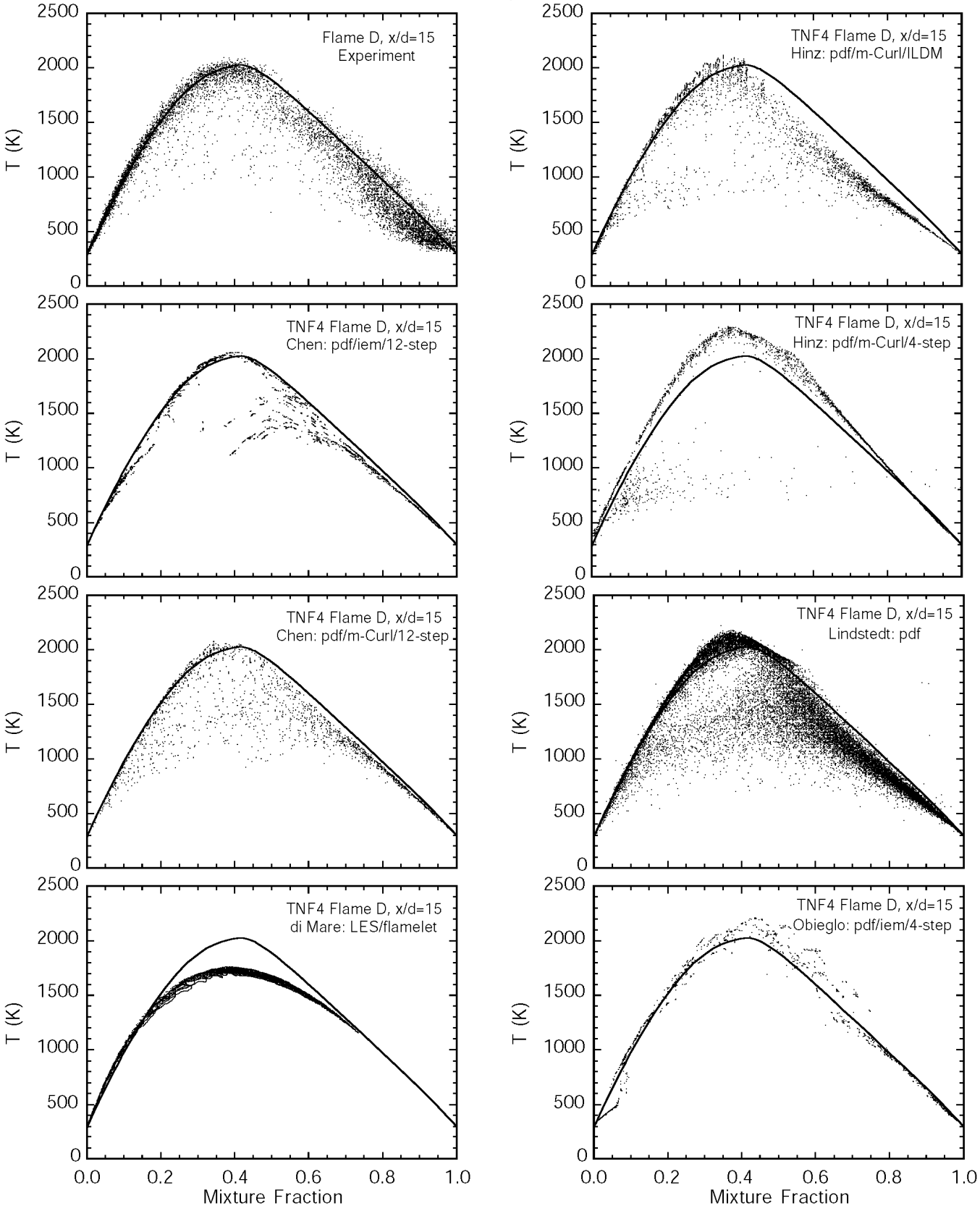

TNF4 Piloted Flame D: Temperature Scatter Plots at x/d=30

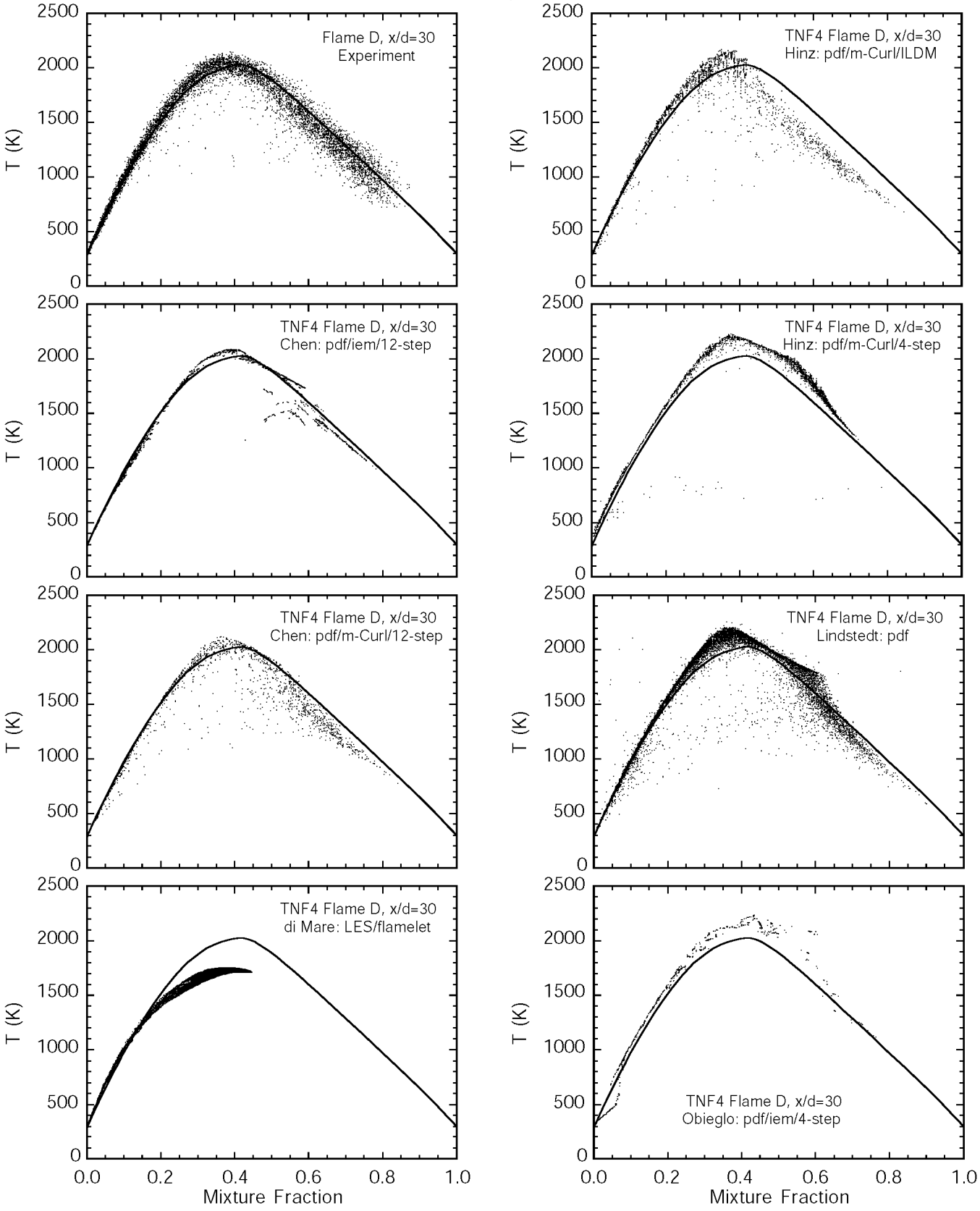

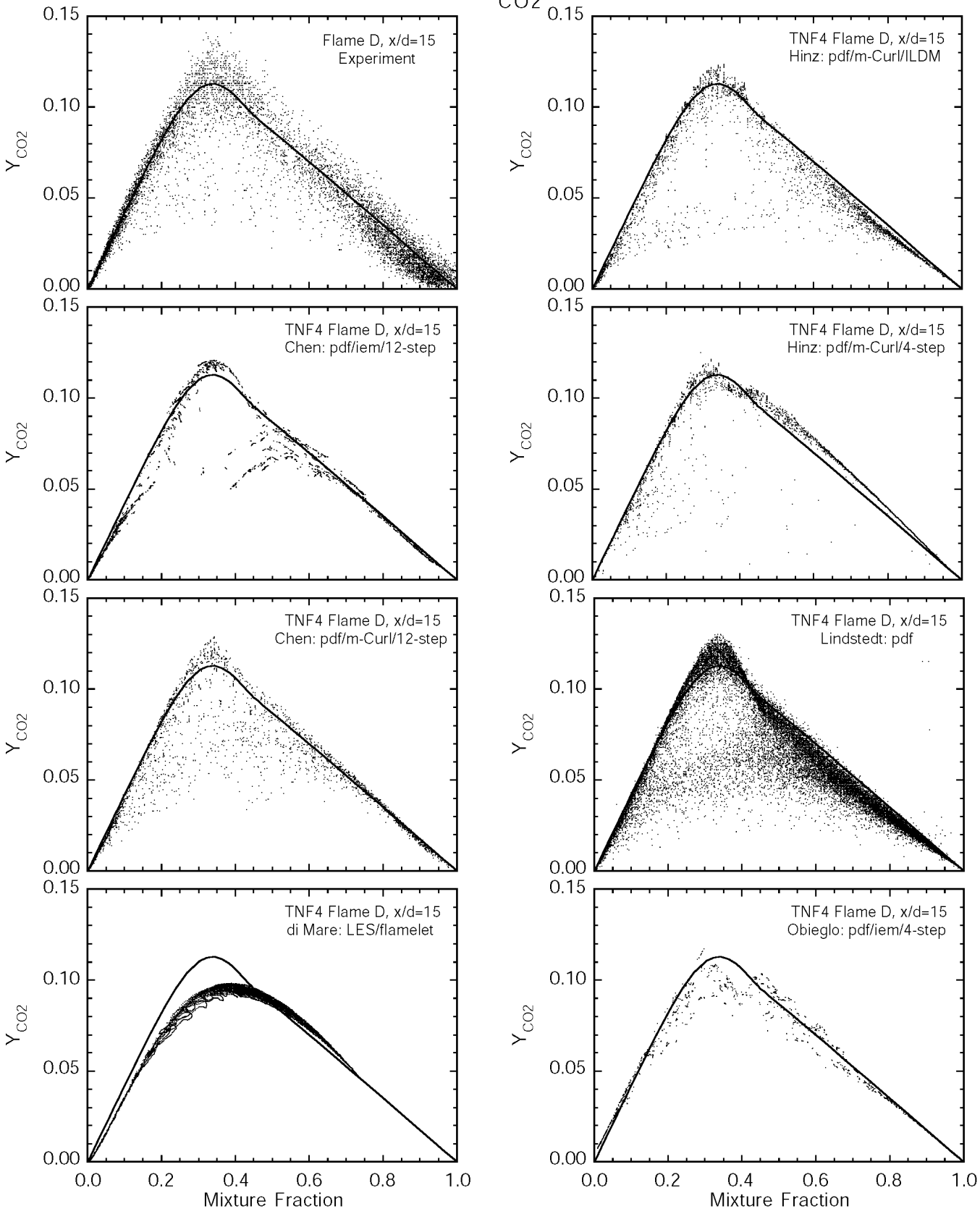
TNF4 Piloted Flame D: Y_{CO2} Scatter Plots at x/d=15
Flame D, x/d=15
Experiment
TNF4 Flame D, x/d=15
Hinz: pdf/m-Curl/ILDM
TNF4 Flame D, x/d=15
Chen: pdf/iem/12-step
TNF4 Flame D, x/d=15
Hinz: pdf/m-Curl/4-step
TNF4 Flame D, x/d=15
Chen: pdf/m-Curl/12-step
TNF4 Flame D, x/d=15
Lindstedt: pdf
TNF4 Flame D, x/d=15
di Mare: LES/flamelet
TNF4 Flame D, x/d=15
Obieglo: pdf/iem/4-step
Y_{CO2}
0.00
0.05
0.10
0.15
0.0
0.2
0.4
0.6
0.8
1.0
Mixture Fraction

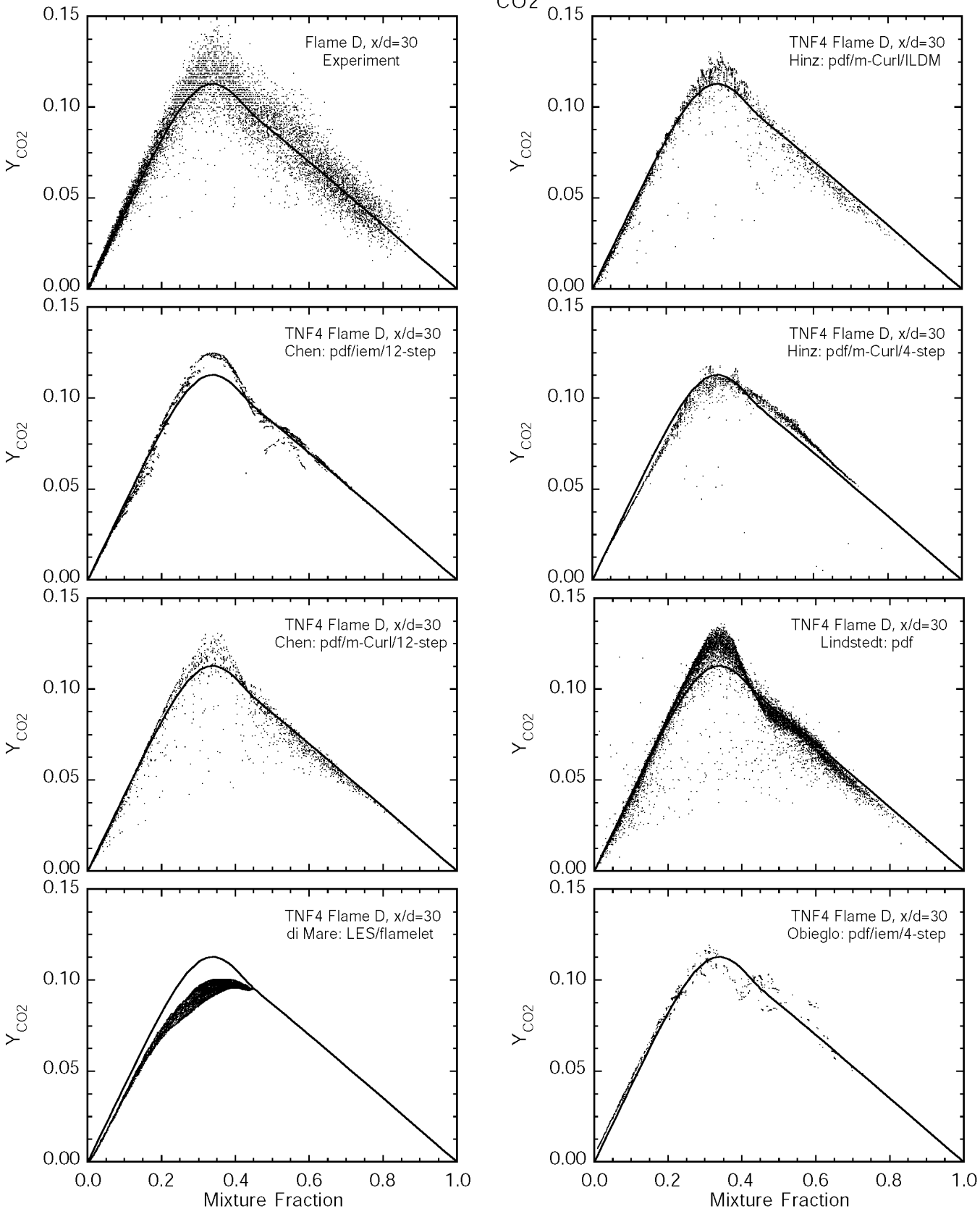
TNF4 Piloted Flame D: Y_{CO2} Scatter Plots at x/d=30
Flame D, x/d=30
Experiment
TNF4 Flame D, x/d=30
Hinz: pdf/m-Curl/ILDM
TNF4 Flame D, x/d=30
Chen: pdf/iem/12-step
TNF4 Flame D, x/d=30
Hinz: pdf/m-Curl/4-step
TNF4 Flame D, x/d=30
Chen: pdf/m-Curl/12-step
TNF4 Flame D, x/d=30
Lindstedt: pdf
TNF4 Flame D, x/d=30
di Mare: LES/flamelet
TNF4 Flame D, x/d=30
Obieglo: pdf/iem/4-step
Y_{CO2}
0.00
0.05
0.10
0.15
0.0
0.2
0.4
0.6
0.8
1.0
Mixture Fraction

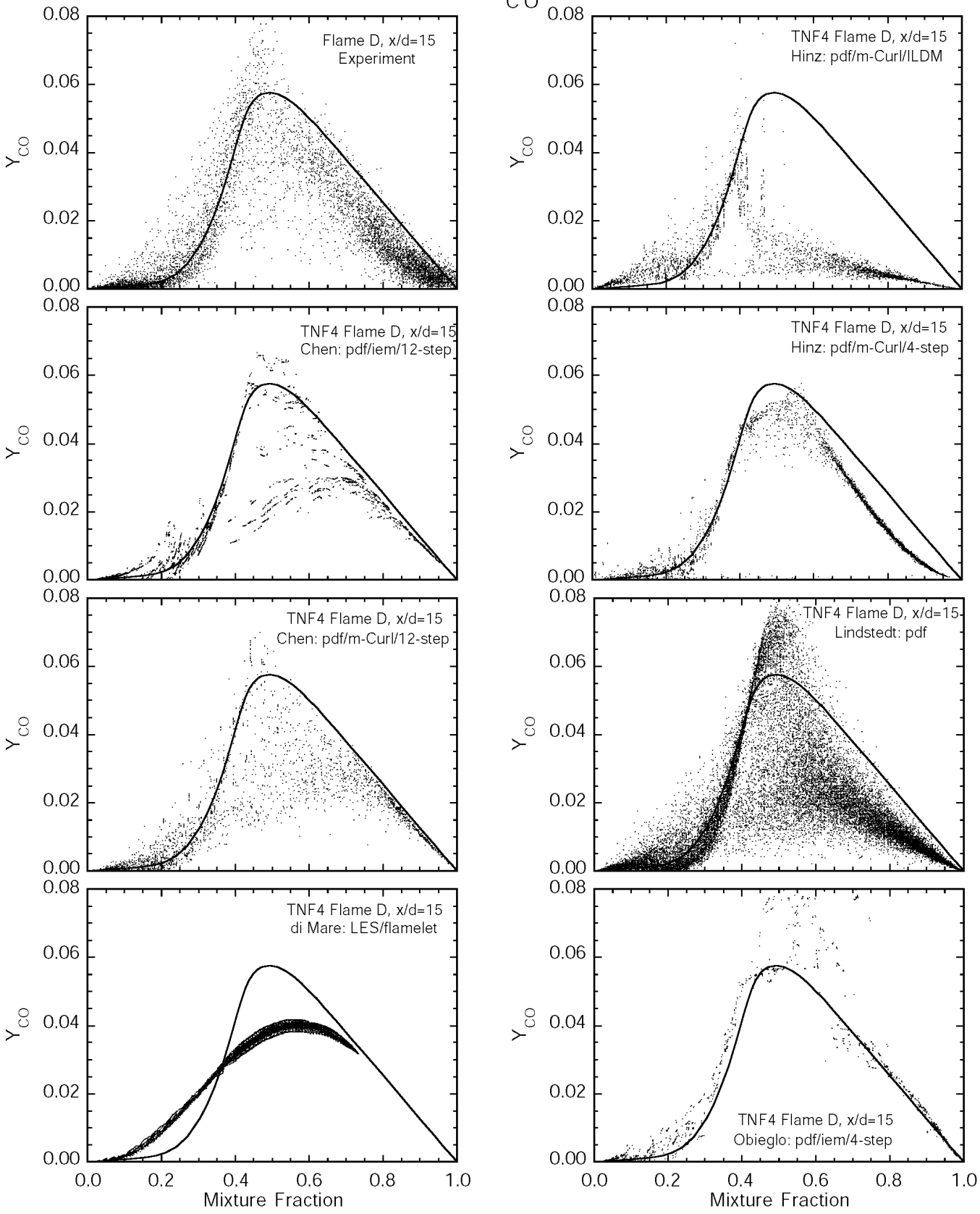
TNF4 Piloted Flame D: Y_{CO} Scatter Plots at x/d=15
Flame D, x/d=15
Experiment
TNF4 Flame D, x/d=15
Hinz: pdf/m-Curl/ILDM
TNF4 Flame D, x/d=15
Chen: pdf/iem/12-step
TNF4 Flame D, x/d=15
Hinz: pdf/m-Curl/4-step
TNF4 Flame D, x/d=15
Chen: pdf/m-Curl/12-step
TNF4 Flame D, x/d=15
Lindstedt: pdf
TNF4 Flame D, x/d=15
di Mare: LES/flamelet
TNF4 Flame D, x/d=15
Obieglo: pdf/iem/4-step
Y_{CO}
0.00
0.02
0.04
0.06
0.08
0.0
0.2
0.4
0.6
0.8
1.0
Mixture Fraction

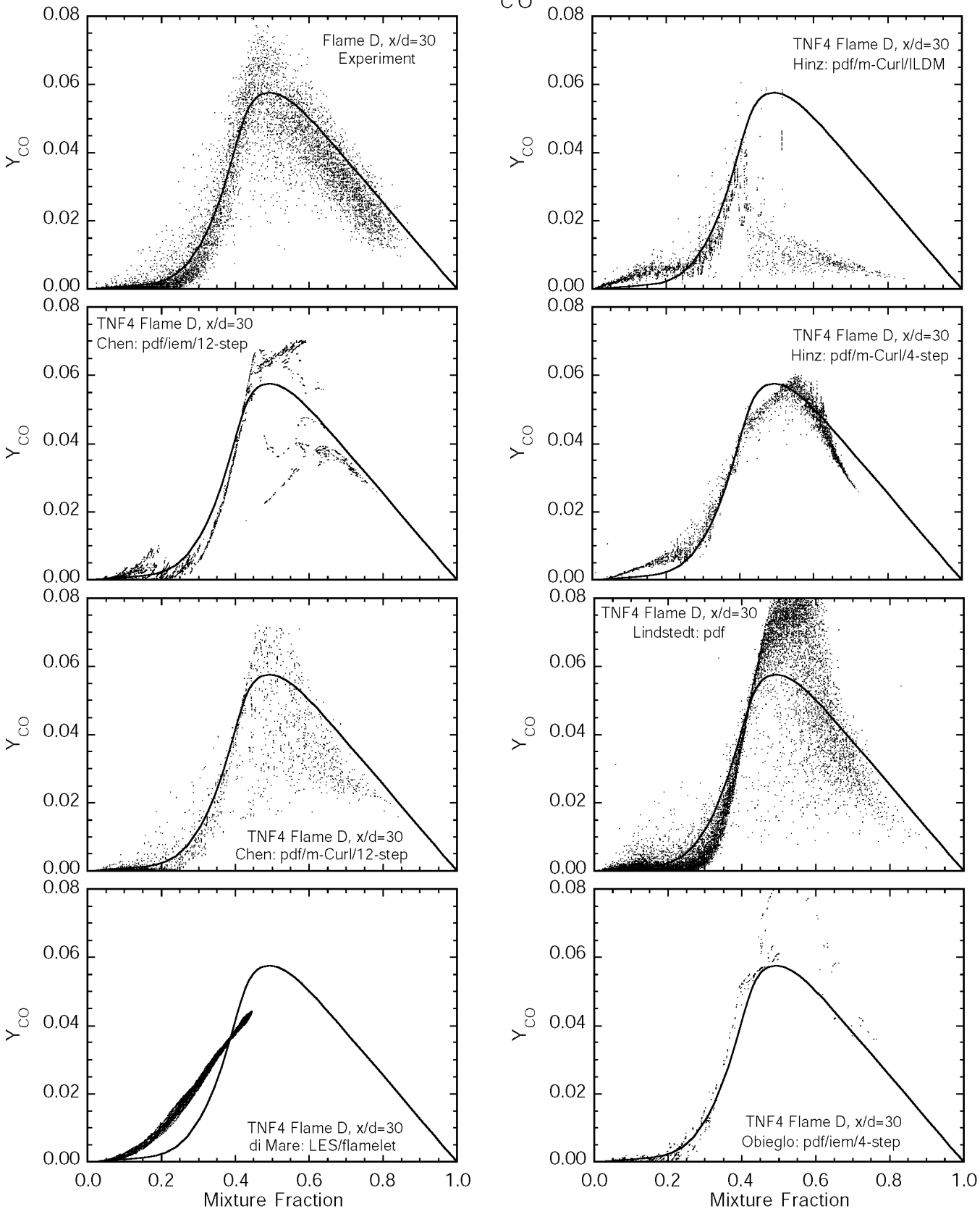
TNF4 Piloted Flame D: Y_{CO} Scatter Plots at x/d=30
Flame D, x/d=30
Experiment
TNF4 Flame D, x/d=30
Hinz: pdf/m-Curl/ILDM
TNF4 Flame D, x/d=30
Chen: pdf/iem/12-step
TNF4 Flame D, x/d=30
Hinz: pdf/m-Curl/4-step
TNF4 Flame D, x/d=30
Chen: pdf/m-Curl/12-step
TNF4 Flame D, x/d=30
Lindstedt: pdf
TNF4 Flame D, x/d=30
di Mare: LES/flamelet
TNF4 Flame D, x/d=30
Obieglo: pdf/iem/4-step
Y_{CO}
0.00
0.02
0.04
0.06
0.08
0.0
0.2
0.4
0.6
0.8
1.0
Mixture Fraction

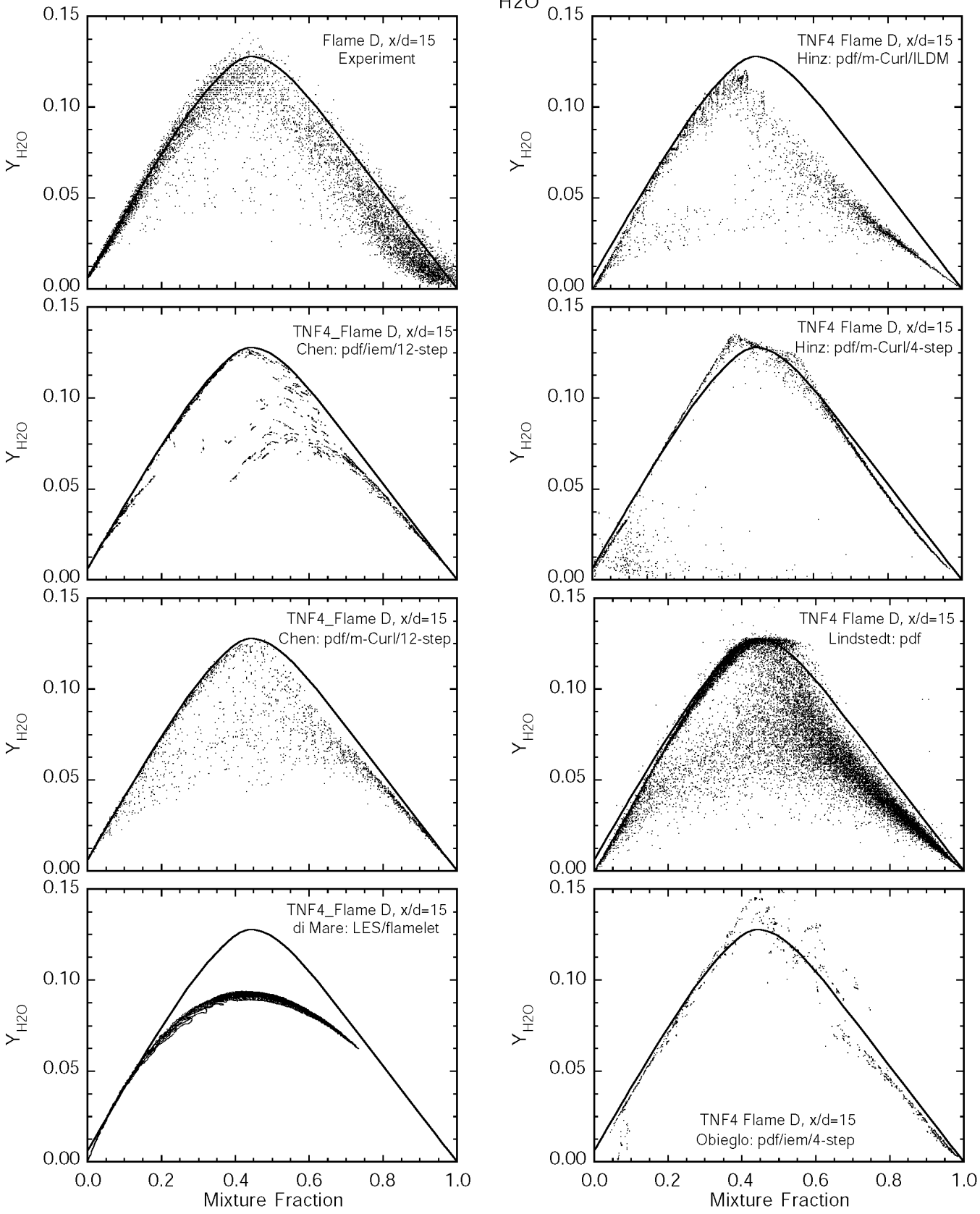
TNF4 Piloted Flame D: Y_{H2O} Scatter Plots at x/d=15
Flame D, x/d=15
Experiment
TNF4 Flame D, x/d=15
Hinz: pdf/m-Curl/ILDM
TNF4_Flame D, x/d=15
Chen: pdf/iem/12-step
TNF4 Flame D, x/d=15
Hinz: pdf/m-Curl/4-step
TNF4_Flame D, x/d=15
Chen: pdf/m-Curl/12-step
TNF4 Flame D, x/d=15
Lindstedt: pdf
TNF4_Flame D, x/d=15
di Mare: LES/flamelet
TNF4 Flame D, x/d=15
Obieglo: pdf/iem/4-step
Y_{H2O}
0.00
0.05
0.10
0.15
0.0
0.2
0.4
0.6
0.8
1.0
Mixture Fraction

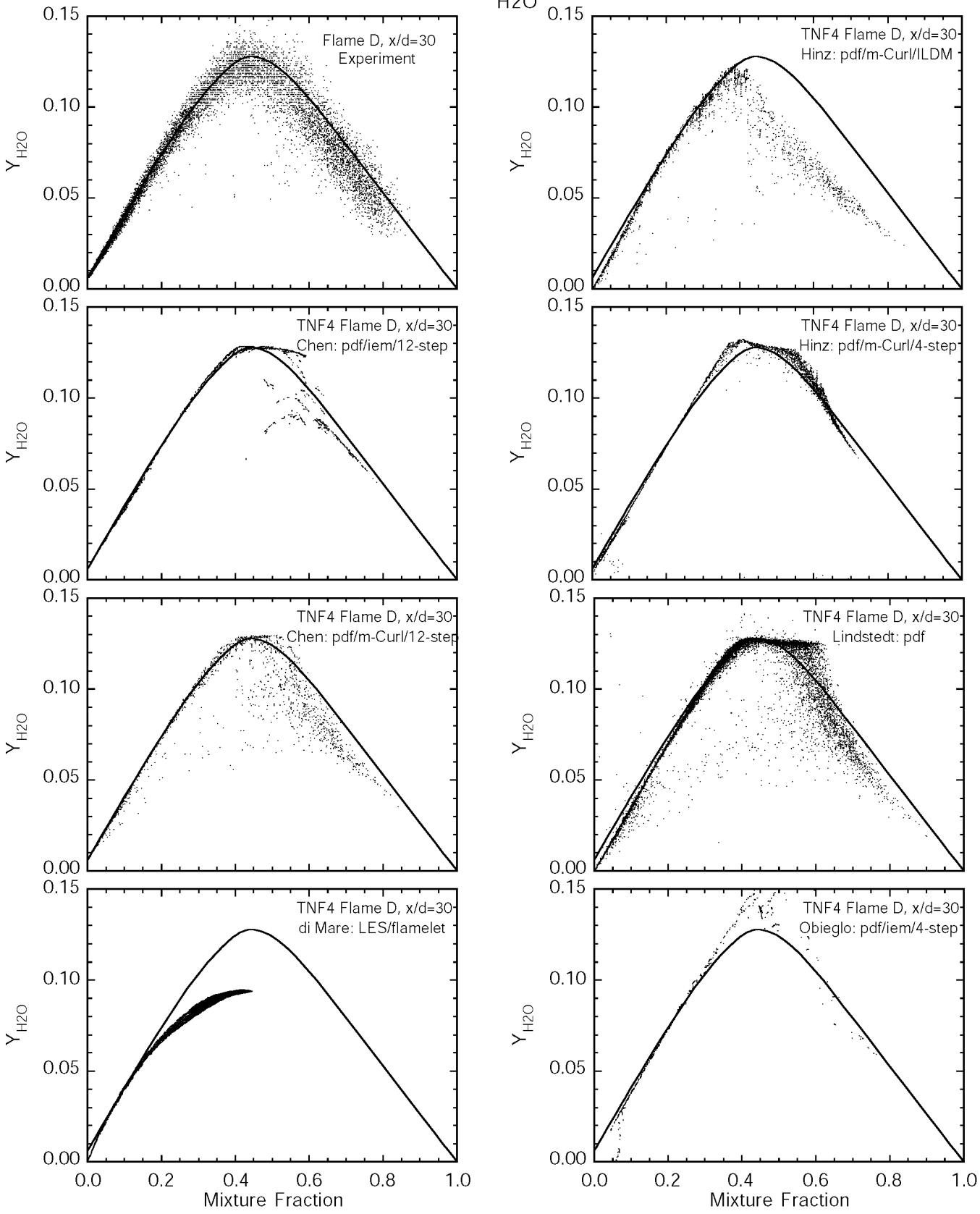
TNF4 Piloted Flame D: Y_{H2O} Scatter Plots at x/d=30
Flame D, x/d=30
Experiment
TNF4 Flame D, x/d=30
Hinz: pdf/m-Curl/ILDM
TNF4 Flame D, x/d=30
Chen: pdf/iem/12-step
TNF4 Flame D, x/d=30
Hinz: pdf/m-Curl/4-step
TNF4 Flame D, x/d=30
Chen: pdf/m-Curl/12-step
TNF4 Flame D, x/d=30
Lindstedt: pdf
TNF4 Flame D, x/d=30
di Mare: LES/flamelet
TNF4 Flame D, x/d=30
Obieglo: pdf/iem/4-step
Y_{H2O}
0.15
0.10
0.05
0.00
0.0
0.2
0.4
0.6
0.8
1.0
Mixture Fraction

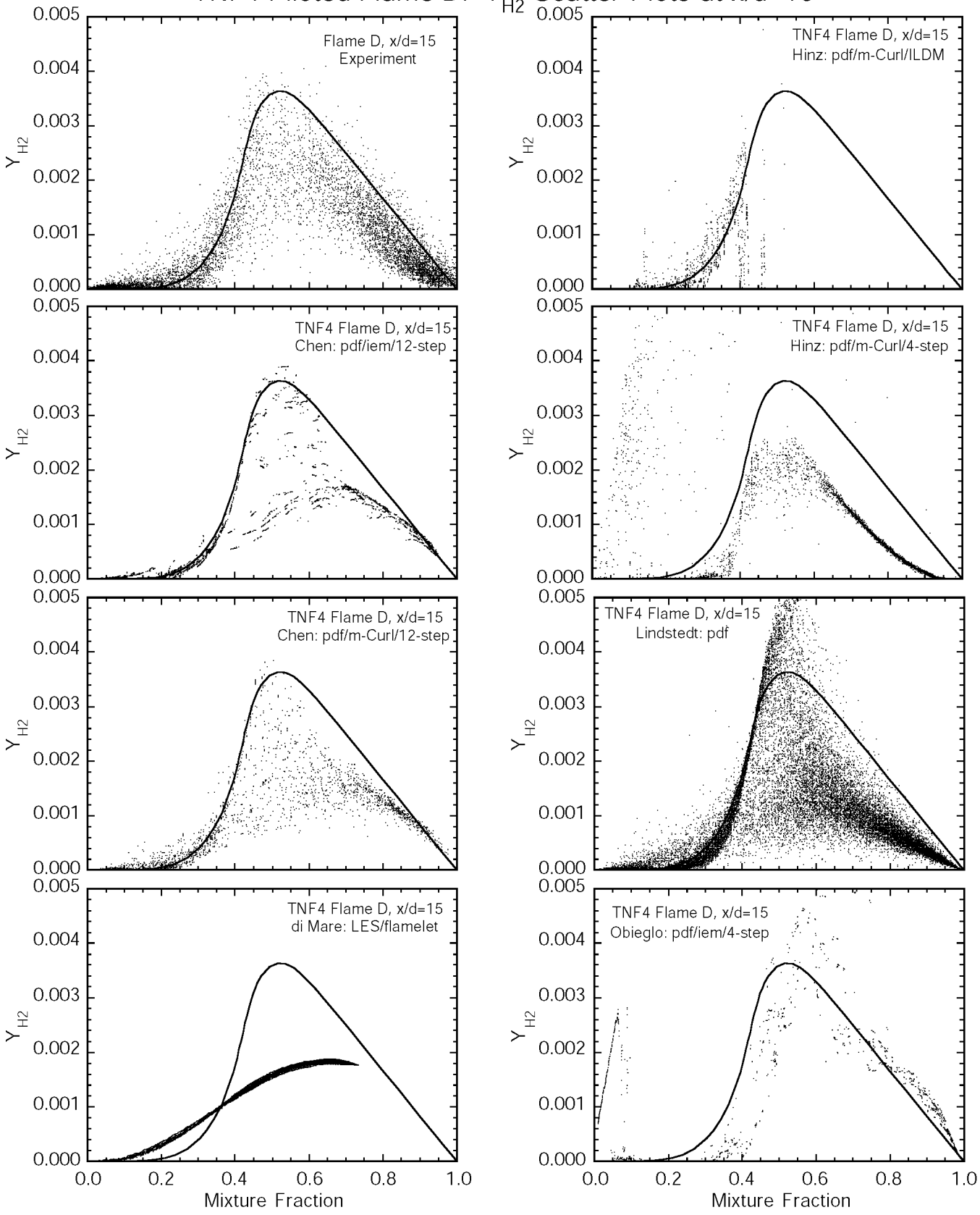
TNF4 Piloted Flame D: Y_{H2} Scatter Plots at x/d=15
Flame D, x/d=15
Experiment
TNF4 Flame D, x/d=15
Hinz: pdf/m-Curl/ILDM
TNF4 Flame D, x/d=15
Chen: pdf/iem/12-step
TNF4 Flame D, x/d=15
Hinz: pdf/m-Curl/4-step
TNF4 Flame D, x/d=15
Chen: pdf/m-Curl/12-step
TNF4 Flame D, x/d=15
Lindstedt: pdf
TNF4 Flame D, x/d=15
di Mare: LES/flamelet
TNF4 Flame D, x/d=15
Obieglo: pdf/iem/4-step
Y_{H2}
0.000
0.001
0.002
0.003
0.004
0.005
0.0
0.2
0.4
0.6
0.8
1.0
Mixture Fraction

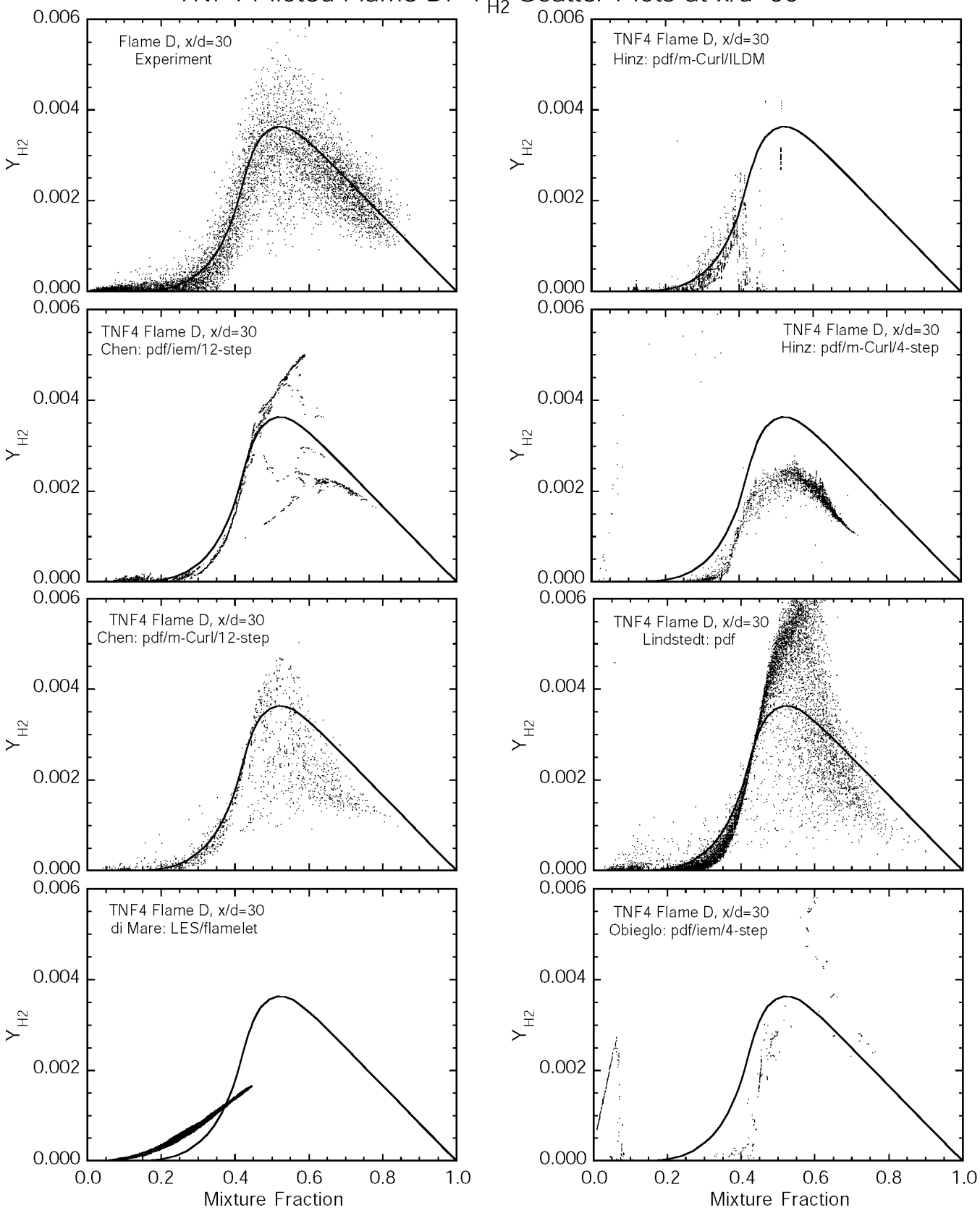
TNF4 Piloted Flame D: Y_{H2} Scatter Plots at x/d=30
Flame D, x/d=30
Experiment
TNF4 Flame D, x/d=30
Hinz: pdf/m-Curl/ILDM
TNF4 Flame D, x/d=30
Chen: pdf/iem/12-step
TNF4 Flame D, x/d=30
Hinz: pdf/m-Curl/4-step
TNF4 Flame D, x/d=30
Chen: pdf/m-Curl/12-step
TNF4 Flame D, x/d=30
Lindstedt: pdf
TNF4 Flame D, x/d=30
di Mare: LES/flamelet
TNF4 Flame D, x/d=30
Obieglo: pdf/iem/4-step
Y_{H2}
0.000
0.002
0.004
0.006
0.0
0.2
0.4
0.6
0.8
1.0
Mixture Fraction

TNF4 Piloted Flame D: Y_{OH} Scatter Plots at x/d=15

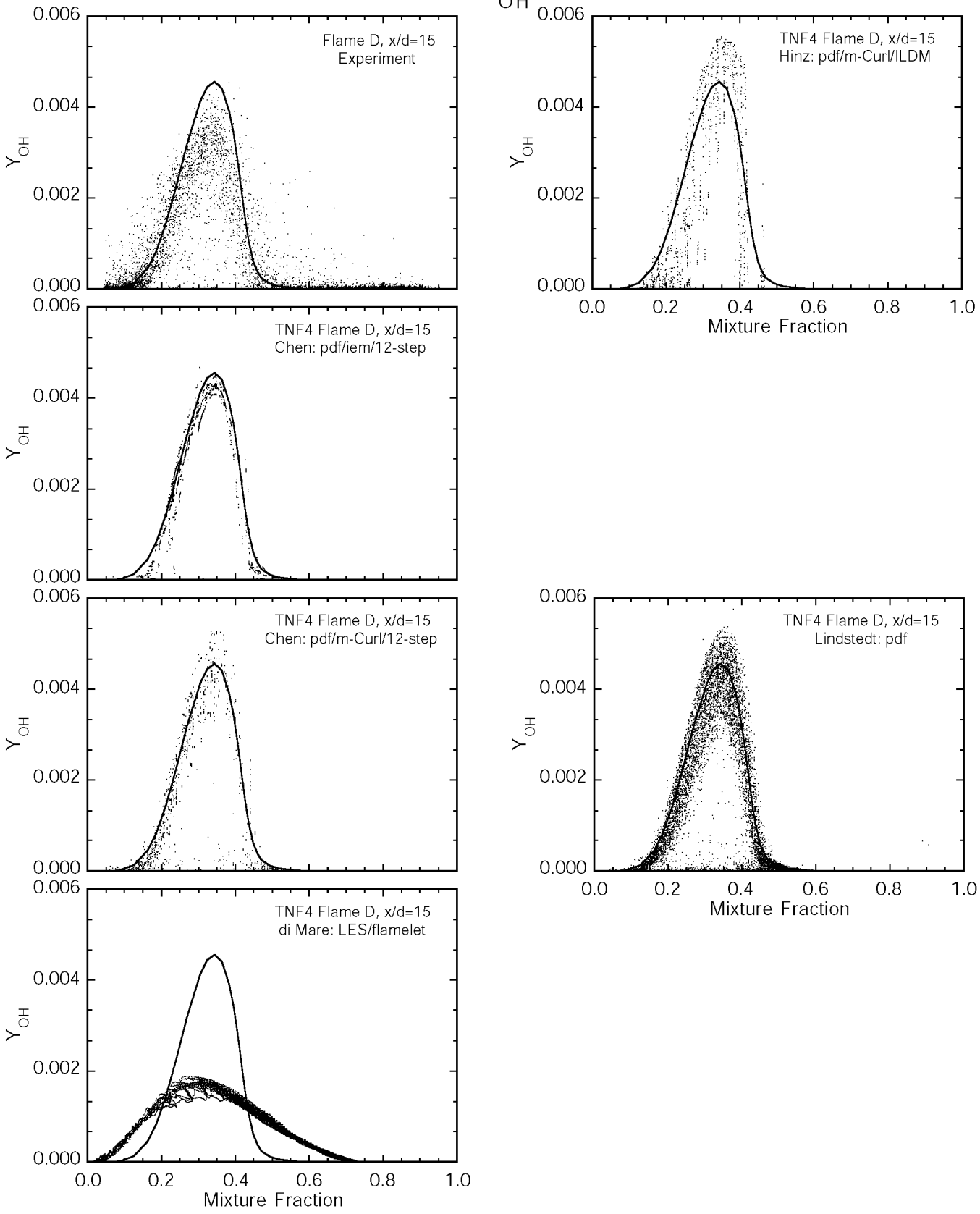

TNF4 Piloted Flame D: Y_{OH} Scatter Plots at x/d=30

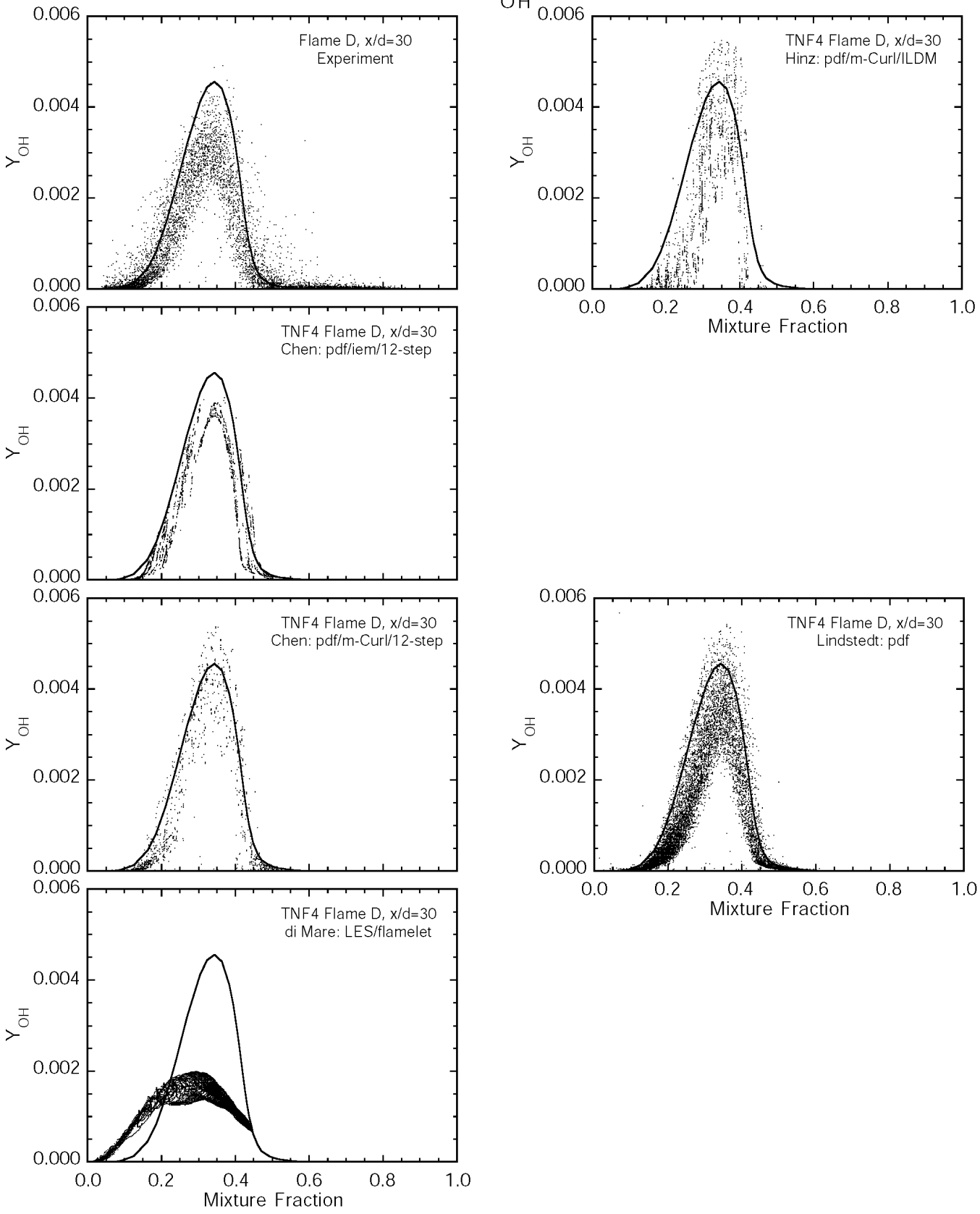

Comparison Plots: Flame E

Piloted Flame E: Axial Profiles of Axial Velocity, Mixture Fraction, and Temperature

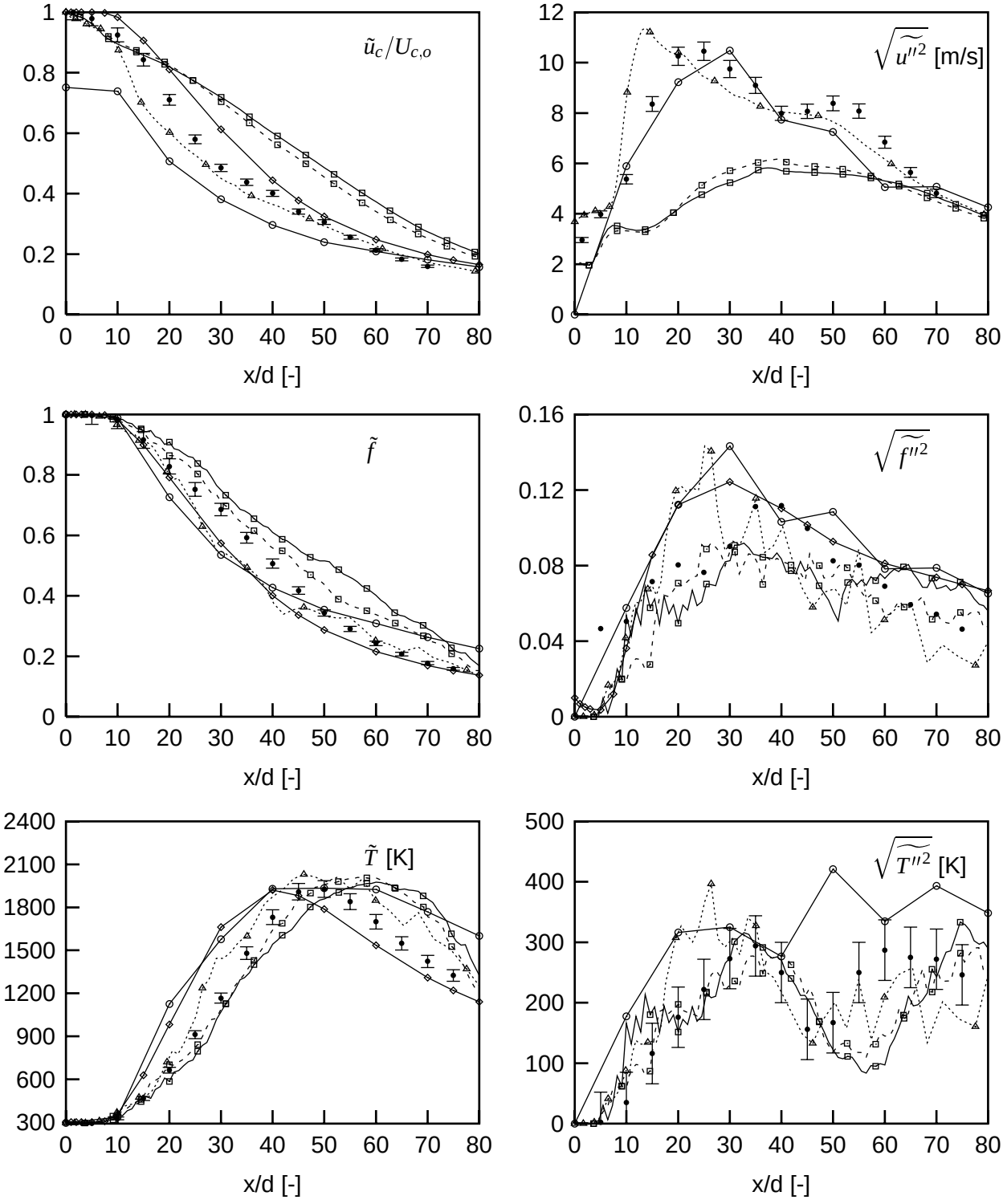

Piloted Flame E: Axial Profiles of Species Mass Fractions

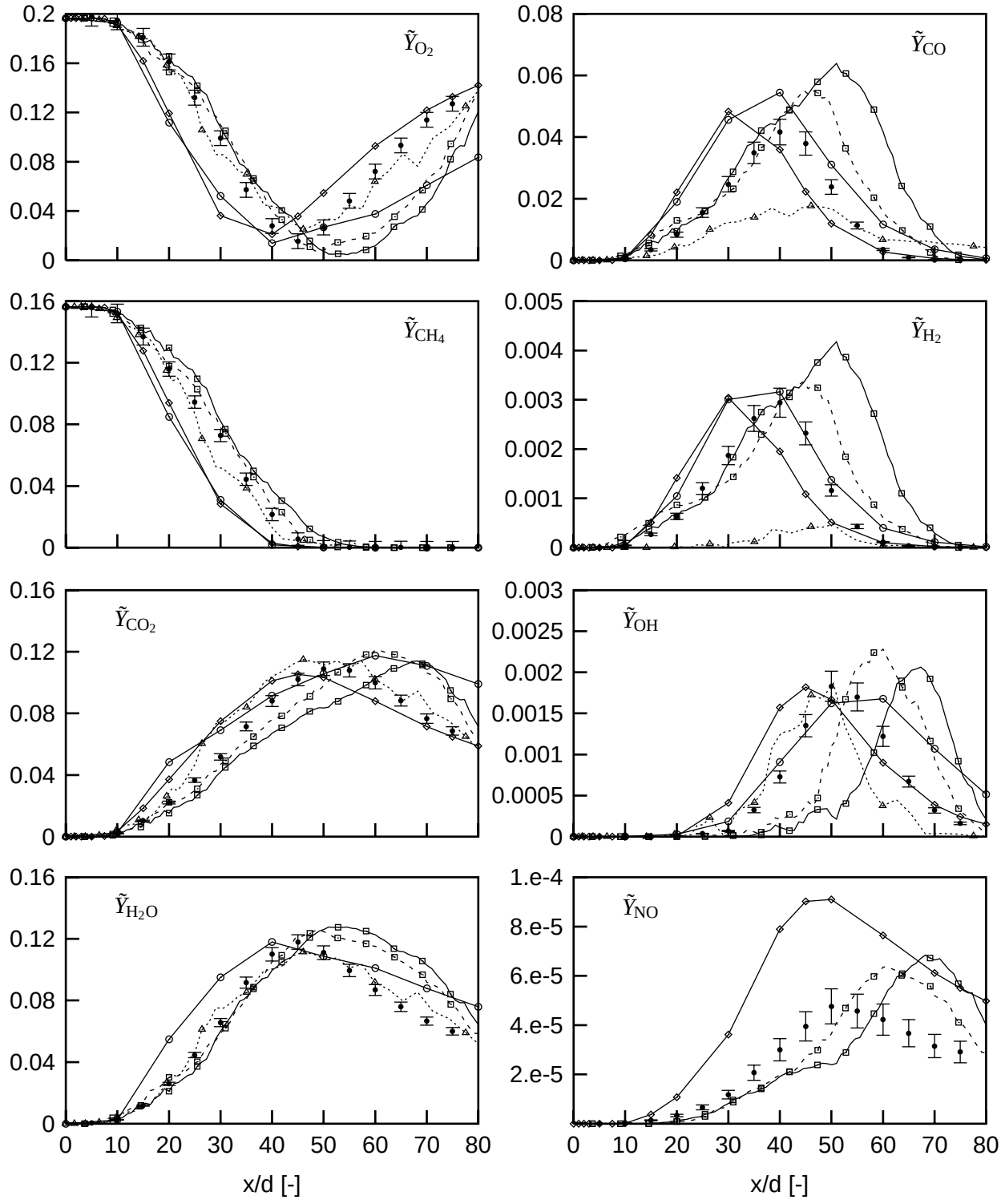

Piloted Flame E: Radial Profiles of Velocity and Shear Stress at x/d=15, 45

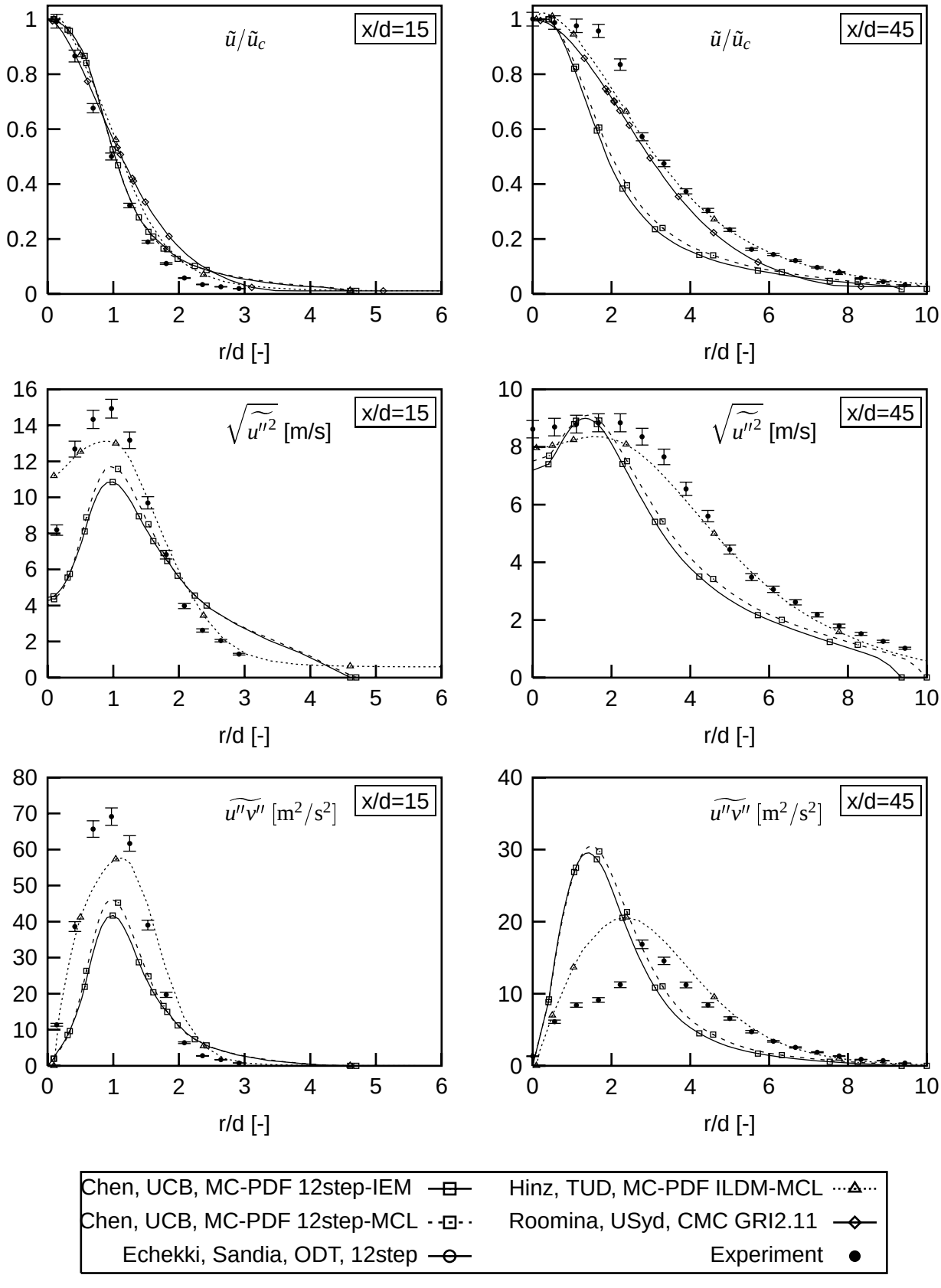

Piloted Flame E: Radial Profiles of Scalars at x/d=15

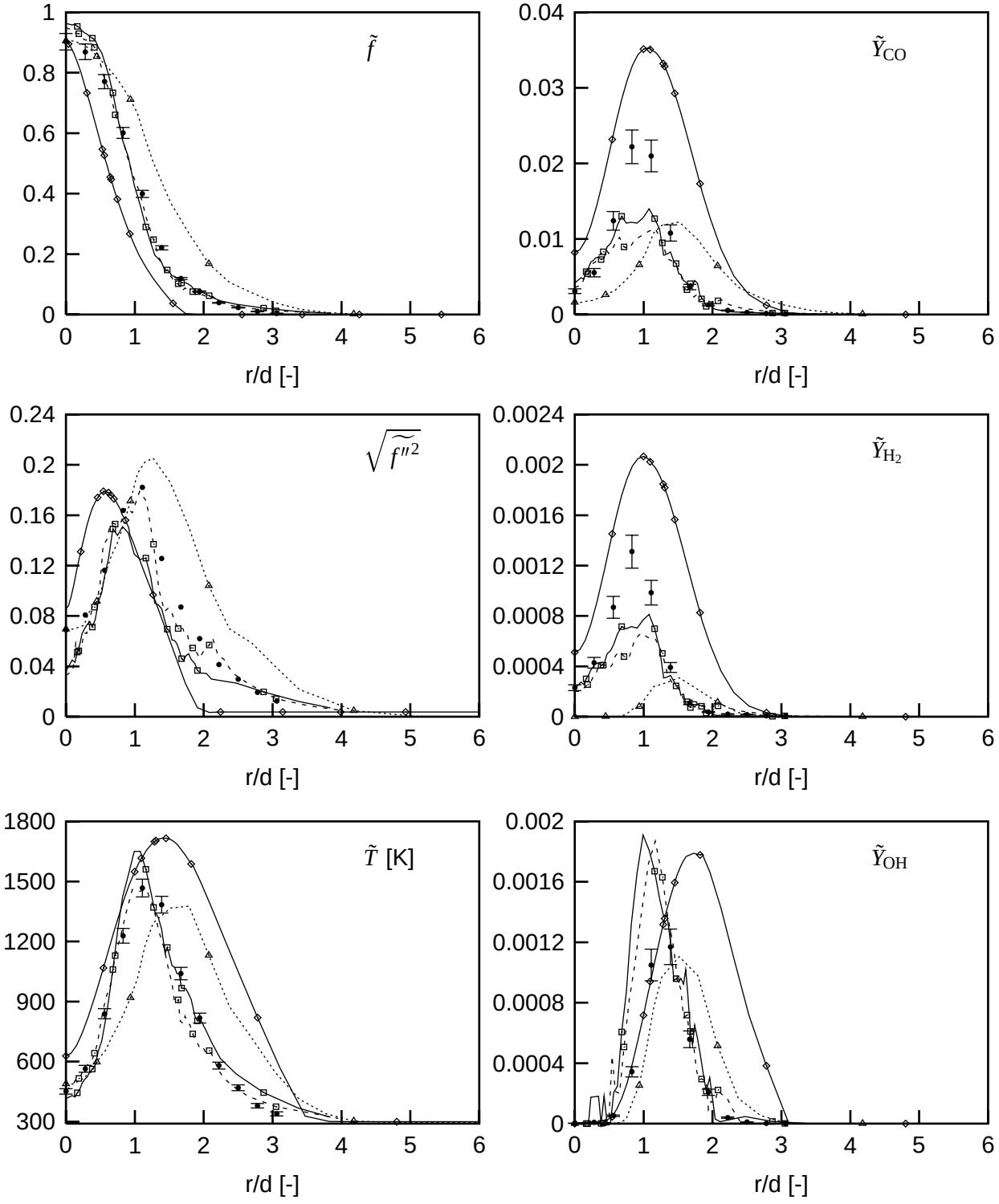

Piloted Flame E: Radial Profiles of Scalars at x/d=30

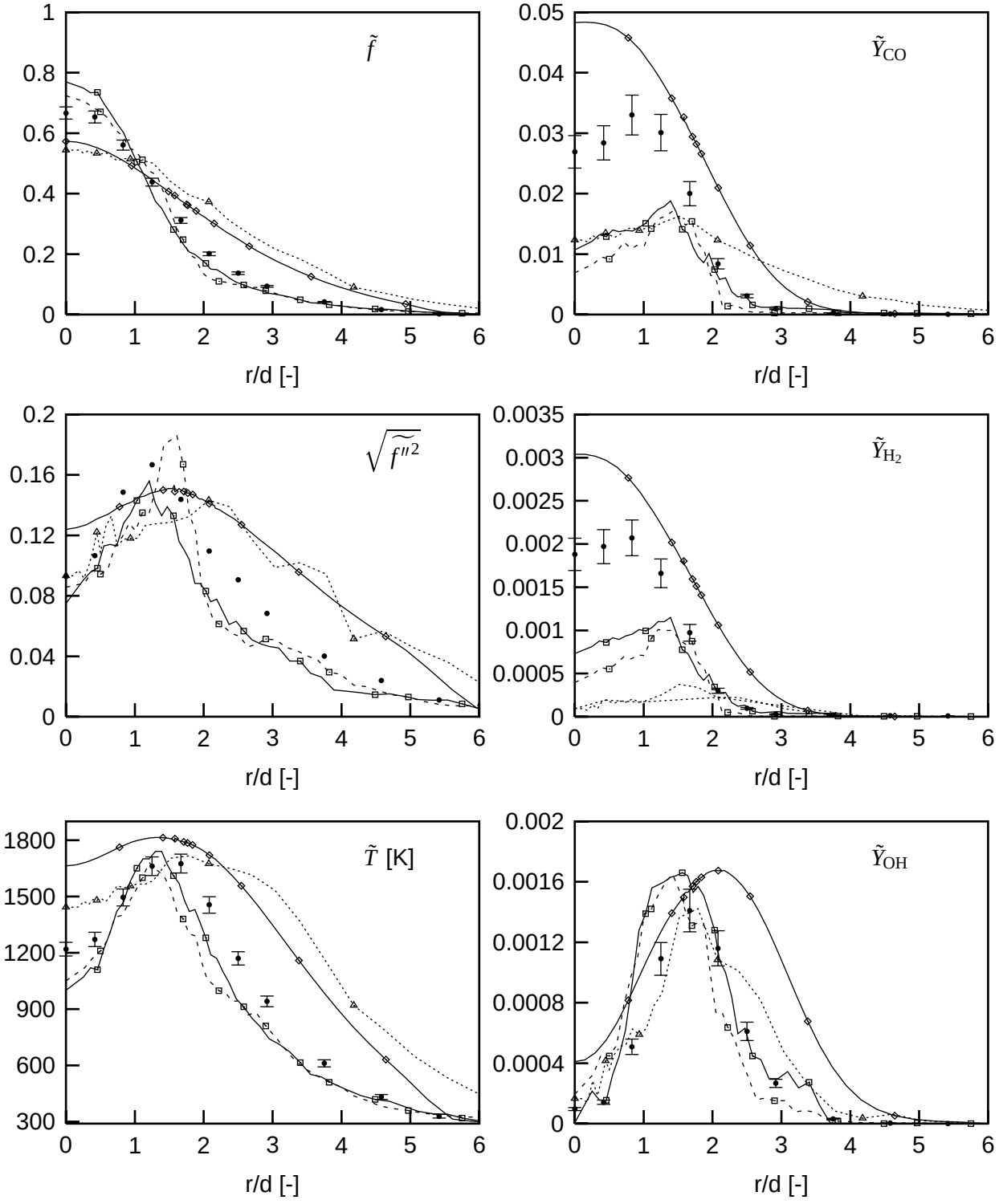

Piloted Flame E: Radial Profiles of Scalars at x/d=45

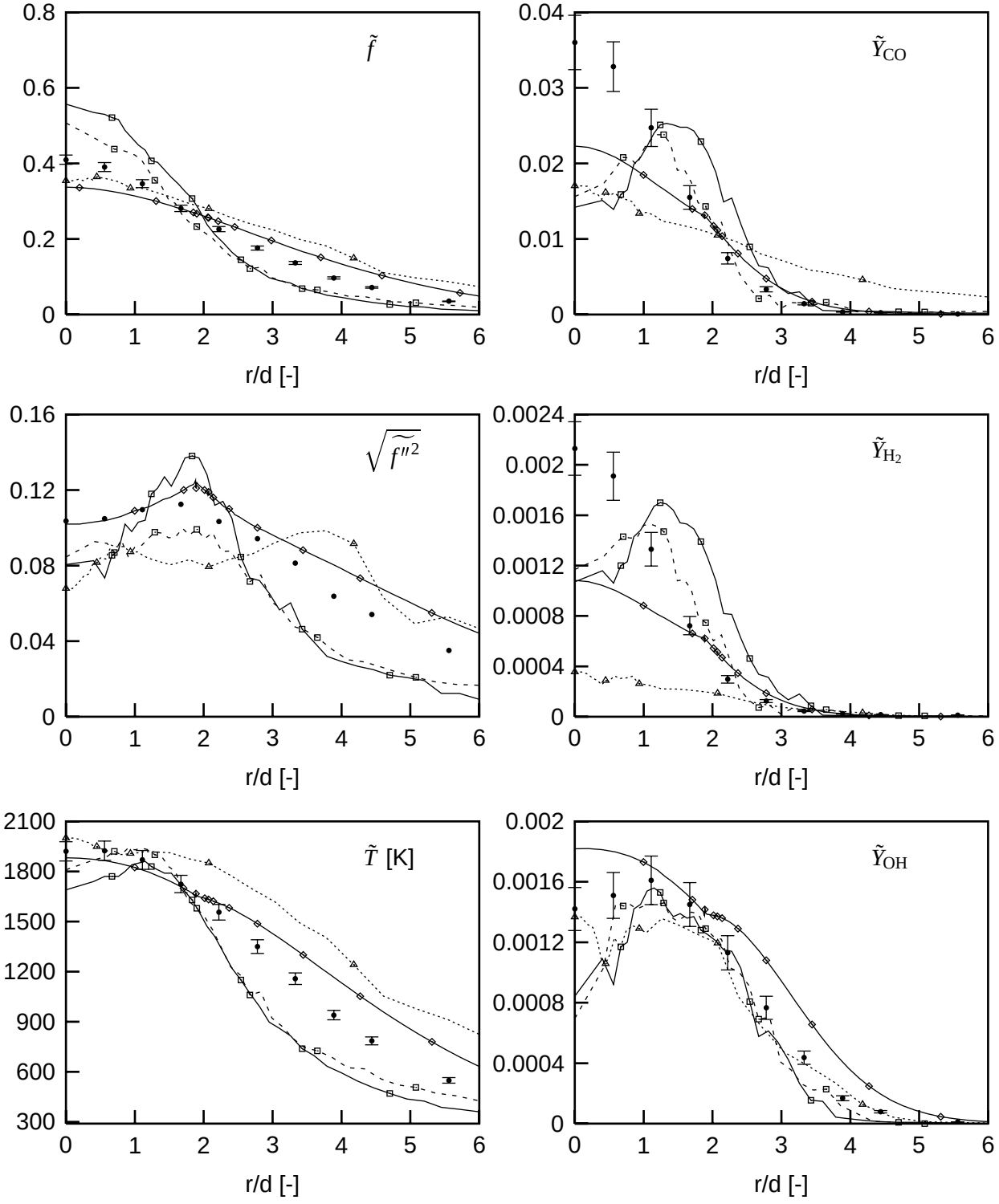

Piloted Flame E: Conditional Means at x/d=15

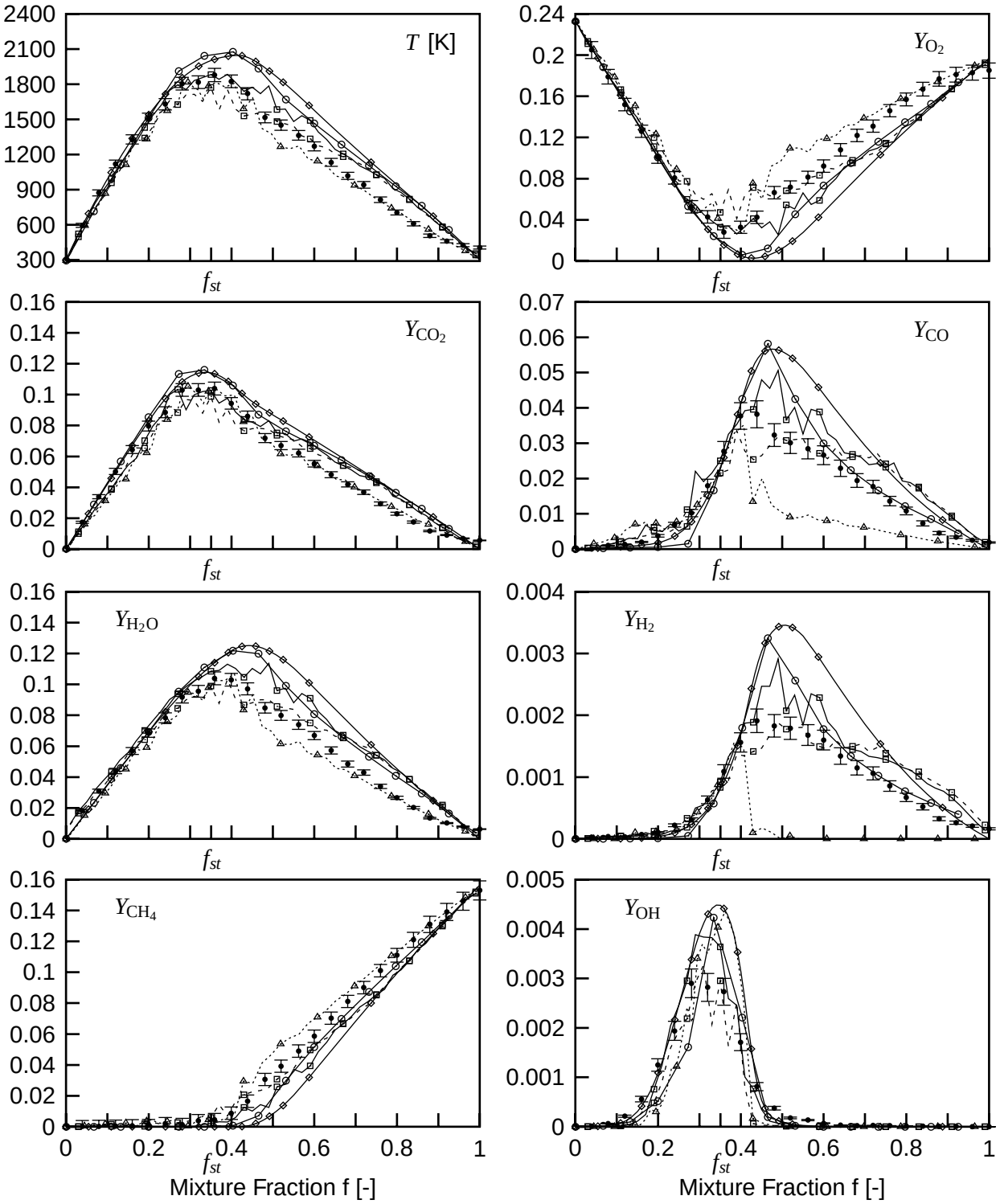

Piloted Flame E: Conditional Means at x/d=30

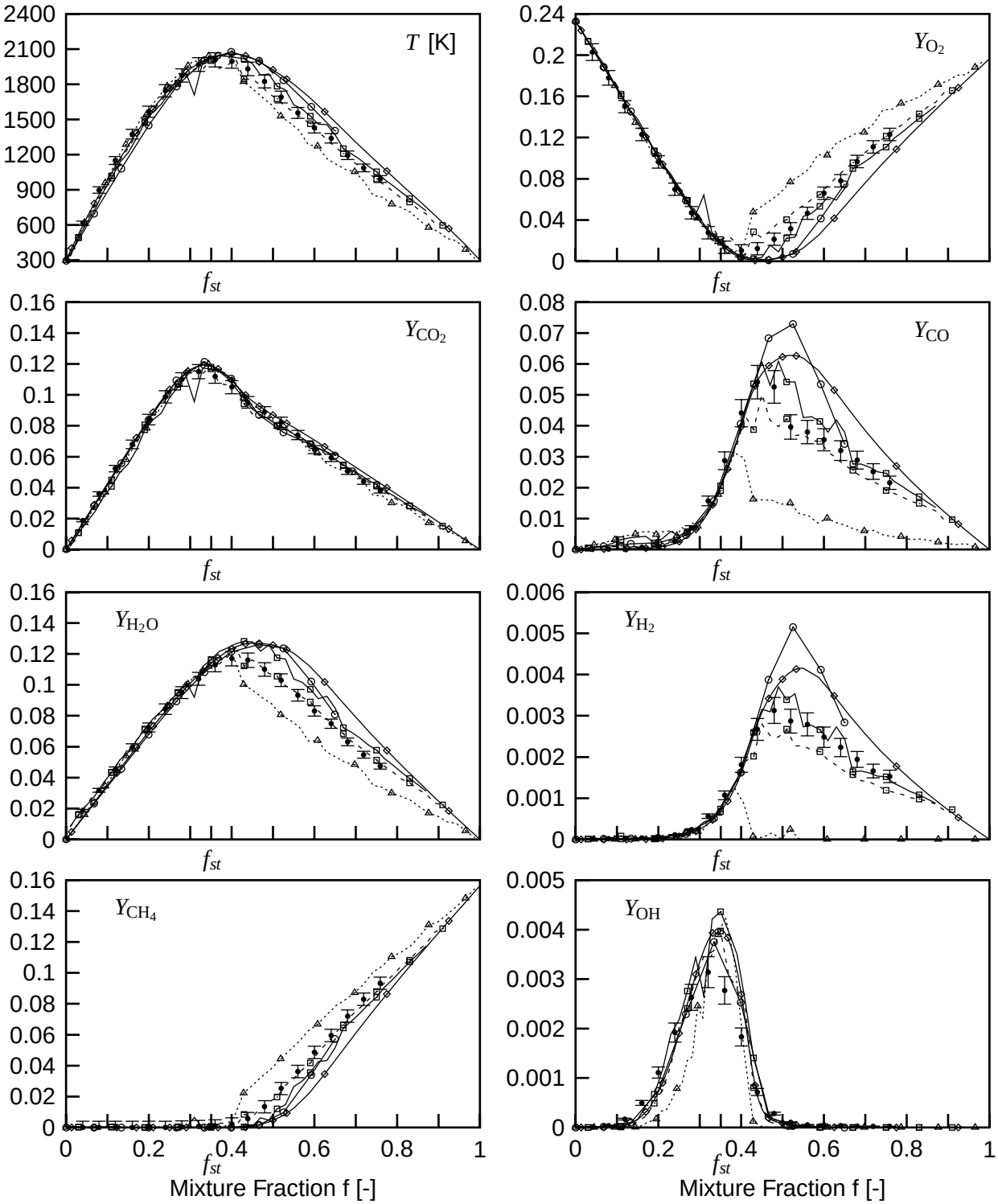

Piloted Flame E: Conditional Means at x/d=45

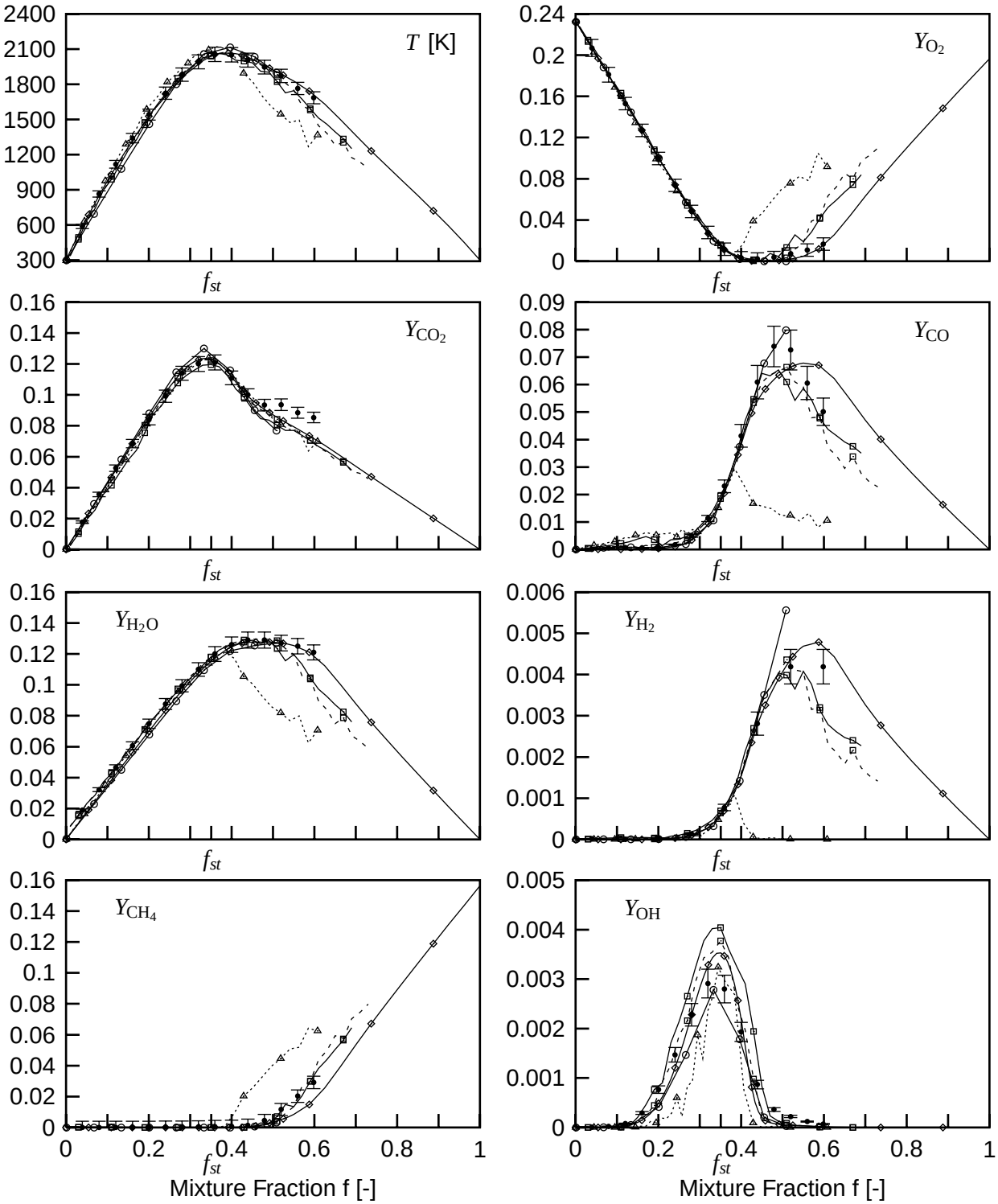

Piloted Flame E: Scatter Plots of Temperature [K] at x d=15, 30

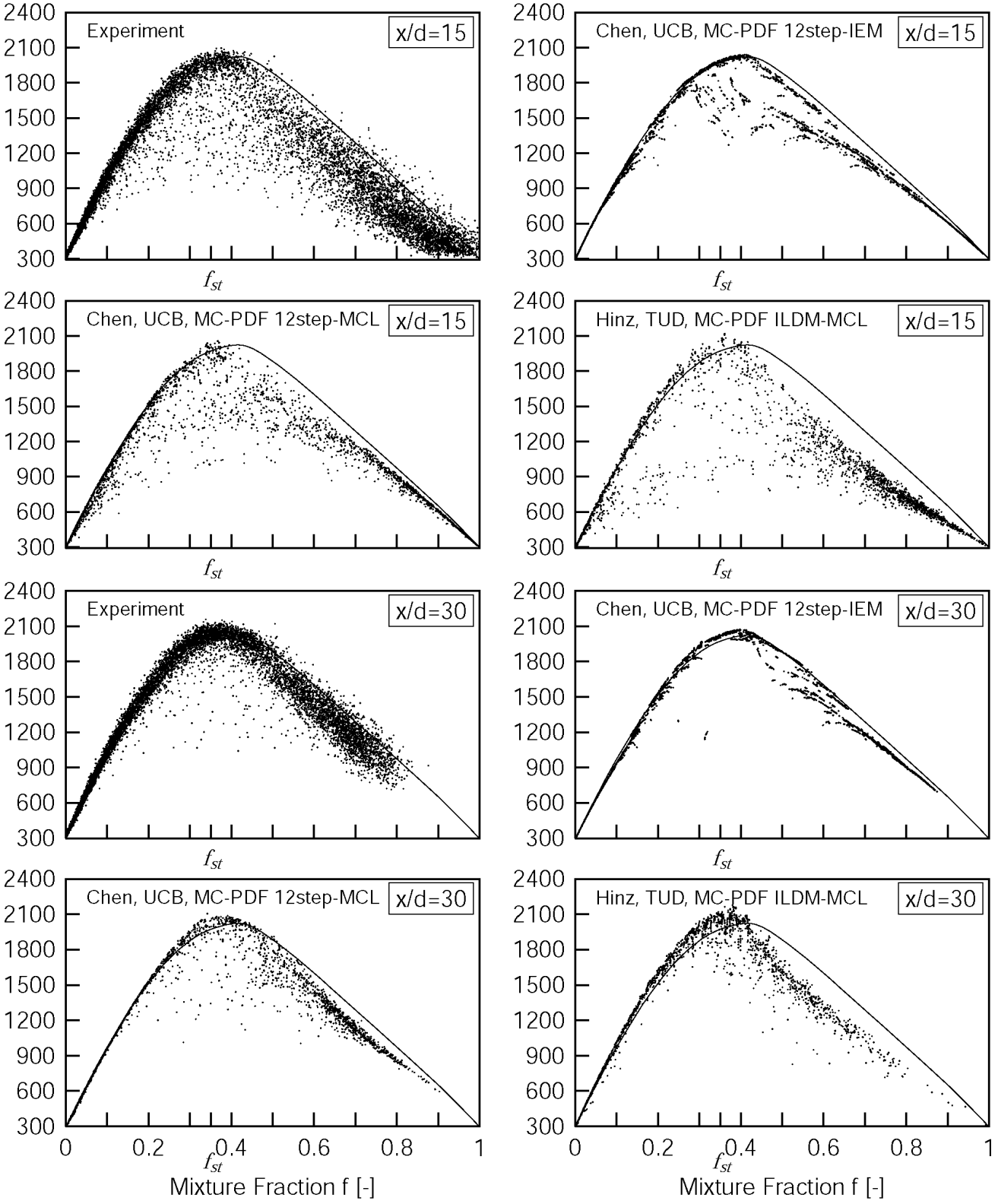

Piloted Flame E: Scatter Plots of Mass Fraction of CO_2 at x d=15, 30

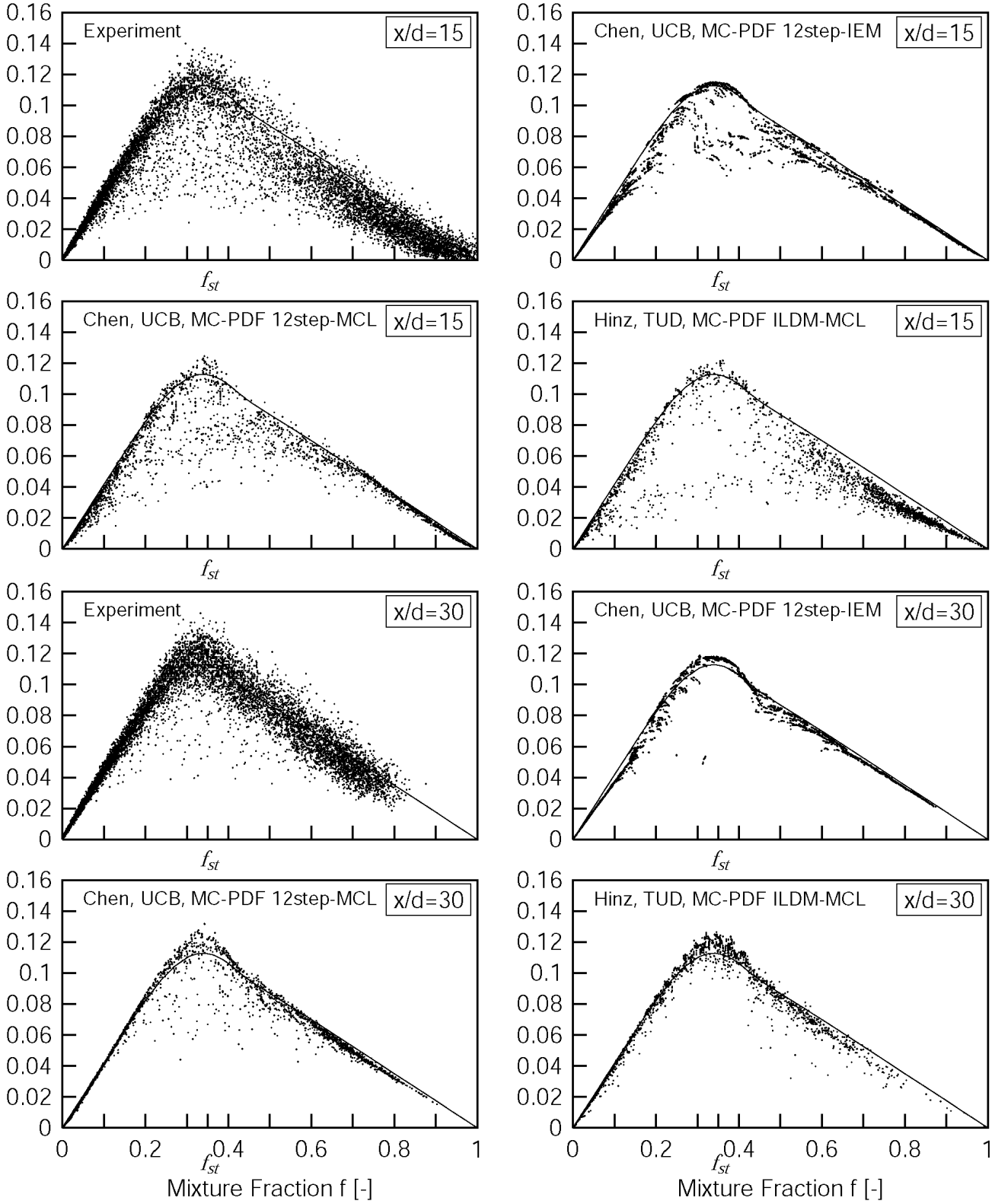

Piloted Flame E: Scatter Plots of Mass Fraction of CO at x d=15, 30

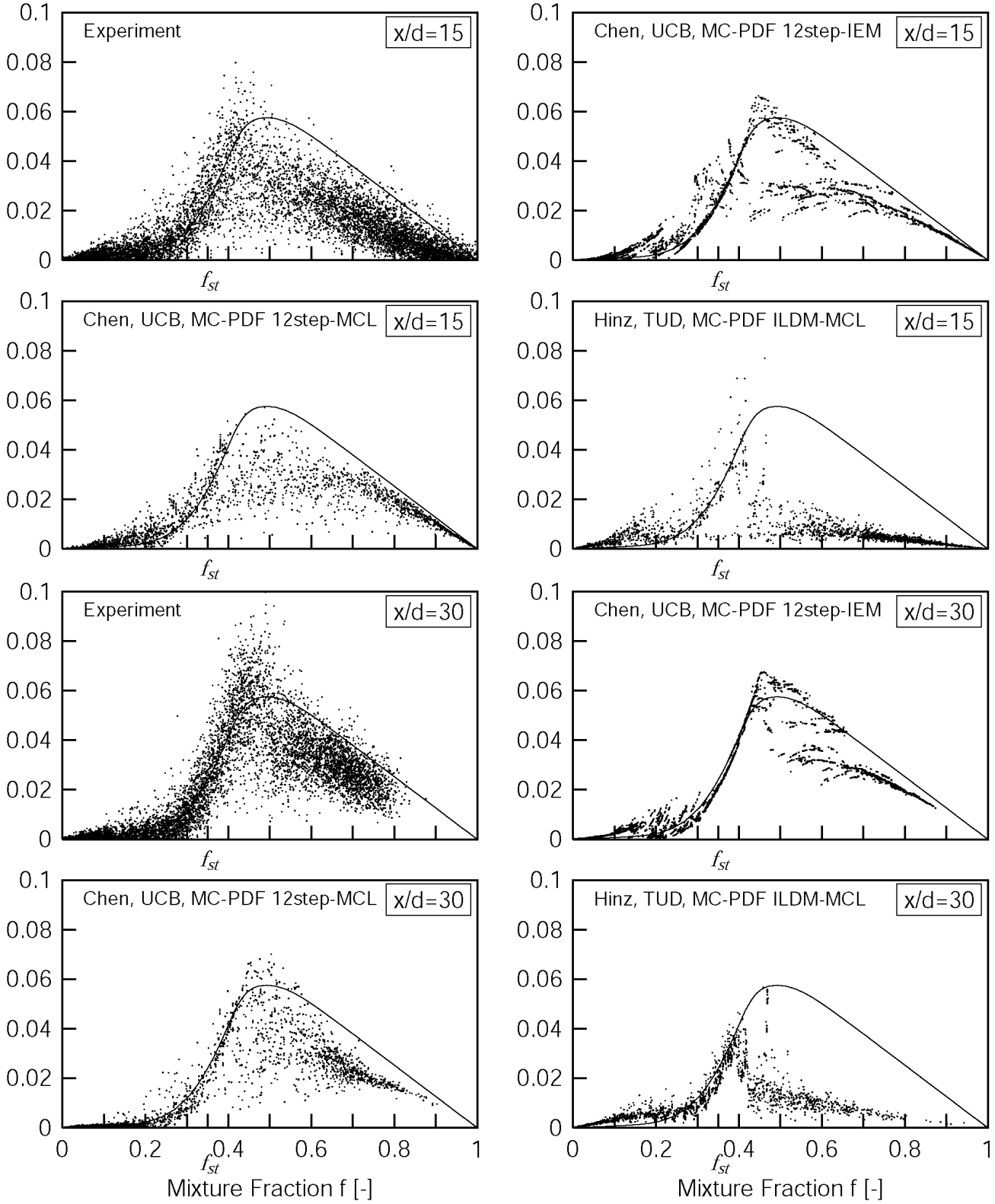

Piloted Flame E: Scatter Plots of Mass Fraction of H_2O at x d=15, 30

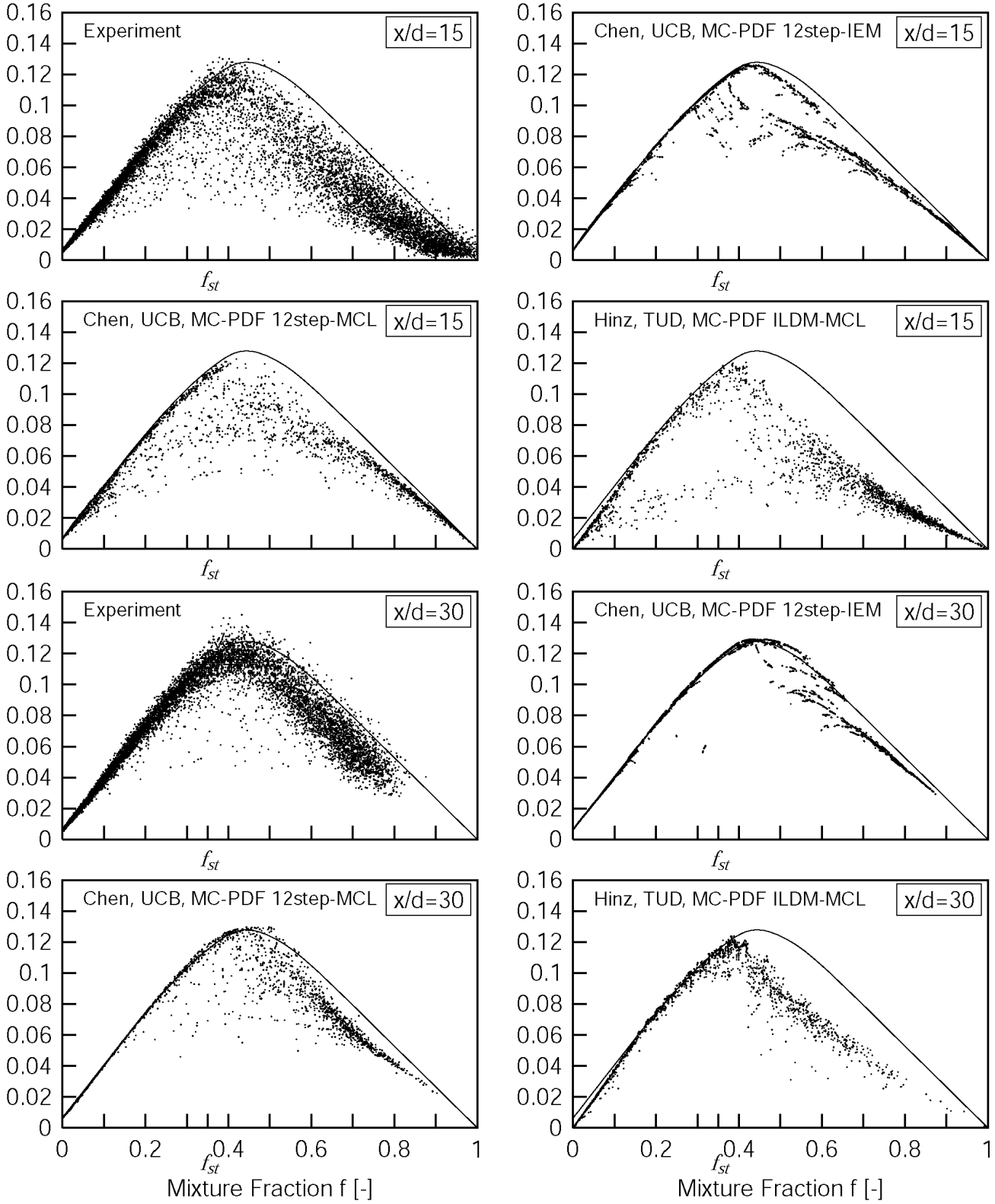

Piloted Flame E: Scatter Plots of Mass Fraction of H_2 at x d=15, 30

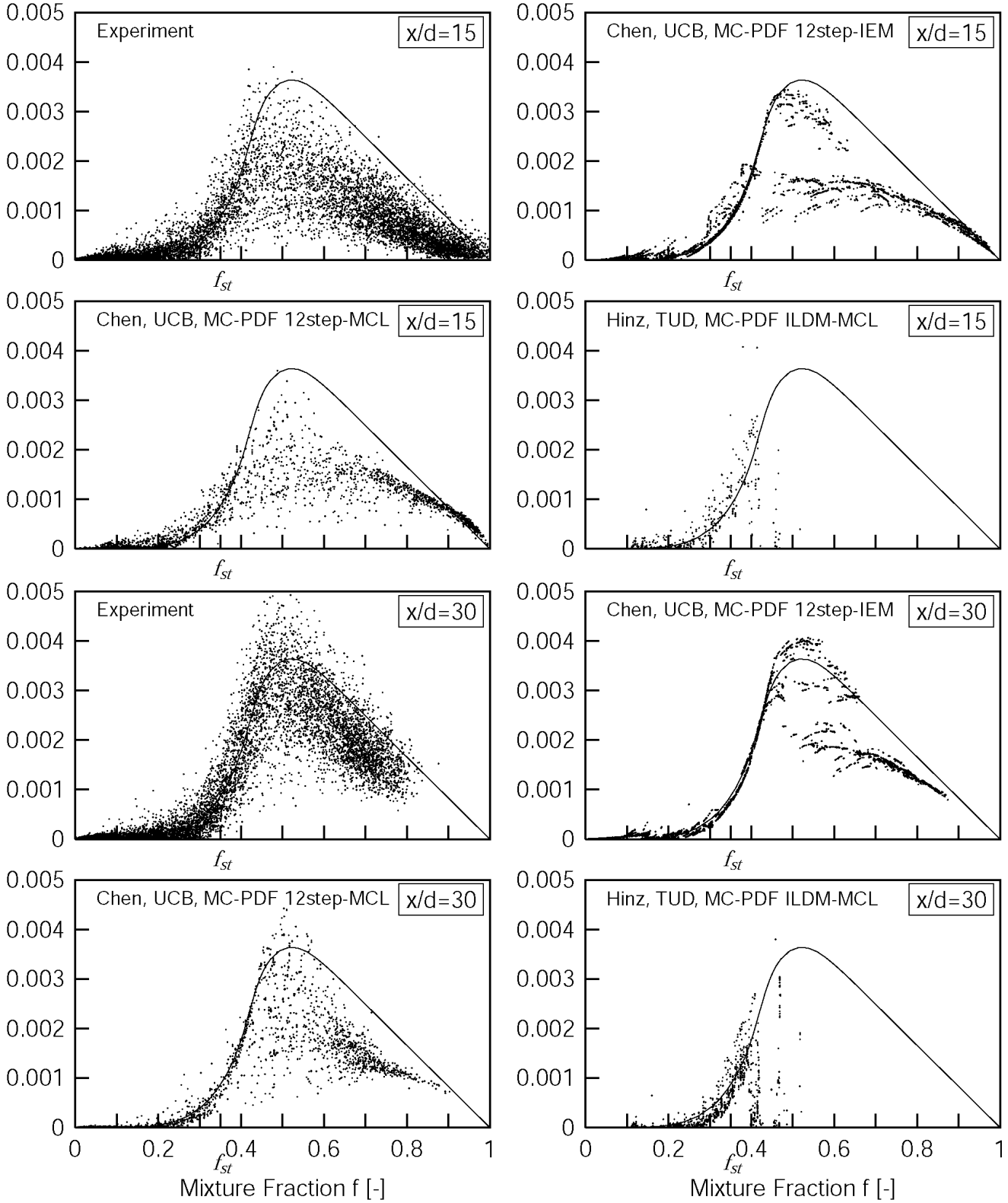

Piloted Flame E: Scatter Plots of Mass Fraction of OH at x d=15, 30

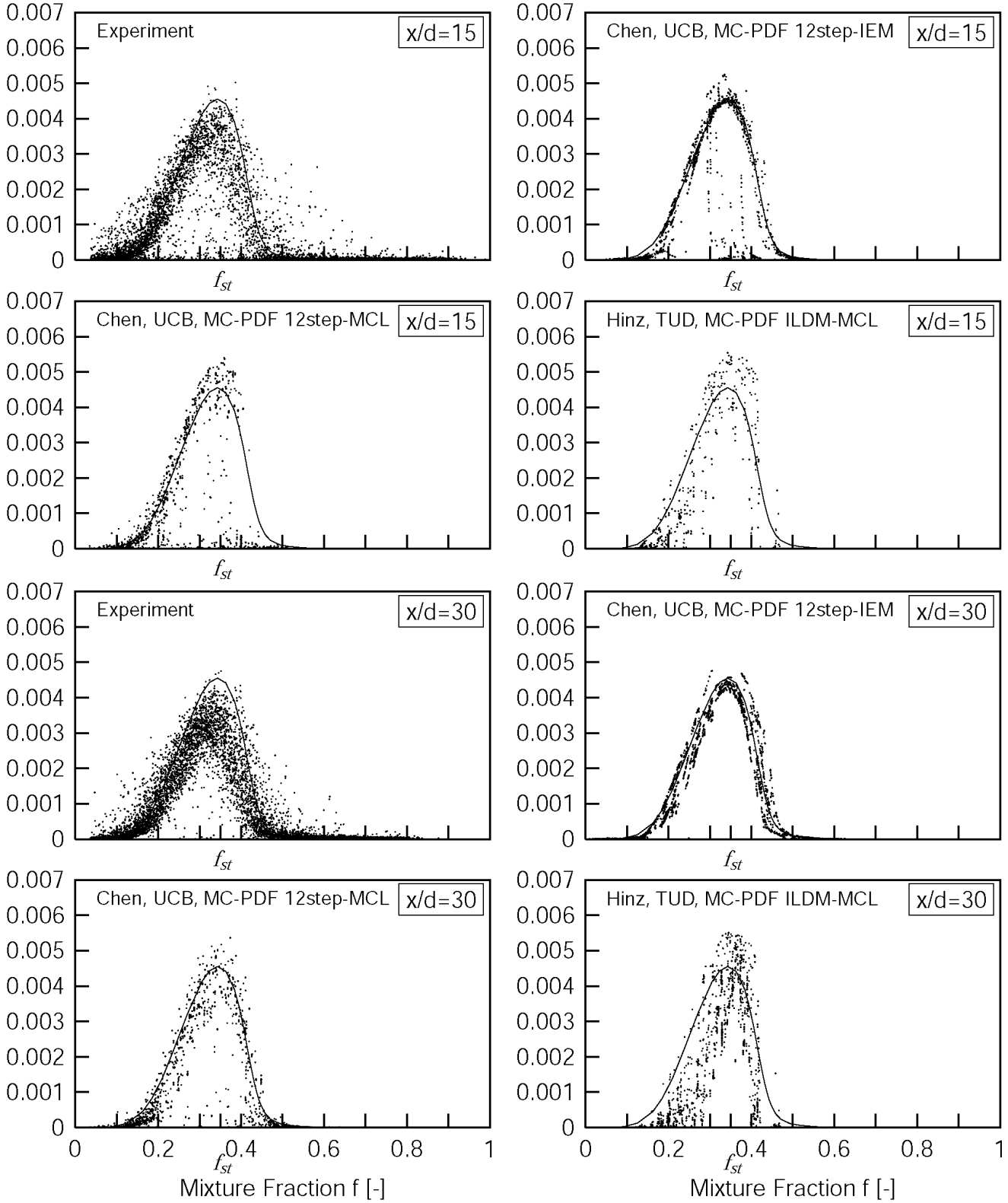

Comparison Plots: Flame F

Piloted Flame F: Axial Profiles of Axial Velocity, Mixture Fraction, and Temperature

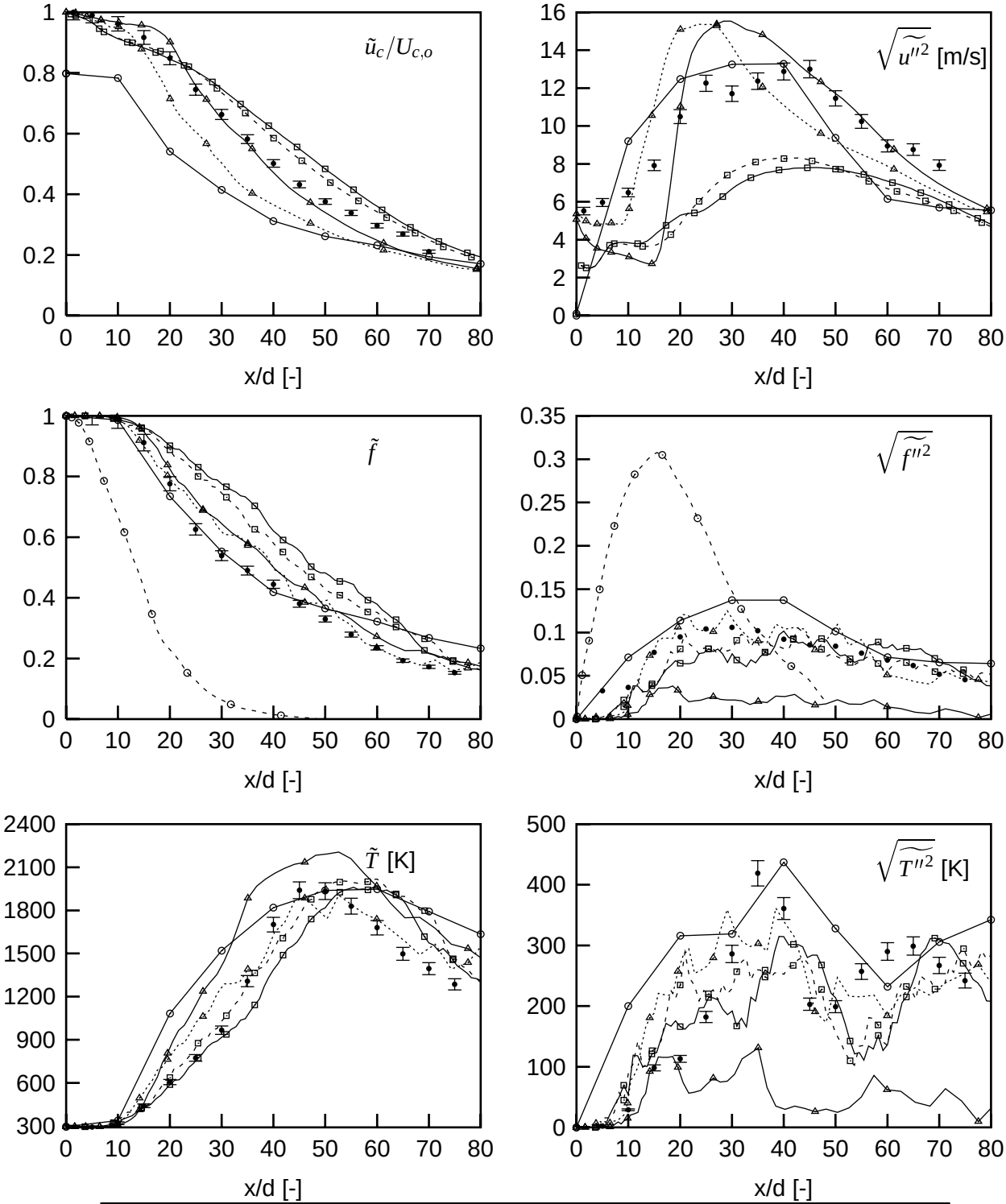

Piloted Flame F: Axial Profiles of Species Mass Fractions

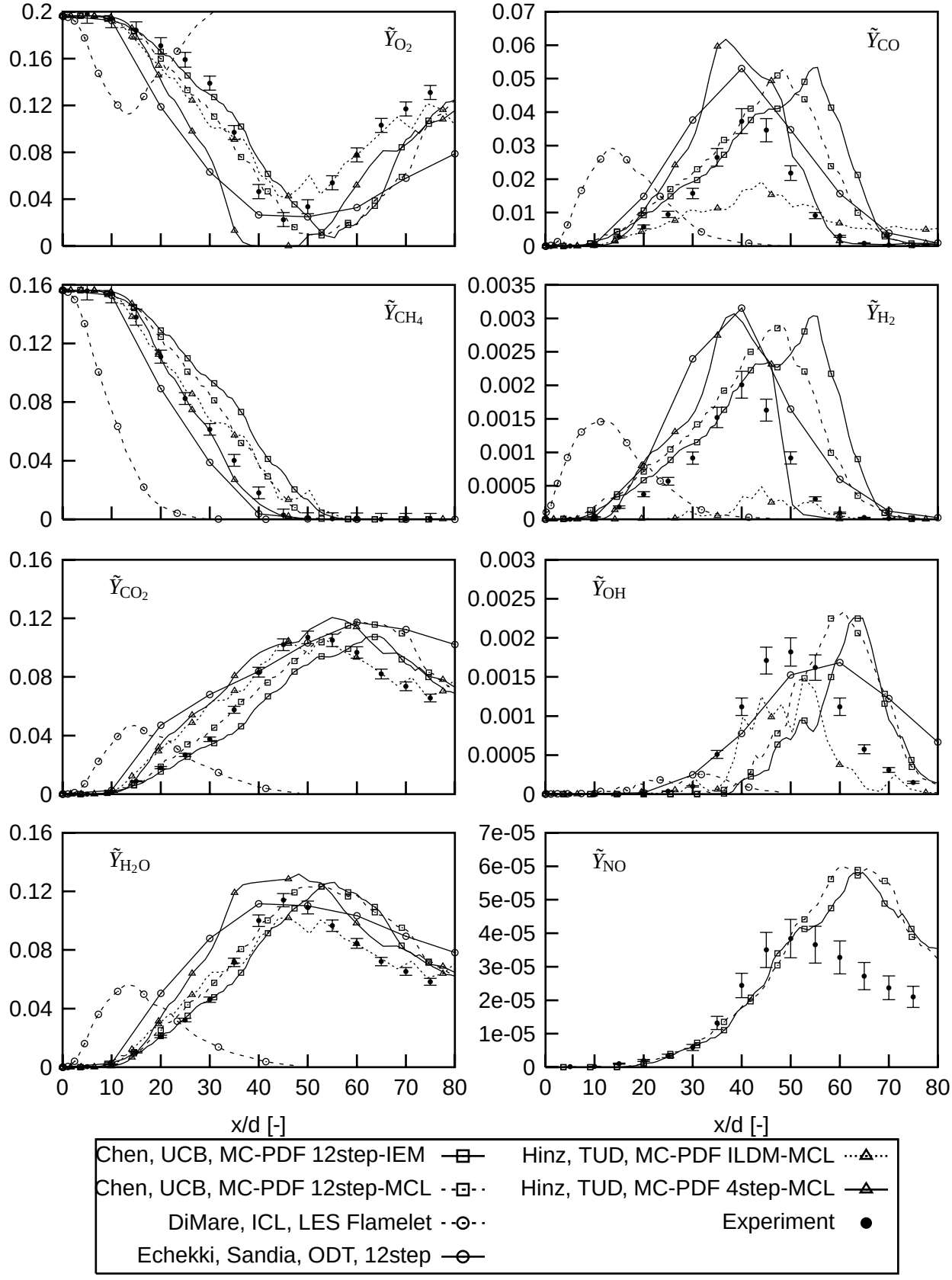

Piloted Flame F: Radial Profiles of Velocity and Shear Stress at x/d=15, 45

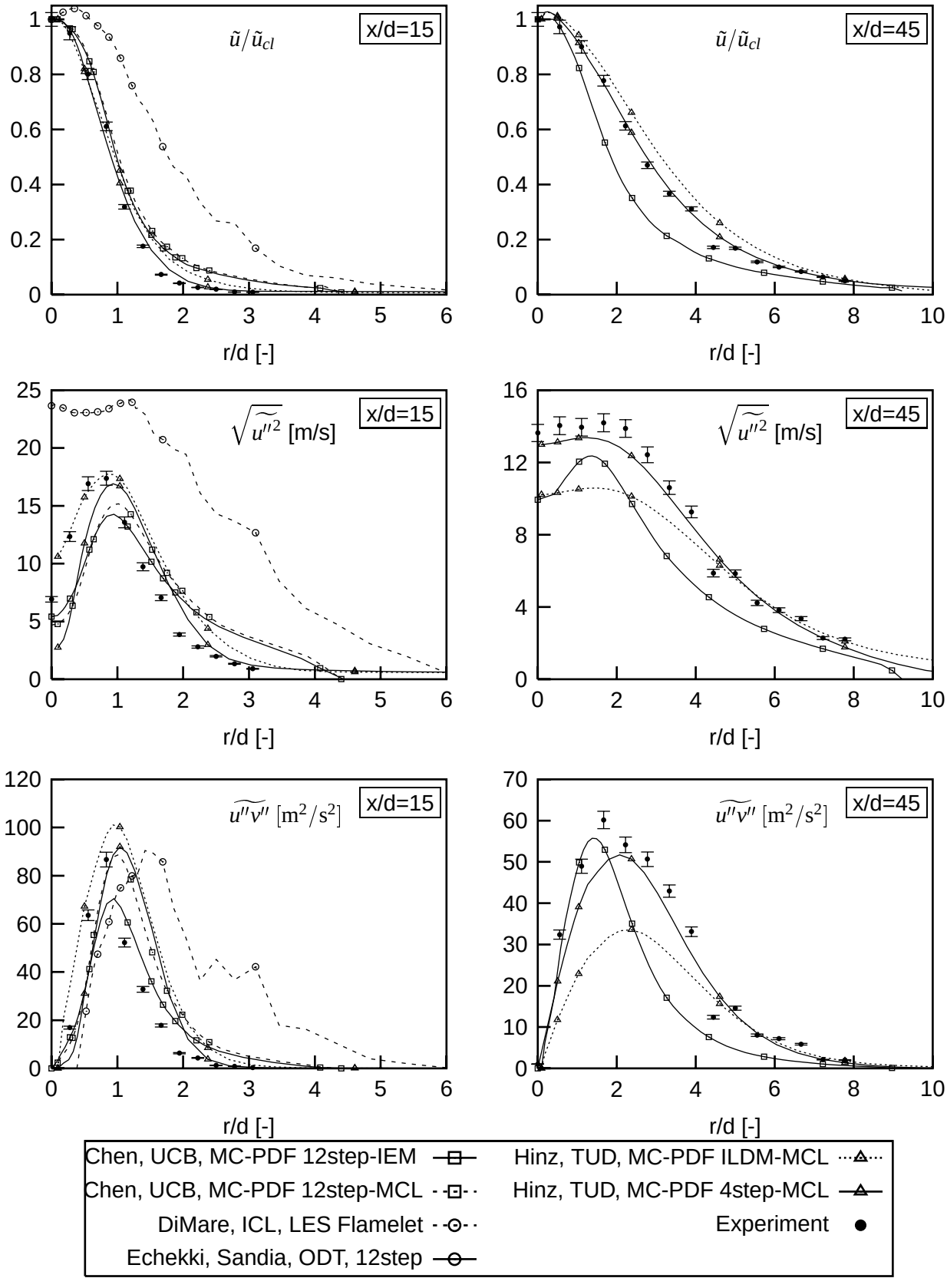

Piloted Flame F: Radial Profiles of Scalars at x/d=15

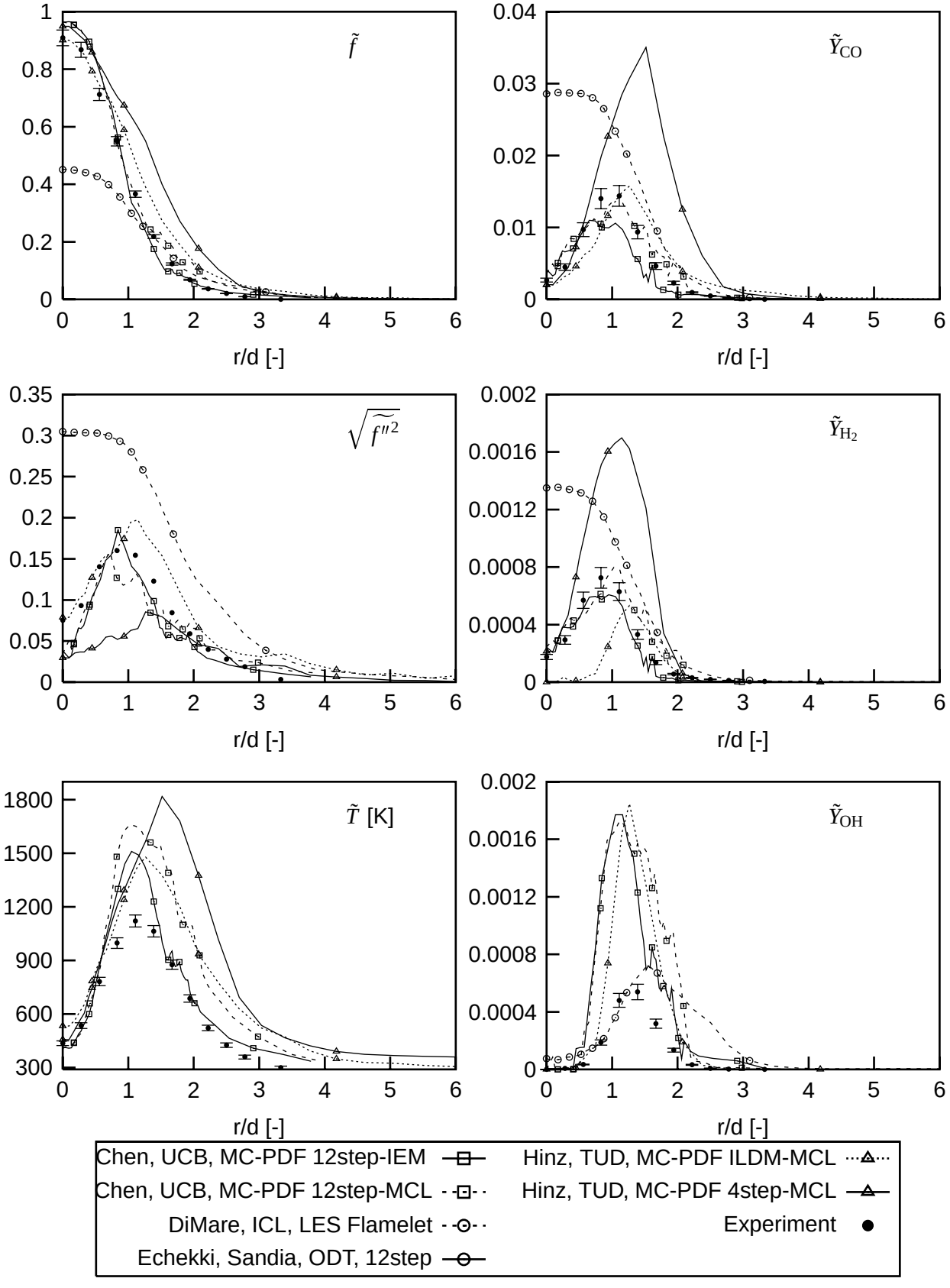

Piloted Flame F: Radial Profiles of Scalars at x/d=30

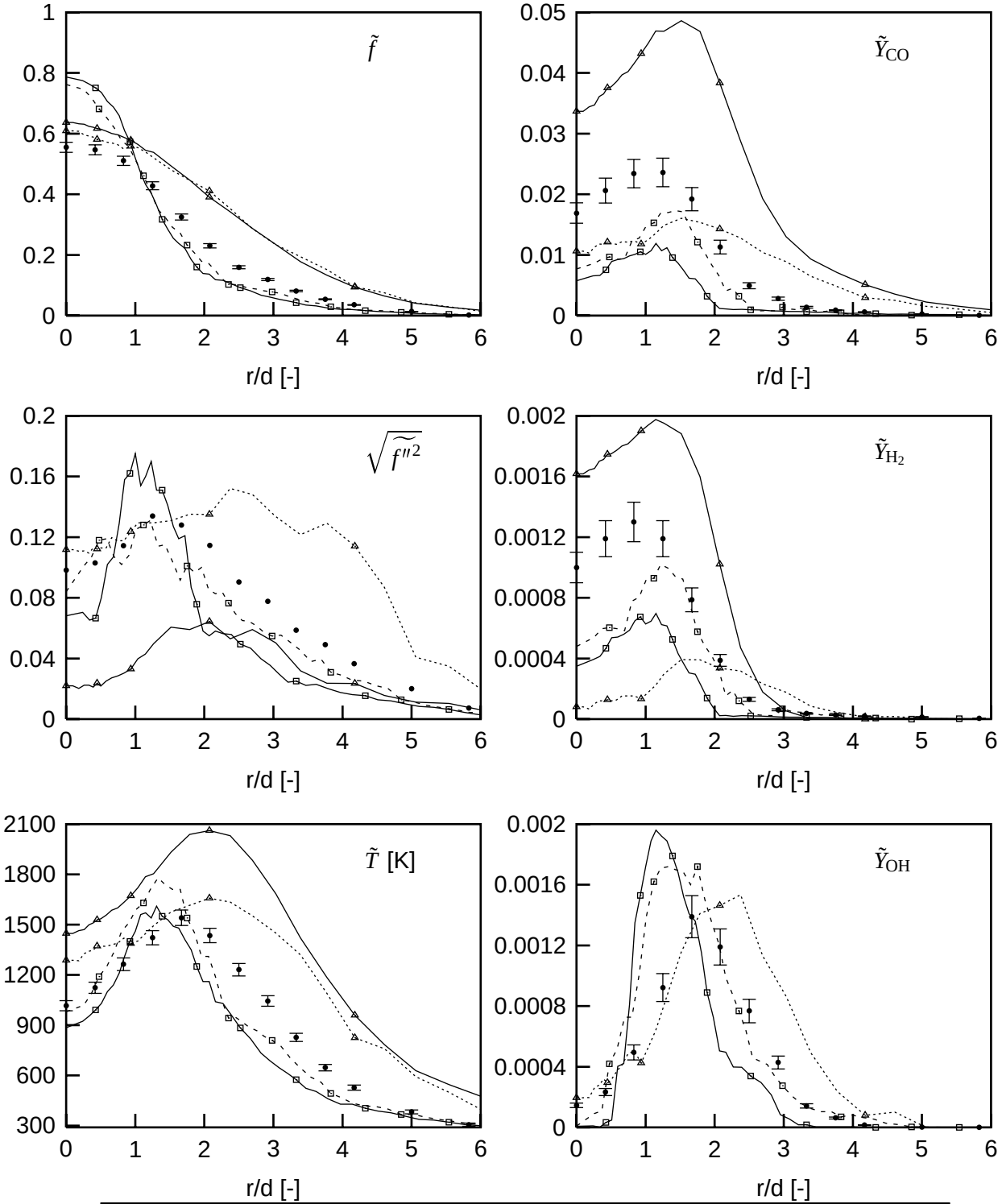

Piloted Flame F: Radial Profiles of Scalars at x/d=45

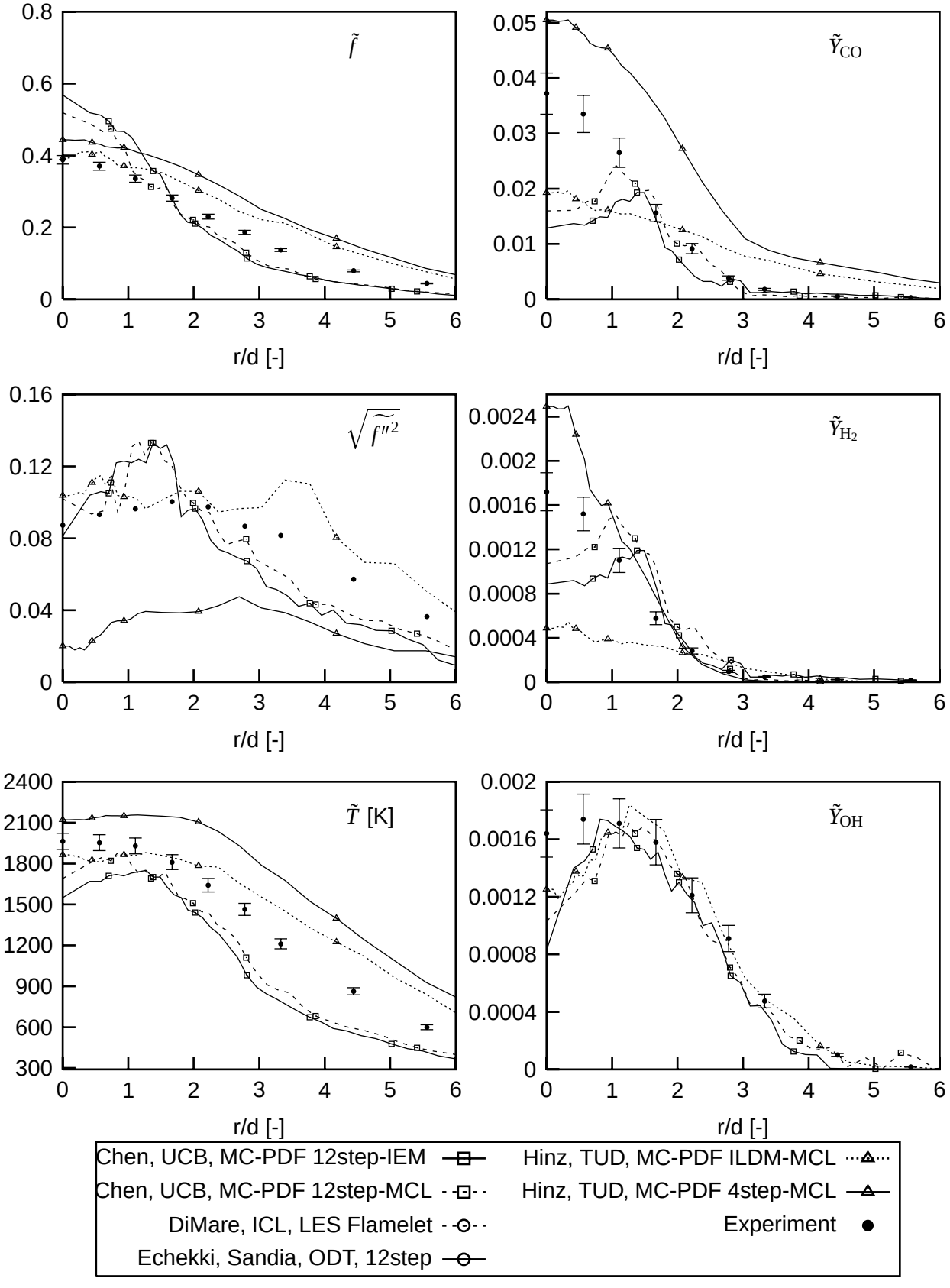

Piloted Flame F: Conditional Means at x/d=15

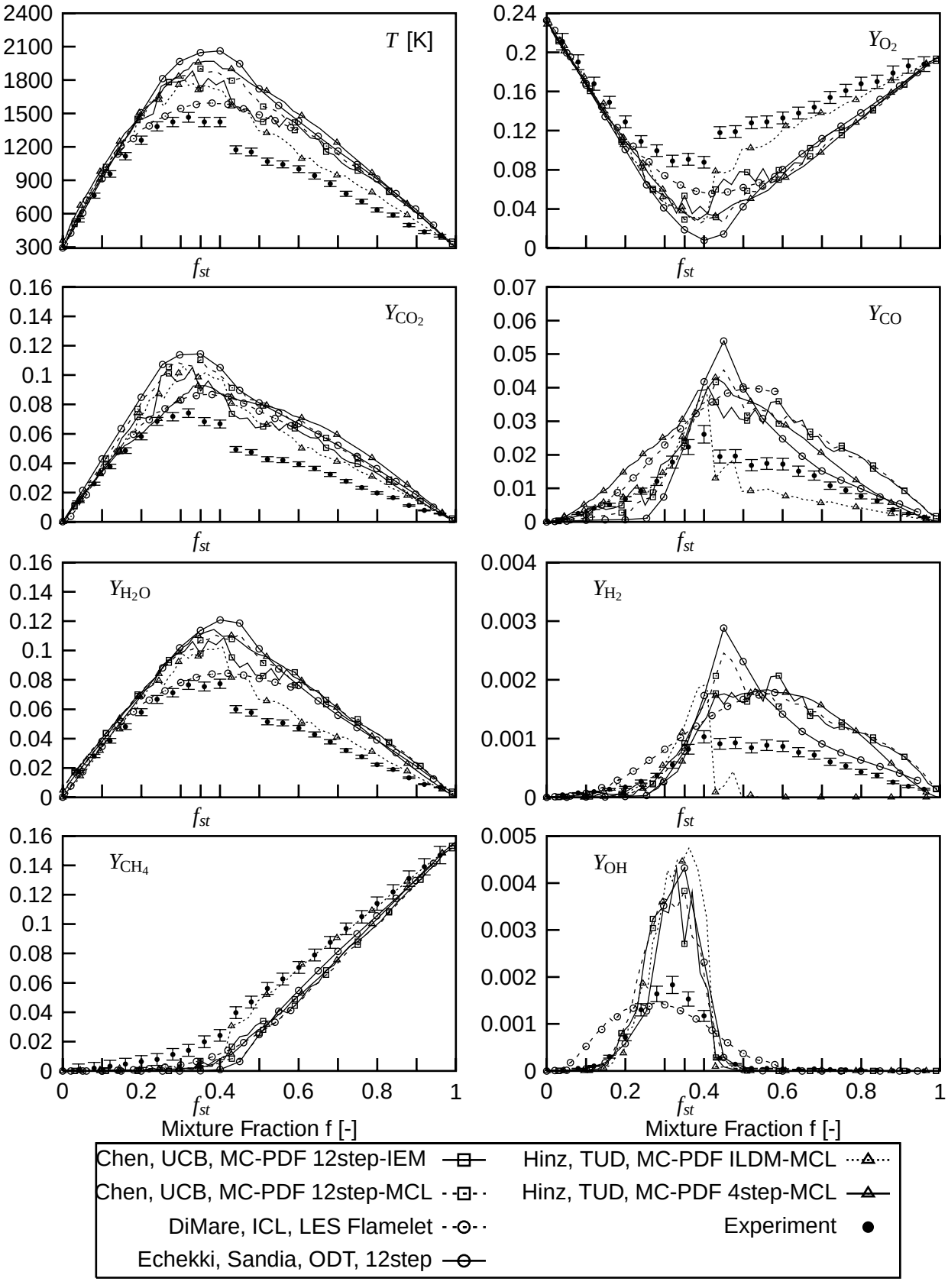

Piloted Flame F: Conditional Means at x/d=30

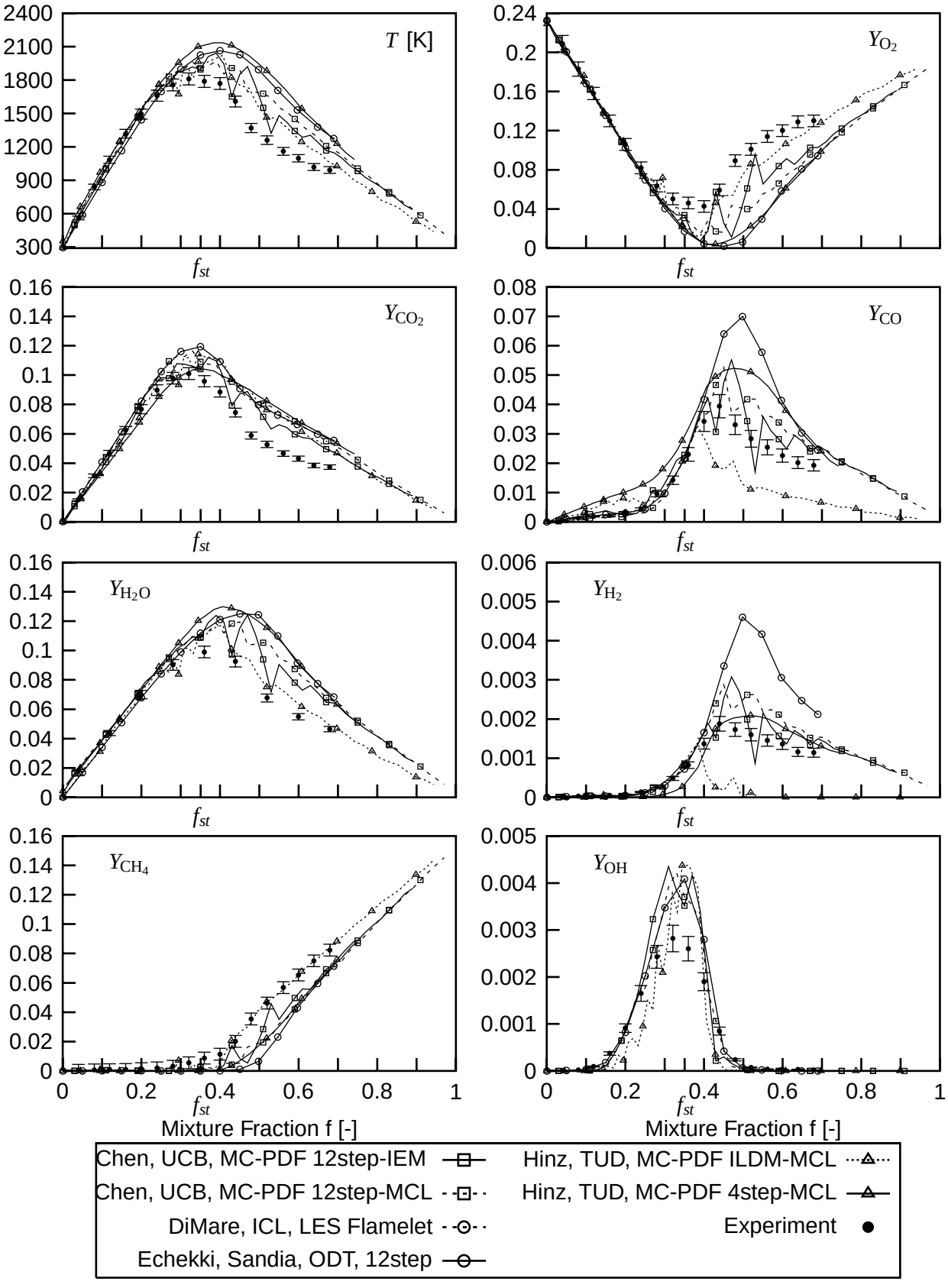

Piloted Flame F: Conditional Means at x/d=45

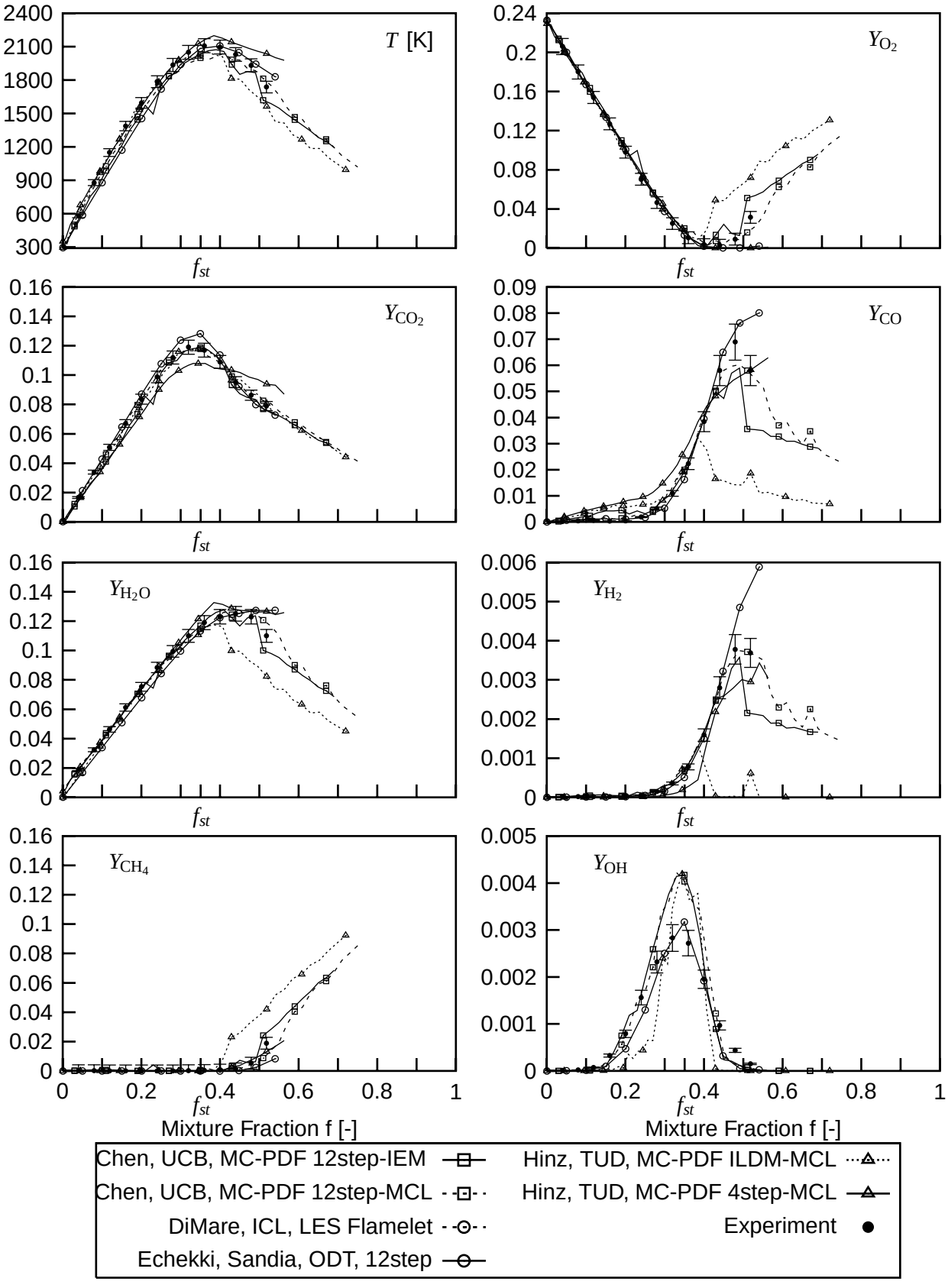

Piloted Flame F: Scatter Plots of Temperature [K] at x d=15

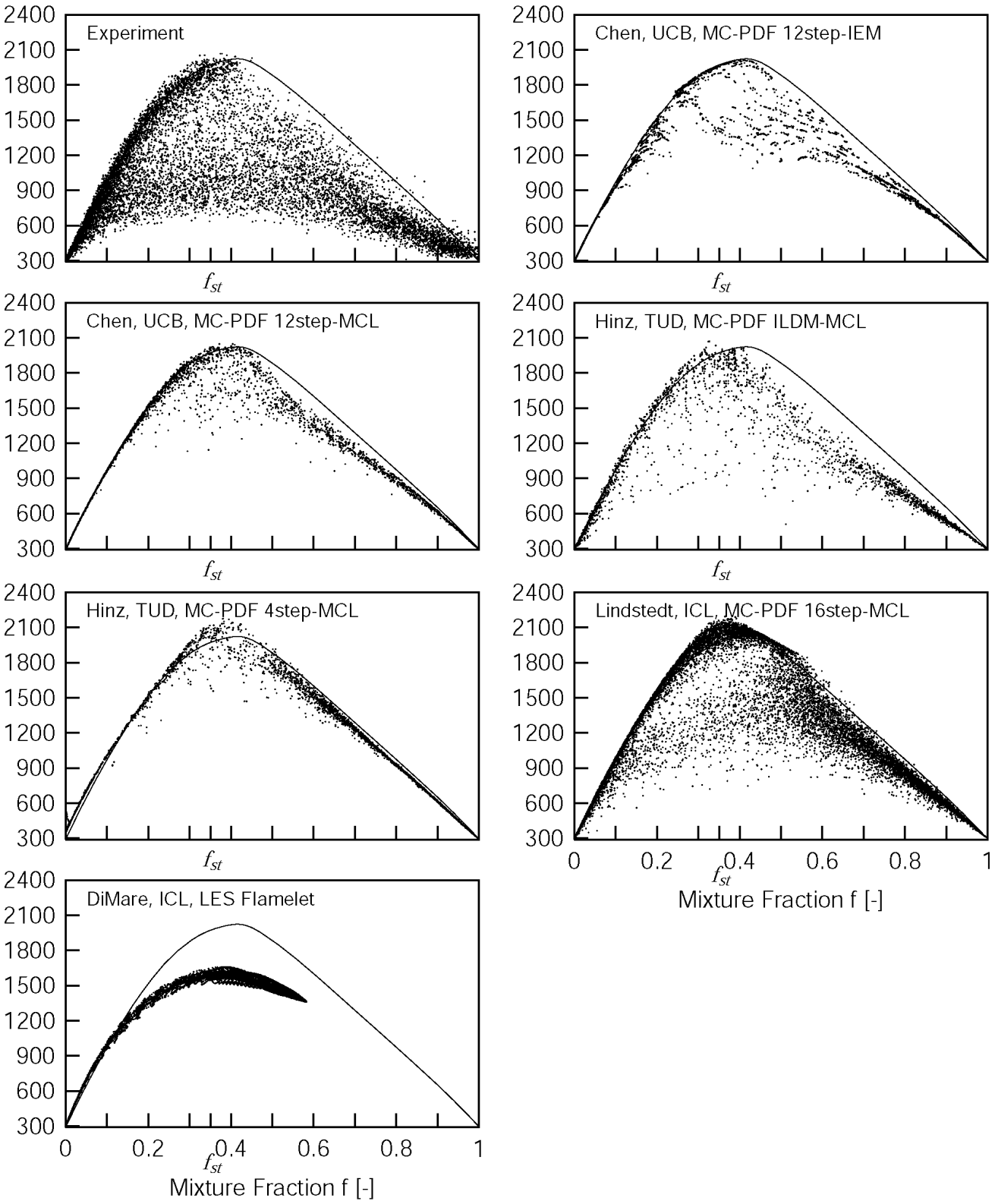

Piloted Flame F: Scatter Plots of Temperature [K] at x d=30

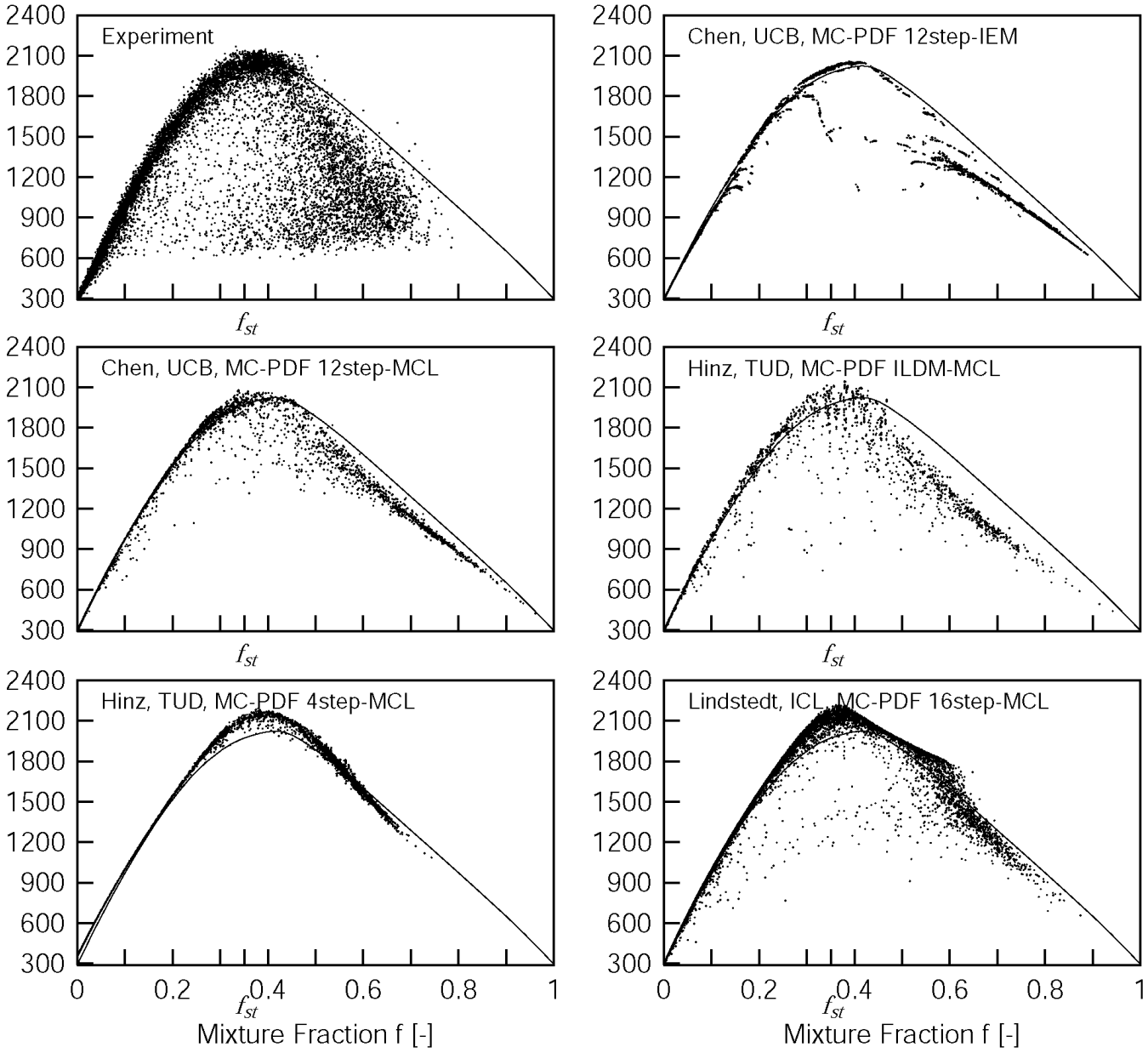

Piloted Flame F: Scatter Plots of Mass Fraction of CO_2 at x d=15

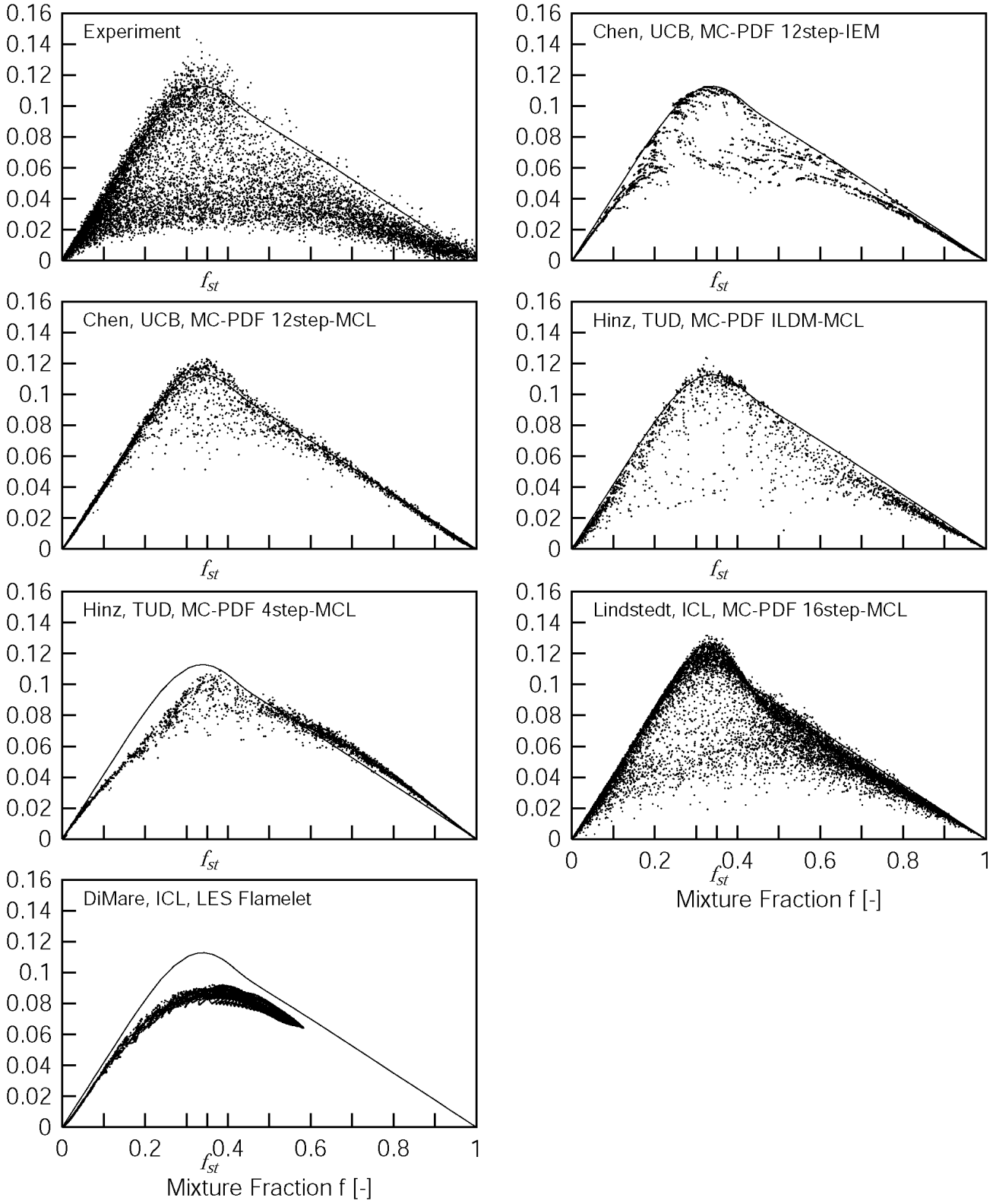

Piloted Flame F: Scatter Plots of Mass Fraction of CO_2 at x d=30

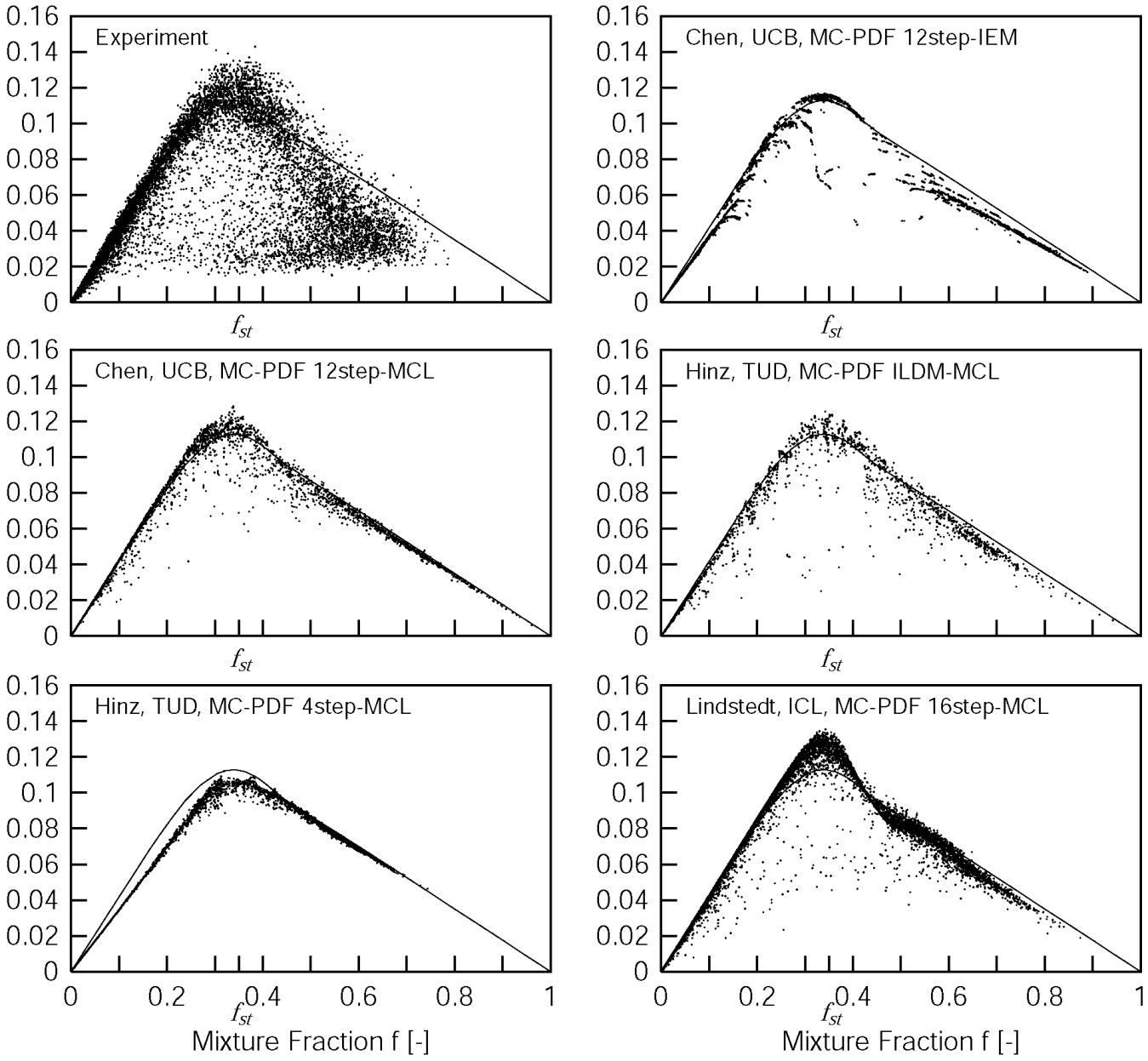

Piloted Flame F: Scatter Plots of Mass Fraction of CO at x d=15

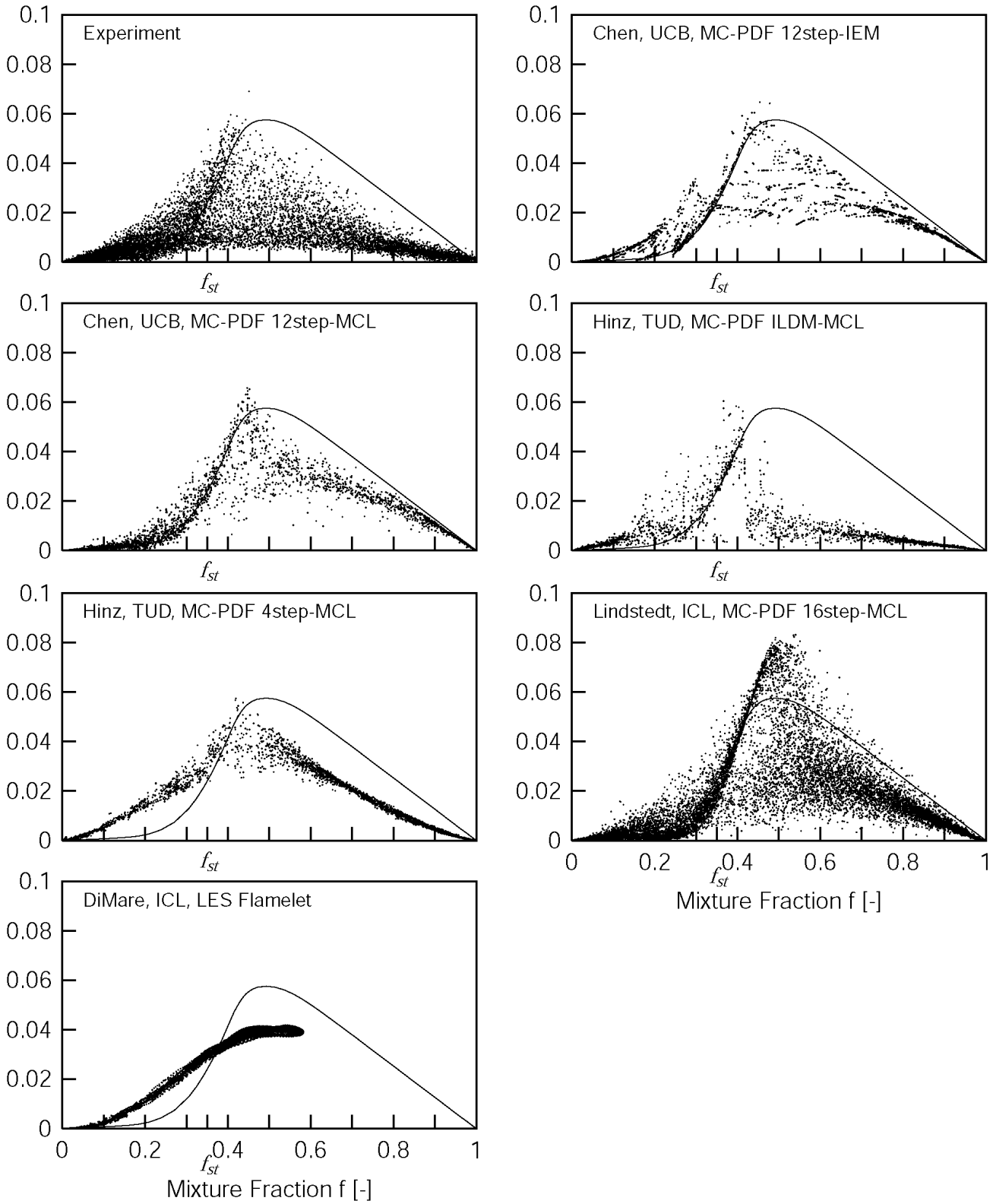

Piloted Flame F: Scatter Plots of Mass Fraction of CO at x d=30

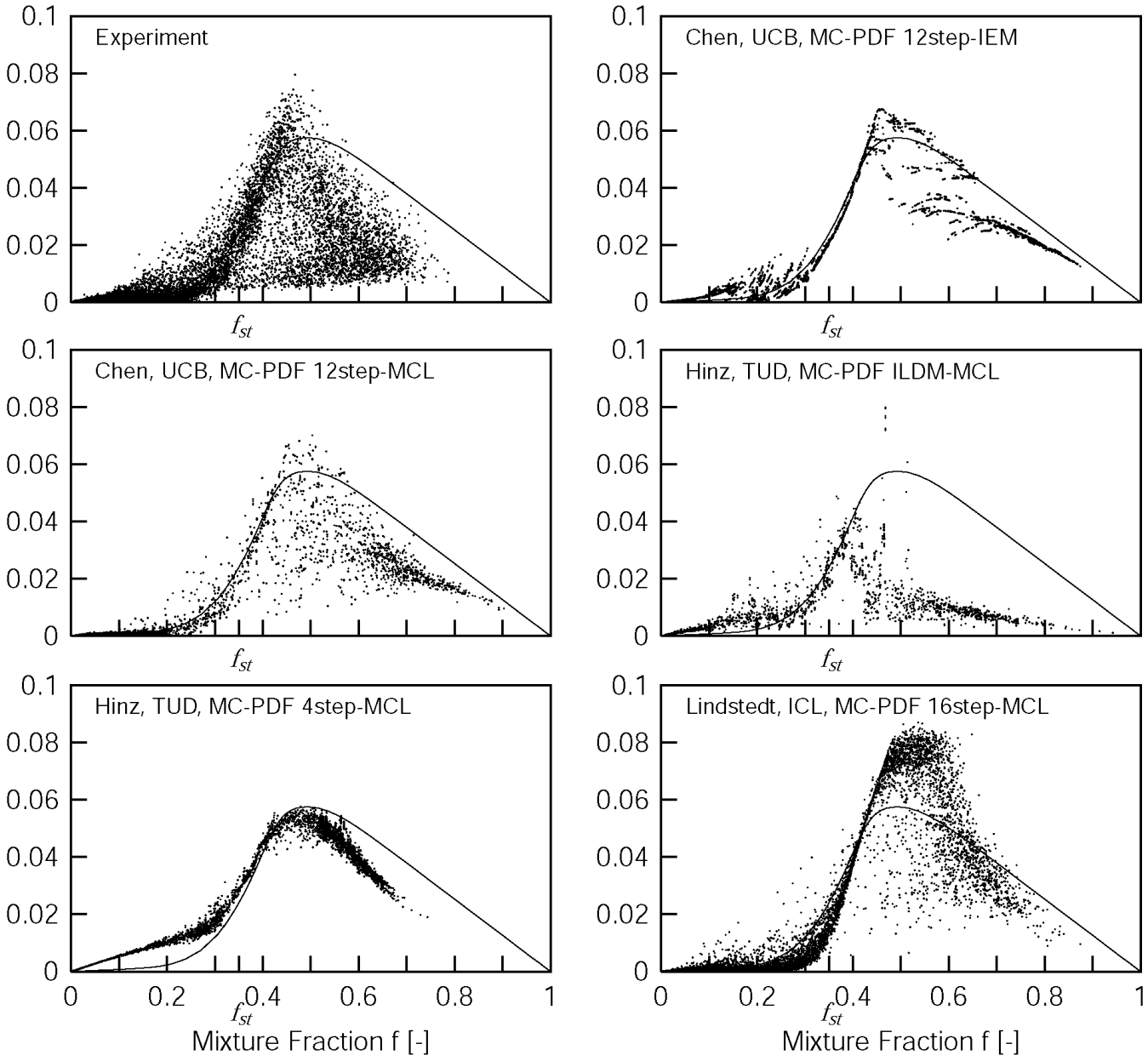

Piloted Flame F: Scatter Plots of Mass Fraction of H_2O at x d=15

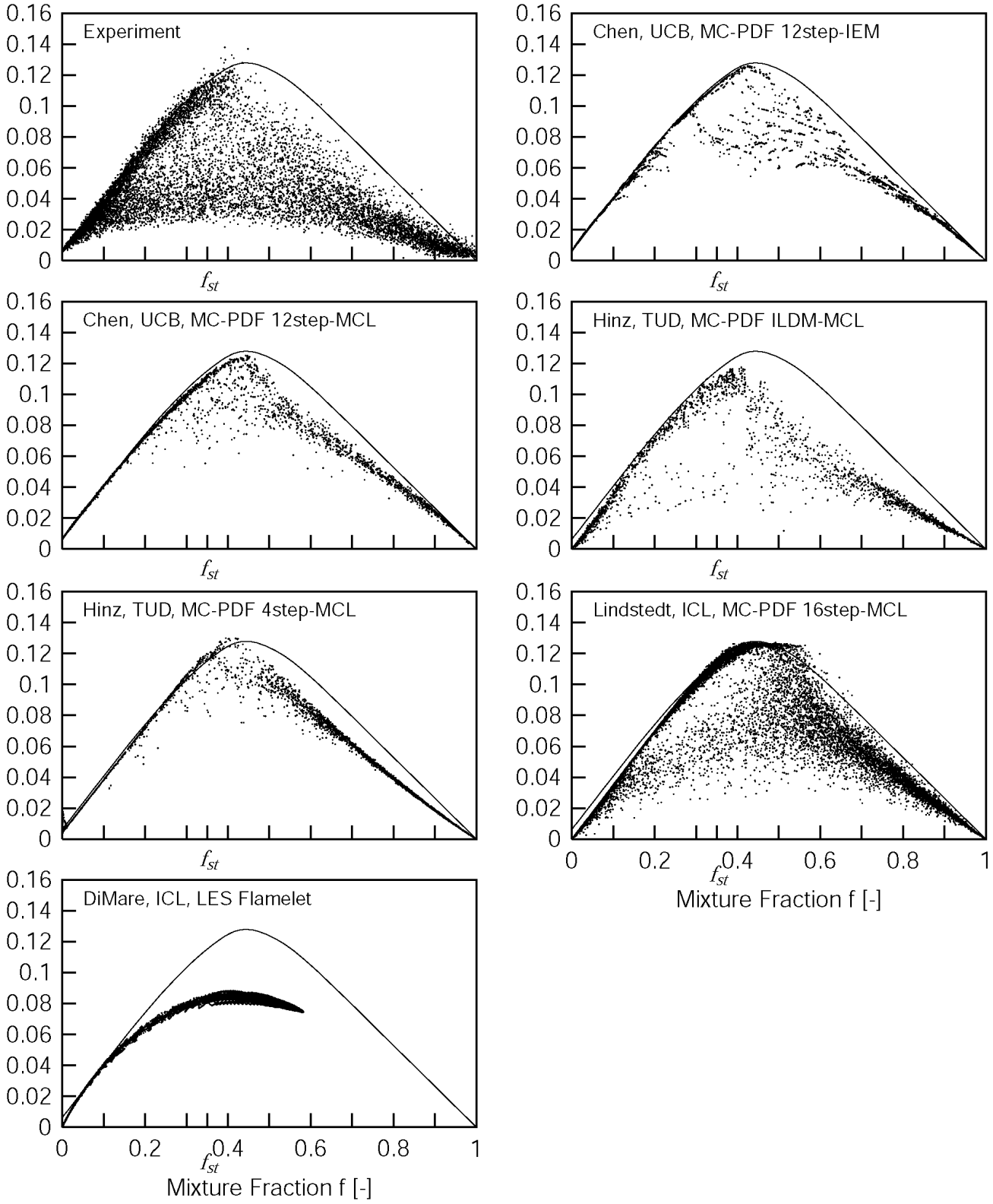

Piloted Flame F: Scatter Plots of Mass Fraction of H_2O at x d=30

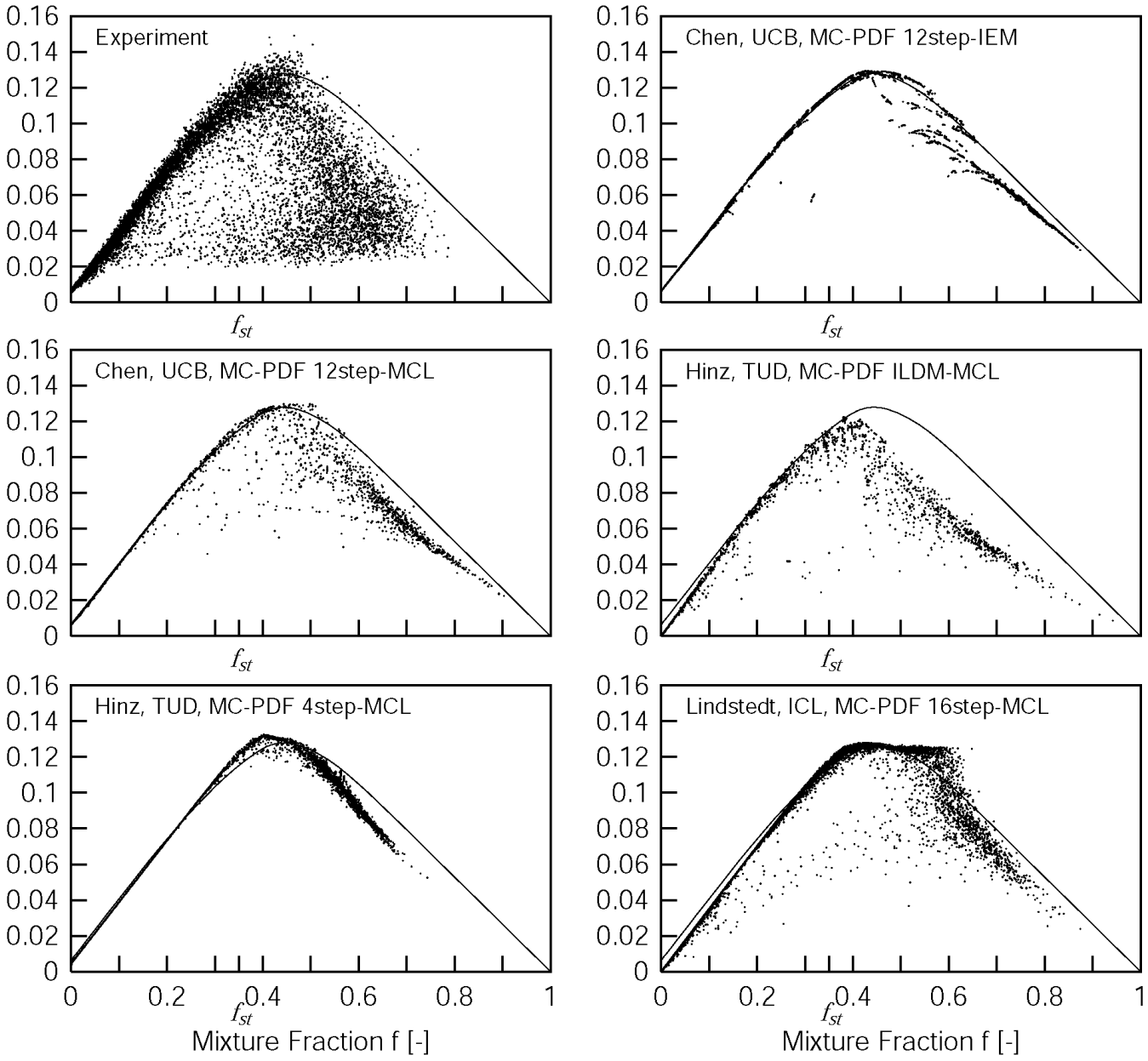

Piloted Flame F: Scatter Plots of Mass Fraction of H_2 at x d=15

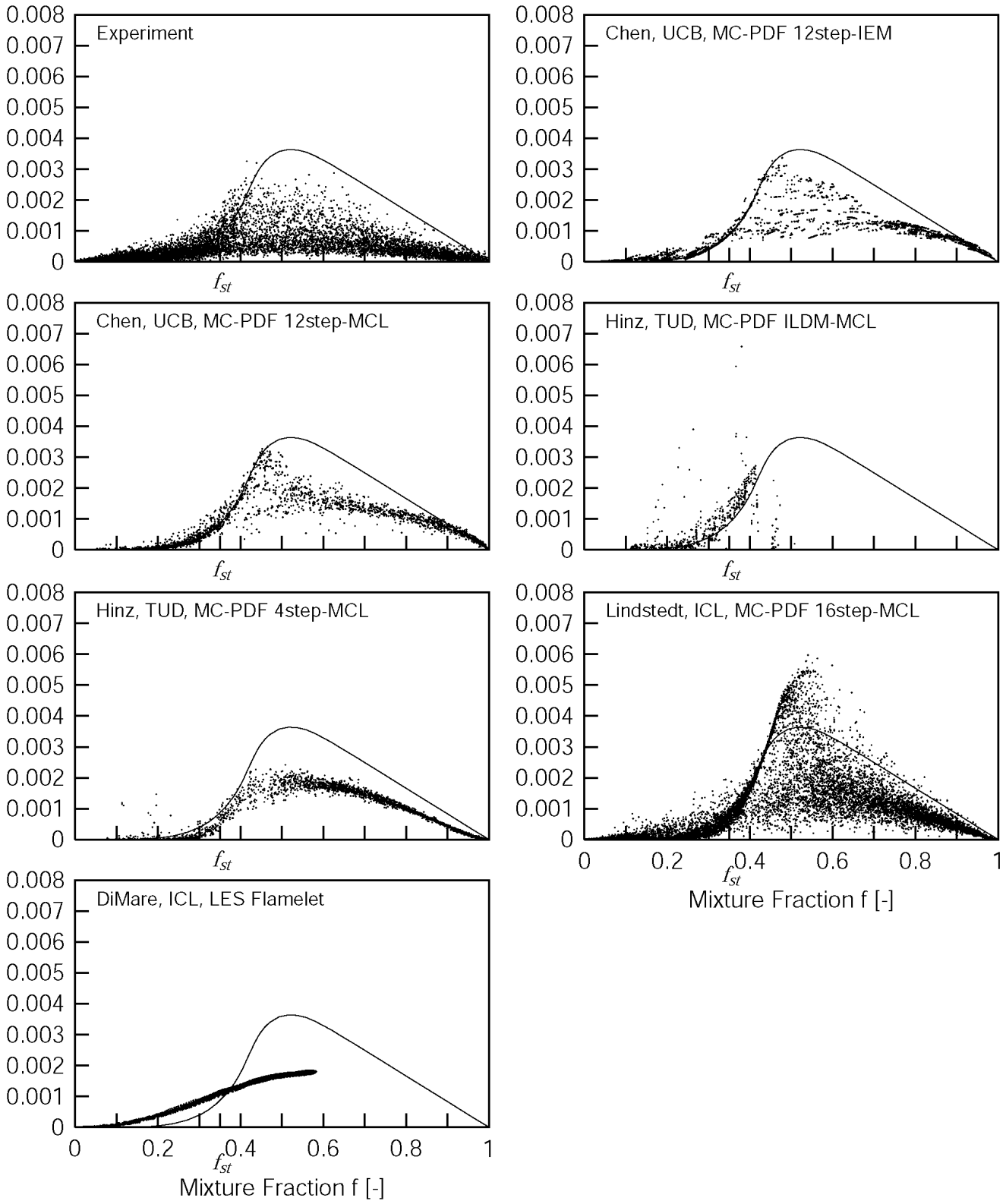

Piloted Flame F: Scatter Plots of Mass Fraction of H_2 at x d=30

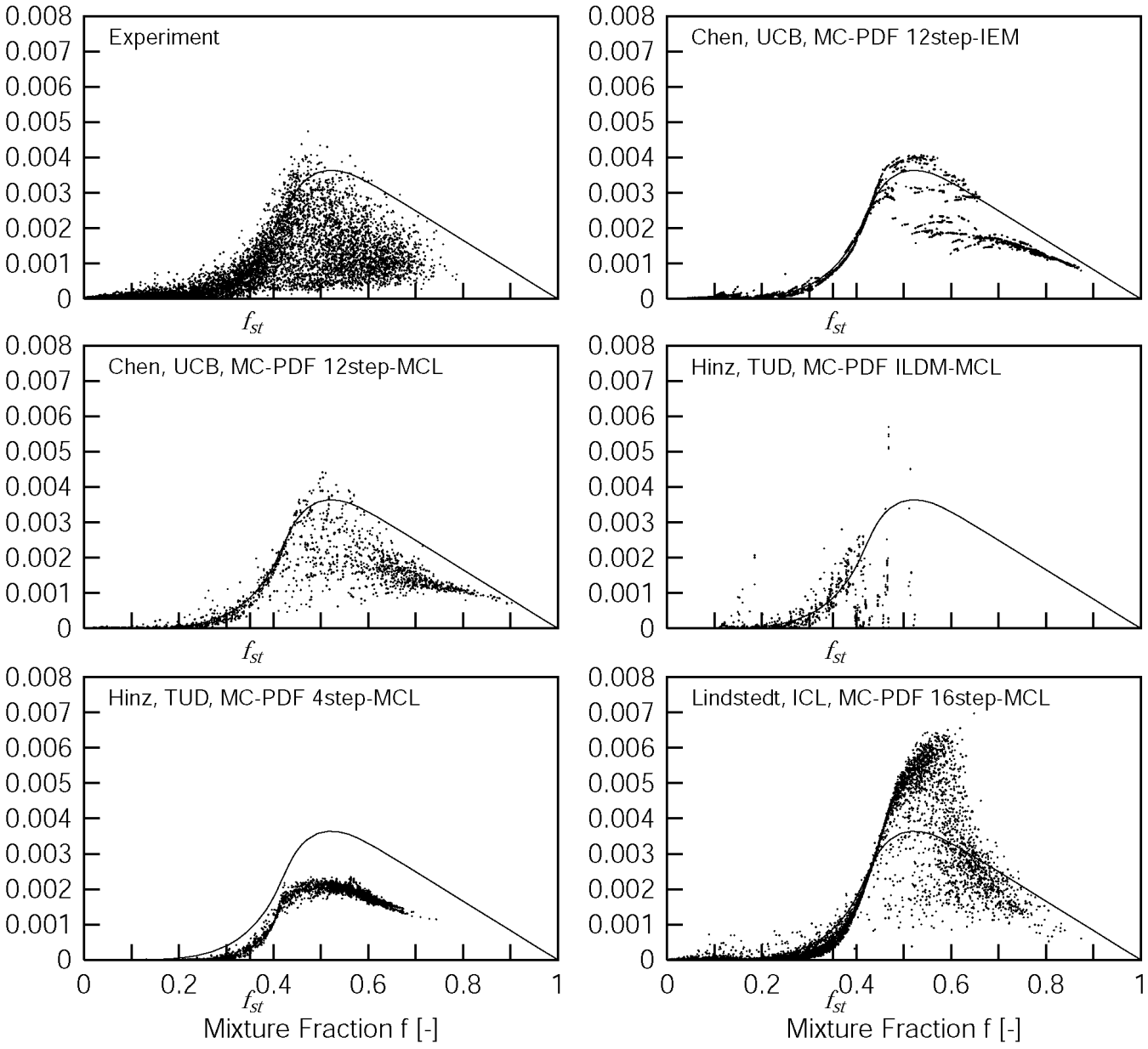

Piloted Flame F: Scatter Plots of Mass Fraction of OH at x d=15

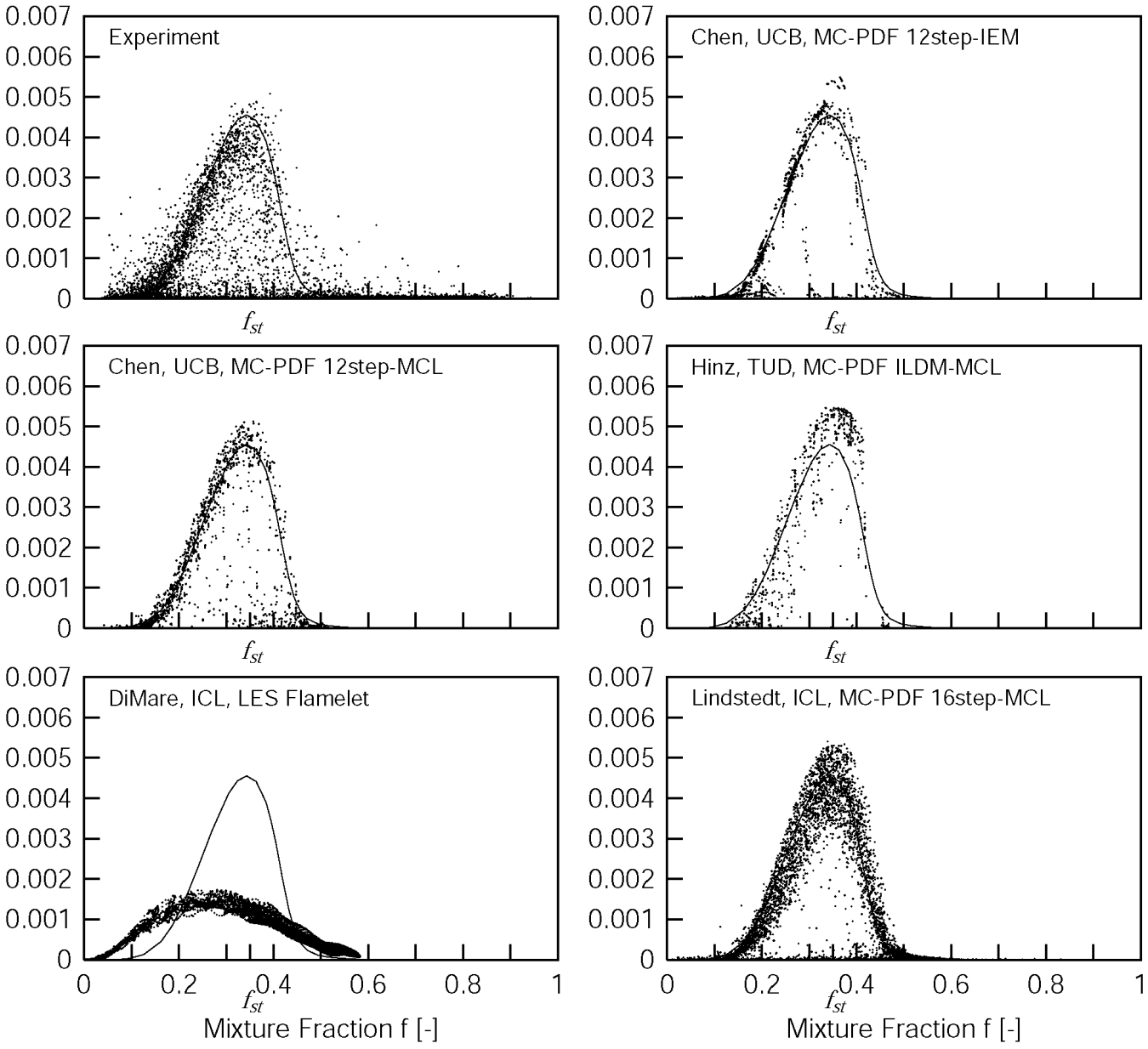

Piloted Flame F: Scatter Plots of Mass Fraction of OH at x d=30

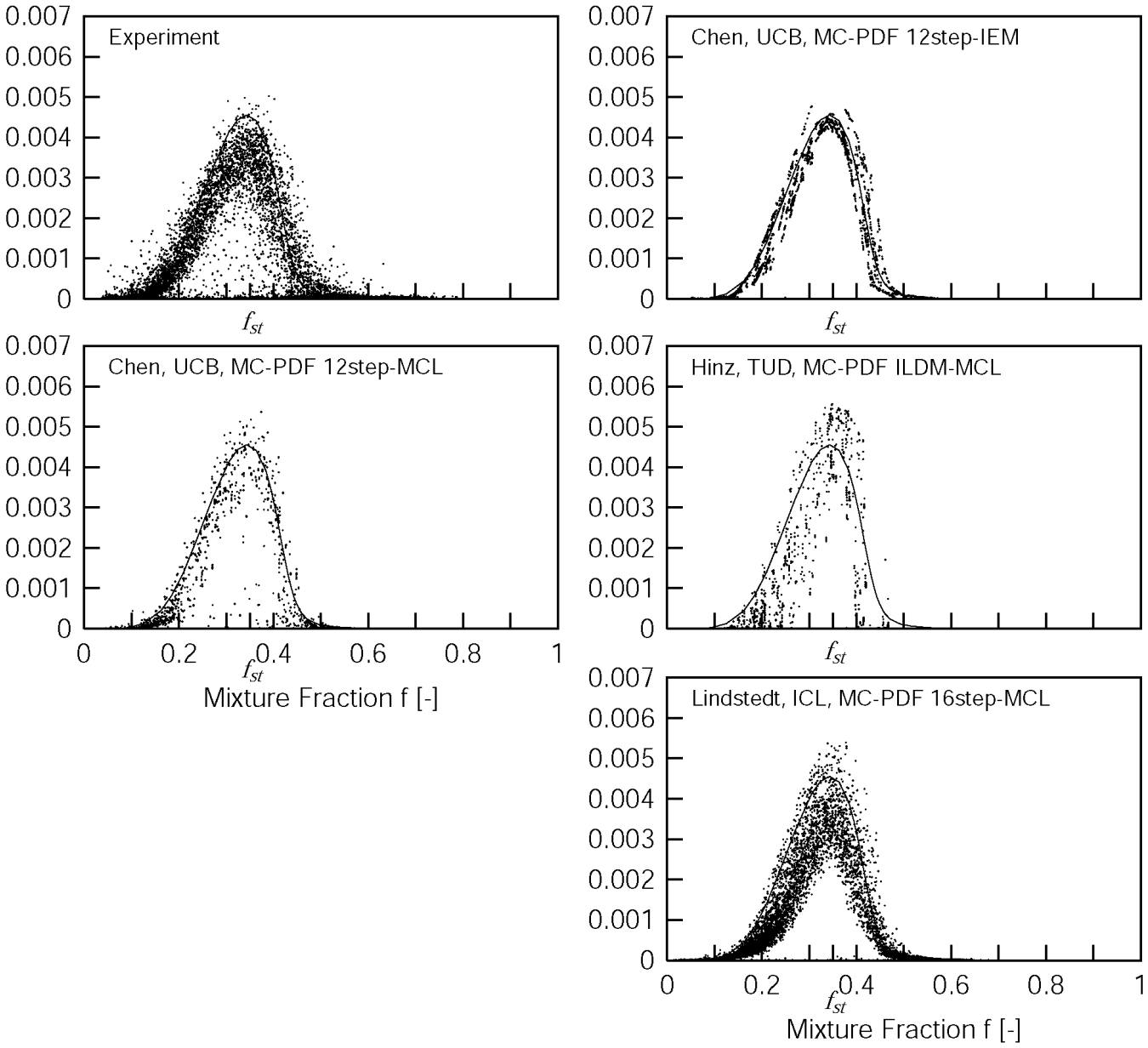

Comparison Plots: Conditional PDF's

(Flames D, E, F)

Piloted Flames D, E, F: Conditional PDF's of Temperature [K] at x/d=15
Mixture Fraction Interval: 0.30 < f < 0.40

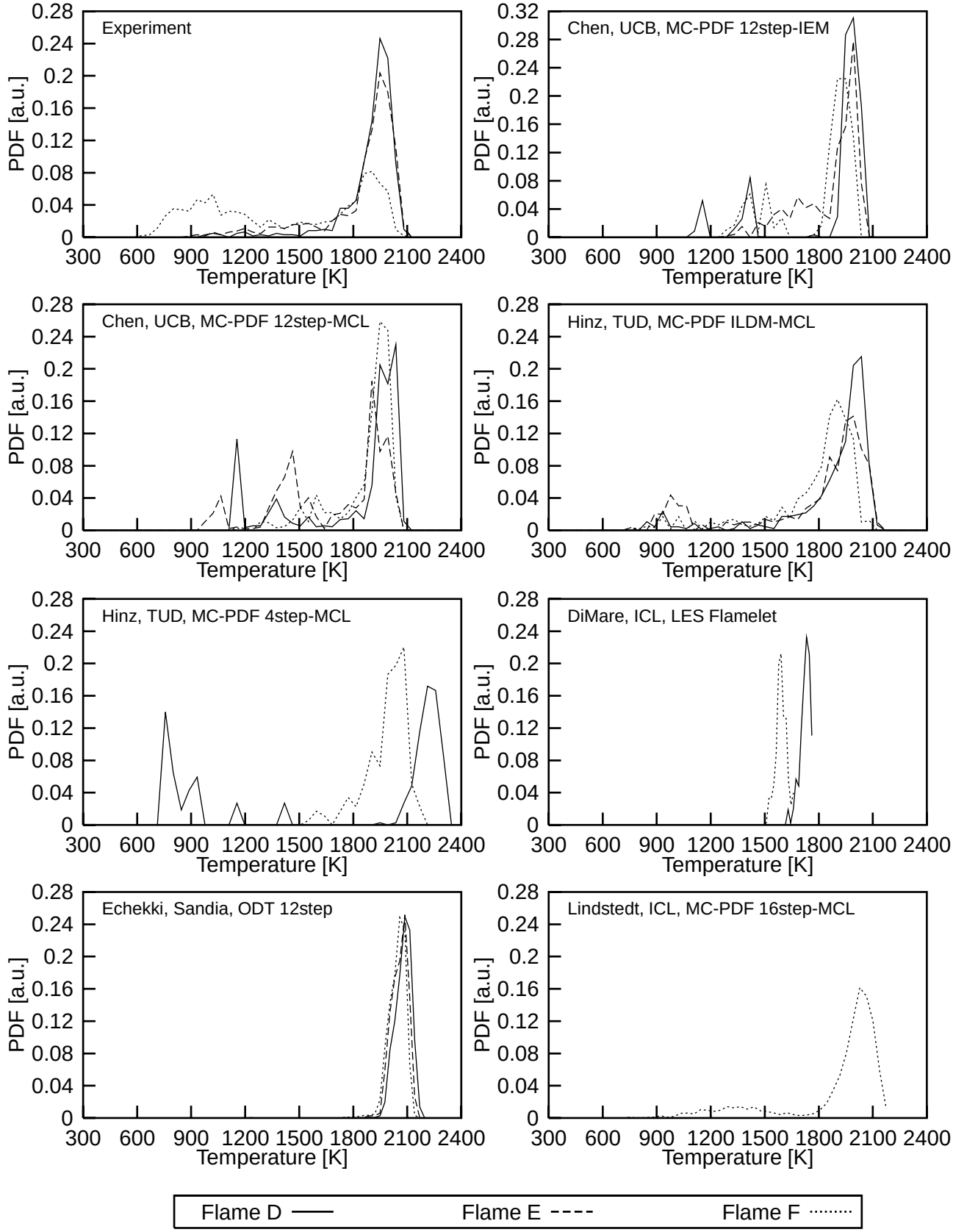

Piloted Flames D, E, F: Conditional PDF's of Temperature [K] at x/d=30
Mixture Fraction Interval: 0.30 < f < 0.40

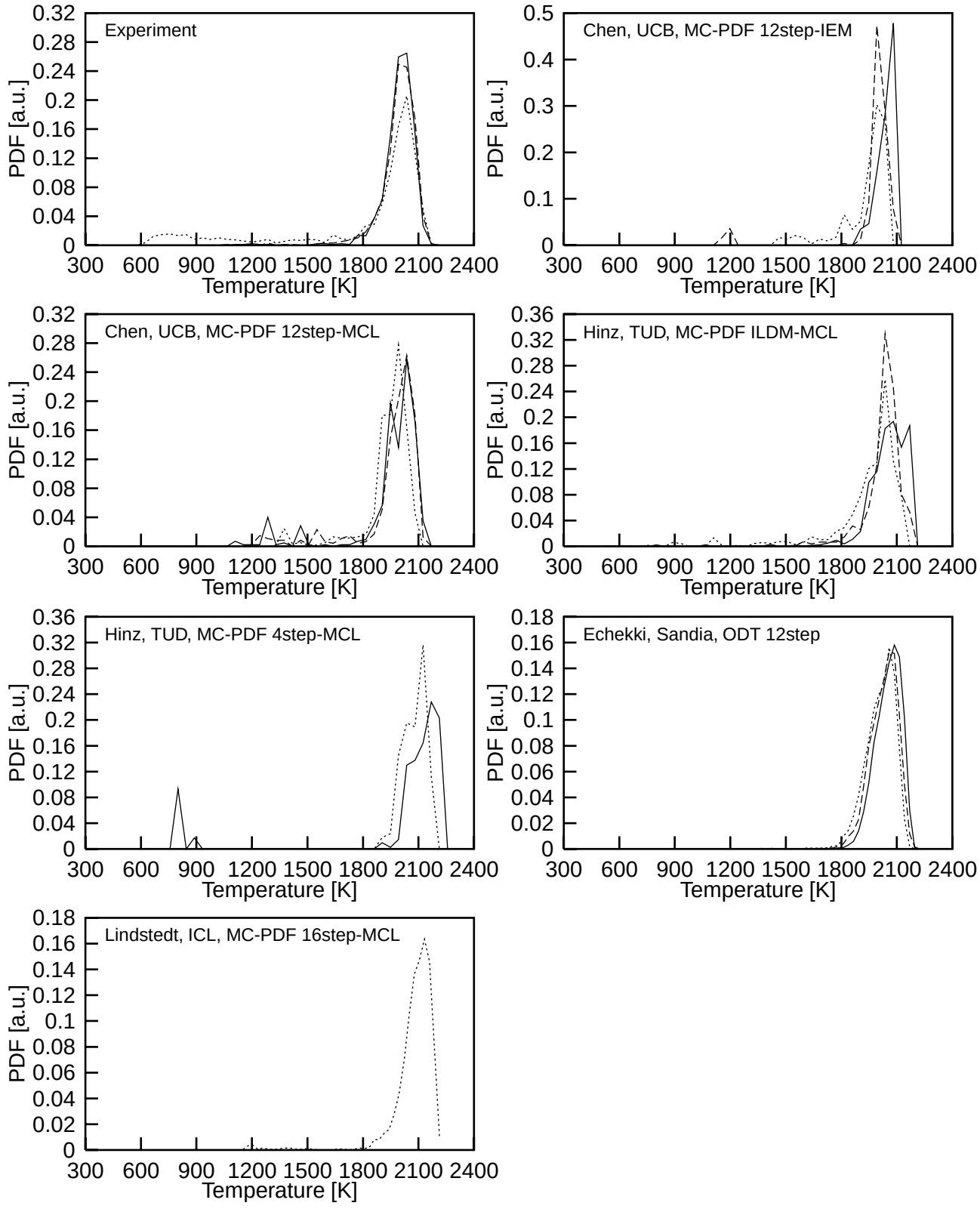

Piloted Flames D, E, F: Conditional PDF's of Mass Fraction of H_2O at x/d=15
Mixture Fraction Interval: $0.35 < f < 0.45$

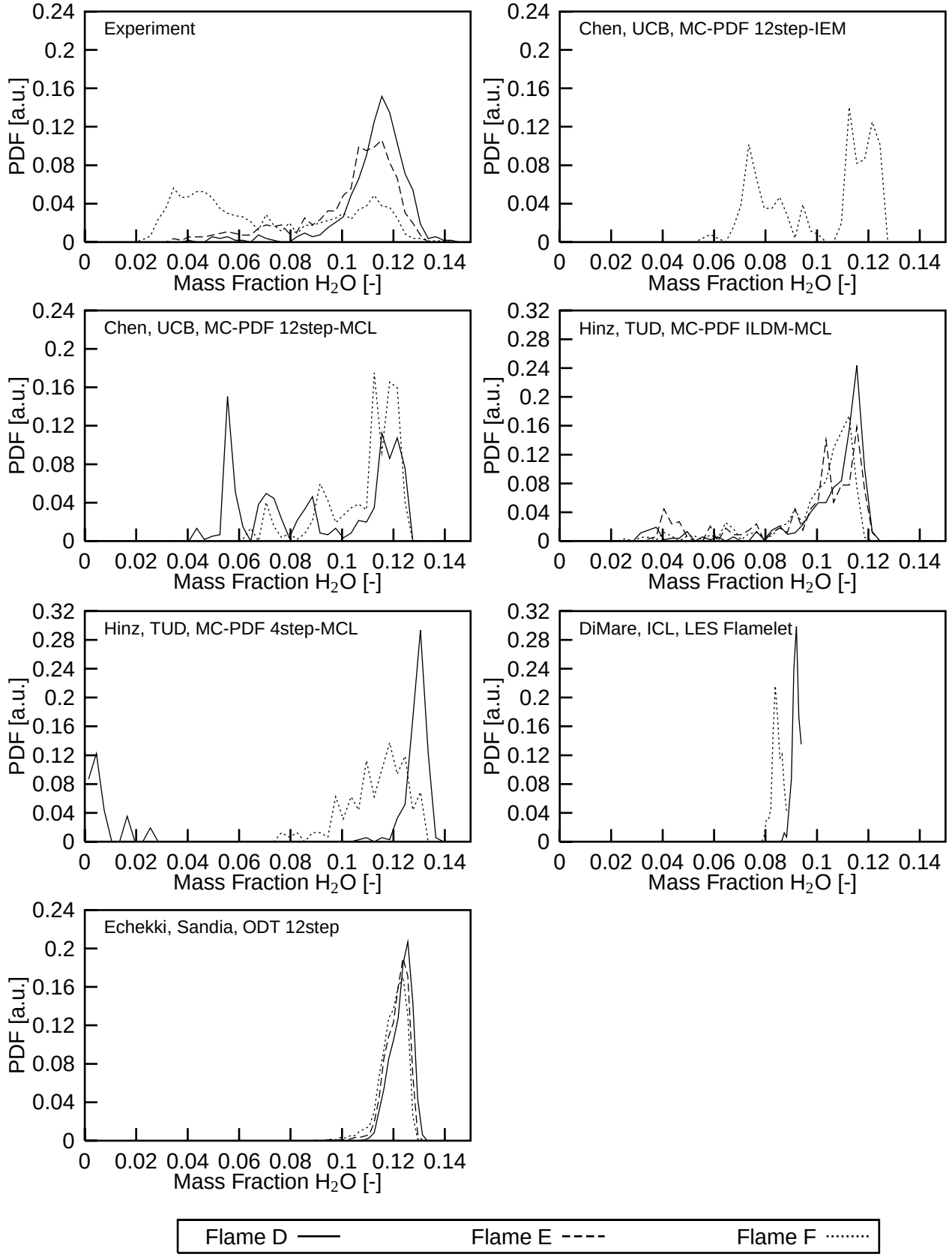

Piloted Flames D, E, F: Conditional PDF's of Mass Fraction of H_2O at x/d=30
Mixture Fraction Interval: $0.35 < f < 0.45$

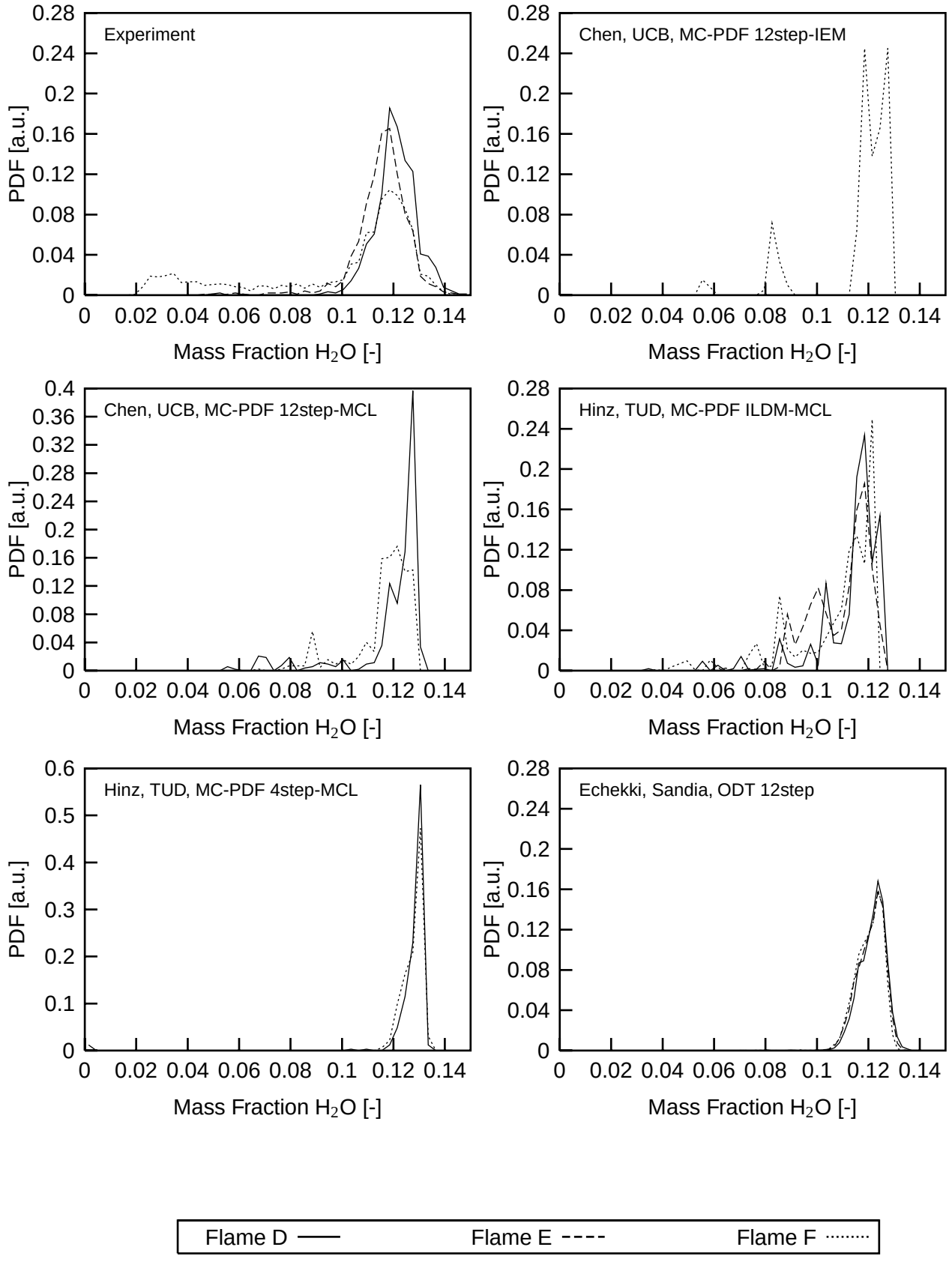

Piloted Flames D, E, F: Conditional PDF's of Mass Fraction of CO_2 at x/d=15
Mixture Fraction Interval: $0.30 < f < 0.40$

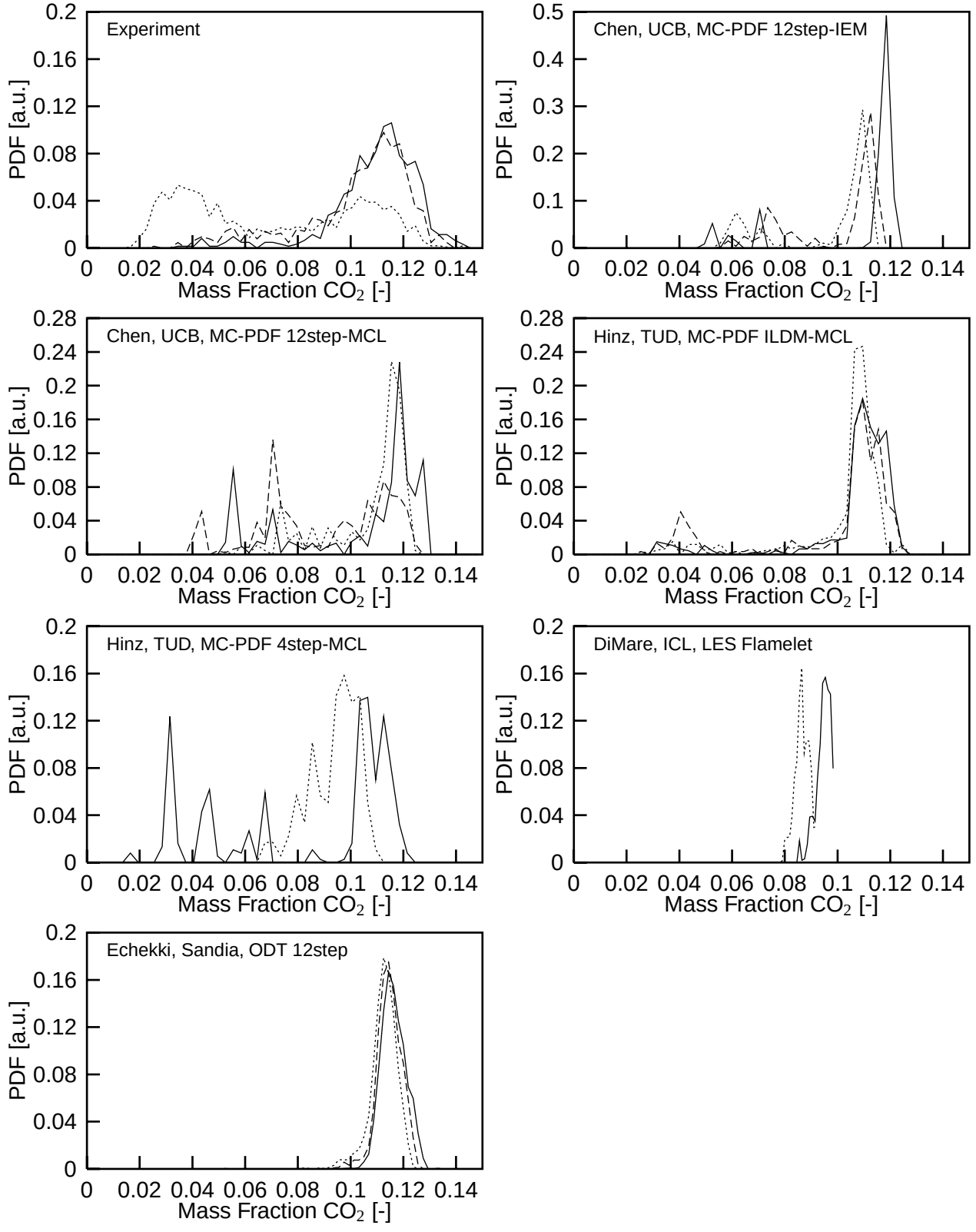

Piloted Flames D, E, F: Conditional PDF's of Mass Fraction of CO_2 at x/d=30
Mixture Fraction Interval: $0.30 < f < 0.40$

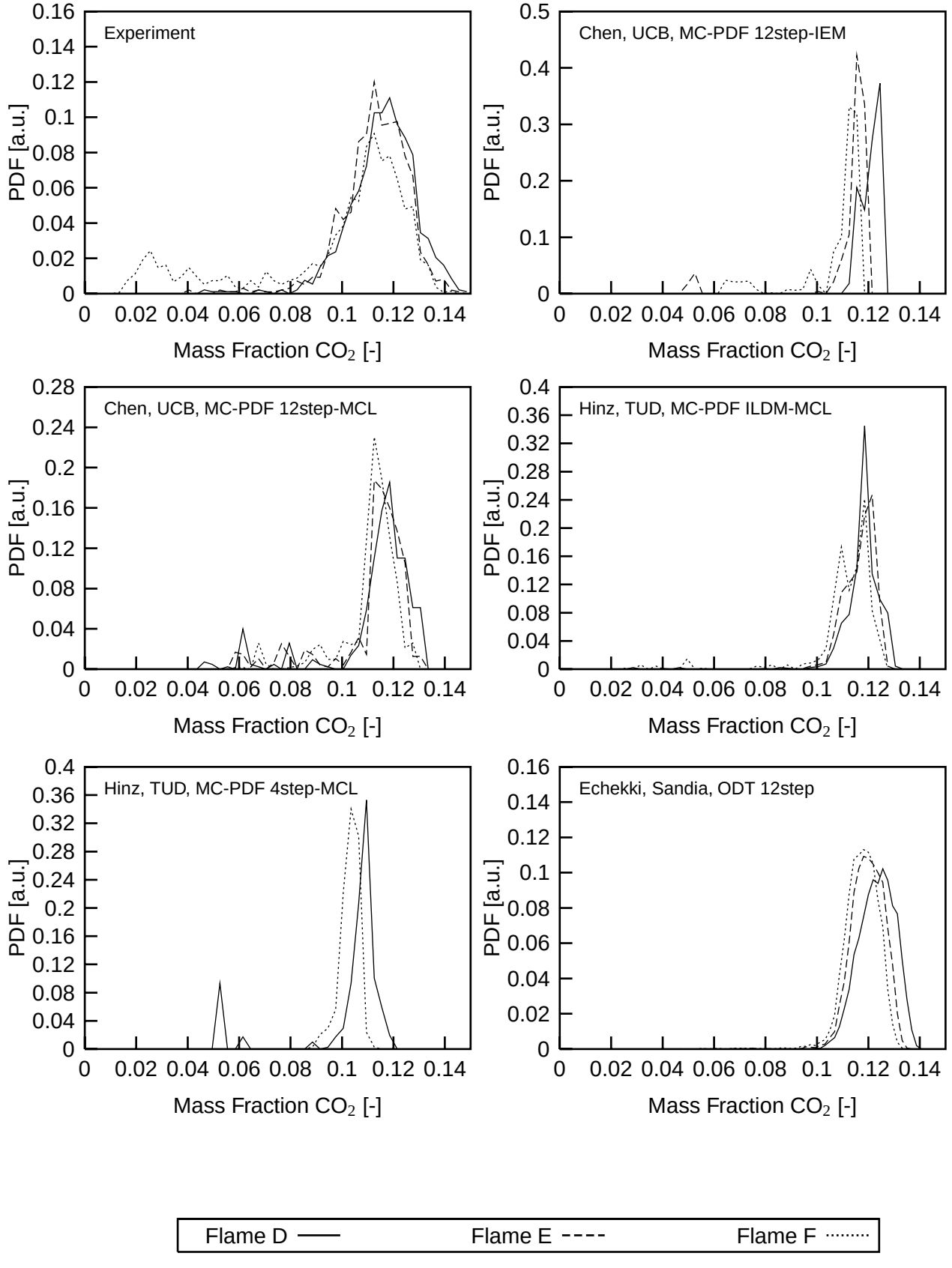

Piloted Flames D, E, F: Conditional PDF's of Mass Fraction of OH at x/d=15
Mixture Fraction Interval: 0.28 < f < 0.36

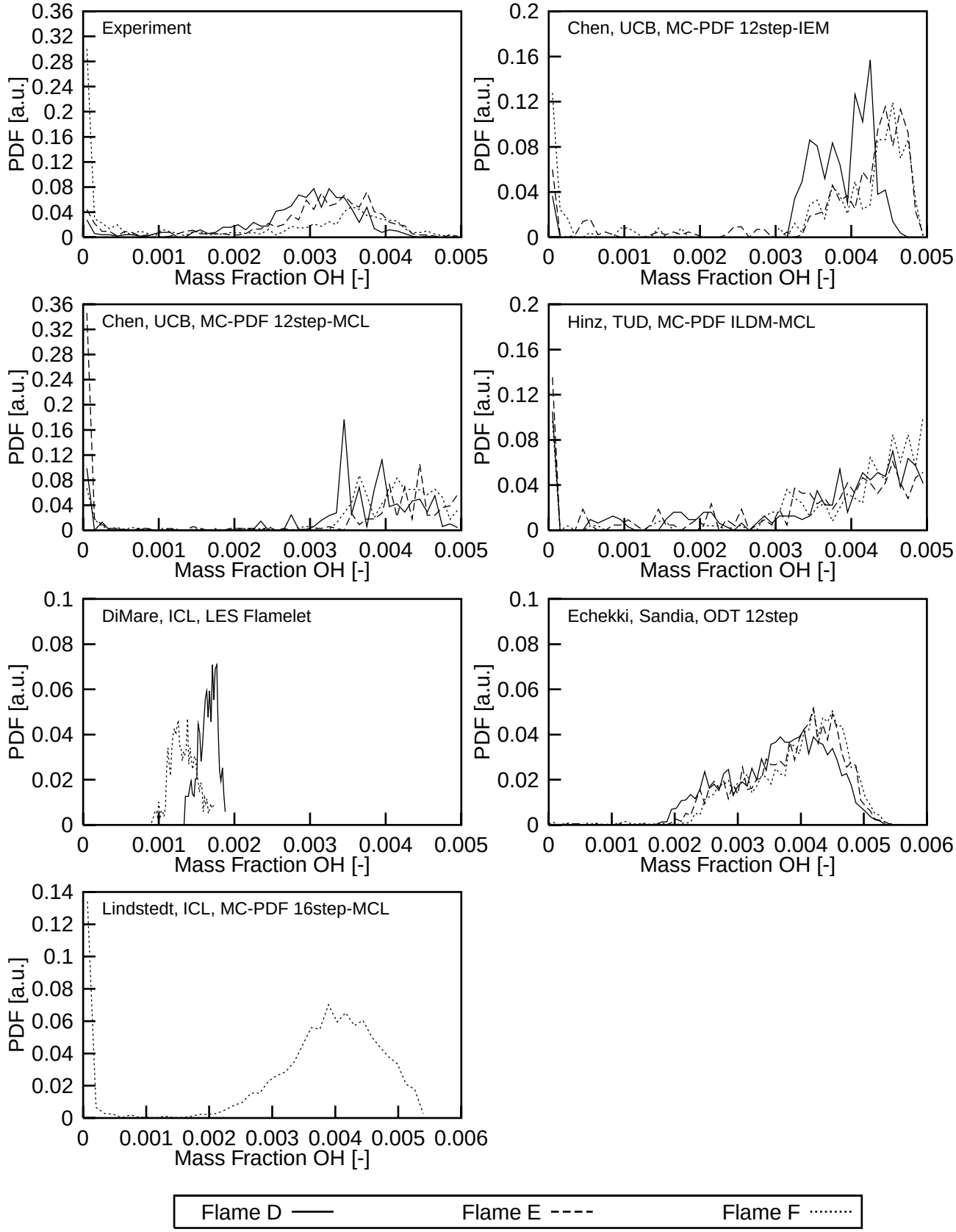

Piloted Flames D, E, F: Conditional PDF's of Mass Fraction of OH at x/d=30
Mixture Fraction Interval: 0.28 < f < 0.36

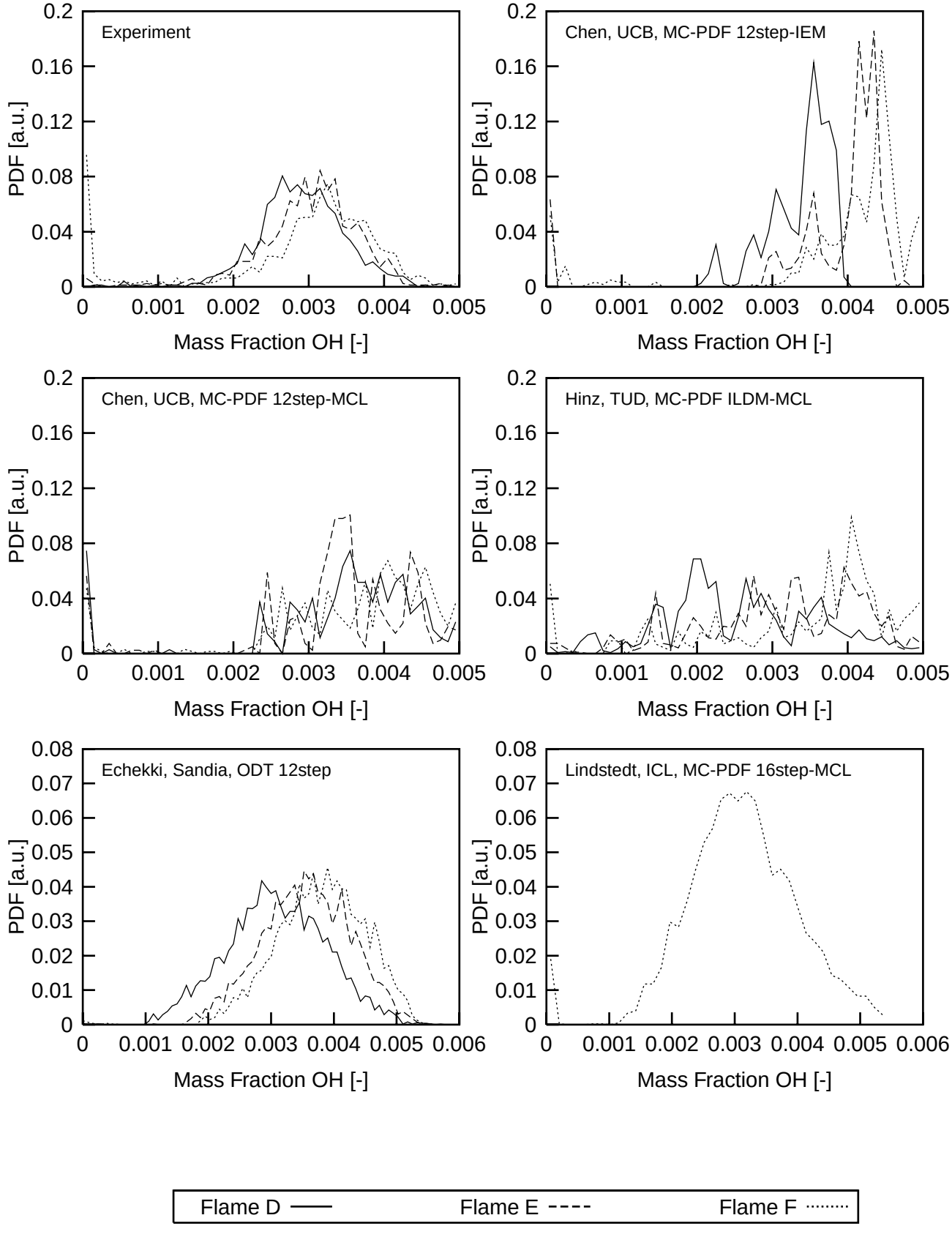

Piloted Flames D, E, F: Conditional PDF's of Mass Fraction of CO at x/d=15
Mixture Fraction Interval: 0.43 < f < 0.53

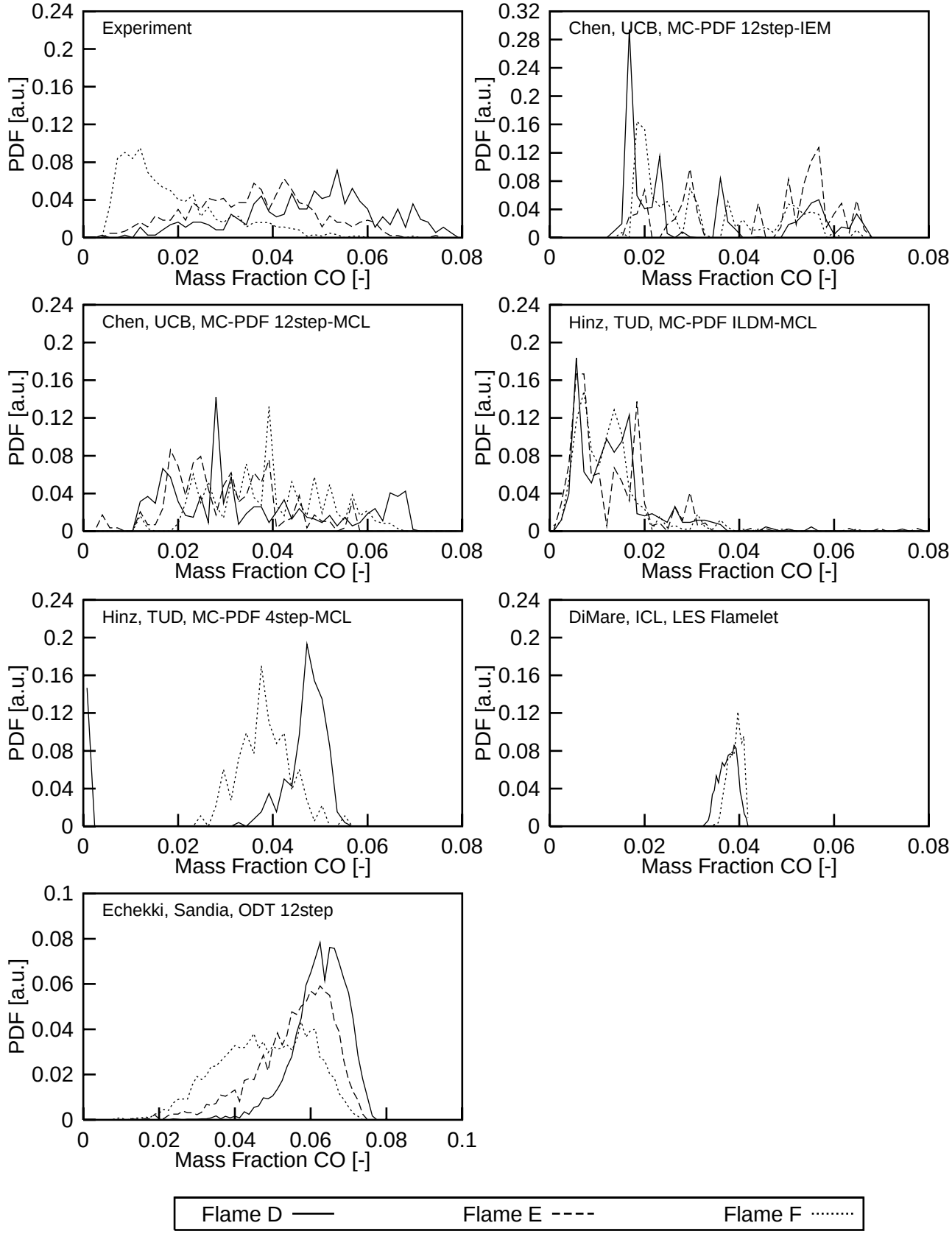

Piloted Flames D, E, F: Conditional PDF's of Mass Fraction of CO at x/d=30
Mixture Fraction Interval: 0.43 < f < 0.53

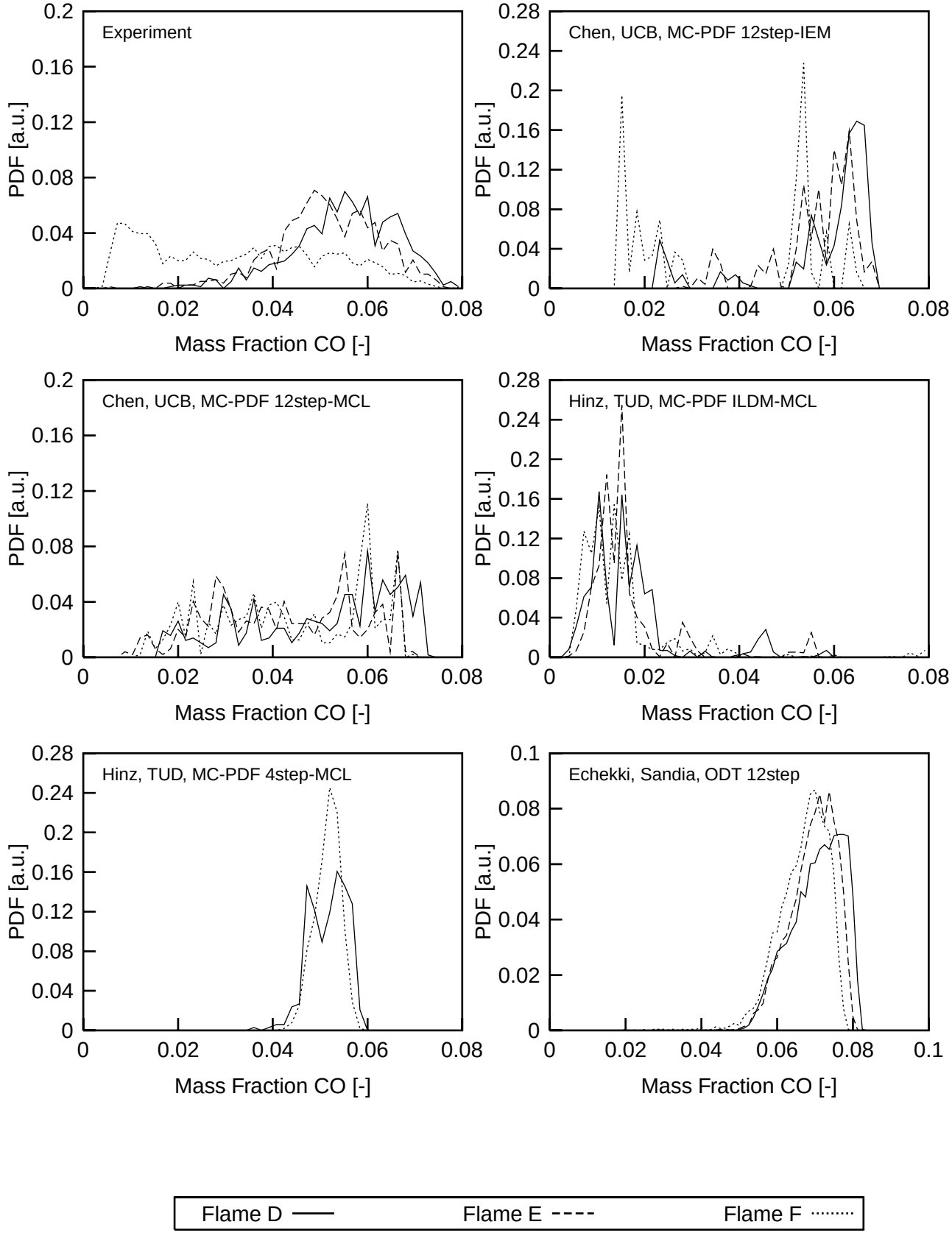

Piloted Flames D, E, F: Conditional PDF's of Mass Fraction of H_2 at x/d=15
Mixture Fraction Interval: $0.48 < f < 0.58$

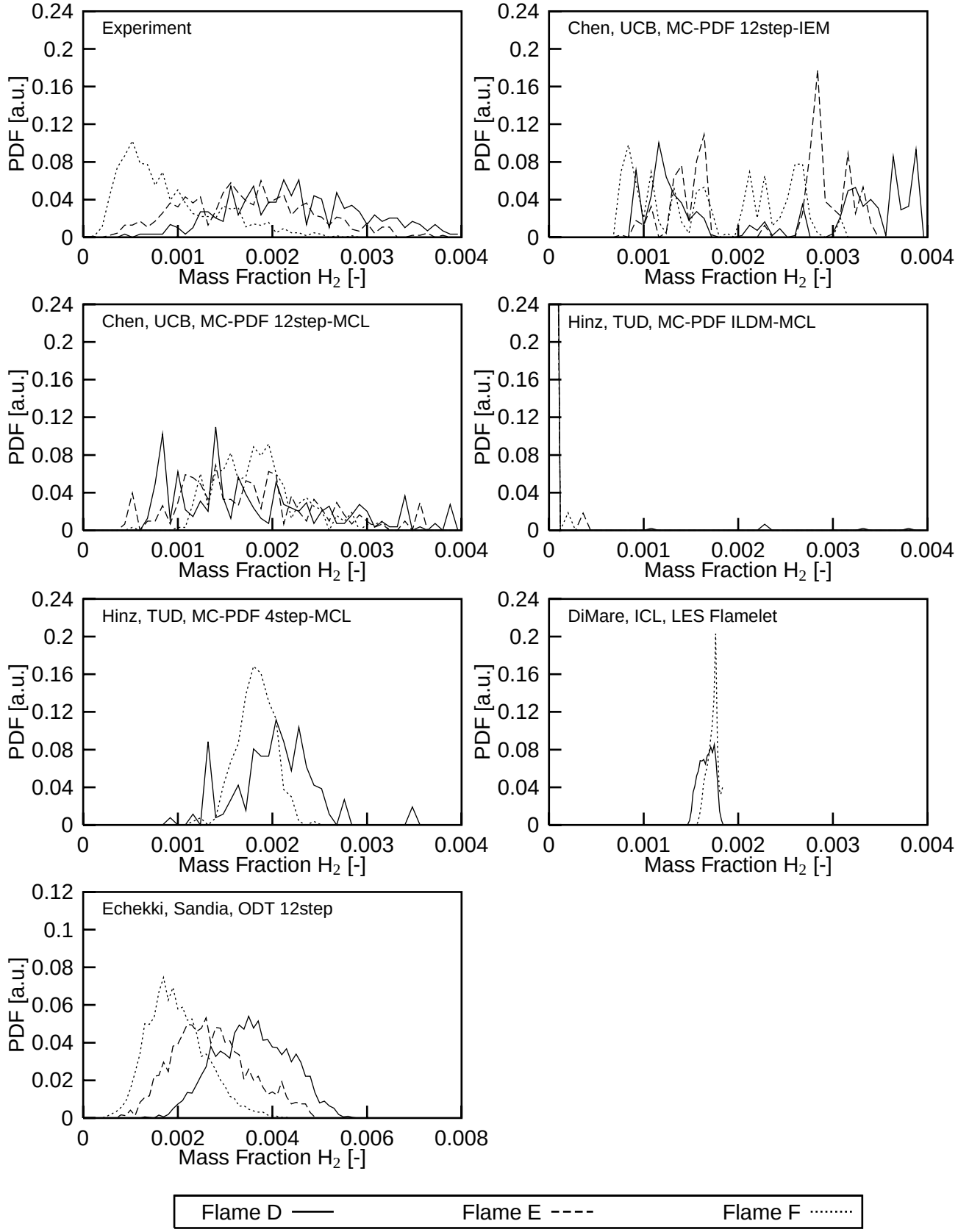

Piloted Flames D, E, F: Conditional PDF's of Mass Fraction of H_2 at x/d=30
Mixture Fraction Interval: $0.48 < f < 0.58$

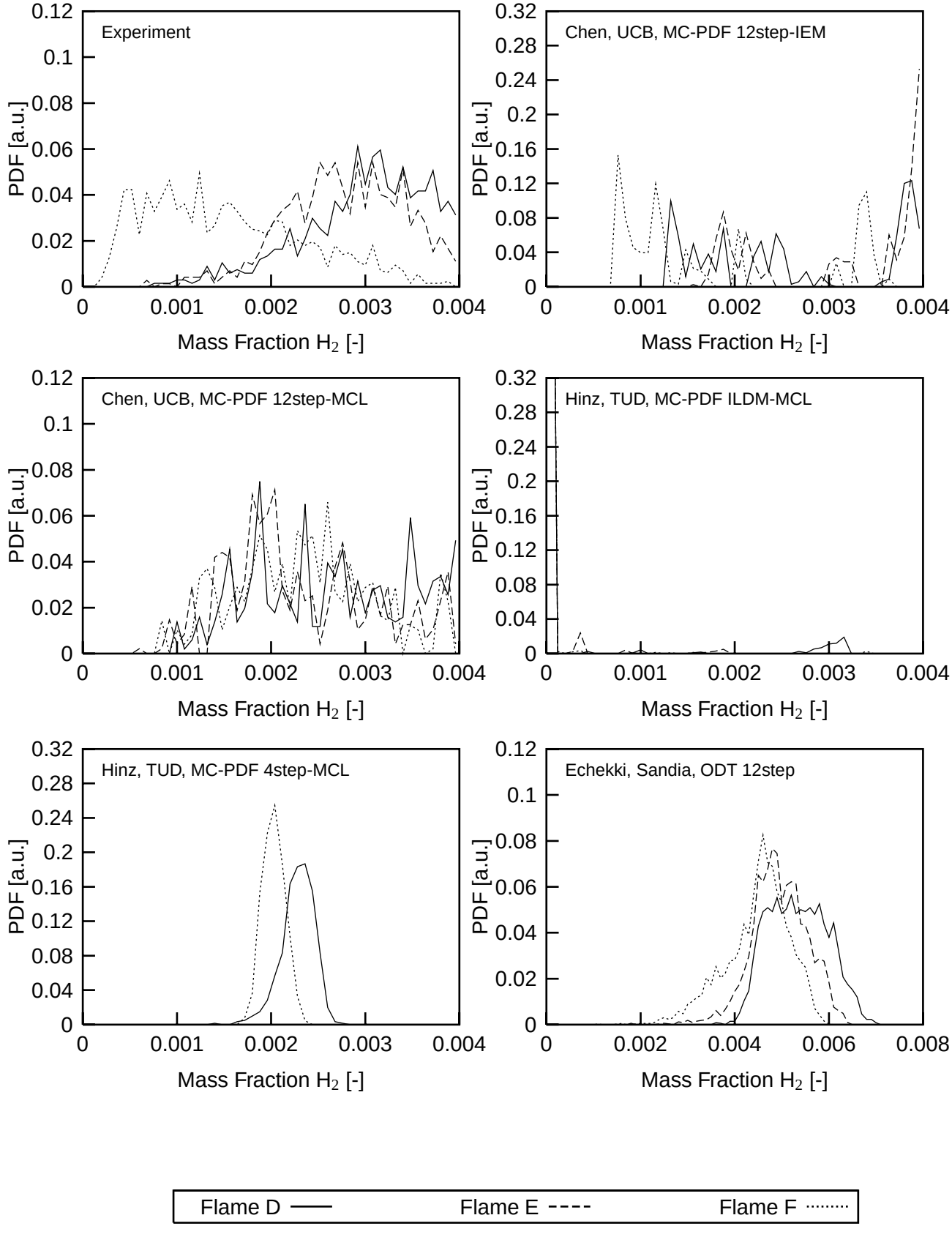

Piloted Flames D, E, F: Conditional PDF's of Mass Fraction of NO at x/d=15, 30
Mixture Fraction Interval: 0.33 < f < 0.41

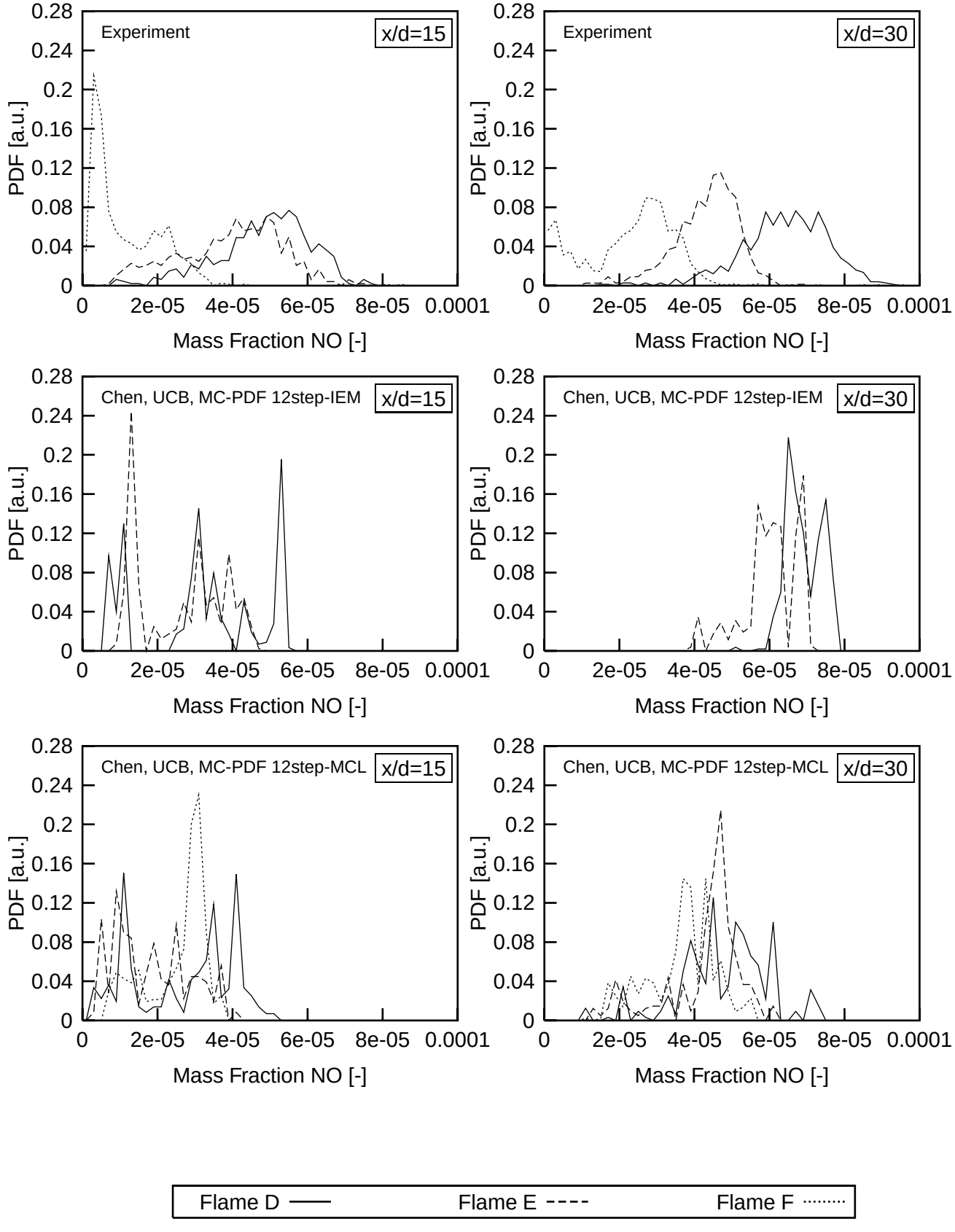

SECTION 2

Bluff-Body Flames

Problems and Numerical Issues in Computing Bluff-Body Stabilised Flows

At the Third Workshop in 1998, calculations for bluff-body stabilised jets and flames were presented using two standard models of turbulence: k-ϵ and Reynolds Stress models. Results were shown for the standard constants as well as for cases where $C_{\epsilon 1}$ was modified from 1.44 to 1.6. Comparisons of the flow, mixing and temperature fields (where appropriate) were made for the recirculation zone as well for other downstream locations.

The conclusion was that regardless of the value of the constant used, there are still significant discrepancies with the experimental results. While the modified k-ϵ or RS models gave improved results, the improvements are not uniform over the flow and mixing fields for both reactive and non reactive flows. There were even instances were the standard models gave better comparisons with the data than the modified ones. It was clear, therefore, that there are basic long-term limitations with these engineering approaches.

The objective for this workshop was to encourage modelers to compute bluff-body stabilised flows using "advanced" approaches. Given the time constraint, it became clear that this configuration poses a more difficult numerical problem than was originally anticipated and that it was too premature to aim for comparisons of advanced computations at this stage. Hence the title of this session was changed as shown above and the groups involved in computing these flows were invited to present a short talk on the problems and the difficulties they encountered and the tricks and fixes they applied in attempting these computations. This is intended to create an environment of collaboration where delegates can benefit from the experience of the speakers who will, in turn benefit from the feedback.

There are four groups who agreed to share their experience with this meeting:

Presenter	Approach	Group	Institution
F. di Mare	LES	W.P. Jones	Imperial College
A. Gill	LES	Bish/Prasad	Fluent
T. Peeters	PDF	D. Roekaerts	Delft
Jenny/Muradoglu	PDF	S. Pope	Cornell

SECTION 3

Poster Abstracts

ABSTRACTS

P. Bajaj, A. Obieglo, J. Gass
Numerical Simulation of a Piloted Methane/Air Flame (Flame D) using a Finite−Volume−Monte Carlo−PDF and Steady State Flamelet Codeˆ

R.S. Barlow, R.W. Schefer, P.C. Miles
New CRF Phase II Laboratory for Turbulent Combustionˆ

C.−P. Chou, J.−Y. Chen
On k−ε and Reynolds Stress Models for Opposed−Jet Turbulent Mixing/Reacting Flowˆ

P.J. Coelho, N. Peters
Numerical Simulation of a Turbulent Piloted Methane/Air Jet Flame using a Laminar Flamelet Modelˆ

T. Ding, T.H. van der Meer, M. Versluis
Time−resolved PLIF Measurement in the Delft turbulent diffusion flamesˆ

J.F. Driscoll, J.M. Donbar, C.D. Carter
Methods to Assess Large Eddy Simulations and Flame Surface Density Models ˇ Using Images of Reaction Zonesˆ

T. Echekki, A.R. Kerstein
One−Dimensional Turbulence Simulation of Piloted Methane−Air Jet Diffusion Flamesˆ

H. Forkel, J. Janicka
An Efficient Method for Large−Eddy Simulation of Turbulent Diffusion Flamesˆ

G.M. Goldin
Application of a Laminar Flamelet Model for Turbulent Combustion Simulations in a Gas Turbine Combustorˆ

J.C. Hewson, T. Echekki, A.R. Kerstein
One−Dimesional Turbulenceˆ Modeling of Turbulent $CO/H_2/N_2$ Jet Flamesˆ

A. Hinz, J. Janicka
Numerical Investigation of Turbulent Piloted Methane/Air Jet Flames using Monte Carlo PDF Methodˆ

C. Hollmann, E. Gutheil
A Flamelet Model for Turbulent Spray Diffusion Flames using a Laminar Spray Flame Library^

Y. Ikeda, J. Kojima, T. Nakajima
The Time and Spatial Resolved Measurement of Flame Emission for Analysis Local Flame−Front Structure^

P. Jenny, M. Muradoglu, S.B. Pope, D.A. Caughey
Towards PDF Simulations of Complex Reacting Flows ˘ A Consistent Hybrid Algorithm^

O. Keck, W. Meier, W. Stricker
Spontaneous Raman Scattering in Confined Swirling Natural Gas Flames: Temperature and Species Concentrations from the TECFLAM Burner^

T. Landenfeld, J. Janicka
Modelling of turbulence−chemistry interaction with a multivariate presumed (−PDF method^

R.P. Lindstedt, S.A. Louloudi, E.M. Vaos
Joint scalar PDF Monte Carlo simulations of CH_4/Air turbulent jet diffusion flames with comprehensive chemistry^

A. Mbiock, T. Peeters, D. Roekaerts
Computation of bluff−body inert and reactive flows^

W. Meier, R.S. Barlow, Y.−L. Chen
The Turbulent DLR $CH_4/H_2/N_2$ Jet Diffusion Flame: More Results from Raman/LIF Measurements^

M. Muradoglu, P. Jenny, S.B. Pope, D. A. Caughey
PDF Calculations of Non−reacting and Reacting Turbulent Bluff−Body Flows^

H. Niemann, B. Schramm, J. Warnatz
Application of ILDM−reduced mechanisms in laminar and turbulent flames^

H. Pitsch, H. Steiner
Large−Eddy Simulation of a Turbulent Piloted Methane/Air Diffusion Flame (Sandia Flame D)^
H. Pitsch, E. Riesmeier, N. Peters
Unsteady Flamelet Modeling of a Piloted Methane−Air Jet Flame (Sandia Flame D)^

M.R. Roomina, R.W. Bilger
Conditional Moment Closure (CMC) Predictions of a Methane−Air Piloted Jet Flame (Flame E)ˆ

D. Thévenin, R. Baron
Direct Simulations of Turbulent Non−Premixed Flames with Detailed Chemistryˆ

J. Xu, S.B. Pope
PDF/ISAT Calculations of of Piloted−Jet Non−premixed Methane Flamesˆ

A. Yuasa, J.−Y. Chen, O. Ukai
Numerical Simulation of Sandia Piloted CH_4/Air Jet Flame using the Monte Carlo Joint−Scalar PDF Methodˆ

Numerical Simulation of a Piloted Methane/Air Flame (Flame D) using a Finite-Volume - Monte Carlo-PDF and Steady State Flamelet Code

P. Bajaj, A. Obieglo, J. Gass
Institute of Energy Technology, ETH Zurich
Laboratory of Thermodynamics in Emerging Technologies
LOW C2, ETH-Zentrum, 8092 Zurich, Switzerland

We present results of the numerical simulation of a piloted Methane/Air Flame (flame D) using a Finite Volume - Monte Carlo-PDF Code and a steady state laminar flamelet model. The motivation of carrying out the simulation is the partially premixed nature of the methane/air flame. Such calculations can help in the further development of the existing model in order to predict the partially premixed turbulent flames. The results were obtained with a hybrid solution for the flow field and the thermo chemical variables are solved with an Eulerian composition PDF and Flamelet assumption respectively [1],[2].

The computational grid has been refined around the centre axis and nozzle exit. The boundary conditions have been defined according to the documentation.The flow field is solved with a finite volume code which is based on a finite element method (CFX-TASCflow). The turbulence closure is done with a $k-\varepsilon$ model with *Pope*-correction [3] where the standard constants according to Launder [4] are taken, except for the turbulent viscosity which was set as it has been suggested from the last workshop.

For the PDF-transport equation a four-step-mechanism [5] with eight species was used for modelling the chemistry. The system is described with the mixture fraction and mass concentrations of $n_{\mathrm{CH_4}}, n_{\mathrm{CO}}, n_{tot}$ and n_{H} which are calculated in a pre-processing and stored in tables [6]. During the computation the values are read out from the tables with an interpolation algorithm. The mixing model in the presented results is the *IEM* model and the number of particles was 64 per cells.

The results have shown, that a good agreement of calculations and experiments has been obtained in mixture fraction space. Indeed there are some discrepancies in predicting the right flame length. In order to find out the influence of the parameters some new calculations have been done. One calculation is done using modified Curl model. In another calculations the number of particles in each cell has been varied. Results of the computations will be presented.

In the Flamelet model the favre mean values of the species mass fraction equation is of the kind

$$\tilde{Y_n} = \int_0^1 \int_0^\infty Y_n(Z,\chi) P(Z) P(\chi) d\chi dZ \tag{1}$$

where Z denotes the mixture fraction, χ the scalar dissipation rate, $\tilde{Y_n}$ the mean mass fraction of the species. The statistical independence of Z and χ is assumed in the model. The flamelet library is generated with the detailed mechanism published by Peter-Rogg [7] using the code FLAMIX [8]. This code is derived from the Sandia's opposed code, named OPPDIF and is the extension to the CHEMKIN package. In the model a beta PDF is assumed for the mixture fraction and a log normal PDF for the scalar dissipation rate. The results obtained are to be discussed in the poster. The calculations are also performed using the GRI 2.11 mechanism for methane/air combustion.

Fig 1.a shows the comparison of both the computational results along with the experimental data for the OH mass fraction profile. The C1-C2 mechanism over predicts the OH mass fraction compared to the results obtained by using GRI 2.11 combustion mechanism. The prediction of the flame length (for both mechanism), using this steady state

model, is incorrect. The problem lies in the existing model, which was developed for the pure non premixed flames. These unexpected results give motivation for using this methane/air partially premixed flame as a test flame for the modification of the existing flamelet model. The aim of the continuing work is to predict the structure of the partially premixed methane/air turbulent flame.

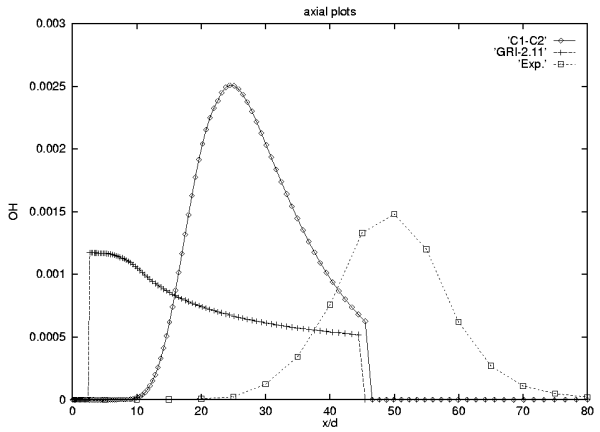

1.a OH Profiles along the centerline - Flamelet calculations

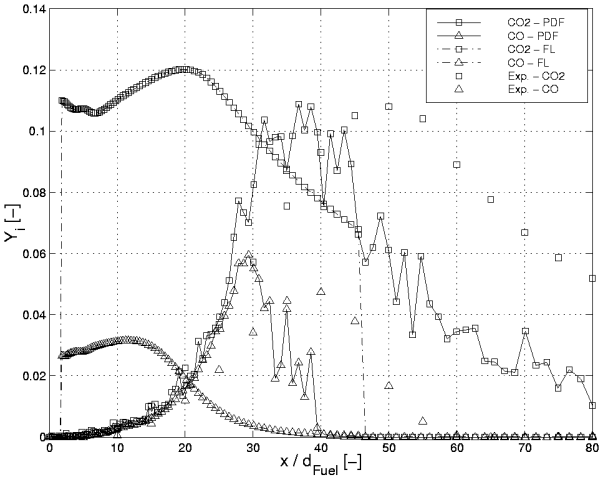

1.b CO and H_2O Profiles along centerline for PDF and Flamelet calc.

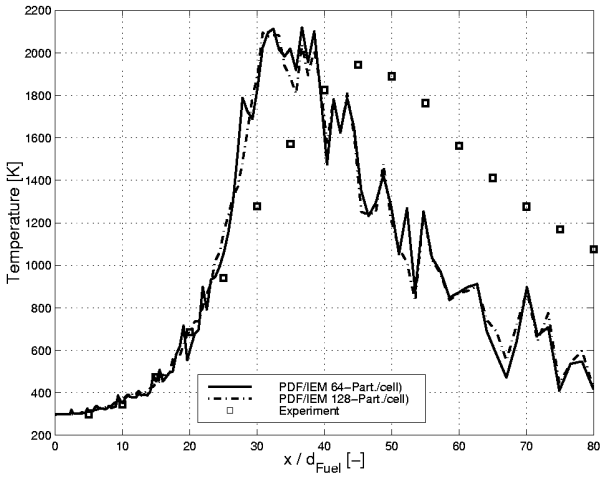

1.c Effect of variation of the Particle number on the Flame structure (PDF)

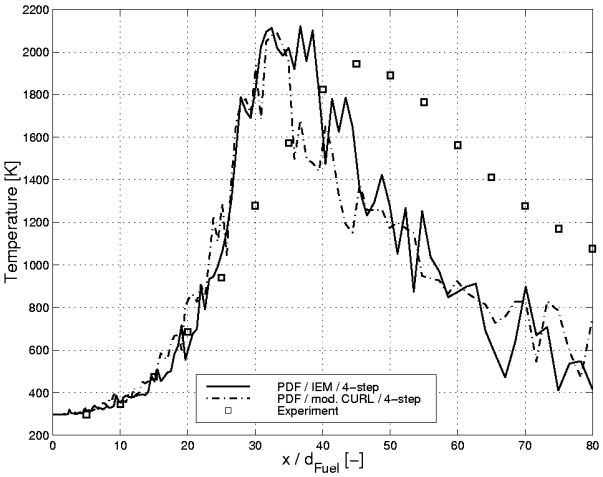

1.d Effect of variation of the Mixing models on the Flame structure (PDF)

Figure 1: *Computational Results*

References

[1] Laxander, A. (1996), *PhD thesis*, TU Stuttgart
[2] Ferreira, J.C. (1996), *PhD thesis*, ETH, Zurich
[3] Pope, S.B.(1978), *AIAA Journal*,16, pp. 279-281
[4] Launder, B.E., Spalding,D.B. (1974), *Comput. Methods Appl. Mech. Engrg.*, 3, pp. 269-289
[5] Rogg, B. (1991),*Lecture Notes in Physics*, 384, pp. 159-192
[6] Chen, J.Y.,Kollmann,W., Dibble,R.W. (1989) *Combust. Sci. and Techn.*, 64, pp. 315-346
[7] Peters, N., Rogg, B. (1993), Red. Kin. Mech. for Appl. in Comb. Systems. Springer, Berlin.
[8] Ferreira, J.C. (1996), Internal report, LTNT, ETH, Zurich, Switzerland.

NEW CRF PHASE II LABORATORY FOR TURBULENT COMBUSTION

R. S. Barlow, R. W. Schefer, and P. C. Miles
Sandia National Laboratories
Livermore, California
USA

Sandia's Combustion Research Facility is undertaking a significant expansion of its laboratory capabilities. This Phase II of the CRF includes a new dual laboratory that will emphasize experiments in turbulent flames, both nonpremixed and premixed. The Turbulent Combustion Laboratory (TCL) is currently under construction and will include two independent flow facilities with matched capabilities for supporting a variety of burner configurations. One of these facilities will be dedicated to scalar measurements that will extend beyond the current point measurement capabilities of the current Turbulent Diffusion Flame (TDF) lab. The other facility will support measurements of velocity, using LDV and PIV, and the spatial structure of turbulent flames, using PLIF imaging and combinations of PLIF and PIV. Our intent in developing this laboratory is to provide a single location where a range of state-of-the-art diagnostics may be applied to fully characterize a given flame or burner configuration. This laboratory has been funded by the Department of Energy with the understanding that it will be operated with a strong emphasize on collaborative interactions with visiting researchers. We expect that most of these visitor interactions will be developed in the context of the TNF Workshop and similar collaborative groups that promote a strong connection between experimental and computational research.

The scalar measurements will be based on a combination of line imaging of Rayleigh scattering, spontaneous Raman scattering, and two-photon LIF of CO over a length of approximately 8 mm. We plan to intersect this line with two sheets of laser light for PLIF imaging of small regions (1-2 cm on a side). This will provide information on the orientation of the instantaneous flame front relative to the measured line-Raman image. For the line-Raman measurements we have been collaborating with the Engine Combustion Research group at the CRF on the development of a high-speed mechanical shutter system that eliminates the need for an image intensifier to gate out flame luminosity. This shutter serves as the entrance slit of an imaging spectrograph (SPEX 270M), and is integrated into the spectrograph housing as shown in Fig. 1. Gating of 9 ms (FWHM) is achieved with a 0.8-mm wide slit in a wheel that rotates at 21,000 rpm.

We have recently demonstrated this shutter and spectrograph in combination with a back-illuminated CCD detector by obtaining line measurements of Raman scattering in a laminar jet flame of CH_4/air, as shown in Fig.1, right side. The fuel jet composition is 25% CH_4 and 75% air, the same as used in the Sandia piloted flame series that is a target for the TNF Workshop. Single-shot and averaged images were obtained using a laser energy of roughly 450 mJ/pulse at 532 nm. The length of the image along the laser beam was 12.5 mm, extending from the jet centerline out to the coflowing air. The resulting CCD image has radius as one dimension and wavelength as the second dimension. Figure 2 shows spectra of Raman scattering plus fluorescence interference from three radial locations in an averaged (500 shots) line-Raman image of the laminar flame. The interference spectrum includes the distinct C_2 Swan band structure, a broadband component, and a few distinct features, such as those surrounding the H_2 Raman band, that have yet to be identified. This information on the nature of the interference spectrum will be useful in correcting for interferences in single-shot measurements in turbulent hydrocarbon flames. Single-shot measurements use on-chip binning to maximize the SNR.

The TCL will make use of four doubled Nd:YAG lasers (over 900 mJ/pulse from each) and the latest CCD detectors. We expect to obtain better spatial resolution and better SNR than is currently achieved with the point measurements in the TDF lab. We hope to achieve a spatial resolution of 400 microns (or better) with sufficient SNR to allow useful measurement of fixture fraction gradients that can be related to the local scalar dissipation in turbulent flames.

Fig. 1. Mechanical shutter/imaging spectrograph combination (left) and configuration for demonstration experiment on laminar jet flame (right).

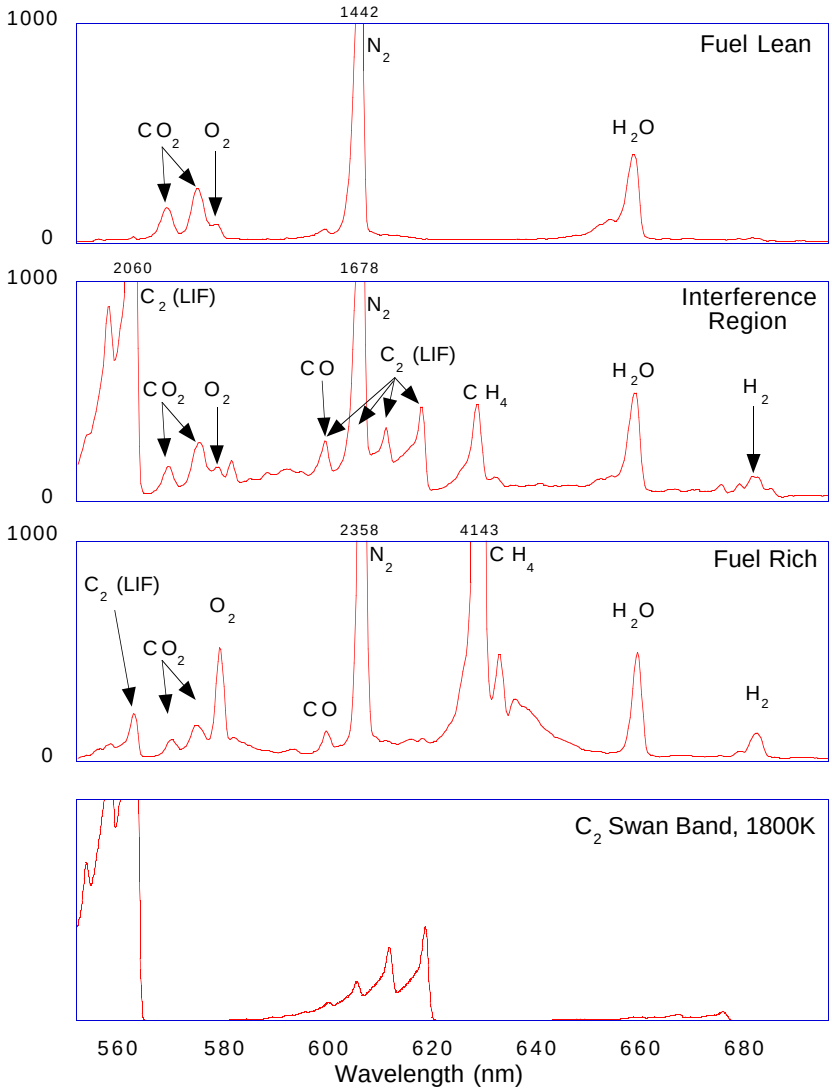

Fig. 2. Averaged spectra (top three) of Raman scattering and hydrocarbon fluorescence interference at three locations (fuel lean, interference region, and fuel rich) along the imaged line through the laminar flame. The lower graph is a calculated C_2 fluorescence spectrum (provided by Y.-L. Chen). Single-shot measurements use on-chip binning to integrate over the Raman bands.

On $\tilde{\kappa}$ - $\tilde{\epsilon}$ and Reynolds Stress Models for Opposed-Jet Turbulent Mixing/Reacting Flows

Chen-Pang Chou and J.-Y. Chen
Department of Mechanical Engineering, University of California
Berkeley, CA 94720
and
Rolf Hoffmann and Johannes Janicka
Fachgebiet für Energie- und Kraftwerkstechnik, Technische Universität Darmstadt
Germany

Abstract

Turbulent opposed jet flows offer simplicity in experimental studies as well as in mathematical formulations. In addition, opposed jet flows exhibit salient characteristics, such as dominant normal velocity gradients and a strong anisotropic turbulence production. These features distinct turbulent opposed jet flows from the widely studied turbulent free shear flows. Moreover, turbulent opposed jet flows present a challenge to the predictions of turbulence intensities especially when the $\tilde{\kappa}$-$\tilde{\epsilon}$ eddy viscosity model is employed. The short global residence time of opposed jet flows also complicates the turbulent mixing of scalars. In the present study, performance of the $\tilde{\kappa}$-$\tilde{\epsilon}$ eddy viscosity model and a Reynolds stress model are compared against the experimental data by Mastorakos for turbulent opposed jet flows. Since chemical kinetics is not focused in this study, a flamelet model is used for coupling the flow calculations. The mean density is determined by a presumed-shape pdf (probability density function) with a pre-calculated density table. The results showed that the simple gradient model can lead to negative turbulent intensities when the density change is large. The second moment closure is preferred for predicting turbulent opposed jet flows. Also explored in this study are the dependence of scalar field on mean strain rate and initial turbulence intensity and the level of complexity needed for adequate scalar modeling, *e.g.*, using a gradient model or transport equations for the turbulence-scalar interaction. The widely assumed value of mechanical-to-scalar time scale ratio, $C_D = 2$, is found not adequate for opposed jet flows. As revealed by the modeled transport equation for the scalar dissipation rate, C_D varies substantially throughout the flow field. Since inclusion of the scalar dissipation rate equation is computationally more expensive, a value of 8 is recommended for simple fixed-C_D calculations. The C_D value is also critical for the molecular mixing model when the time-consuming pdf transport equation with realistic combustion chemistry is used to predict strong turbulence-chemistry interactions in turbulent opposed jet flows.

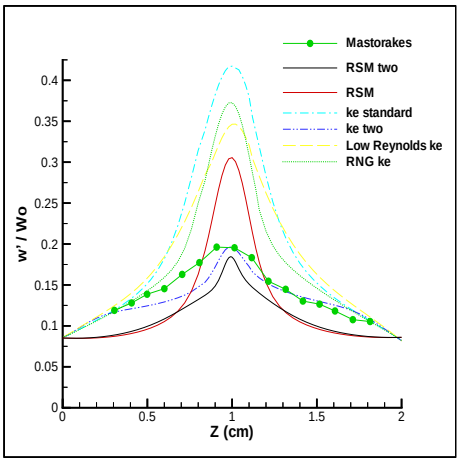

(a) Pure mixing cases: rms of axial velocity predictions

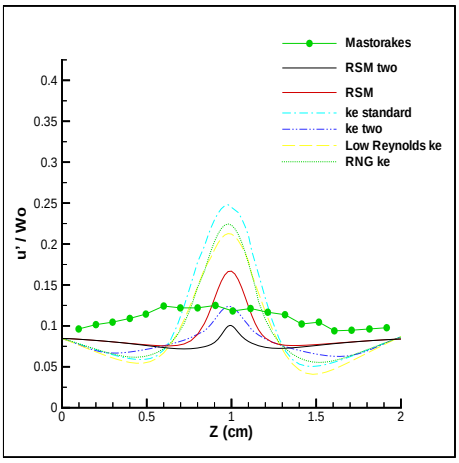

(b) Pure mixing cases: rms of radial velocity predictions

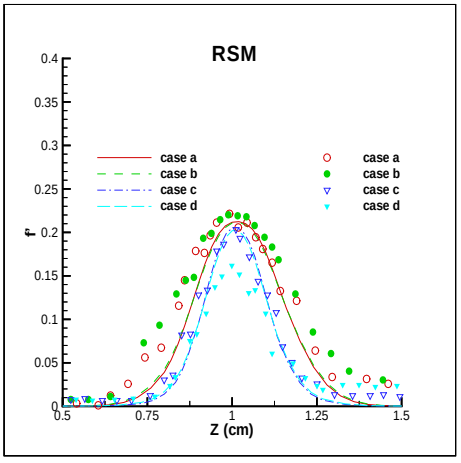

(c) Pure mixing cases: rms of mixture fraction predictions

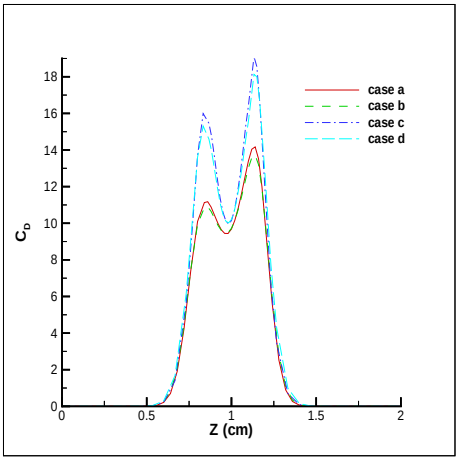

(d) Pure mixing cases: distribution of C_D

Numerical Simulation of a Turbulent Piloted Methane/Air Jet Flame Using a Laminar Flamelet Model

P.J. Coelho (*) and N. Peters (**)

* Instituto Superior Técnico, Technical University of Lisbon, Av. Rovisco Pais, 1049-001 Lisboa, Portugal
e-mail: coelho@vangogh.ist.utl.pt

** Institut für Technische Mechanik, RWTH Aachen, Templergraben 64, 52062 Aachen, Germany
e-mail: N.Peters@itm.rwth-aachen.de

A turbulent piloted methane/air jet flame, the so-called flame D, experimentally studied by Barlow and Frank (1) has been simulated numerically. The experimental data are available in (2). The time-averaged equations for mass, momentum and energy conservation, the Reynolds stress equations and equations for mixture fraction, mixture fraction variance and enthalpy were solved with a finite volume method using the version 4.8 of the Fluent code. The Reynolds stress equations do not include terms that account for variable density effects and no effort was undertaken to improve this. Standard values were used for the constants of the model. The ε equation was modified according to (3) in order to improve the prediction of the spreading rate of the fuel jet.

The combustion models available in Fluent were not activated, and the laminar flamelet model was used and linked to Fluent by means of appropriate user subroutines. A steady flamelet library was generated using RIF (Representative interactive flamelets), an ITM-RWTH in-house code based on the solution of the flamelet equations. Flamelets were computed for several dissipation rates assuming Le=1 for all species. The chemical mechanism, also developed at ITM-RWTH, comprises 49 species and 547 reactions, including those of the NO mechanism. The temperature calculated from flamelet equations was not used, since it does not consider radiation. Instead, an enthalpy equation was solved in the CFD code, and the temperature was obtained from the definition of enthalpy and using the species mass fractions. The enthalpy equation includes a radiative source term, obtained using the optically thin approximation with absorption coefficients for H_2O, CO_2, CO and CH_4 taken from the fit to the RADCAL calculations described in (2). A presumed beta pdf was used to compute mean (Favre averaged) quantities.

Unsteady flamelet calculations were also carried out in a post-processing stage using marker particle transport equations as described in (4). It has been found that the results of the unsteady calculations using marker particles are somewhat dependent on the initial conditions, namely the flamelet profiles and the particle concentration fields at t=0 s. This dependence is larger for the minor species whose concentration is more influenced by unsteady effects. In the data delivered to the present workshop, the unsteady results were obtained considering 6 marker particles (MP) and taking as the initial condition steady flamelet profiles (SFP). The region where there are particles at t=0 s is restricted to the range $Z_{st} < Z < 1.4Z_{st}$, where Z is the Favre averaged mixture fraction and Z_{st} is the stoichiometric mixture fraction. This region is subdivided into 6 subregions, according to the local scalar dissipation rate, and each marker particle is assigned and initialized only in one subregion. In addition, this poster includes two other sets of unsteady calculations using 10 marker particles. In one set the initial profiles are assumed as Burke-Schumann profiles (BSP) and the particles are initialized in the range $Z_{st} < Z < 1.4Z_{st}$. In the other set, initial Burke-Schumann profiles are again assumed and the initialization range is $0.5Z_{st} < Z < 1$.

The predicted mixture fraction and temperature along the centreline, shown in Fig. 1, are in good agreement with the data, but the radial profiles (not shown here) suggest that the spreading rate of the jet is slightly overestimated despite the modification of the ε equation following (3). The centreline mass fraction profiles displayed in Fig. 2 show that unsteady flamelet calculations yield an improvement of the predictions. This is particularly evident for CO, H_2 and NO, but also the prediction of the major species is improved. The initial conditions of the unsteady calculations only marginally influence the mass fraction of the major species, but the influence is important in the case of the minor species. In general, the mass fractions computed using Burke-Schumann initial profiles are closer to the measurements than those computed using steady flamelet initial profiles. In all cases, however, the OH and NO mass fractions are overpredicted. This and the conditional means (not shown here) suggest that the reaction mechanism may be responsible for part of the discrepancies found between measurements and predictions of these species.

Acknowledgments

The financial support given by the Portuguese Ministry of Science and Technology to the sabbatical leave of P.J. Coelho at RWTH in the framework of the FMRH programme is acknowledged.

References

[1] Barlow, R.S. and Frank, J.H., 27th Symposium (Int.) on Combustion, pp. 1087-1095, 1998.

[2] http://www.ca.sandia.gov/tdf/Workshop.html

[3] Pope, S.B., AIAA J., Vol. 16, No 3., pp. 279-281, 1978.

[4] Barths, H., Peters, N., Brehm, N., Mack, A., Pfitzner, M. and Smiljanovski, V., 27th Symposium (Int.) on Combustion, 1998.

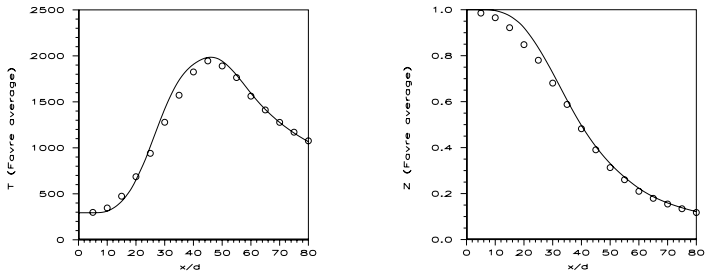

Figure 1 - Predicted (solid lines) and measured (symbols) centreline profiles of temperature and mixture fraction.

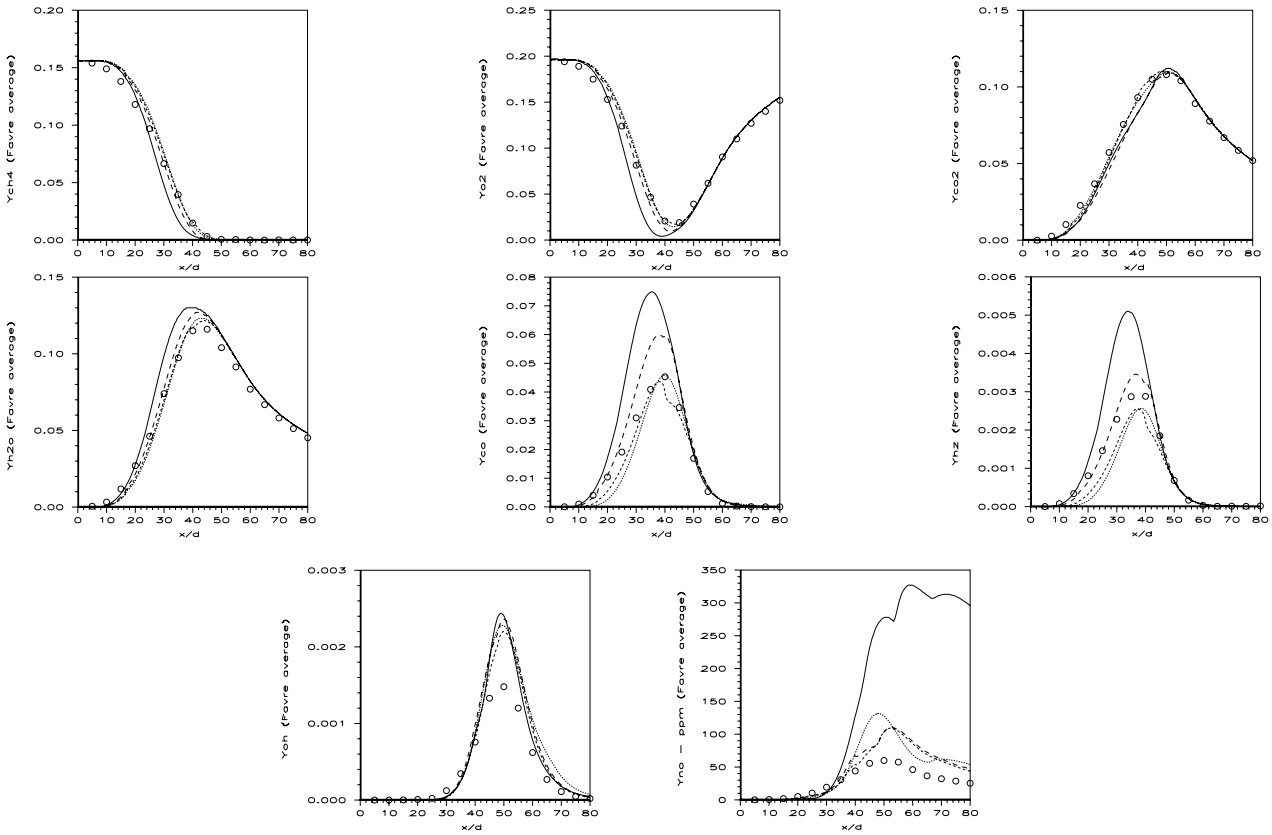

Figure 2 - Predicted and measured centreline profiles of species mass fractions

——— : steady flamelets

– – – : unsteady flamelets, 6 MP, SFP,$Z_{st} < Z < 1.4Z_{st}$

- - - - - : unsteady flamelets, 10 MP, BSP,$Z_{st} < Z < 1.4Z_{st}$

..... : unsteady flamelets, 10 MP, BSP,$0.5Z_{st} < Z < 1$

Poster Abstract

TNF99 workshop

Time-resolved PLIF measurement in the Delft turbulent diffusion flames

T.Ding, Th. H. van der Meer, M. Versluis

Delft University of Technology, Faculty of Applied Sciences, Thermal and Fluids Sciences Section, Lorentzweg 1, Delft 2628CJ, The Netherlands
(Fax: +31-15-2781204, E-mail: tieying@ws.tn.tudelft.nl)

J. Hult, M. Aldén, C.F. Kaminski

Division of Combustion Physics, Lund Institute of Technology, Box 118, S-22100 Lund, Sweden
(Fax: +31-15-2781204, E-Mail: clemens.kaminski@forbrf.lth.se)

Time-resolved planar laser induced fluorescence (PLIF) imaging of the OH radical is presented in the Delft flames III and IV. We report on the measurement of sequential PLIF OH images in our Delft flames, by using the ultra high repetition rate laser system and fast framing rate camera detector at the Lund Laser Centre (LLC), Division of Combustion Physics. The laser system consists of 4 double pulsed YAG lasers and a dye laser. With the fast camera it is possible to record 8 frames with a minimal time separation of 1 μs. Several phenomena which are characteristic for turbulent flames were captured and their evolution tracked in time. The volumetric expansions of the OH structures were observed, the transition from laminar to turbulent flow, the processes of extinction and re-ignition, the formation of vortices and the structural development of the flame could all be followed. By comparing the PLIF data to the corresponding emission images, some 3 dimensional phenomena could be extracted. Different temporal and spatial scales of the turbulent structures could be tracked by varying the time separations between events in a recorded sequence, ranging from ~100 μs to several ms.

Methods to Assess Large Eddy Simulations and Flame Surface Density Models - Using Images of Reaction Zones

James F. Driscoll[1], Jeffrey M. Donbar[2], and Campbell D. Carter[3]

[1]University of Michigan, Ann Arbor MI
[2] Air Force Research Lab, AFRL/PRSS, Wright-Patt. AFB, OH
[3]Innovative Scientific Solutions, Dayton OH

Some quantities are identified which can be used to assess whether or not the fundamental assumptions associated with a particular model of a nonpremixed jet flame are realistic. Quantities which are sensitive to the physical structure of the flame, and which were measured, include:

1. Surface density	- of the thin, wrinkled reaction zone
2. Wrinkledness	- of the reaction zone, which differs from surface density
3. Thickness	- of the instantaneous, thin reaction zone
4. Strain rate	- on the reaction zone
5. Curvature	- of the reaction zone
6. Stretch rate	- quantifying the area increase due to turbulence, and
7. Wavelength of wrinkles	- on the reaction zone, compared to Taylor, integral scales
8. Strength	- of the reaction zone, based on radical concentrations
9. Stoichiometric contour	- instantaneous location with respect to vortices,
10. Large vortex locations	- with respect to reaction zones
11. Conditioned mean velocity	- on the reaction zone
12. Extinguished fraction	- of the reaction zone.

Measurements of the above parameters were made as a function of the streamwise distance (x) in a turbulent jet flame at a high Reynolds numbers (18,600 and 9,100). Diagnostics used were simultaneous CH-OH PLIF imaging, and simultaneous CH-PIV imaging.

Results show that an ideal way to image the instantaneous stoichiometric contour is to record simultaneous CH-OH images and then to identify the CH-OH boundary. This makes it possible to measure the flame surface density (Σ), which has a typical value of 0.2 mm^{-1}. Surface density is shown to be related to the turbulent brush thickness and the degree of wrinkling. The reaction zone that is associated with fuel decomposition (i.e., the CH layer) remains thin and rarely exceeds 1 mm, even near the tip of the high Reynolds number flame. CH layers in the turbulent flame are not thicker than the CH layers in the laminar jet flame at the same x/d location. In fact, CH layer thickness is insensitive to Reynolds number and the level of turbulence. This implies that turbulence does not broaden the CH reaction zone. Thus one assumption employed by flamelet models (i.e. thin fuel decomposition zones) is realistic. CH layer thickness increases from 0.4 to 0.8 mm in the x direction, which is expected because scalar gradients decrease in the x direction.

Results also show that the in-plane components of the strain rate can be measured along the wrinkled stoichiometric contour by employing simultaneous CH PLIF and PIV diagnostics. Strain rate is a source term in the equation for flame surface density, thus strain explains how turbulence increases

both the flame surface area and the volumetric reaction rate. Taylor scales were resolved at three locations, and corrections due to small scales were 10%, based on data obtained for two values of spatial resolution. The out-of-plane contribution is nearly equal to the measured in-plane value. Instantaneous strain rates are highly intermittent, with large peak values exceeding 10,000 s^{-1} and an average value (1,600 s^{-1}) that is only one-sixth of the peak value. Strain rates oscillate at 10 kHz, with a period that approximately equals the crossing time of integral scale eddies. Due to the short residence time of each eddy, the CH layer thickness and CH concentrations do not respond to the high frequency components of the strain field and they do not follow quasi-steady-state predictions. Only a small fraction of the strain effectively acts on the flame, while the remaining strain varies too rapidly in time. Mean strain rates do not decrease in the streamwise direction and they increase more rapidly with jet velocity than is predicted, due to flame wrinkling.

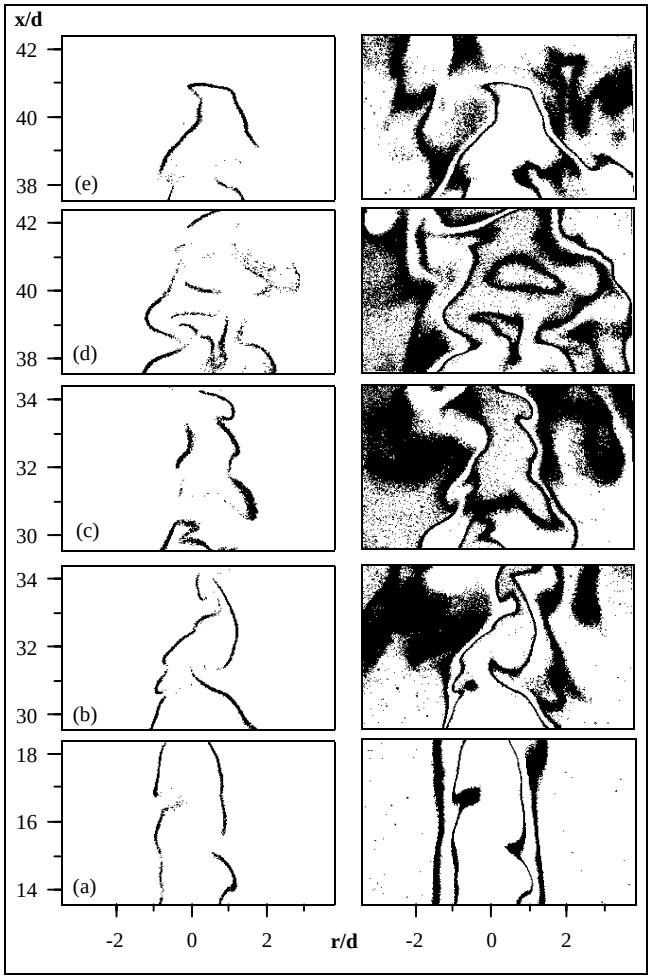

Figure 1. Structure of the CH reaction zone (left images) and the simultaneous OH reaction zone (right images) in the high Reynolds number (18,600) jet flame

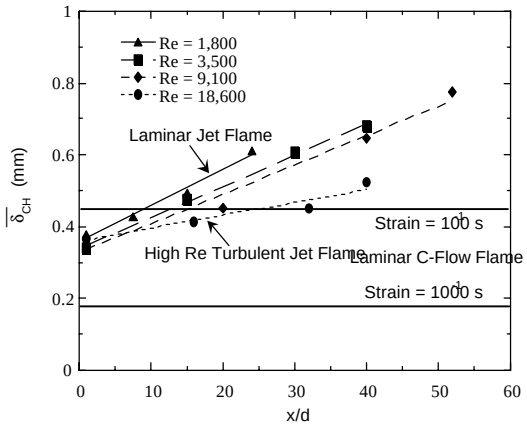

Figure 2. Mean thickness of the CH layers, a measure of the fuel decomposition reaction zone, for Re of 18,600, 9,100, 3,500 and 1,800.

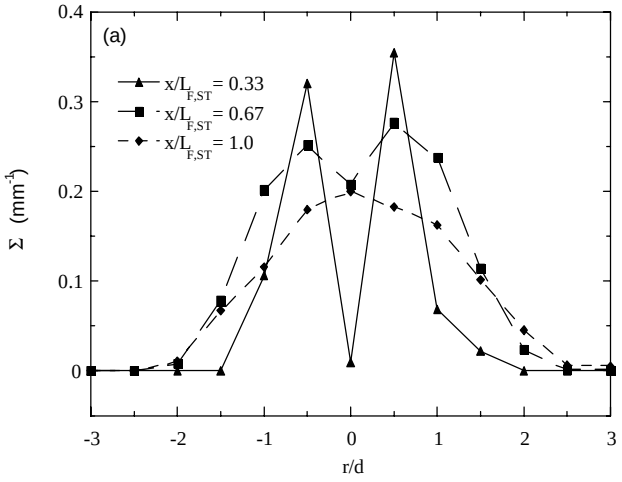

Figure 3. Flame Surface Density (Σ) measured using the CH-OH boundary to mark the stoichiometric contour for the high Reynolds number (18,600) flame.

One-Dimensional Turbulence Simulation of Piloted Methane-Air Jet Diffusion Flames

Tarek Echekki and Alan R. Kerstein

Sandia National Laboratories
Livermore, CA 94551-0969, USA

Temporal simulations of turbulent nonpremixed piloted methane-air flames (flames D, E and F in the Sandia experiments) are performed using the One-Dimensional Turbulence (ODT) model [1]. The calculations of temporally and spatially resolved thermochemical scalars on a 1D domain transverse to the mean flow include a 12-step chemistry model for methane-air [2]. Mixture averaged transport models are implemented using the CHEMKIN library. The solution of the streamwise velocity provides a measure for the local shear, which is used to 'drive' the turbulence.

Single and multiple simulated realizations of the piloted flame are performed to (i) evaluate qualitatively the model predictions of the piloted flame structure and the mechanisms of entrainment, turbulent mixing and finite-rate chemistry, and (ii) compare with experiment for quantitative evaluation of scalar statistics.

The simulations are shown to reproduce the qualitative structure of the piloted jet diffusion flame. The OH concentration field from a single realization of flame F is compared to an averaged field in Fig. 1. The averaged field highlights the distinction between pilot-assisted burning up to 20 jet diameters downstream, followed by self-sustained burning fed by air entrained from the coflow.

The rendering of stirring events (Fig. 1) shows that the model reproduces a number of known features of turbulent shear flow structure. The initialization of turbulence along the fluid interfaces of highest shear is evident. Between the high-shear regions, the nonturbulent core of the inner jet and the pilot flow is delineated. Farther downstream the merging of these regions and the onset of a 'turbulent cascade,' with smaller eddies trailing larger ones, and associated 'spatial intermittency' are seen.

Comparison of ODT results with measurements in flames D, E and F are based on jet centerline profiles, radial profiles at various downstream distances and conditional pdf's at the corresponding downstream distances. Using the same model formulation and parameter values employed in a previous study of hydrogen-air flames [3], good agreement is obtained for the axial evolution of the mean and fluctuations of the scalars, including features of the rms fluctuations that reflect turbulence-chemistry interactions. However, the model predicts significantly less extinction than the experiment for flame F. Despite this limitation, which is also observed in condititional statistics and conditional pdfs based on radial profiles, reasonable agreement between computation and experiment is found.

Figure 2 shows the conditional pdfs of OH mass fraction at $x/d = 7.5$, 15, 30 and 45. As observed in the experiment [4], there is a discernable shift of OH means towards higher mass fractions as the Reynolds number is increased. The computations show some extinction, in particular in flame F, at x/d of 7.5. However, little extinction is detected in the computation at $x/d = 15$ and 30 in contrast with experimental observations [4]. Additional comparisons between experiment and computations are presented in the poster.

References

[1] Kerstein, A.R., One-Dimensional Turbulence: Model Formulation and Application to Homogeneous Turbulence, Shear Flows, and Buoyant Stratified Flows, in press *J. Fluid Mech.* (1999).

[2] http://www.princeton/~cklaw/kinetics/12-step.

[3] Echekki, T., Kerstein, A.R., Chen, J.Y., Dreeben, T.D., 'One-Dimensional Turbulence' Simulation of Turbulent Jet Diffusion Flames: Model Formulation and Illustrative Applications, submitted for publication to *Combust. Flame* (1999).

[4] Barlow, R.S. and Frank, J.H., Twenty-Seventh Symp. (International) on Combustion, the Combustion Institute, 1998, pp. 1087–1095.

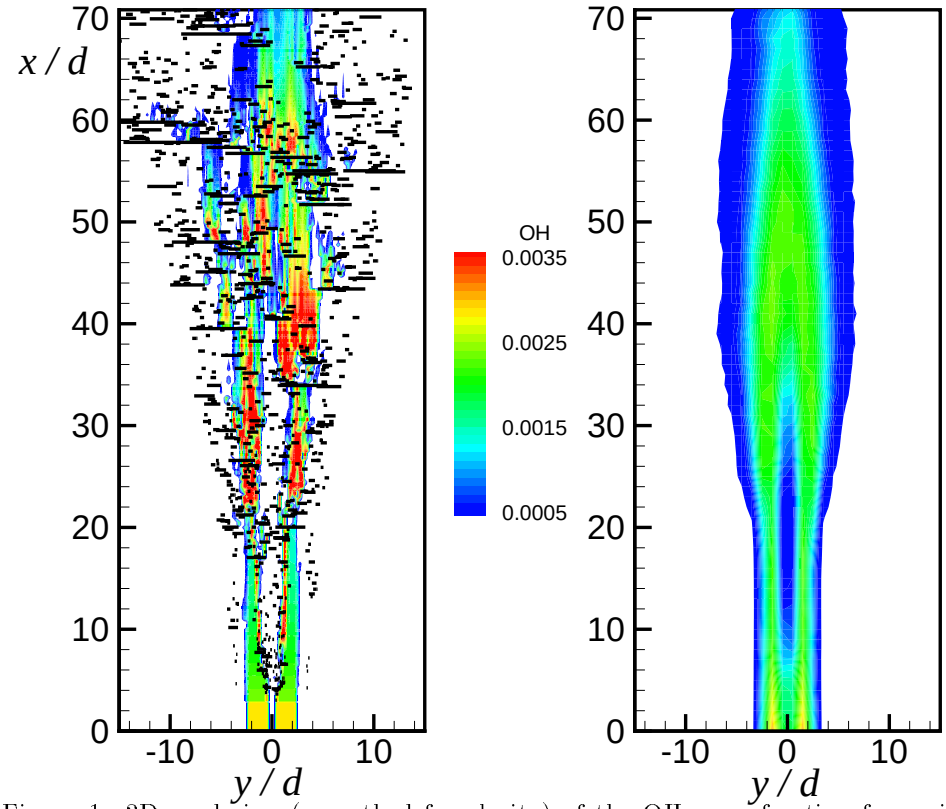

Figure 1: 2D rendering (smoothed for clarity) of the OH mass-fraction for a single realization (left) and for an average of 100 realizations (right) of flame F. Also shown on the single realization is a rendering of stirring events (horizontal line segments) that represent turbulent eddies in the simulations. The 1D domain corresponds to the y axis. Its temporal evolution is converted to downstream distance from the jet inlet, corresponding to the x axis.

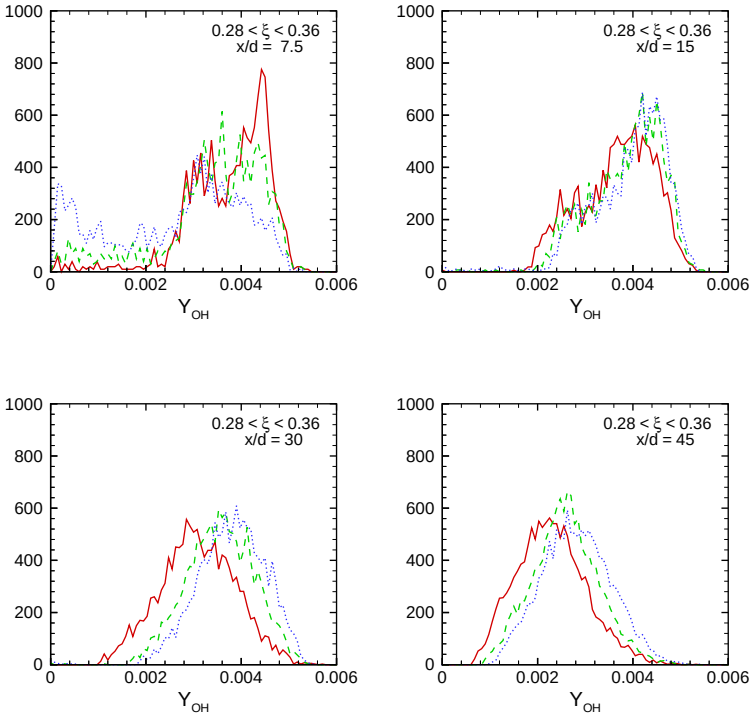

Figure 2: Conditional pdf's of OH mass fraction for flames D, E and F and downstream distances x/d = 7.5, 15, 30 and 45. (Solid): flame D, (Dashed): flame E, (Dotted): Flame F.

An Efficient Method for Large-Eddy Simulation of Turbulent Diffusion Flames

Hendrik Forkel, Johannes Janicka

Fachgebiet Energie- und Kraftwerkstechnik, Technische Universität Darmstadt
Petersenstr. 30, D–64287 Darmstadt, Germany

phone: +49-6151/16 2502, fax: +49-6151/16 6555, e-mail: ekt@hrzpub.tu-darmstadt.de
WWW: http://www.tu-darmstadt.de/fb/mb/ekt

Introduction

Large-eddy simulation (LES) is a method with great potential for the simulation of turbulent diffusion flames. Since velocity fluctuations are resolved down to filter width, an accurate description of mixing, the driving mechanism of combustion in such systems, is possible. Because LES of recting flows requires to address variations of density in time, a time integration procedure different from the constant density case is needed.

One possibility is to solve the equations for compressible fluids (e. g. [1]), but then the speed of sound puts limits on time step size and the numerical costs for simulations of low Mach-number flows are higher than for a method assuming incompressibility. In [2] an example for the latter is presented and applied to the simulation of a turbulent non-premixed flame, but *ad hoc* modifications were needed to stabilise the calculation. Considering the fact, that even recent papers on LES and combustion assume the density to be constant ([3], [4]), the lack of an efficient and stable method becomes clear.

In the current paper a time integration procedure for LES of incompressible, reacting flows is presented, that aims on overcoming the described deficiencies. The method has been used for the simulation of a turbulent hydrogen diffusion flame and by comparison with experimental data it will be shown, that a high grade of accuracy is achieved.

A LES Method for Non-Premixed Combustion

The method is based on the pressure correction scheme that is well known for LES of constant density flows, and extends it to handle spacial and temporal density variations. The local chemical composition of the fluid is described by solving a transport equation for the Favre-filtered (i. e. density weighted filtered) mixture fraction $\tilde{f}$. Density, viscosity, temperature and species mass fractions are evaluated assuming chemical equilibrium. Since the mixture fraction field can not be resolved completely, sub-grid fluctuations are taken into account. The shape of the sub-grid PDF is presumed (β-function) and the dependent scalars are evaluated as functions of $\tilde{f}$ and its sub-grid variance $\overline{f''^2}$. An approximation for $\overline{f''^2}$ is calculated from the resolved fluctuations. Density varies in time, so $\frac{\partial \bar{\rho}}{\partial t}$ does not vanish in the continuity-equation, but appears as a source in the Poisson-equation for pressure. Because the conserved scalar is $\overline{\rho f}$, not $\tilde{f}$, when integrating the mixture fraction equation in time, the need to split $\overline{\rho f}$ into $\bar{\rho}$ and $\tilde{f}$ arises. Hence, the non-linear equation

$$F\left(\tilde{f}\right) \equiv \bar{\rho}\left(\tilde{f}, \overline{f''^2}\right) \cdot \tilde{f} = \overline{\rho f} \tag{1}$$

has to be solved for every grid cell at each stage of the time integration.

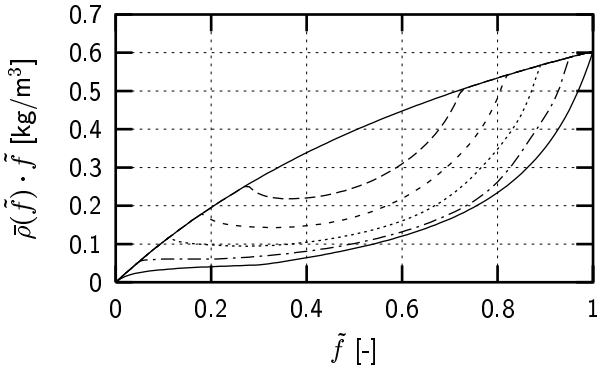

Figure 1: $\overline{\rho f}$ as a function of $\tilde{f}$ and $\overline{f''^2}$. lines bottom to top: $\overline{f''^2} = 0$, 0.05, 0.1, 0.15, 0.2, 0.25 (fuel: 50% vol. H_2 and N_2 each, oxidator: air)

F is not monotonous for some range of $\overline{f''^2}$ and there may be up to three solutions (figure 1). In order to find the physically correct one, the interval $[0, 1]$ is split into subintervals of monotonous F. Then for each subinterval the unique solution, if there is one, is determined. After doing this, all solutions of (1) are known and the one closest to $\tilde{f}^{\text{old}}$ at the last time step is chosen to be the new value. If all chemistry information is available from a pre-calculated table, this procedure can be implemented very efficiently, in particular the intervals of monotonous F can be calculated in advance.

Due to spatial discretisation of the transport equations using non-diffusive central schemes, high frequency errors are introduced to all quantities. Because acoustic modes are neglected according to the assumption of incompressibility, these are removed from density by relaxation in time. A relaxation time of $5 \cdot 10^{-4}$ seconds turned out to be adequate. It should be stressed, that the method for splitting up $\overline{\rho f}$ can be applied to other chemistry models as well, e. g. to the laminar flamelet approach, and is not restricted to equilibrium chemistry.

Application to a Test Case

The considered flow is a turbulent jet diffusion flame defined as test case "H3" for the Second International Workshop on Measurement and Computation of Turbulent Non-Premixed Flames [5]. A mixture of H_2 and N_2, 50% vol. each, is discharging from a circular nozzle (diameter $D = 8$mm) at 34.8 m/s into air co-flowing at 0.2 m/s. Reynolds-number is $\text{Re}_b = 10,000$. Experimental data and a detailed description of the setup is available from [6]. For the computation a zylindrical domain of $48.2D$ length and $30D$ radius was disretised using $257 \times 32 \times 60$ grid cells. In figure 2 the results achieved by LES utilising the presented method are compared to measurements. The agreement of axial and radial profiles is very good, though calculated temperature fluctuations near the axis are somewhat to high.

Conclusions

A method has been proposed for LES of reacting flows. Though density is assumed to be independent of pressure (incompressibility), its spacial and temporal fluctuations due to changing chemical composition and temperature are treated. The simulation of a well documented non-premixed flame veryfied that the method is capable of high accuracy.

The authors gratefully acknowledge the financial support of DFG "Graduiertenkolleg Modellierung und numerische Beschreibung technischer Strömungen" (contract no. GRK-91-1).

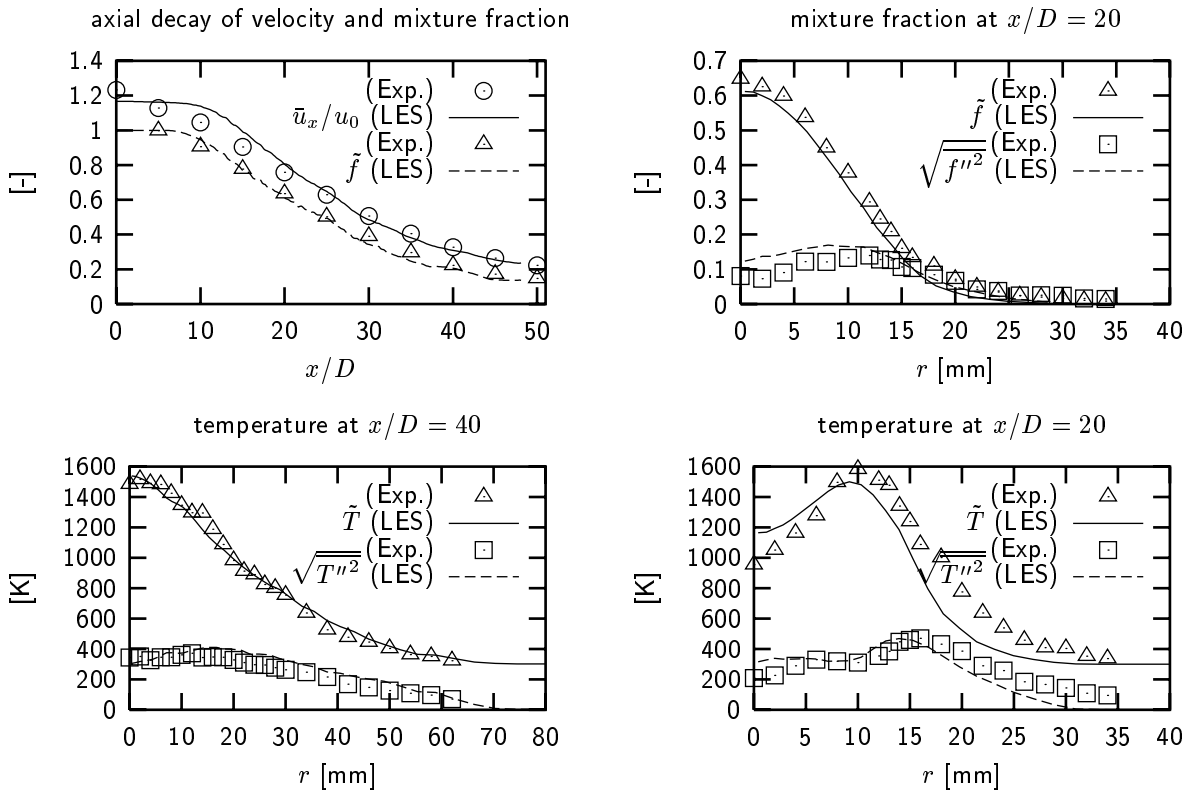

Figure 2: Scalars: Favre-means and resolved fluctuations. Axial decay and radial profiles at selected positions.

References

[1] Möller S.I., Lundgren E. and Fureby C., in *Twenty-Sixth Symposium (International) on Combustion*, pp. 241–248. The Combustion Institute (1996).

[2] Branley N. and Jones W.P., in *Proceedings of the Eleventh Symposium on Turbulent Shear Flows*, pp. 21-1 – 21-6, Grenoble, France (1997).

[3] Cook A.W. and Riley J.J., *Combustion and Flame* 112:593–606 (1998).

[4] Jaberi F.A., Colucci P.J., James S., Givi P. and Pope S.B., *J. Fluid Mech.* (1998), submitted.

[5] Barlow R., *International Workshop on Measurement and Computation of Turbulent Nonpremixed Flames*, http://www.ca.sandia.gov/tdf/Workshop.html ().

[6] Fachgebiet für Energie- und Kraftwerkstechnik, Technische Universität Darmstadt, http://www.tu-darmstadt.de/fb/mb/ekt/flamebase/Welcome.html, *Flame Data Base for Turbulent Nonpremixed Flames* (1997).

[7] Forkel H. and Janicka J., "Large-Eddy Simulation of a Turbulent Hydrogen Diffusion Flame," to be presented at the 1st International Symposium on Turbulence and Shear Flow Phenomena, Santa Barbara, CA, USA (1999).

Application of a Laminar Flamelet Model for Turbulent Combustion Simulations in a Gas Turbine Combustor

Graham M. Goldin, Ph.D.
gmg@fluent.com

Fluent, Inc.
10 Cavendish Court
Lebanon, NH 03766-1442

Accurate modeling of turbulent combustion remains a formidable task for CFD. In particular, addressing the coupling of turbulence and chemistry that exists via highly non-linear reaction rate terms is a key element in simulating these complex reactive systems. An increasingly popular strategy for modeling turbulent non-premixed combustion is to apply a conserved scalar or *mixture fraction* based approach, typically assuming equilibrium chemistry. By addressing the moments of thermodynamic and chemical quantities via an assumed-shape PDF formulation, turbulence-chemistry interactions may be treated formally. An extension of this mixture fraction approach for addressing non-equilibrium chemistry is referred to as the laminar flamelet model. By assuming a steady, laminar opposed-flow diffusion "flamelet" as the local, canonical structure governing combustion, local straining of the flame may be included in the analysis. Look-up tables and an assumed-shape PDF formulation analogous to those used in the equilibrium chemistry PDF approach are used. This approach allows non-equilibrium chemistry effects to be included in the analysis and can provide more accurate predictions of temperature and radical concentrations as well as indications of local extinction.

This poster presents results from the application of the laminar flamelet model in the software code FLUENT V5 to the GE LM-1600 gas turbine combustor. The annular combustion chamber consists of 18 non-premixed, natural gas swirl nozzles. The combustor produces 12.8 MW of power with a 19:1 pressure ratio at full load. Numerical simulations were performed on a 3-D, 20 degree sector consisting of 286,000 hexahedral cells in a multiblock structured arrangement. Turbulence closure was achieved using the standard k-ε model. Laminar flamelet calculations consisted of 22 chemical species and 104 elementary reactions modeled after the GRI-MECH 1.22 mechanism. Differential diffusion (*Le* effects) were included. Sub-equilibrium peak flame temperatures and super-equilibrium *O*-atom concentrations, consistent with observed influences of non-equilibrium chemistry, are seen in the laminar flamelet results. The effects of equilibrium chemistry departures are further demonstrated by comparisons of *NO* flux measurements exiting the combustor with numerical predictions for different combustor loads. *NO* post-processing results from the laminar flamelet simulations compare much better with experimental measurements than *NO* predictions from simulations using the equilibrium chemistry PDF approach.

The author would like to gratefully acknowledge the contributions of Nova Research and Technology, Calgary Canada, in preparing this work.

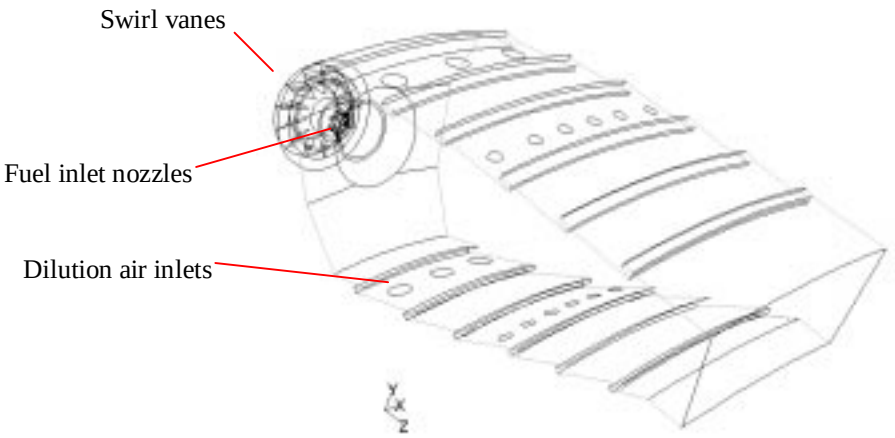

Figure 1. Combustor geometry.

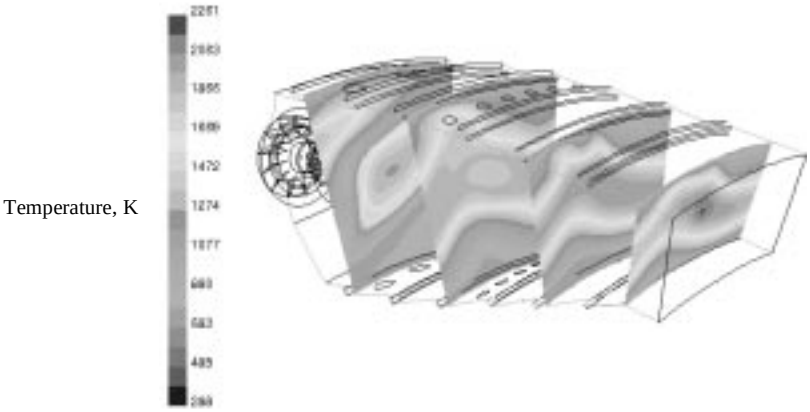

Figure 2. Contours of mean temperature (K) predicted by the laminar flamelet model (full load).

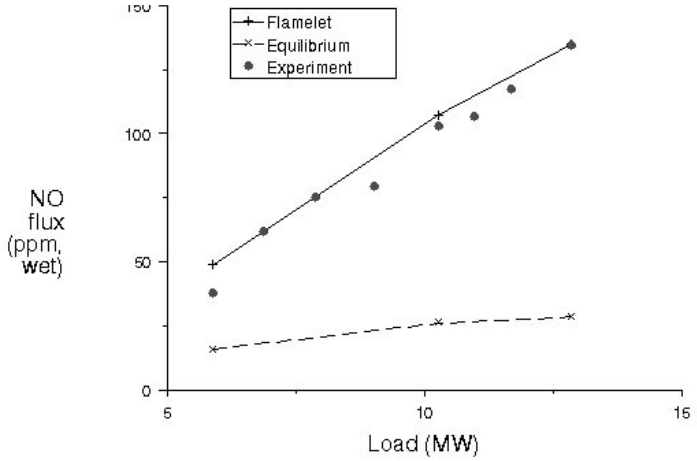

Figure 3. Plot of NO flux at the combustor exit versus load. Results are plotted for the laminar flamelet model, equilibrium chemistry PDF model and experimental measurements.

"One-Dimensional Turbulence" Modeling of Turbulent $CO/H_2/N_2$ Jet Flames

John C. Hewson, Tarek Echekki, and Alan R. Kerstein
Sandia National Laboratories, Livermore, CA 94551-0969

The one-dimensional turbulence (ODT) formulation of Kerstein [1] is used to model the spatial evolution of various jet flames studied in the present workshop series. The model resolves the full range of scales in a single dimension, providing exact treatment of chemical reaction and molecular mixing at Reynolds and Damkohler numbers not accessible to DNS. Advective processes are modeled as a stochastic process using triplet maps to emulate the effect of turbulent straining of the flow field. In this manner, turbulent mixing acts to steepen gradients in locally inhomgeneous regions. The ODT model incorporates two order-unity constants to relate the characteristic eddy rate to the local shear rate and the total elapsed time for nonstationary flows. The same values of these constants appear to give good results for jet flames of H_2/N_2, $CO/H_2/N_2$, and CH_4/air mixtures, though it may be possible to fine tune these constants through comparison with additional sensitive data.

This poster describes the modeling of the $CO/H_2/N_2$ flames A and B of Barlow et al [2]. These flames have the same Reynolds numbers (16700), but nozzle diameters differ by a factor of 1.7, and characteristic time scales (U/d) differ by a factor of 0.35. The present should be considered to be preliminary results as there are still unresolved issues related especially to the initial conditions.

The ODT calculation is carried out by evolving in time a series of one-dimensional Lagrangian fields and ensemble averaging the results. The initial time corresponds to the nozzle exit while downstream locations are found from an integral convective velocity. At the origin (nozzle) a laminar flame profile is mapped to a region approximately 2 mm wide corresponding to the thickness of the blunt nozzle wall to initialize the computation. The initial velocity profile corresponds, at present, to the normalized measured velocity profile for the ETH-Zurich 20% He/80%H2 flame.

Conditional means shown on the following page indicate quite reasonable agreement with measurements of Barlow et al [2]. Trends from flame A to B of higher temperatures, lower superequilibrium radical concentrations and less reactant leakage are correctly captured; the trends correspond to lower scalar dissipation rates in flame B. Evidence in the plots for x/d=40 indicates that the ODT predicts a scalar dissipation rate that is lower than the measurements. It is unclear whether this is attributable to the model constants or to the mapping from temporal to spatial locations. The latter possibility arises because agreement of ODT predictions at x/d=40 with measurements at x/d=50 is much better.

For flame A the ODT predicts some local extinction occuring primarily below x/d=10. By x/d=20, all stoichiometric mixtures have reignited and the only evidence of prior extinction is in lean pockets. This is evident in the conditional means for CO where some nonnegligible CO is observed to the lean side of stoichiometric. There are no measurements below x/d=20, but the measurements at x/d=20 do not show evidence of prior fuel leakage. These phenomena are much more evident in scatter plots to be shown on the full poster. Preliminary analysis indicates that local extinction may be sensitive to some of the model constants and also the viscous cutoff; it is also sensitive to the chemical mechanism. The model constants and the viscous cutoff affect the large and small (molecular) scale mixing rates, respectively.

References

[1] A. R. Kerstein. One-dimensional turbulence: Model formulation and application to homogenous turbulence, shear flows, and buoyant stratified flows. *J. Fluid Mech.*, accepted 1999.

[2] R. S. Barlow, G. J. Fiechtner, C. D. Carter, and J.-Y. Chen. Experiments on the scalar structure of turbulent $CO/H_2/N_2$ jet flames. *Combust. Flame*, submitted 1998. Also http://www.ca.sandia.gov/tdf/DataArch/SANDchnWeb/SANDchn.html.

Conditional Means for $CO/H_2/N_2$ Flames A and B
Measurements (symbols) taken from
http://www.ca.sandia.gov/tdf/DataArch/SANDchnWeb/SANDchn.html

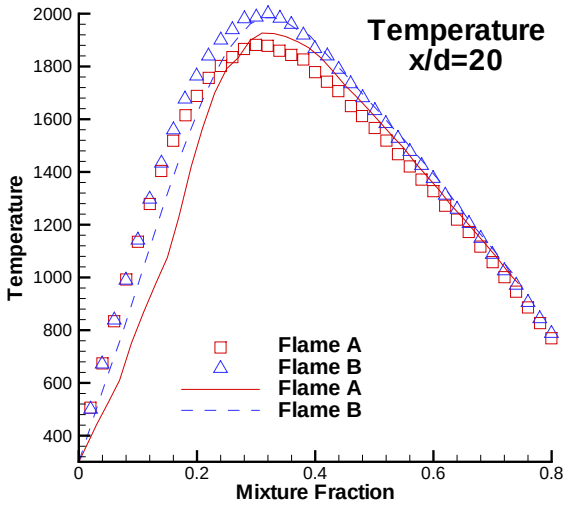

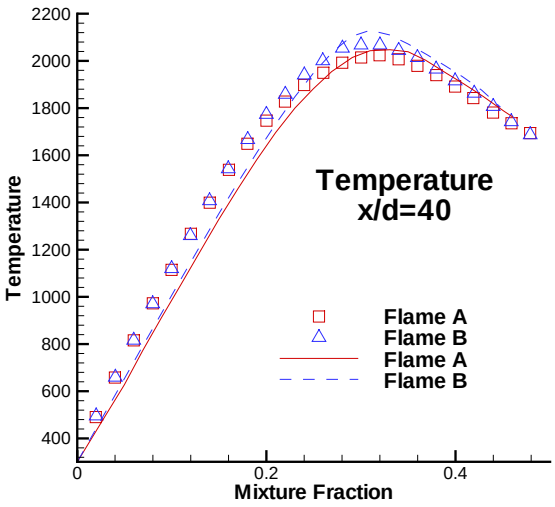

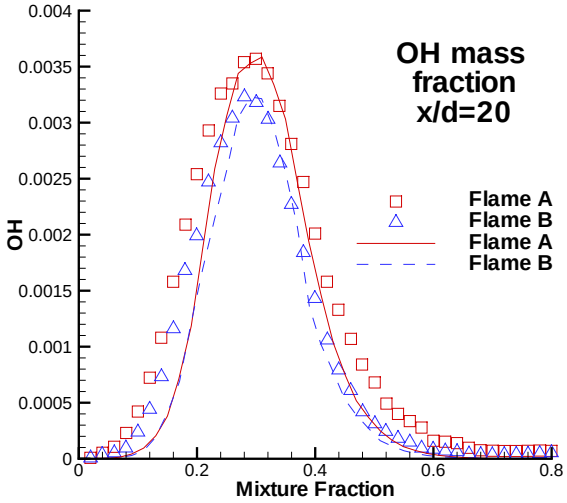

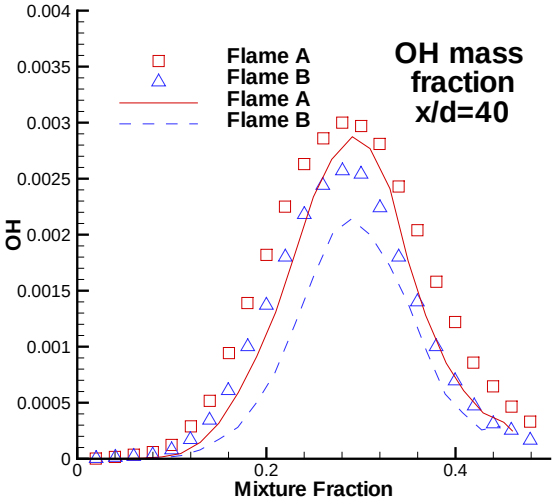

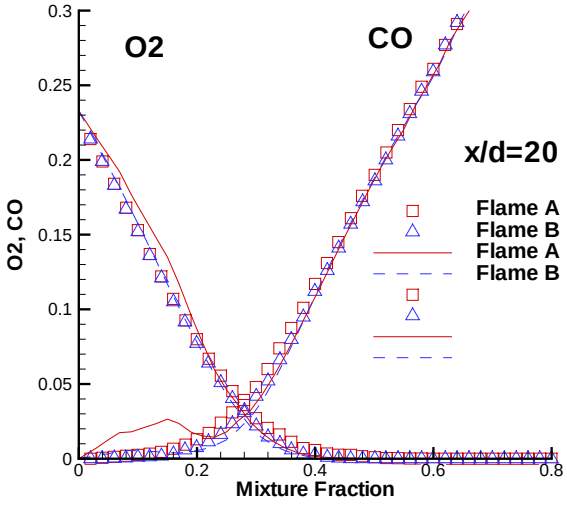

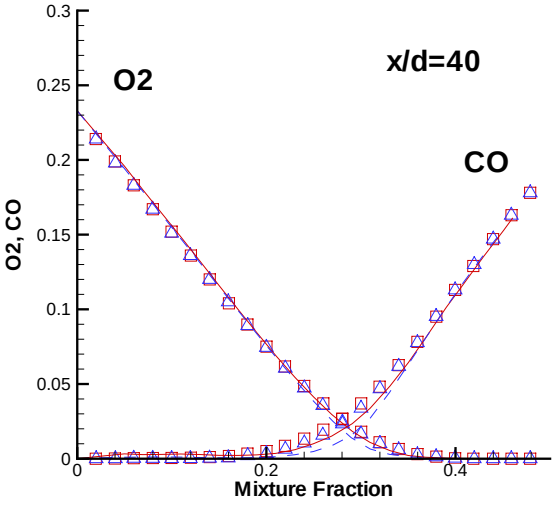

Numerical Investigation of Turbulent Piloted Methane / Air Jet Flames using Monte Carlo PDF Method

Alexander Hinz, Johannes Janicka

FG Energie– u. Kraftwerkstechnik, Technische Universität Darmstadt,
Petersenstr. 30, 64287 Darmstadt, Germany
phone: +49-6151/16 2502, fax: +49-6151/16 6555, e-mail: ekt@hrzpub.tu-darmstadt.de

The focus of this work is on the prediction of local extinction effects in turbulent jet diffusion flames. The series of the piloted methane / air flames (Flame D, E, F) [1] at increasing Reynolds number serve as subject of the investigation.

The method bases on the coupling of a Monte-Carlo code solving for the Eulerian composition PDF and a 2D elliptic finite-volume CFD code solving for the velocity field (Hybrid method). Besides a gradient diffusion approximation for the unclosed conditional expectation of velocity fluctuations, the following models are used throughout the investigations:

Diffusion in Scalar Space: Modified Curl model [2]: A number of particles is randomly picked out of the ensemble and pair-wisely mixed where the weighting factors are given by a random number between zero and one.

Chemistry Mechanism: Based on a Intrinsic-Low-Dimensional-Manifold (ILDM) [3] stored in a look-up table. Parameterization is given by mixture fraction f and reaction progress variables Y_{CO_2} and Y_{H_2O}.

Turbulence Model: Reynolds stress model by Jones and Musonge [4] in its modified version by Jones [5].

Assuming axis-symmetry, the grid consists of $N_x \times N_y = 80 \times 70$ nodes, condensed near the centerline and the burner, $L_x \times L_y = 140\,d \times 70\,d$. The computation takes about 100 h on an ALPHA lx533 including the process of evolving stably burning flame.

The detection of local extinction is based on scatter plots and conditional PDF's of temperature and mass fraction of H_2O, Y_{H_2O}. As a reference a flamelet solution with $a = 100 s^{-1}$ is added to the scatter plots. The analysis of the conditional PDF's reveals an increasing probability of lower temperature and water as the Reynolds number is raised.

REFERENCES

[1] Barlow R. and Frank J., in *Twenty-Seventh Symposium (International) on Combustion,* pp. 1087–1095. The Combustion Institute (1998).

[2] Janicka J., Kolbe W. and Kollmann W., *Journal of Non-Equilibrium Thermodynamics* 4:47–66 (1979).

[3] Maas U. and Pope S., in *Twenty-Fourth Symposium (International) on Combustion*, pp. 103–112. The Combustion Institute (1992).

[4] Jones W.P. and Musonge P., *Physics of Fluids* 31(12):3589–3604 (1988).

[5] Jones W.P., in Libby P.A. and Williams F.A., eds., *Turbulent Reacting Flows*, pp. 309–374, Academic Press, London, San Diego, New York (1994).

Conditional PDF's of Temperature and Y_{H_2O}

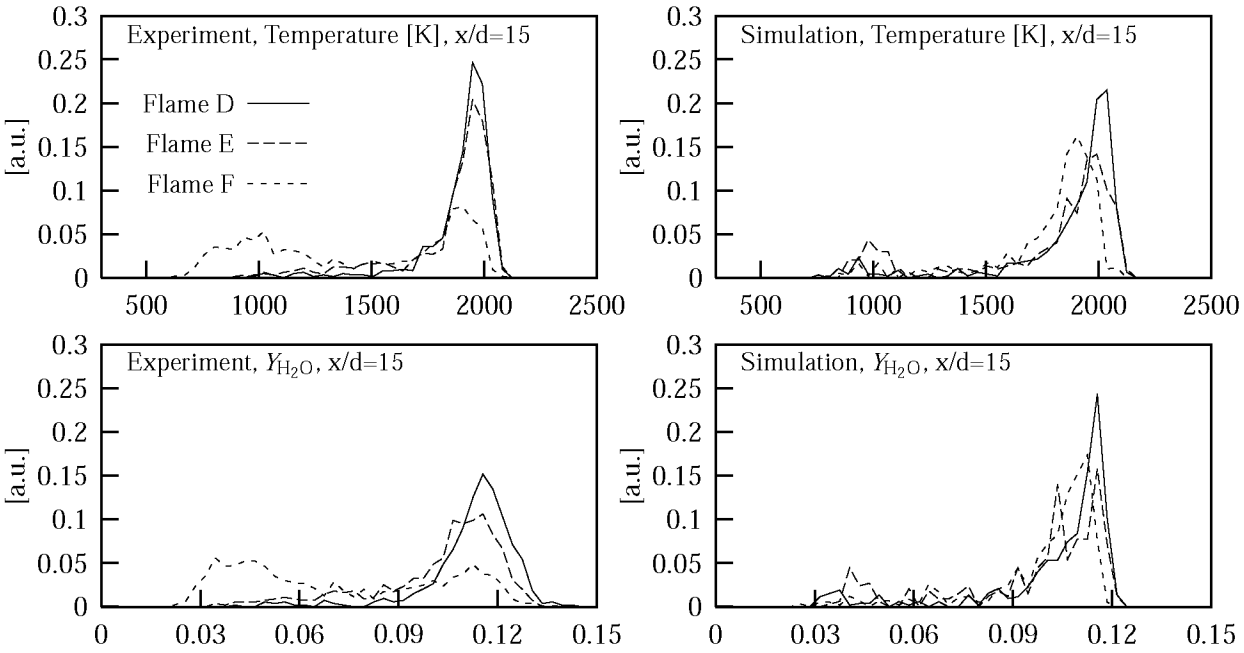

Scatter Plots of Temperature [K]

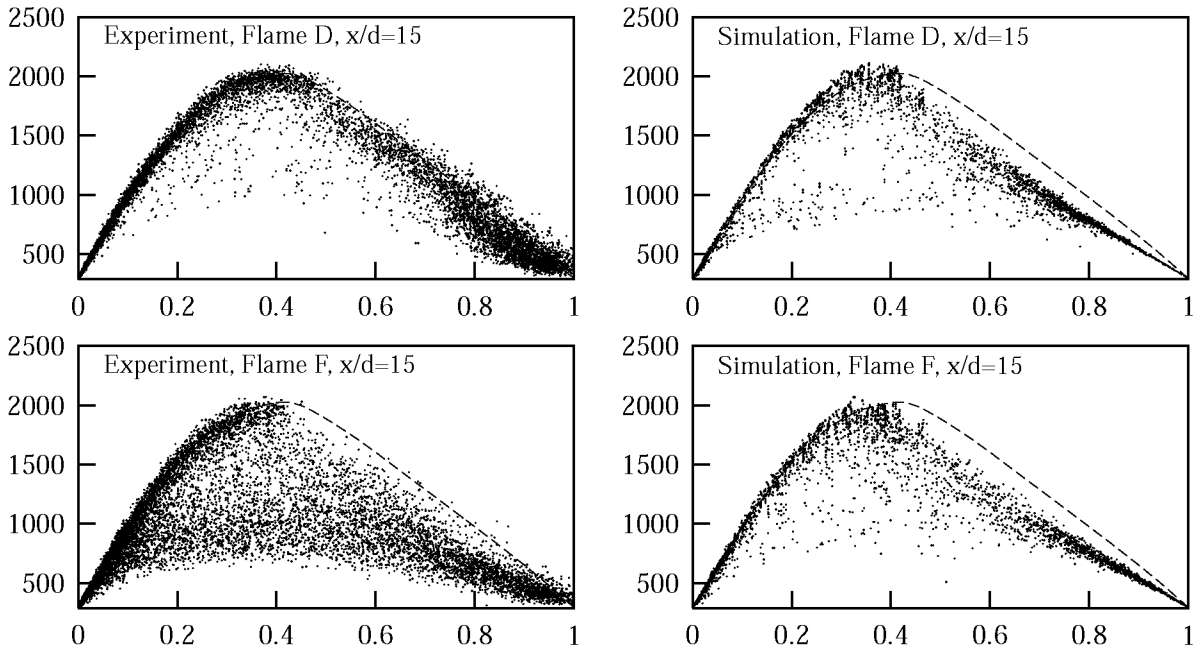

A Flamelet Model for Turbulent Spray Diffusion Flames Using a Laminar Spray Flame Library

C. Hollmann, E. Gutheil

Interdisziplinäres Zentrum für Wissenschaftliches Rechnen, Universität Heidelberg, Im Neuenheimer Feld 368, 69120 Heidelberg, Germany

A flamelet model for turbulent spray diffusion flames is presented that includes effects of vaporization in the formulation of the mixture fraction and its variance [1]. Furthermore, the model is extended to include laminar structures of spray flames to consider the effect of vaporization on the laminar flame structure. For fixed pressure and both temperature and composition of the inlet streams, the structure of laminar gas flames may be described by the mixture fraction and the strain rate; the structure of spray flames also depends on the initial droplet size, velocity, dispersity of the spray, and equivalence ratio at the spray inlet. The non-monotonicity of mixture fraction with space associated with the non-premixedness of air with gaseous fuel introduces additional requirements if laminar spray flames are to be considered in the turbulent spray flame model.

The presentation consists of two parts: First, the structure and extinction of laminar spray flames need to be precalculated. This includes the development of an appropriate model for these flames. Second, the turbulent spray diffusion flame is simulated where the flamelet model is incorporated.

The study concerns both structures of laminar spray flames and turbulent spray diffusion flames where the fuel methanol is used. The laminar flame structures are computed with a code that is developed by Gutheil and Sirignano [3]. It includes detailed transport as well as a detailed chemical reaction mechanism for methanol/air comprising 23 species and 168 elementary reactions [4]. The model is suitable to consider both mono- and polydisperse sprays [5].

Figure 1 presents the structure of a laminar spray flame where some characteristics discussed in the first section are shown. The scalar dissipation rate attains two local maxima where the one at the stagnation point is shifted to the air side of the configuration if droplets cross the stagnation plane as

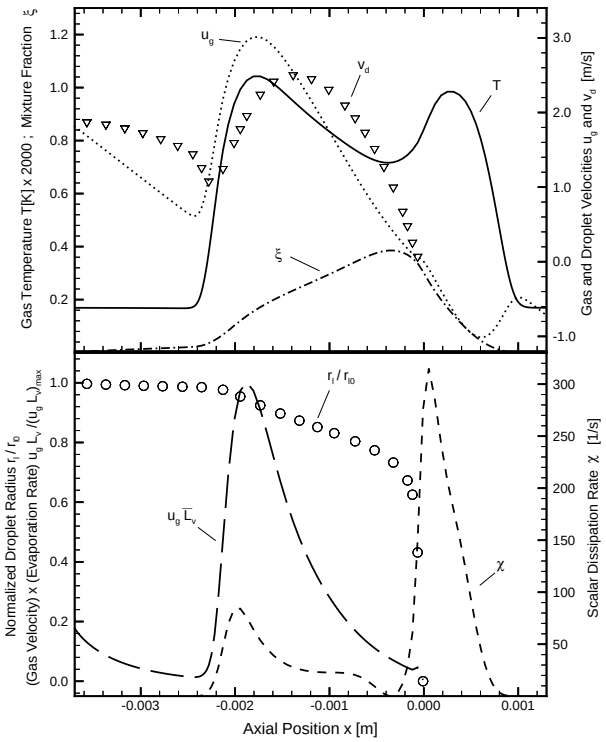

Figure 1: Structure of a laminar spray flame at elevated strain [2].

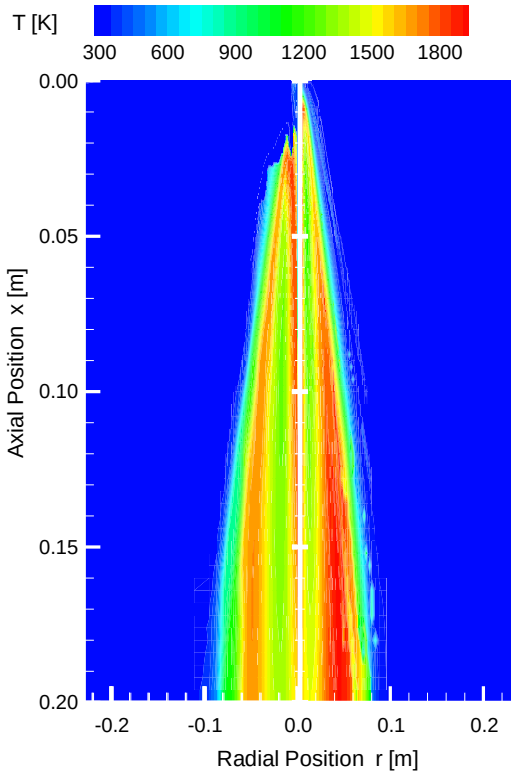

Figure 2: Flame structure of a turbulent spray jet flame [2] calculated with a laminar gas flame library (left) and with a laminar spray flame library (right).

extinction is approached. The laminar flame structure is spitted at the position where the maximum mixture fraction is located in order to introduce a well defined matching of laminar and turbulent flame characteristics. The left part is used where droplets are present in the turbulent flame, and the gas side of the laminar structure is employed where droplets have completely vaporized.

The structure of the turbulent jet flame obtained using laminar spray flame structures is shown in the right part of Fig. 2. It may be compared with the model including a laminar gas flame library (left part). The more advanced model is free of parameter adjustment, and it is suitable to predict the correct flame structure where the flame interacts with the spray close to the injector, at the centerline, and at the jet boundary. The model using a laminar gas flame library includes a cut-off temperature of 700 K which produces the artificial lift-off seen in the left part of Fig. 2. Moreover, the study shows a comparison of the results with experiments performed by McDonell and Samuelsen [6].

References

[1] Hollmann, C., Gutheil, E., *26th Symp. (Int.) on Combustion*, The Combustion Institute, Pittsburgh, 1687-1695, 1996.

[2] Hollmann, C., Gutheil, E., *Combust. Sci. and Tech.*, 135: 175-192, 1998.

[3] Gutheil, E., Sirignano, W. A., *Combust. and Flame*, 113: 92-105, 1998.

[4] Gutheil, E., *Combust. and Flame*: 93, 239-254 (1993).

[5] Schlotz, D., Gutheil, E., *Modeling of Laminar Mono- and Bidisperse LOX/H_2 Spray Flames for Cryogenic Condistions*, 15th ILASS Conference, Toulouse, July 5-7, 1999, France.

[6] McDonell, V.G., Samuelsen, G.S., *Detailed Data Set: PDI and IRES Measurements in Methanol Sprays Under Reacting and Nonreacting Conditions, Case A–C*, UCI Combustion Laboratory Report UCI–ARTR–90–17A–C, 1990.

4th International Workshop on Measurement and Computation
of Turbulent Nonpremixed Flames

The Time and Spatial Resolved Measurement of Flame Emission for Analysis Local Flame-Front Structure

Yuji IKEDA, Jun KOJIMA and Tsuyoshi NAKAJIMA,
Department of Mechanical Engineering, Kobe University

Summary

The turbulence-chemistry interaction is central to understanding turbulent combustion. Various efforts have been made to investigate the turbulence characteristics and reaction rate in turbulent premixed and nonpremixed flames. In order to understand physics of turbulent combustion it has been carrying out by numerous laser techniques such as LDV, PDA, PIV, LIF, CARS and so on. Mixture fraction, temperature and flame front structure can be measured by these laser diagnostics in spite of their large body. Especially, LIF took a great part of combustion diagnostics that can show a radical concentration such as OH and CH, and its flame shape [(1)], but is incapable of observing flame front movement or measuring its velocity, due to the low frequency of the laser pulses. For understanding of chemical reaction rate and fine spatial flame front structure, many spectroscopic measurement of flame emission such as OH*, CH* or C2* have been applied for, however, the conventional spectroscopic methods can observe not local field but whole field of flame emission zone. So that the fundamental previous combustion spectroscopic method [(2)] could not describe local turbulence-flame interaction and its evolution in time.

We have been focusing on detail measurement of flame spectra in time series with a developed Cassegrain Optics [(3)], which has very small measurement volume less than 100μm in diameter at a local point. Local chemiluminescence measurement combined with LDV or PIV can allow us to examine the local structure and intensity of the local OH*,CH* and C2* reaction zone with turbulent scale and its intensity in time series.

In our previous study, the local chemiluminescences measurement of OH*, CH* and C2* were carried out in a fundamental bunsen laminar and turbulent premixed methane flames (Re<14000) and internal combustion engines. The profile of OH*,CH* and C2* radical and its dependence on equivalence ratio were examined in a laminar premixed flame, and also the local flame front thickness and local flame velocity in a certain intensity of turbulence were determined in a turbulent premixed flame, and then flame propagation speed and its flame structure could be observed in a SI engine[(4)].

In the present study, we tried to apply this local spectroscopy method to fundamental diffusion flame (weak turbulence) and to illustrate the structure of local reaction zone compared with that of premixed flame. Figure 1 shows the comparison with the flame emission spectra at certain local point (spatial resolution: less than 0.1mm) and that from the bulk of burner rim. Intensity peak of OH*, CH* and C2* emission can be observed with a certain level of background emission in the bulk emission spectra, which results from high temperature or soot flame, but only clearly strong peak of OH*, CH* and C2* emission were observed in local flame spectra. Figure 2 shows that the local flame spectra at different point in diffusion flame. The intensity of OH* and CH* emission become lower as measurement point shift to upper position. It means the local reaction process and temperature are different according to location in a flame. Figure 3 shows the intensity profiles of chemiluminescent radicals in a laminar diffusion flame. It is clearly show that the intensity distribution of OH*, CH* and C2* are different from each other at all location.

As conclusions, it is found that the local reaction rate or radical distribution can be examined using local chemiluminescence measurement. This method is valuable for local interaction between turbulent diffusion and chemical reaction in nonpremixed flame.

(1) Nguyen, Q.-V. and Paul, 26th Symposium (International) on Combustion, pp.-357-364, 1996.
(2) Gaydon, A.G., The *spectroscopy of flames* , Chapman and Hall, 1957.
(3) Akamatsu, T., Wakabayashi, T., Tsushima, S., Katsuki, M., Mizutani, Y., Ikeda, Y., Kawahara, N. and Nakajima, T., *Measurement Science Technology*, 1999, submitted.
(4) Ikeda, Y., Ichi, S., Nakai, H. and Nakajima, T., The Fourth International Symposium on Diagnostics and Modeling of Combustion in Internal Combustion Engines, COMODIA98, pp.411-416, 1998.

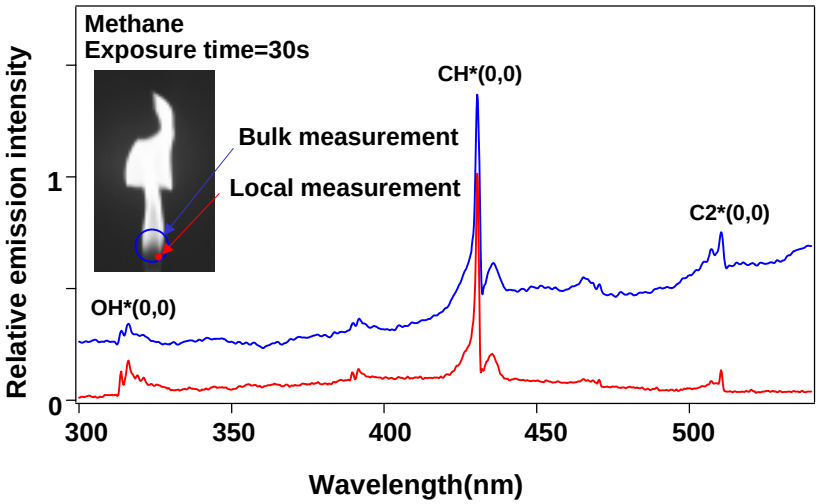

Fig.1 Flame spectra at a local point and the bulk of flame zone in a diffusion flame

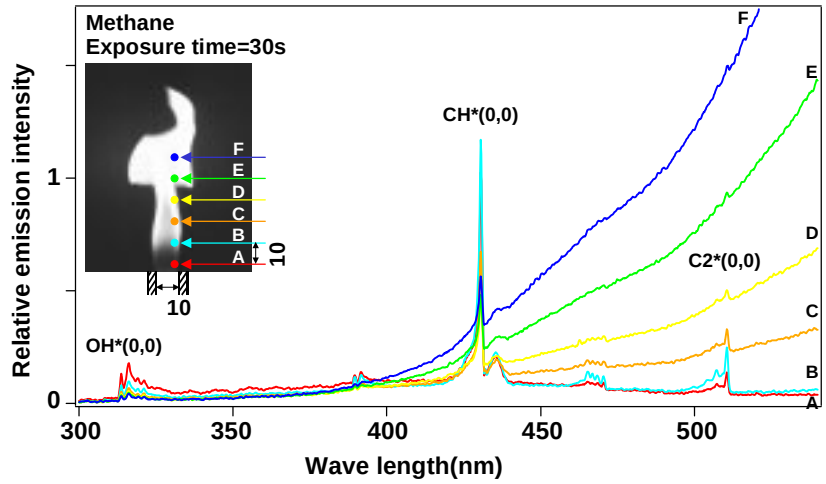

Fig. 2 Local flame spectra at different positions in a diffusion flame

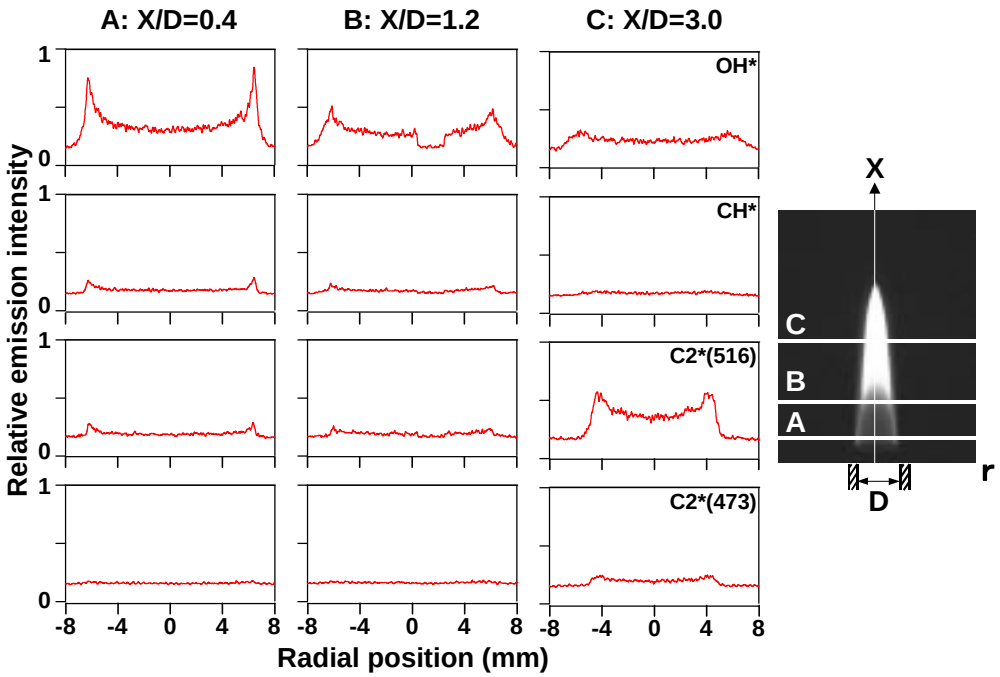

Fig. 3 Distribution of chemiluminescent radicals in laminar diffusion flame

Towards PDF Simulations of Complex Reacting Flows- A Consistent Hybrid Algorithm

Patrick Jenny, Metin Muradoglu, Stephen B. Pope and David A. Caughey

Sibley School of Mechanical and Aerospace Engineering

Cornell University

Ithaca, NY 14853

Abstract

Accurate simulations of turbulent recirculating flows like the bluff body stabilized flow provide a great challenge for turbulence models and since many flow problems of this type are found in industry a considerable effort has been made to improve the predictions. Here the suitability of PDF (probability density function) methods for this class of problems is investigated and a new hybrid algorithm to solve the joint velocity-frequency-composition PDF transport equation is presented.

Opposed to second moment closure models PDF methods have the great advantage that the turbulent transport and the chemical source terms are in closed form and do not have to be modeled[1]. Furthermore the full shape of the PDF is considered, not only first and second statistical moments. Since the PDF evolves in a high dimensional space it is in general infeasible to use finite volume or finite difference schemes and therefore particle methods (which are much better suited for high dimensional problems) are widely used for PDF simulations[2].

Although stand alone particle algorithms for joint velocity-frequency-composition PDF methods have been successfully applied to simulate numerous reacting and non-reacting flow problems of industrial interest, such simulations are relatively expensive due to the

large number of particles which is necessary to reduce the statistical error and the bias error[3]. To improve the efficiency and to make the method feasible for more complex flows a new hybrid algorithm has been developed. The same joint PDF transport equation is solved, but the mean density, the Favre averaged velocity and the Favre averaged sensible total energy per unit volume are computed separately (by solving the Reynolds averaged Navier-Stokes equations using a finite volume scheme; the turbulent fluxes, the energy source term of the chemical reactions and the thermodynamic properties of the fluid are computed by a particle method). In general these fields are much smother than the corresponding ones extracted from the particles and, if used in the particle method, the statistical error can be reduced significantly. A time averaging scheme allows not only to further reduce the statistical error, but also the bias error is reduced. The hybrid algorithm can be described as follows: First the particle and finite volume data are initialized. Then the finite volume scheme is advanced by n_{fv} sub steps before the particle method is advanced by $n_{particle}$ sub steps. Then first and second moments are extracted from the new particle field and a time averaging technique is applied. Unless the algorithm has reached statistically stationary state a further loop starting with the finite volume scheme is performed, while the new time averaged fields are used. The algorithm is called loose coupled, if $n_{fv,particle} > 1$ and tight coupled, if $n_{fv,particle} = 1$. The optimal choice of n_{fv} and $n_{particle}$ is one subject of our further research. The details of the hybrid method can be found in [4].

To compare the performance of the new hybrid algorithm (tight coupled) with a stand alone particle method asymptotic studies of both algorithms have been performed (using the same piloted jet flame test case and the same models) and it is shown that for a given accuracy the hybrid algorithm is approximately 20 times faster. The robustness of the scheme is demonstrated by inert bluff body stabilized flow simulations. Although a relatively simple velocity model is applied the results compare very well with experiments. This

test case shows that PDF methods are a very promising approach for complex turbulent flow simulations.

References

[1] S.B. Pope, PDF methods for turbulent reactive flows, *Prog. Energy Combust. Sci.* **11**, pp.119-192 (1985)

[2] S.B. Pope, Lagrangian PDF methods for turbulent flows, *Ann. Rev. Fluid Mech.* **26**, pp.23-63 (1994)

[3] J. Xu and S.B. Pope, Numerical studies of PDF/Monte Carlo methods for turbulent reactive flows, *J. Comput. Phys.* (Accepted for publication) (1998)

[4] P. Jenny, S.B. Pope, M. Muradoglu and D.A. Caughey, A Hybrid Algorithm for the Joint PDF Equation of Turbulent Reactive Flows, *submitted to Journal of Computational Physics* **1999**.

Spontaneous Raman Scattering in Confined Swirling Natural Gas Flames: Temperature and Species Concentrations from the TECFLAM Burner

Olaf Keck, Wolfgang Meier, Winfried Stricker

Institut für Verbrennungstechnik
DLR Stuttgart, Pfaffenwaldring 38, D-70569 Stuttgart

Summary

Swirling flows allow a fast and efficient mixing of fuel and oxidizer and are, thus, often applied in practical systems. On the other hand, a number of problems arise in the mathematical simulation of these flames and the improvement of CFD codes is a challenge in modern combustion research. The main goal of this work has been a comprehensive qualitative and quantitative characterization of confined swirling diffusion flames with different swirl numbers and air/fuel ratios. The experimental data from these well-defined flames form the basis of a better understanding of the behavior of swirling flames and the improvement of theoretical models.

The measured data sets consist mainly of the joint probability density functions (PDFs) of the temperature, mixture fraction, and major species concentrations determined by spontaneous Raman scattering. The overall behaviour of the flames and effects like unreactedness and temperature depression due to the cooling of hot products by wall contact are discussed.

Burner and Flames

Swirling natural gas/air flames with a thermal load of 150 kW were stabilized in the confined TECFLAM swirl burner [1]. Natural gas and swirling air are supplied to the flame through annular nozzles with i.d. 20 mm, o.d. 26 mm, and i.d. 30 mm, o.d. 60 mm, respectively. The amount of swirl, i.e. the swirl number of the air stream, can be changed by a movable block inside the burner [2]. Flames with an overall air/fuel ratio of 1.2 and swirl numbers 0.9, 1.13, 1.4, and 1.8 have been investigated in detail.

The water cooled burner housing has an inner diameter of 500 mm, a height of 1200 mm, and a top with an annular slit for the exhaust gas. The optical access is provided by four quartz windows.

Measuring Technique

Sponteneous Raman scattering has been applied to simultaneously determine the temperature and the species concentrations of CH_4, H_2, O_2, N_2, H_2O, CO_2, and CO in pointwise single shot measurements with a spatial resolution of 0.6 mm. Because all major species have been detected, the mixture fraction could also be deduced from the experimental data. The excitation source was a flashlamp pumped dye laser (λ=489 nm, 2 μs pulse duration, 2.5 J pulse energy) and the scattered light

was detected by an array of 10 photomultiplier tubes after wavelenghts separation in a spectrograph [3].

The experimental setup and the calibration and correction procedure have been optimized to achieve highly accurate and reliable data. The flames were investigated at typically 120 locations. At each location 300 single-pulse measurements were performed from which the joint PDFs were determined.

Results

In order to yield a general quantitative characterization of the flames, radial profiles of the mean values and rms fluctuations of the temperature, concentrations, and mixture fractions have been extracted from the PDFs at 8 different heights. These profiles reflect, for example, the position and downstream development of the mixing zone, the turbulence intensity, and the overall temperature level. The two recirculation zones of the flames, i.e. the inner one near the flame axis and the burner mouth and the outer one which reaches from the flame region to the burner walls, can be clearly distinguished in the profiles. The inner one exhibits temperatures close to 2000 K and near stoichiometric burnt mixtures, whereas the outer one contains exhaust gas with temperatures around 1200 K and with a mixture fraction value that corresponds to the air/fuel ratio of 1.2.

A deeper insight into the turbulence-chemistry interaction and the thermochemical state of the flame was gained from the correlations between various quantities. The scatterplots of temperature vs. mixture fraction revealed, for instance, the coexistence of unreacted fuel and oxidizer, even for stoichiometric mixtures in regions of intensive mixing. Furthermore, the temperature reduction due radiation, flame stretch, and wall contact could be quantified from these correlations.

For a swirl number of 1.8 the average temperature is 100 - 200 K lower than in flames with lower swirl numbers. This effect is explained by a faster mixing and the small influence of higher strain rates. In addition, the poster will discuss comparisons between our data and theoretical and experimental results obtained by other research groups for identical flames.

[1] www.tu-darmstadt.de/fb/mb/ekt/tecflam/

[2] F. Holzäpfel, B. Lenze, W. Leuckel: Twenty-Sixth Symposium on Combustion/The Combustion Institute, p.187 (1996)

[3] V. Bergmann, W. Meier, D. Wolff, W. Stricker: Appl.Phys. B 66, 489 (1998)

Modelling of turbulence-chemistry interaction with a multivariate presumed β-PDF method

Tilo Landenfeld, Johannes Janicka

FG Energie– u. Kraftwerkstechnik, Technische Universität Darmstadt,
Petersenstr. 30, 64287 Darmstadt, Germany
phone: +49-6151/16-2157, fax: +49-6151/16-6555, e-mail: ekt@hrzpub.tu-darmstadt.de

A turbulence-chemistry interaction model based on presumed probability density functions (PDF) has been developed. It is capable of predicting major and minor species distributions in turbulent diffusion flames. However, favourable CPU time requirements from simpler approaches are retained opposed to the clearly more expensive PDF methods.

The approximation of the joint PDF as a product of one-dimensional β-PDF's (see Janicka and Kollmann [1]) is enabled by normalization of the composition space. Hereby, the assumption of statistical independence of the composition space variables is validated by a statistical analysis of a Monte Carlo PDF simulation (see Landenfeld *et al.* [2] and figure 1). Combined with a reduced mechanism using intrinsic low-dimensional manifolds (ILDM), the method has been successfully applied to model the turbulent mixing and scalar field of a turbulent piloted methane/air flame (flame D, see Barlow and Frank [3]). Assuming axis-symmetry, the grid consists of $N_x \times N_y = 80 \times 70$ nodes, condensed near the centerline and the burner, $L_x \times L_y = 140\,d \times 70\,d$. Results of the simulations in form of conditional means of scalars are compared to experimental data (figure 2).

The applied sub-models can be summarized:

Turbulence Model: The second order moment closure of Jones and Musonge [4] in its revised form [5] is employed to model this redistribution term. The model of Daly and Harlow [6] for the turbulent transport and the model of Jones [7] for the fluctuating density-velocity correlation are used.

Chemistry Mechanism: Based on an Intrinsic-Low-Dimensional-Manifold (ILDM), a method developed by Maas and Pope [8], thermochemical properties are stored in a look-up table. Parameterization is given by mixture fraction f and reaction progress variables Y_{CO_2} and Y_{H_2O}.

Turbulence-Chemistry Interaction: The composition space $\boldsymbol{\phi} = (f, Y_{CO_2}, Y_{H_2O})$ is transformed via the normalizing relation $Y^*_\alpha = Y_\alpha / Y_{\alpha,\mathrm{eq}}(f)$, where the index eq denotes the value adopted in the fast chemistry limit. The PDF integration $\tilde{\varphi} = \int \varphi(\phi^*)\tilde{P}(\phi^*)\, d\boldsymbol{\phi}^*$ with a presumed PDF, its shape given alternatively by

- $\tilde{P} \approx \tilde{P}_\beta(f)\tilde{P}_\beta(Y^*_{CO_2})\tilde{P}_\beta(Y^*_{H_2O})$ (complete statistics) or
- $\tilde{P} \approx \tilde{P}_\beta(f)\tilde{P}_\delta(Y^*_{CO_2})\tilde{P}_\delta(Y^*_{H_2O})$ (reduced statistics),

is performed as pre-processing and stored in a look-up table. In the CFD code transport equations for means and variances of $\phi_j = (f,$ Y_{CO_2} and $Y_{H_2O})$ are solved. The thermochemical properties such as density $\overline{\rho}$ and chemical source terms $\overline{\dot{w}}$, needed within the CFD run, are economically accessed through linear interpolation from the look-up table. Details are given in Hinz *et al.* [9].

The conditional means shown in figure 2 are evaluated with

$$\langle \varphi | f = \zeta \rangle = \frac{\sum_j \langle \varphi(r_j) | f = \zeta \rangle P_f(r_j, \zeta)}{\sum_j P_f(r_j, \zeta)} \quad \text{with} \quad \langle \varphi(r_i) | f = \zeta \rangle = \int \varphi(Y_\alpha^*) P_{Y_\alpha^*} \, dY_\alpha^* \, .$$

REFERENCES

[1] Janicka J. and Kollmann W., *Combust. Flame* 44:319–336 (1982).

[2] Landenfeld T., Hinz A. and Janicka J., in *Joint Meeting of the British, German and French Sections*, pp. 1–3, Nancy (1999), The Combustion Institute.

[3] Barlow R.S. and Frank J., in *Twenty-Seventh Symposium (International) on Combustion*, pp. 1087–1095. The Combustion Institute (1998).

[4] Jones W.P. and Musonge P., *Phys. Fluids* 31(12):3589–3604 (1988).

[5] Jones W.P., in Libby P.A. and Williams F.A., eds., *Turbulent Reacting Flows*, pp. 309–374, Academic Press, London, San Diego, New York (1994).

[6] Daly B.J. and Harlow F.H., *Phys. Fluids* 13(11):2634–2649 (1970).

[7] Jones W.P., in *Prediction Methods for Turbulent Flows*, vol. 1979-02, Von Karman Institute for Fluid Dynamics (1979).

[8] Maas U. and Pope S.B., *Combustion and Flame* 88:239–264 (1992).

[9] Hinz A., Landenfeld T., Hassel E.P. and Janicka J., in Rodi W. and Laurence D., eds., *Engineering Turbulence Modelling and Experiments*, vol. 4, pp. 831–840 (1999).

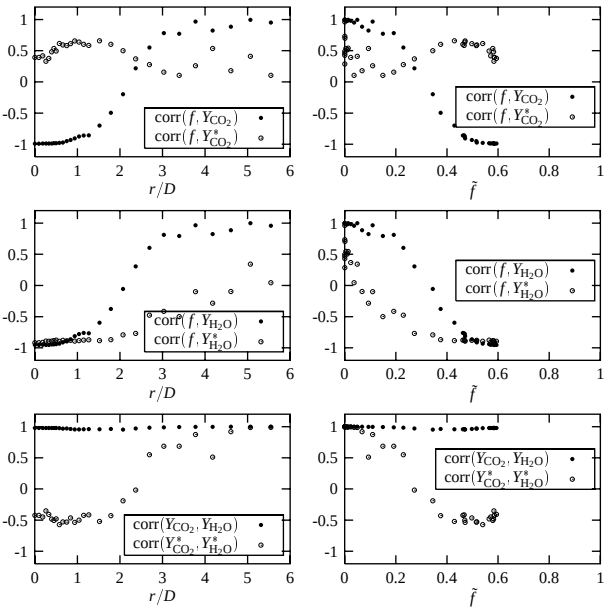

Figure 1: Correlation coefficient $\mathrm{corr}(\phi_1, \phi_2) = \widetilde{\phi_1'' \phi_2''} / (\widetilde{\phi_1''^2} \widetilde{\phi_2''^2})^{1/2}$ evaluated for normalized and unaltered composition space at plane $x/D = 30$.

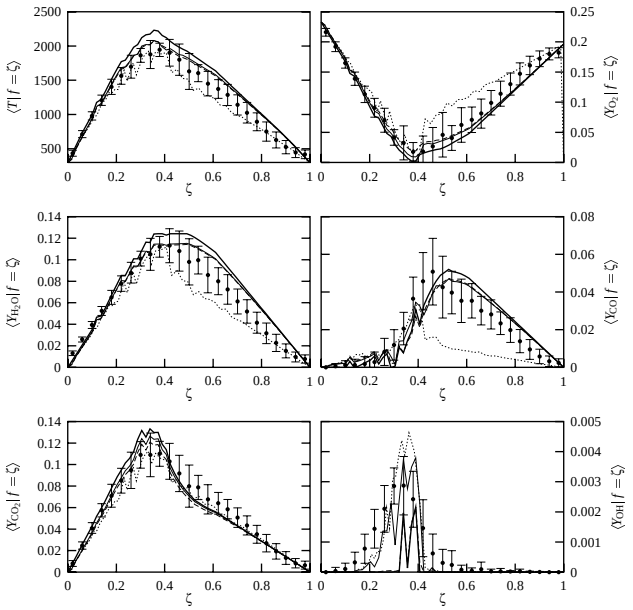

Figure 2: Conditional means of mass fractions and temperature at plane $x/D = 15$ (——, complete statistics; – – –, reduced statistics; - - - -, Monte Carlo PDF; ——, equilibrium chemistry; •, experiment with rms).

Joint scalar PDF Monte Carlo simulations of CH_4/Air turbulent jet diffusion flames with comprehensive chemistry

R.P.Lindstedt, S.A.Louloudi and E.M.Vaos

e-mail:p.lindstedt@ic.ac.uk

Imperial College of Science,Technology and Medicine
Mechanical Engineering Department
London SW7 2BX, U.K.

Two piloted *CH_4:Air* turbulent diffusion flames investigated experimentally by Barlow and co-workers [1,2] have been modelled using a transported Probability Density Function (PDF) approach closed at the joint scalar level. The flames have Reynolds numbers of ∼22400 (Flame D) and ∼44800 (Flame F) respectively. The burner geometry features axisymmetric fuel jets with mean velocities of 63.1 and 126.2 m/s and an ambient air-coflow of 0.9 m/s. Both flames are stabilised by a fuel-lean (ϕ=0.77) premixed pilot flame with a velocity of 11.4 m/s.

In the present study the velocity field is modelled using the SSG (Speziale, Sarkar and Gatski [3]) second moment closure. The $C_{\epsilon 2}$ constant in the dissipation rate equation is adjusted from 1.92 to 1.8 in order to improve the predicted spreading rate. Scalar mixing is modelled using the modified Curl's model of Janicka and Kollmann [4]. The equations are solved using a Monte Carlo approach featuring moving particles in a Lagrangian frame (eg. Hulek and Lindstedt [5]). The flames are assumed adiabatic and computed using an implicit parabolic formulation with 70 cross stream cells with each containing on average 600 (Flame D) or 800 (Flame F) particles. About 10000 axial steps are used to cover 80 jet diameters. The approximate CPU time is two weeks with 800 particles/cell and the time is reduced to 2 days with 100 particles/cell. The chemistry [6] is based on the work of Lindstedt and co-workers [7,8] and the systematically reduced form used in the present work features 48 species of which 16 are treated as independent scalars.

The agreement with experimental data is mostly excellent. Conditional averages of experimental and computational (40 bins) mass fractions are presented for *CH_4, CO, O_2, OH, CO_2* and *NO* in Figs. 1-2.

Encouragingly, the predicted CO levels at x/D=7.5 and x/D=15 coincide with the experimental data and, in addition, the OH level is in very good agreement with the measurements. The NO concentrations at x/D=7.5 are also in excellent agreement with data. Further downstream, however, NO levels are overpredicted by up to a factor of ~ 3 (e.g. x/D=15). The latter overprediction may predominantly be attributed to the adiabatic assumption leading to excessive temperatures as shown in Fig. 3.

References

[1] Barlow, R.S. and Frank, J.H., 27^{th} *Symposium (Int.) on Combustion*, pp.1-17 (1998).
[2] www.ca.sandia.gov/tdf/Workshop.html
[3] Speziale, C.G., Sarkar, S. and Gatski, *JFM* 227:245-272 (1991).
[4] Janicka, J. and Kollmann, W., *J. Non-equilib. Thermodyn.* 4-47 (1978).
[5] Hulek, T. and Lindstedt, R.P, *Combust. Sci. Tech.* 136:303-331 (1998).
[6] Leung, K.M. and Lindstedt, R.P., *Brite Euram Contract 95-0056, Final Report,* April 1999.
[7] Sick, V., Hildenbrand, F. and Lindstedt, R.P., 27^{th} *Symposium (Int.) on Combustion*, pp.1401-1409(1998).
[8] Juchmann, W., Latzel, H., Shin, D.I., Peiter, G., Dreier, T., Volpp, H.R., Wolfrum, J., Lindstedt, R.P. and Leung, K.M., 27^{th} *Symposium (Int) on Combustion*, 469-476 (1998).

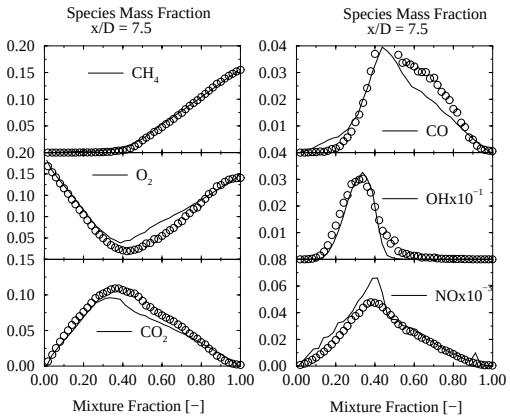

Figure 1: *Radial species profiles in mixture fraction space at x/D=7.5. The circles and lines are conditional averages of experimental [2] and computed data.*

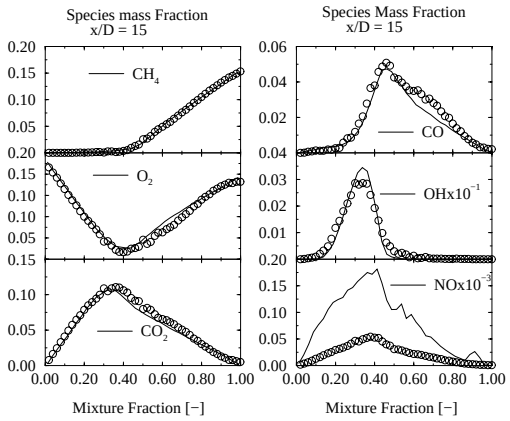

Figure 2: *Radial species profiles in mixture fraction space at x/D=15. The circles and lines are conditional averages of experimental [2] and computed data.*

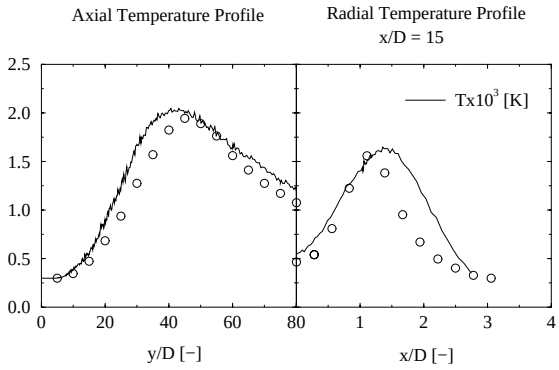

Figure 3: *Axial and radial temperature profile at x/D=15 in mixture fraction space. The circles and lines represent experimental [2] and computed data.*

Computation of bluff-body inert and reactive flows

Aristide Mbiock, Tim Peeters and Dirk Roekaerts
Thermal and Fluids Sciences, Delft University of Technology, The Netherlands

Bluff-body inert and reactive flows are considered using second moment closure and PDF methods as a continuation of previous studies [1]. In the present study, we use the modified coalescence/dispersion model for the scalar micro mixing in combination with the constrained-equilibrium chemistry model. The performance of this and other approaches was examined earlier in Refs. [2-4] using a one block domain computation in bluff-body and piloted turbulent flame configurations. The objective of Ref. [1] and of this work is to contribute to the study of the bluff-body test cases of the TNF workshops by providing results obtained using a new version of the finite volume code, using multi-blocks domain decomposition, in combination with either assumed shape or Monte Carlo PDF methods. For the inert flow, a Monte-Carlo PDF is used together with the standard k-ε model in the finite volume code. For the reactive case, assumed beta probability density function is used together with the basic Differential Reynolds-Stress model. Comparisons between model predictions and available measurement data are given.

The computations were performed upon partitioning the 0.04m x 0.25m main physical domain using a relatively coarse 76 (radial) x 96 (axial) grid. Constant boundary conditions were set 0.05m upstream of the burner tip. For the inert flow, the C_2H_4 fuel was injected through the burner with a bulk velocity of 62 m/s and a co-flow air velocity of 20 m/s was used. The predictions of radial profiles of mean velocity and velocity fluctuations at 20 nozzle and 40 nozzle diameter downstream the bluff body are shown in Fig. 1 and Fig. 2. For the reactive flow, a mixture of CH_4 and H_2 was injected through the burner with a bulk velocity of 118 m/s and a co-flow air velocity of 40 m/s was used. The radial profiles of mean velocity and velocity fluctuations at 26 nozzle and 60 nozzle diameter downstream the burner tip are plotted in Fig. 3 and Fig. 4. The overall agreement between predictions of flow field and experimental data is seen to be reasonable in these first nozzle diameters. The rate at which these flames spread were, however, over predicted after these diameters. Further tests are been undertaken for assessing the predictions of temperature and species concentrations with the novel multi-blocks implementation.

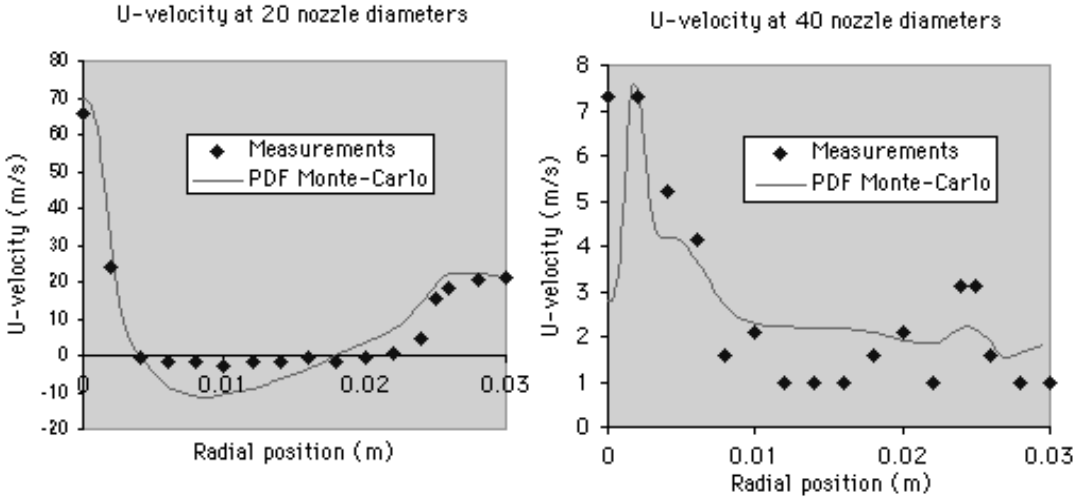

Fig 1. Inert flow: mean velocity profiles at x/D=20,40

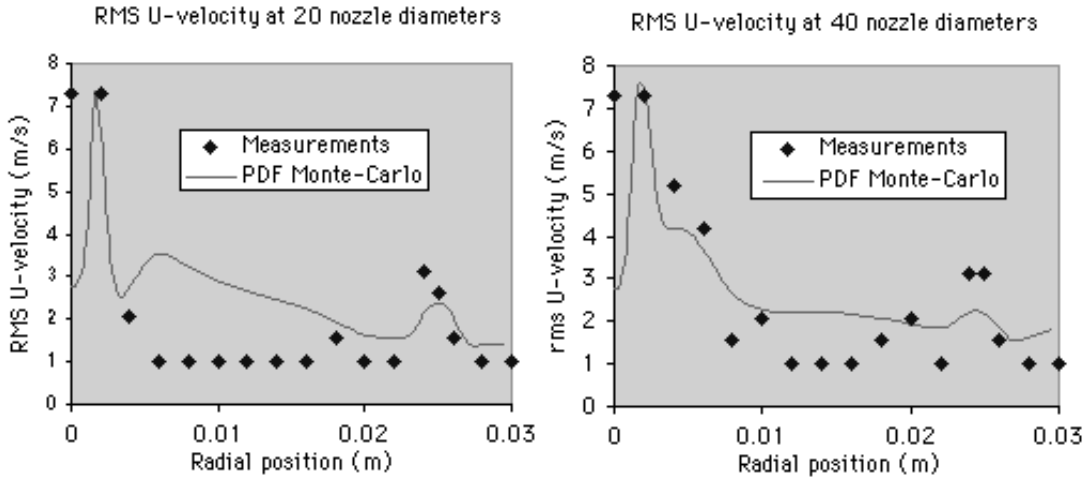

Fig. 2: Inert flow: rms fluctuations of velocity profiles at x/D=20,40

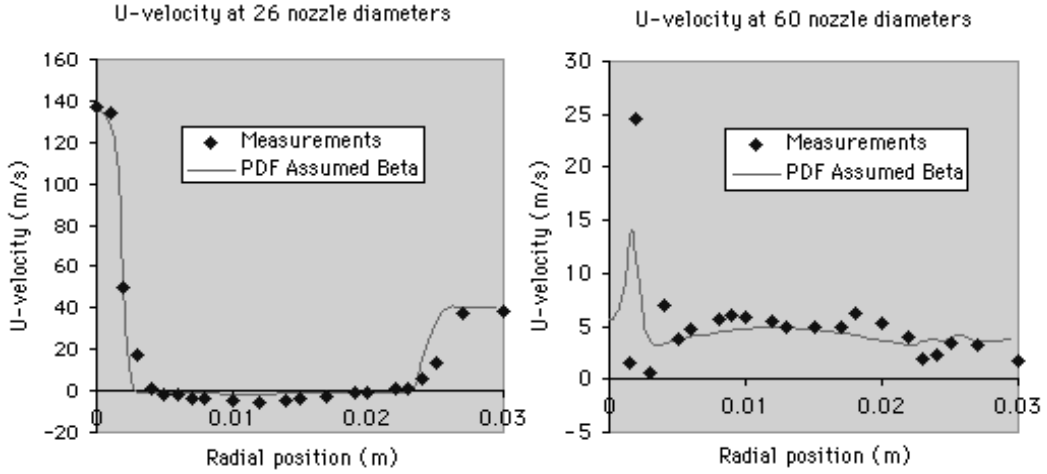

Fig. 3: Reactive flow: mean velocity profiles at x/D=26,60

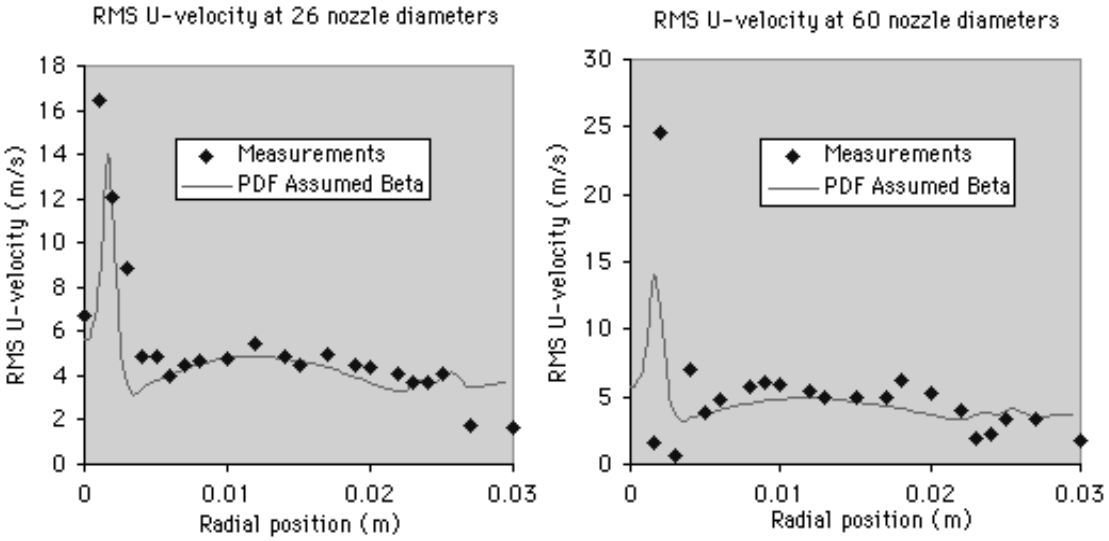

Fig. 4: Inert flow: rms fluctuations of velocity profiles at x/D=26,60

References

1. T. W. J. Peeters, H. A. Wouters and D. Roekaerts ,Second moment closure and PDF calculations of a bluff-body stabilized CH4/H2 flame, In: Proceedings of the Third International Workshop on Measurement and Computation of Turbulent Nonpremixed Flames, Boulder – Colorado, 1998
2. H.A. Wouters, Lagrangian Models for Turbulent Reacting Flows, Ph. D. Thesis, Delft University of Technology, 1998
3. P.A. Nooren, Stochastic modelling of turbulent natural-gas flames, Ph.D. Thesis, Delft University of Technology, 1998
4. P. A. Nooren, H. A. Wouters, T. W. J. Peeters, D. Roekaets, U. Maas and D. Schmidt , Monte Carlo PDF modelling of a turbulent natural-gas diffusion flame, Combustion Theory and Modelling, 1, 79-96, 1997

The Turbulent DLR $CH_4/H_2/N_2$ Jet Diffusion Flame: More Results from Raman/LIF Measurements

Wolfgang Meier*, Robert S. Barlow, Ying-Ling Chen****

* DLR-Institut für Verbrennungstechnik, Stuttgart, Germany
** Sandia National Laboratories, Livermore, California, USA

The DLR jet flame (fuel composition: 33.2% H_2, 22.1% CH_4, 44.7% N_2, 8 mm nozzle diameter, Re=15200) was one of the target flames at the Third TNF Workshop, and results from 2D LIF and pointwise multispecies Raman measurements were compared with results from different model calculations. As a special feature, the gas composition of the flame provides an insight into the hydrocarbon chemistry in turbulent flames without sacrifycing the simple flow field of a free jet, i.e. the flame is not stabilized by a pilot or bluff body.

At the present TNF Workshop, more detailed results from Raman/LIF investigations, performed at the TDF lab of the Sandia National Laboratories, are presented including joint PDFs of temperature, major species mass fractions, mixture fraction, and NO and OH mass fractions. In addition, the CO mass fractions have been measured by two-photon LIF, which yields a better accuracy compared to spontaneous Raman scattering.

The poster will focus on experimental results and address three issues: (1) A comparison of the Raman results obtained in Stuttgart and Sandia including a discussion of deviations due to environmental conditions and experimental techniques. (2) A detailed characterization of the thermochemical state of the flame. The correlations between various quantities are displayed as scatter plots or conditionally averaged data and give an insight into the turbulence-chemistry interaction. In the lower part of the flame, a few events of local flame extinction are observed. The OH concentrations are approx. three times higher than adiabatic equilibrium values at x/D=5 and are decreasing with downstream position, but are still well above the adiabatic level at x/D=60. In comparison to steady strained laminar flame calculations, the measured CO mole fractions are higher by 10-20% at slightly rich mixtures, but an „overshooting“ of CO concentrations known from pure methane turbulent flames was not observed. The maximum single-shot NO concentrations are around 60 ppm at x/D=5 and 100 ppm at x/D=60. (3) Variation of Reynolds number. In a further investigation, the jet exit velocity was increased by 50% leading to a Re number of 22800, at which the flame was close to extinction. The influence of the higher flow velocity on the overall flame shape, the mixing behaviour, and the turbulence-chemistry interaction is presented and discussed in the poster.

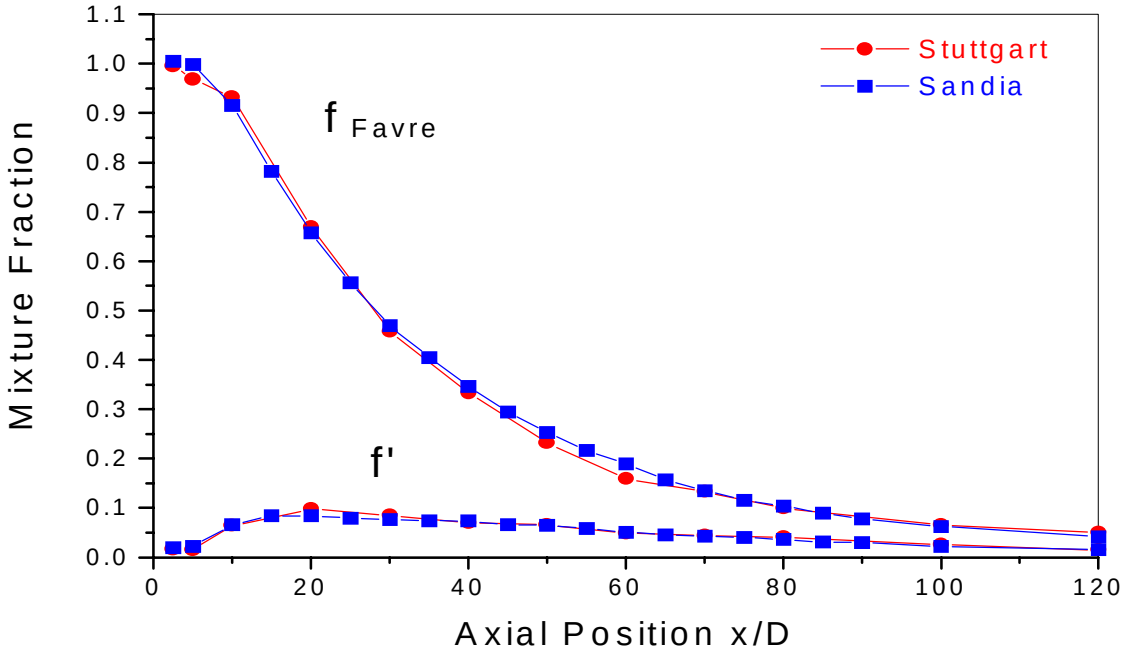

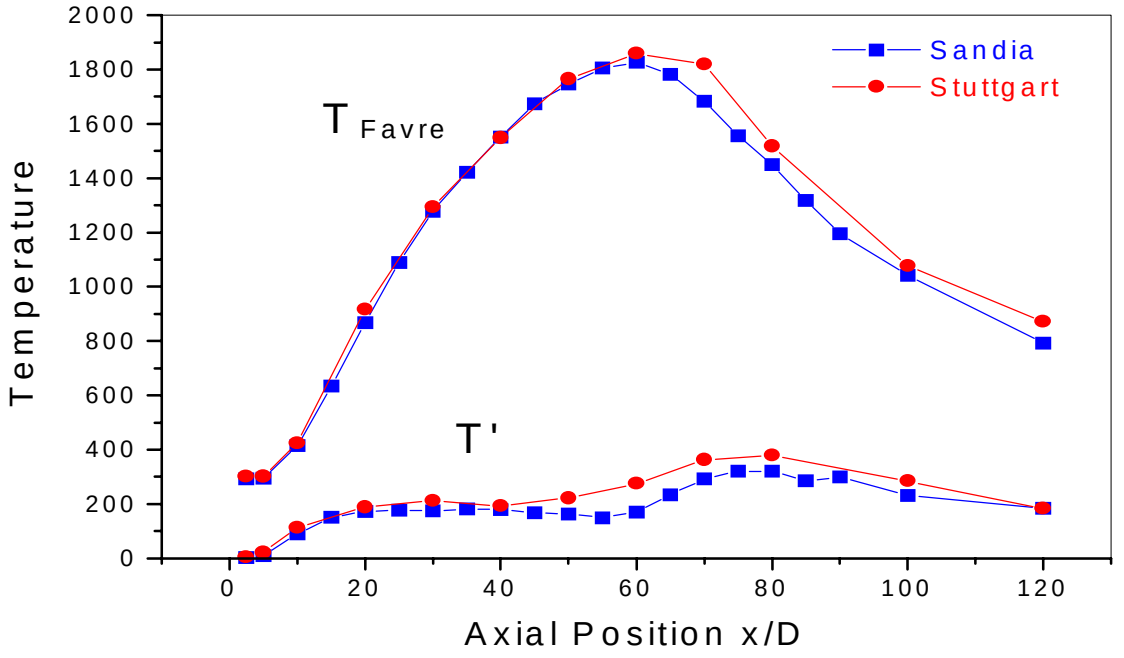

Comparison between axial profiles of mixture fraction and temperature measured in Stuttgart and Sandia in the DLR jet flame.

PDF Calculations of Non-reacting and Reacting Turbulent Bluff-Body Flows

Metin Muradoglu, Patrick Jenny, Stephen B. Pope and David A. Caughey

Sibley School of Mechanical and Aerospace Engineering

Cornell University

Ithaca, NY 14853

Abstract

The non-reacting and reacting turbulent bluff-body flow are studied by a newly developed consistent hybrid Finite-Volume (FV)/ Particle method. In this approach, the conservation equations for mean mass, momentum and energy conservation are solved by a FV method while a particle algorithm is employed to solve the fluctuating velocity-turbulence frequency-compositions joint PDF transport equation. The mean velocity is supplied to the particle code by the FV code which in turn obtains all the Reynolds stresses, the scalar fluxes and the reaction terms needed in the FV code. An important feature of the method is the complete consistency between the set of equations solved by the FV and particle methods.

The coupling between the FV and Particle codes is achieved through the tight and loose coupling strategies. Details of the tightly and loosely coupled algorithms are given by Muradoglu et al.[1] and by Jenny et al.[2] respectively. Both the tightly and loosely coupled hybrid algorithms are used to simulate the non-reacting bluff-body flow[3] and the results for the mean velocities and the r.m.s. fluctuating velocities are compared with the experimental data.

The tightly coupled hybrid method is also applied to the reacting bluff-body stabilized

flame ($CH_4/H_2 - air$ flame) by using a simple flamelet model for the chemistry.

In general, there is a good agreement between calculated results and experimental data for the non-reacting case. It's emphasized that the results for the reacting case is very preliminary and it is too early to make any conclusions about the method based on the results presented.

References

[1] M. Muradoglu, P. Jenny, S.B. Pope, and D.A. Caughey, A Consistent Hybrid Finite-Volume/Particle Method for the PDF Equations of Turbulent Reactive Flows, *Journal of Computational Physics* Accepted for publication **1999**.

[2] P. Jenny, S.B. Pope, M. Muradoglu and D.A. Caughey, A Hybrid Algorithm for the Joint PDF Equation of Turbulent Reactive Flows, *submitted to Journal of Computational Physics* **1999**.

[3] A.R. Masri. http://www.mech.eng.usyd.edu.au/research/energy/

Application of ILDM-reduced mechanisms in laminar and turbulent flames

Holger Niemann, Berthold Schramm, Jürgen Warnatz

Interdisciplinary Center for Scientific Computing
University of Heidelberg,
Im Neuenheimer Feld 368, D-69120 Heidelberg, Germany
niemann@iwr.uni-heidelberg.de

The ILDM-method is a new approach for the generation of reduced chemical mechanisms [1]. The key idea is to consider the fast chemical time scales as relaxed. So "Intrinsic Low-Dimensional Manifolds" (ILDMs) are defined in the chemical state space. In the reactive flow calculation the species composition is constrained to these manifolds. So conservation equations are solved for a small number of reaction progress variables parameterizing the manifold instead of a huge number of species of the detailed mechanism.

The evaluation of the ILDMs is computationally demanding. So it is done only once and the resulting ILDMs are stored in look-up tables. But that introduces the problem of the limited disk and memory space for the ILDM tables [2]. The dimension of the state needed in an industrial application normally exceeds the dimension which can be handled with ILDM tables spanning the whole ILDM space.

The approach of *in-situ* tabulation of the ILDMs, where the calculation of the ILDM table is done during the reactive flow calculation, can overcome that problem [3]. The physics of stiff combustion chemistry normally restricts the solution to a very minor subspace of the ILDM parameter space. So *in-situ* tabulation works well both for laminar flames and turbulent flames where Monte-Carlo methods are used for solving the transport equation of the PDFs.

To make the ILDM method work also for computations using presumed PDFs physical considerations are used on the area accessed by the solution. In many applications the combustion is nearly adiabatic and then the enthalpy would be fixed to the mixture fraction. Non unity Lewis-number effects cause the enthalpy to deviate from this value and potential heat losses to cold walls can also decrease enthalpy. But for combustion configurations with only one fuel and oxidizer stream the enthalpy remains to be banded in a small domain near that value given from mixture fraction. An unstructured tabulation method is used to allow for an tabulation of only those parts of the tabulation domain that are needed in the application.

Here we present the application of precalculated 4-dimensional ILDM tables in simulations of turbulent jet diffusion flames. Different PDF-methods are used to account for turbulent fluctuations. It is not surprising that the simulation using transported PDFs and Monte-Carlo methods produces better results than the simulations using presumed-PDF (beta-functions and Gauss-functions). But the aim of this work is to show the pure applicability of higher dimensional ILDM-tables also in presumed-PDFs when the above assumption is applied.

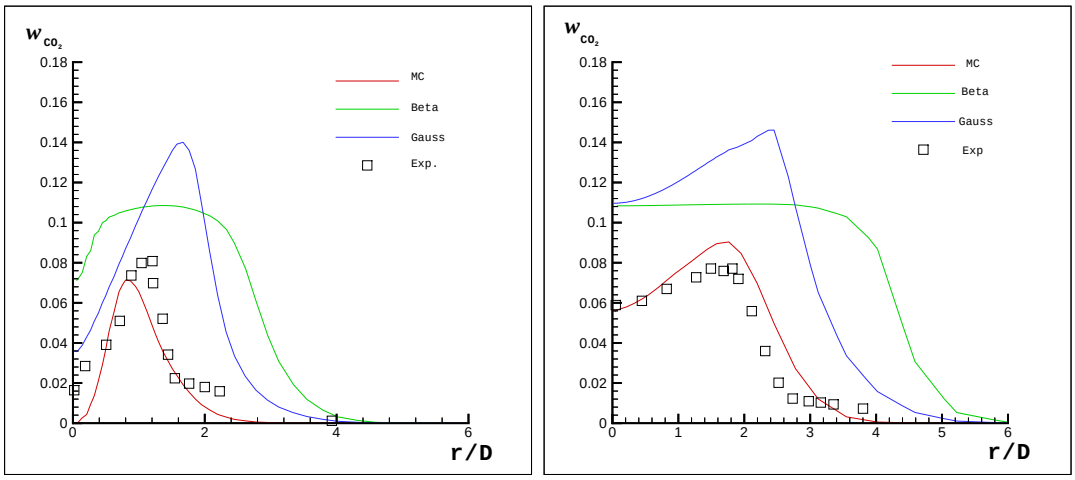

Figure 1: Radial profiles in a free piloted methane jet flame (Masri K-flame [4]). Comparison of experimental results (symbols) with simulations using different assumptions for the PDF (transported PDF [5], presumed PDF using beta-functions [5] and Gauss-functions [6])

References

[1] U. Maas and S. B. Pope. *Combustion and Flame*, 88:239–264, 1992

[2] H. Niemann, D. Schmidt, and U. Maas. *J. Eng. Math.*, 31:131–142, 1997

[3] H. Niemann, J. Warnatz. *W-I-P Poster 27th Int. Comb. Symp.*, 1998

[4] A. Masri, R. W. Dibble, R. W. Bilger *Combustion and Flame* 71:245-266, 1988

[5] B. Schramm *Diplomarbeit* Ruprecht-Karls-Universitt Heidelberg, 1998

[6] O. Fohrmann *Diplomarbeit* Ruprecht-Karls-Universitt Heidelberg, 1998

Large-Eddy Simulation of a Turbulent Piloted Methane/Air Diffusion Flame (Sandia Flame D)

Heinz Pitsch[1], Helfried Steiner[2]

[1]Center for Integrated Turbulence Simulations
e-mail: H.Pitsch@stanford.edu
[2]Center for Turbulence Research
e-mail: steiner@ctr-sgi1.stanford.edu

Department of Mechanical Engineering
Stanford University

While numerical simulations of turbulent flows applying Reynolds averaging techniques solve equations for ensemble averages, Large-Eddy Simulations (LES) offer the opportunity to resolve the large scales of the turbulent motion. For the present study LES simulations for a turbulent, piloted methane/air diffusion flame have been performed and the results are compared to experimental data by Barlow and Frank [1, 2].

The set of equations, which have to be solved in the frame of the current modeling study, can be derived by applying a spatial, density-weighted filter to the continuity equation, the momentum equations, and the mixture fraction transport equation. The unclosed terms in the resulting equations are modeled using an eddy viscosity type model, such that the subgrid-scale fluxes in the momentum equations and the mixture fraction transport equation are given by

$$\widetilde{q}_{ij,t} = -\nu_t \widetilde{S}_{ij} \quad \text{and} \quad \widetilde{q}_{Z,t} = -D_t \nabla \widetilde{Z}\,, \tag{1}$$

where $\widetilde{S}_{ij}$ is the strain tensor and Z is the mixture fraction. The Smagorinsky model is used to obtain the eddy viscosity ν_t, where the Smagorinsky constant is obtained by the Dynamic Model as a function of time and space [3]. This procedure needs no model constants and assures that the turbulent fluxes vanish in the limit of a laminar flow. The subgrid-scale diffusivity D_t is computed assuming a constant turbulent Schmidt number $\mathrm{Sc}_t = 0.7$ as $D_t = \nu_t/\mathrm{Sc}_t$

In the present study a conserved scalar approach is used to describe turbulence-chemistry interactions. The resolved mass fractions of chemical species $\widetilde{Y}_i$ are given by

$$\widetilde{Y}_i(\boldsymbol{x}, t) = \int_Z Y_i(Z, x) \widetilde{P}(Z, \boldsymbol{x}, t) dZ\,, \tag{2}$$

where t is the time, $\boldsymbol{x}$ is the coordinate vector, x is the coordinate in axial direction, and $\widetilde{P}(Z, \boldsymbol{x}, t)$ the Favre pdf of the mixture fraction. Here, $Y_i(Z, x)$ is obtained using the unsteady flamelet model [4, 5] that provides $Y_i(Z, t_f)$, where the flamelet life time t_f can be expressed as function of the axial nozzle distance x [4]. $\widetilde{P}(Z, \boldsymbol{x}, t)$ is presumed to follow a β-function, whose shape is determined by the mean and the subgrid-scale variance of the mixture fraction. Since no transport equation for the mixture fraction variance is solved, this value has to be modeled, which is achieved by using the Dynamic Procedure proposed by Pierce and Moin [6].

In order to solve the unsteady flamelet equations, the temporal development of the scalar dissipation rate has to be specified from the solution of the turbulent flow field. If the mixture fraction dependence of the scalar dissipation rate is presumed as $< \chi | Z > = < \chi_{\mathrm{st}} > f(Z)$, it is sufficient to determine the value at stoichiometric mixture, which can be achieved by [4]

$$\widetilde{\chi} = \int_Z < \chi | Z > \widetilde{P}(Z) dZ\,. \tag{3}$$

However, since in the present study a piloted flame is considered, the mixture fraction dependence cannot be prescribed. This is illustrated in a figure given below showing the scalar dissipation rate at different downstream locations, indicating that the scalar dissipation rate is not a simple function of the mixture fraction. Within the pilot stream, which is at $Z = 0.27$, the scalar gradient, and hence the scalar dissipation rate, is zero. Even at far downstream locations the shape of the scalar dissipation rate is still influenced by the pilot flame. Also, the resolved turbulent motion can clearly be obtained in this figure. In the present model, the conditional average of the scalar dissipation rate as a function of the axial distance from the nozzle $< \chi | Z > (x)$ is computed by the inversion of the integral in Eq. (3). This can be achieved by applying Eq. (3) to all computational cells in azimuthal

direction and determining $< \chi | Z >$ by minimizing the resulting error of the overdetermined system by applying a least squares approach similar to the method of Bushe and Steiner [8].

The spatially filtered scalar dissipation rate, appearing in Eq. (3), is expressed in terms of the eddy diffusivity and the gradient of the resolved mixture fraction following by Girimaji and Zhou [7] as

$$\widetilde{\chi} = 2(D_Z + D_t)\nabla\widetilde{Z}\nabla\widetilde{Z}\,, \tag{4}$$

where D_Z is the molecular diffusivity of the mixture fraction.

Some results of the calculations are presented in a figure given below. Instantaneous solutions of the resolved values for axial velocity and mixture fraction are compared to ensemble averaged experimental data along the centerline. Obviously, the calculations show much more structure of the turbulent flow field than the ensemble averaged data provides.

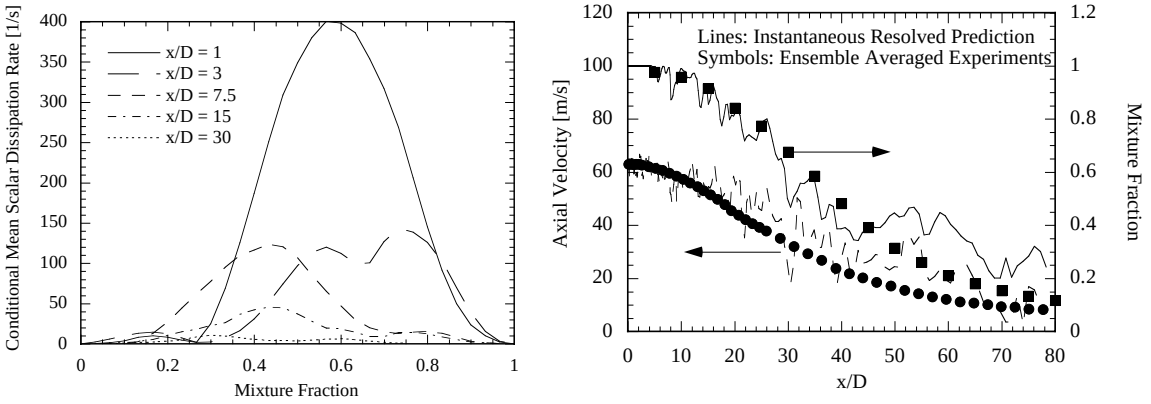

References

[1] Barlow, R. S., Frank, J. H., "Experimental Results on Differential Diffusion in Piloted Methane-Air Jet Flames", 3rd International Workshop on Measurement and Computation of Turbulent Nonpremixed Flames, 1998.

[2] www.ca.sandia.gov/tdf/Workshop.html.

[3] Moin, P., Squires, K., Cabot, W., Lee, S., Phys. Fluids A 3, pp. 2746-2757, 1991.

[4] Pitsch, H., Chen, M., Peters, N., Twenty-Seventh Symposium (International) on Combustion, accepted for presentation, 1998.

[5] Pitsch, H., "Unsteady Flamelet Modeling of Differential Diffusion in Turbulent Jet Diffusion Flames", Comb. Flame, submitted, 1999.

[6] Pierce, C. D., Moin, P., Phys. Fluids A 10, pp. 3041-3044, 1998.

[7] Girimaji, S. S., Zhou, Y., Phys. Fluids A 8, pp. 1224-1236, 1996.

[8] Bushe, W. K., Steiner, H., "Conditional moment closure for large eddy simulation of non-premixed turbulent reacting flows", Phys. Fluids A, accepted for publication, 1999.

Unsteady Flamelet Modeling of a Piloted Methane-Air Jet Flame (Sandia Flame D)

Heinz Pitsch
Center for Integrated Turbulence Simulations
Flow Physics and Computation Division
Department of Mechanical Engineering
Stanford University
e-mail: H.Pitsch@stanford.edu

Elmar Riesmeier, Norbert Peters
Institut für Technische Mechanik
RWTH Aachen
Templergraben 64
52062 Aachen
e-mail: E.Riesmeier@itm.rwth-aachen.de, N.Peters@itm.rwth-aachen.de

An unsteady flamelet model has been applied in a numerical simulation of a steady, turbulent, piloted methane-air diffusion flame (Sandia Flame D), which has experimentally been investigated by Barlow and Frank [1, 2].

Recent studies [3, 4] have shown that transient effects in jet diffusion flames have to be considered, if slow physical or chemical processes such as radiation or the formation of NO_x are of importance.

The unsteady flamelet model applied in the present study is described in detail in Refs. [3, 4]. The flamelet equation for the temperature is of the kind

$$\rho\frac{\partial T}{\partial t}-\rho\frac{\chi}{2}\left(\frac{\partial^2 T}{\partial Z^2}+\frac{1}{c_p}\frac{\partial c_p}{\partial Z}\frac{\partial T}{\partial Z}\right)+\frac{1}{c_p}\left(\sum_{k=1}^{N}h_k\dot{m}_k+\dot{q}_R'''-\mathcal{H}\right)=0\,, \tag{1}$$

where t denotes the time, Z the mixture fraction, T the temperature, χ the scalar dissipation rate, ρ the density, c_p the specific heat capacity at constant pressure, $\dot{q}_R'''$ the rate of radiative heat loss per unit volume. N is the number of chemical species, h_k the enthalpy, and $\dot{m}_k$ the chemical production rate per unit volume of species k. $\mathcal{H}$ accounts for the enthalpy flux by mass diffusion. The flow field has been calculated using the FLUENT code. To incorporate transient effects into the flamelet calculations, only one flamelet is solved for the entire computational domain. This flamelet is thought to be introduced at the nozzle at extinction conditions and traveling downstream with the mean axial velocity at stoichiometric mixture. The temporal evolution of the flamelet is calculated using Eq. (1) and the corresponding equations for the species mass fractions, where the flamelet life time is related to the axial nozzle distance x by

$$t=\int_0^x\frac{1}{u(x')\Big|\left(\widetilde{Z}=Z_{\rm st}\right)}dx'\,. \tag{2}$$

Here, $\widetilde{Z}$ is the Favre average of the mixture fraction, $u(x)\Big|\left(\widetilde{Z}=Z_{\rm st}\right)$ is the axial velocity component at the radial position, where $\widetilde{Z}=Z_{\rm st}$, and the index st refers to stoichiometric conditions. Since the boundary conditions of the flamelet, which are the temperatures and the composition of the fuel and the oxidizer stream, as well as the pressure, remain constant throughout the calculation, the only parameter varying with the flamelet time and thereby influencing the flamelet solution is the scalar dissipation rate, describing the impact of the turbulent flow field on the diffusion flame structure. The scalar dissipation rate used in the flamelet calculation has to be determined from the CFD solution.

In earlier applications of this model [3, 4] the functional dependence of the the scalar dissipation rate and the mixture fraction has been presumed to be that of a semi-infinite mixing layer. This assumption does not hold for the present flame because the pilot has a strong influence on the mixture fraction gradients. Therefore, similar as in Ref. [5], the scalar dissipation rate as a function of mixture fraction is taken as the average of the turbulent mean of the scalar dissipation rate conditioned on the mean mixture fraction at a given nozzle distance.

In a previous study [4] the unsteady flamelet model has been applied to a flame with strong differential diffusion effects and an appropriate model considering these effects has been proposed. Although differential diffusion effects are rather small in the Sandia D flame, Barlow and Frank have demonstrated that these occur in flames A to E, where the obvious effects become smaller with higher Reynolds number and increasing nozzle distance. In the present work the unsteady flamelet model has been applied to Sandia flame D using unity Lewis numbers. However,

calculations applying the proposed model for differential diffusion have also been performed yielding only very little differences in the species mass fraction distribution as shown below.

The calculations have been performed with the GRI mechanism [6]. In the figures given below the results of the numerical simulation for mean and rms of the mixture fraction, and mean values of temperature, CO, H_2, OH, and NO mass fractions are compared with experimental data by Barlow et al. [1, 2] along the centerline. The flow field data, represented by the mean and the rms of the mixture fraction, and also the temperature and the mass fractions of CO, H_2, and OH are predicted reasonably accurate. Slight discrepancies in the maximum values of the species concentrations might be caused by the underprediction of the mixture fraction variance. The agreement of major species, as fuel, oxidizer, and the main products with the experimental data is similar as for the temperature. NO is overpredicted, but still in the right order of magnitude. The last figure shows a comparison of computed temperature profiles with and without differential diffusion effects compared to experimental data at $x/D = 7.5$, revealing that close to the nozzle slight differential diffusion effects occur.

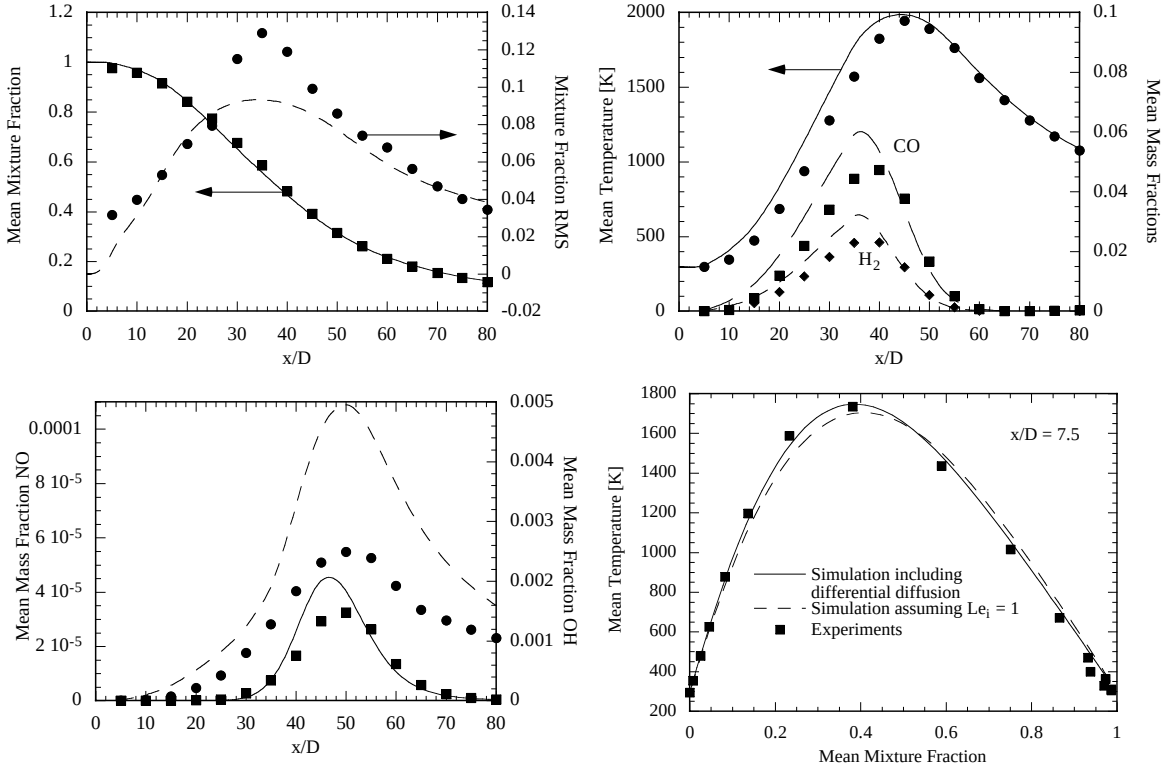

References

[1] Barlow, R. S., Frank, J. H., "Effects of Turbulence on Species Mass Fractions in Methane/Air Jet Flames", Twenty-Seventh Symposium (International) on Combustion, Paper 4A10, 1998.

[2] www.ca.sandia.gov/tdf/Workshop.html.

[3] Pitsch, H., Chen, M., Peters, N., Twenty-Seventh Symposium (International) on Combustion, accepted for presentation, 1998.

[4] Pitsch, H., "Unsteady Flamelet Modeling of Differential Diffusion in Turbulent Jet Diffusion Flames", Comb. Flame, submitted, 1999.

[5] Pitsch, H., Steiner, H., "Large Eddy Simulation of a Turbulent Methane/Air Diffusion Flame (Sandia Flame D)", 4th International Workshop on Measurement and Computation of Turbulent Nonpremixed Flames, 1999.

[6] Bowman, C. T., Hanson, R. K., Davidson, D. F., Gardiner, Jr., W. C., Lissianski, V., Smith, G. P., Golden, D. M., Frenklach, M., Goldenberg, M., http://www.me.berkeley.edu/gri_mech/

Conditional Moment Closure (CMC) Predictions of a Methane-Air Piloted Jet Flame (Flame E)

M. R. ROOMINA[1] and R. W. BILGER

Department of Mechanical and Mechatronic Engineering
The University of Sydney, NSW 2006, AUSTRALIA
E-mail: roomina@cances.atp.com.au; bilger@mech.eng.usyd.edu.au

ABSTRACT

Conditional Moment Closure (CMC) (Klimenko, 1990, Bilger, 1993) is a method for handling turbulence chemistry interactions which is capable of being used with large chemical mechanisms at modest computational cost. The basic idea of the method is that most of the fluctuation in temperature and composition can be associated with one variable and conditional averaging with respect to that variable allows closure of the conditional average chemical reaction rate terms. For the nonpremixed combustion systems considered here, the conditioning variable of choice is the mixture fraction.

CMC has already produced excellent results for several problems of interest. Smith et al. (1992, 1995) have successfully implemented the CMC method for turbulent nonpremixed hydrogen jet flames and reported excellent results for NO predictions. Roomina and Bilger (1998, 1999) have extended application of the CMC method to a turbulent diffusion flame formed from a partially premixed jet of methane and air. They have reported the CMC results for velocity and mixing fields and temperature and species mass fractions including nitric oxide, NO, with a jet Reynolds number of 22400 (Flame D). The comparisons are made with laser diagnostic measurements of Barlow and Frank (1998) and Schneider et al. (1998).

Here we present CMC predictions for jet Reynolds number of 33400 (Flame E). The burner is an axisymmetric jet with a jet nozzle diameter of 7.2 mm and an outer annulus diameter of the pilot of 18.2 mm, centred in a stream of co-flowing air. The jet velocity is 74.4 m/s and the co-flow velocity is 0.9 m/s. The calculations are carried out down to x/D=80. The chemistry is represented by the GRI-Mech 2.11 mechanism. Radiative heat loss is modelled by RADCAL (Sivathanu and Gore, 1993) radiation sub-model. Adiabatic equilibrium compositions are employed for the reactive scalars down to five jet diameters, in order to assure the ignition of the flame in the near-field region due to high mixing rates.

In general, the flow and mixing field predictions are in good agreement with the measurements. The k-ε-g turbulence model somewhat over-predicts the mixing rates near the nozzle. The predicted flame is slightly shorter than that reported in the experiment.

Predictions for the conditional average mass fractions of the major species and of the temperature show good agreement with the measurements on the fuel-lean side of the stoichiometric.

[1] Current address: Centre for Advanced Numerical Computation in Engineering and Science (CANCES), Australian Technology Park, Sydney, Australia.

Discrepancies for these quantities are significant on the fuel-rich side. Apparently, conversion of fuel to intermediates is over-predicted on the rich side of the flame. The discrepancies may be due to inadequacies in the chemical mechanisms tested or in the first-order closure used for the chemical reaction rates. In general the NO predictions are too high, probably as a result of inadequate predictions of the fuel-rich side chemistry noted already for the major species.

Favre averaged statistics are obtained by the weighting of the conditional mean statistics with the local pdf (Clipped Gaussian) over the entire mixture fraction space. Therefore, the quality of predictions for Favre averaged statistics are affected by the quality of both the conditional mean statistics and the pdf of mixture fraction, and hence should not exceed the quality of the conditional averaged predictions. Radial profiles of Favre averaged quantities are in reasonable agreement, particularly at downstream locations.

The overall trends of CMC predictions for flame E are similar to those of flame D. The predictions for flame D show better agreement with the measurements. This is apparently related to the facts that CMC formulation is valid for regions far from ignition and extinction; and a small probability of localised extinction is reported in this flame.

ACKNOWLEDGMENT

This work is supported by the Australian Research Council.

REFERENCES

BARLOW, R.S. and FRANK, J., 1998, available from web site: http://www.ca.sandia.gov/tdf/workshop.html.

BILGER, R.W., *Phys. Fluids* A **5**(2):436-444, 1993.

GRI-Mech 2.11, available from Web site: http://www.me.berkeley.edu/gri_mech/.

KLIMENKO, A.Y., *Fluid Dynamics* **25**:327-334, 1990.

KLIMENKO, A.Y., *Phys. Fluids* **7** (2):446-448, 1995.

ROOMINA, M.R. and BILGER, R. W., *Third International Workshop on Measurement and Computation of Turbulent Nonpremixed Flames,* Boulder, Colorado, 1998.

ROOMINA, M.R. and BILGER, R.W., Conditional Moment Closure (CMC) predictions of a Turbulent Methane-Air Jet Flame, *Combustion and Flame,* 1999 (submitted).

SCHNEIDER,C.,GEISS,S.and HASSEL, E., 1998: http://www.ca.sandia.gov/tdf/workshop.html.

SIVATHANU, Y.R. and GORE, J.P., *Combustion and Flame*, **94**, 265-270, 1993.

SMITH, N.S.A., BILGER, R.W. and CHEN, J.Y., *24th Symposium (International) on Combustion*, The Combustion Institute, pp.263-269, 1992.

SMITH, N.S.A., BILGER, R.W., CARTER, C.D., BARLOW, R.S. and CHEN, J.Y., *Combustion Sci. and Tech.* **105**:357-375, 1995.

DIRECT SIMULATIONS OF TURBULENT NON-PREMIXED FLAMES WITH DETAILED CHEMISTRY

Dominique Thévenin and Romain Baron

Laboratoire E.M2.C., Ecole Centrale Paris and C.N.R.S.,
E-mail : thevenin@em2c.ecp.fr

Poster presentation,
4th International Workshop on Turbulent Nonpremixed Flames, Darmstadt, June 1999

Introduction

The numerical simulation of reactive flows in industrial configurations has progressed at a rapide pace in recent years. There remain nevertheless many uncertainties. The most difficult problem is that available Turbulent Combustion Models very often fail to give an acceptable answer. In order to further increase the impact of numerical predictions on industrial developments, a very good knowledge of the fundamental processes associated with turbulent combustion is required. One possible source of information is given by Direct Numerical Simulations (DNS). We will show results obtained with DNS computations relying on the compressible Navier-Stokes equations in two dimensions taking into account multicomponent transport processes and detailed kinetics. Our DNS code *parcomb* has been described in detail previously [1,2].

Structure of turbulent non-premixed flames

A non-premixed flame of hydrogen diluted in nitrogen and air is first computed in a one-dimensional configuration with *parcomb*. Resulting profiles are then used to initialize the two-dimensional computation by superimposing the turbulent velocity field, and the evolution of the flame with time is observed. A uniform grid spacing of 50 μm is used in both directions for the cases presented here. The initial turbulence field corresponds to $u' = 2.46$ m.s^{-1} and $\Lambda = 1.32$ mm, with resulting turbulent Reynolds number $Re_t = 210$.

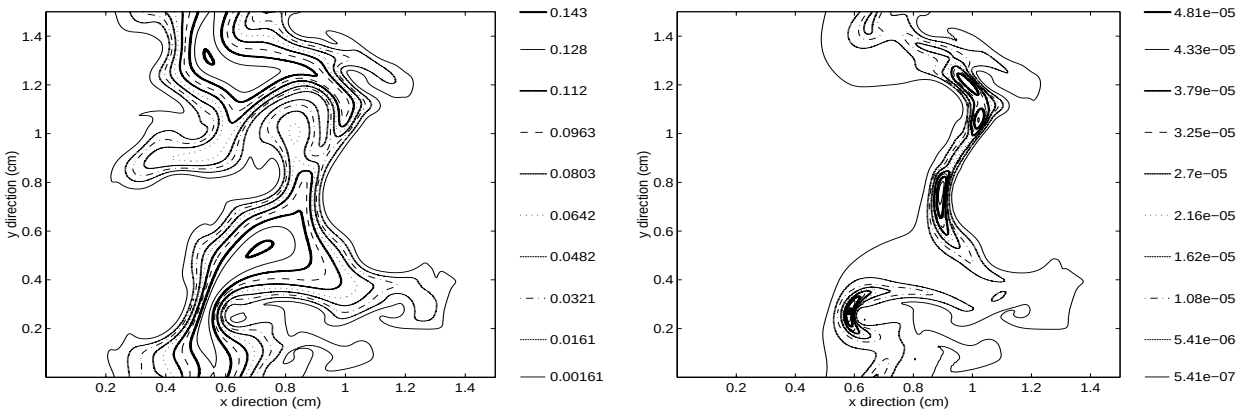

Figure 1: Turbulent non-premixed hydrogen-air flames in homogeneous isotropic turbulence. Instantaneous H_2O mass fractions (left) and H_2O_2 mass fractions (right) are displayed.

The computation is carried out using 8 processors of a CRAY T3E. Total computing time on one node is about 80 hours. All results are presented for a time corresponding to 1.9

times the large-eddy turn-over time Λ/u', which is deemed enough to obtain full coupling between turbulence and chemistry. This same computation has been repeated 10 times.

Figure 1 reveal that the flame is highly contorted by the turbulent velocity field, and it is clear from these plots that the chemical species behave very differently, leading to serious difficulties in the interpretation. The complexity of these features explains the necessity of using adequate post-processing tools to extract any relevant information.

Post-processing

A detailed post-processing package has been recently developed to analyze in detail our DNS results [3]. These procedures allow for example the computation of the flame front position and limits according to user-given definitions, the computation of flame surface area and thickness, of curvature, strain and stretch rates and of propagation speeds. Correlations between all these quantities and physical variables are also determined, along with probability density functions.

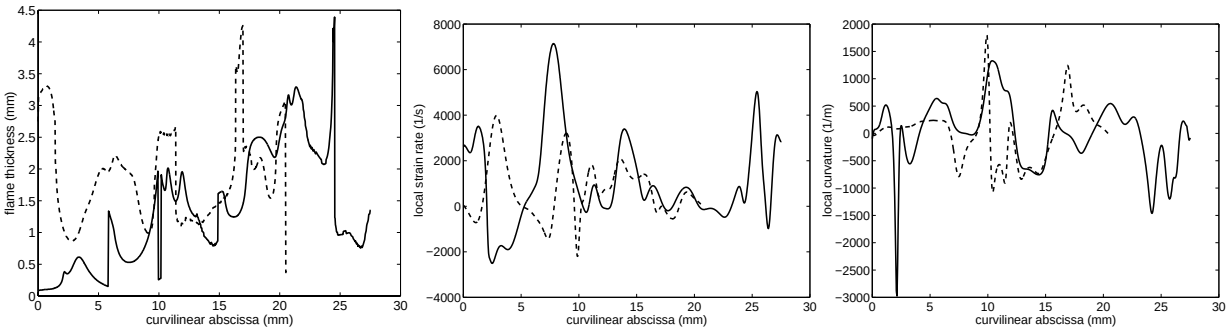

Figure 2: Post-processing results for Flame 1 (solid line) and Flame 2 (dashed line). Flame thickness defined with the H_2 mass fraction (left), strain rate (middle) and curvature (right), all variables plotted versus the curvilinear abscissa along the flame front.

Conclusions

A parallel code and accompanying post-processing package has been developed to investigate turbulent non-premixed flames using Direct Numerical Simulations and detailed models for chemical and transport processes. We hope that a thorough post-processing will help in developing more accurate Turbulent Combustion Models in the future.

References

[1] Thévenin, D., Behrendt, F., Maas, U., Przywara, B. and Warnatz, J. (1996) Development of a parallel direct simulation code to investigate reactive flows. *Comput. Fluids* **25**, 485-496.

[2] Thévenin, D., van Kalmthout, E. and Candel, S. (1997) Two-dimensional direct numerical simulations of turbulent diffusion flames using detailed chemistry. In *Direct and Large-Eddy Simulation II*, (Chollet, J.P., Voke, P.R. and Kleiser, L., Eds.), Kluwer Academic Publishers, 343-354.

[3] Thévenin, D., and Baron, R. (1999) Investigation of turbulent non-premixed flames using Direct Simulations with detailed chemistry. In *INI/ERCOFTAC Conference on Direct and Large-Eddy Simulation*, Cambridge, p.3.4.

PDF/ISAT Calculations of of Piloted–Jet Non–Premixed Methane Flames

J. Xu and S.B. Pope
Sibley School of Mechanical and Aerospace Engineering
Cornell University, Ithaca, NY 14853
email: xujun@mae.cornell.edu, pope@mae.cornell.edu

In this study, a joint velocity–composition–turbulence frequency PDF (JPDF) model is used to simulate piloted–jet non-premixed flames of methane, namely Flame D and F [1]. In this JPDF model, the PDF transport equation is modelled and solved in accordance with Monte Carlo methods, and the model is independent of any RANS based models by providing the information of turbulence scale through a stochastic model of turbulence frequency. The augmented reduced mechanism (ARM) for methane oxidation [6] is used and calculated by the *in situ* adaptive tabulation (ISAT) algorithm [3].

Taking the Lagrangian view, the fluid is modelled by an ensemble of stochastic particles. Each particle has its own position $\mathbf{X}^*(t)$, velocity $\mathbf{U}^*(t)$, turbulence frequency $\omega^*(t)$ and compositions $\boldsymbol{\phi}^*(t)$ ($\boldsymbol{\phi}^*(t) \equiv \{\phi^*_\alpha(t), \alpha = 1, 2, \cdots, \sigma\}$) at time t. First of all, the convection process is simulated by the particle movement,

$$d\mathbf{X}^*(t) = \mathbf{U}^*(t)dt. \tag{1}$$

The evolution of particle velocities is then modelled by the stochastic differential equation (SDE) of the Langevin type. The model considered here is the generalized Langevin model (GLM) [2] with an additional term T_i^* denoting pressure transport

$$dU_i^* = -\frac{1}{\langle\rho\rangle}\frac{\partial\langle P\rangle}{\partial x_i}dt + G_{ij}\left(U_j^* - \widetilde{U_j}\right)dt + T_i^*dt + (C_0 k\Omega)^{1/2}\,dW_i, \tag{2}$$

where ρ and P are fluid density and pressure, respectively, and '$\widetilde{\ }$' denotes a density–weighted mean quantity, for example $\widetilde{\mathbf{U}} = \langle\rho\mathbf{U}\rangle / \langle\rho\rangle$. The model constant $C_0 = 2.1$, $k \equiv \frac{1}{2}\widetilde{u_i'' u_i''}$ ($u_i'' \equiv U_i - \widetilde{U_i}$) is the turbulence energy, Ω is the conditional turbulence frequency [7] and $\mathbf{W}$ is an isotropic Wiener process. The model is completed by providing expressions for the tensor $\mathbf{G}$ and $\mathbf{T}$ [2, 7].

To provide a time scale, a stochastic model for the turbulence frequency ω^* of particles has been developed [7]. The turbulence frequency is defined in such a way that the product of the turbulence energy k and the mean frequency $\widetilde{\omega}$ equals to the mean dissipation of energy ϵ. Alternatively, $\widetilde{\omega}$ is equivalent to the quantity used in the k-ω model [8]. The model is written as

$$d\omega^* = -C_{\omega 3}(\omega^* - \widetilde{\omega})\Omega dt - S_\omega \Omega\omega^* dt + (2C_{\omega 3}C_{\omega 4}\widetilde{\omega}\Omega\omega^*)^{1/2}\,dW, \tag{3}$$

where model constants are $C_{\omega 3} = 1.0$ and $C_{\omega 4} = 0.25$. In Eq.(3), the source term S_ω is of the form

$$S_\omega = C_{\omega 2} - C_{\omega 1}\frac{\mathcal{P}}{k\Omega}, \tag{4}$$

where $\mathcal{P} \equiv -\widetilde{u_i'' u_j''}\frac{\partial\widetilde{U_i}}{\partial x_j}$ is the production of k, $C_{\omega 1} = 0.56$ and $C_{\omega 2} = 0.90$.

Finally, the conservation equation for the αth particle composition ϕ_α is constituted of two parts: the micro-mixing process M_α ,and the chemical reaction S_α:

$$d\phi_\alpha^* = \left[S_\alpha(\boldsymbol{\phi}^*(t)) + M_\alpha(t)\right]dt. \tag{5}$$

There exist several different models of $\mathbf{M}$. The model adopted here is the most advanced EMST model developed by Subramaniam and Pope [5]. The feature of this model is that it performs mixing locally in the composition space.

The efficient computation of chemical reaction rate $\mathbf{S}$ is a big challenge to the modelling of complex turbulent reacting flows, in particular those that are near extinction. In such cases, the computation of a detailed chemistry mechanism which involves tens of species (say 16 species in a skeletal mechanism for methane) is desired. Obviously, this dramatically increases the computational cost. The recently developed ISAT algorithm is such an efficient approach that can speed up the computation of reaction rate by a factor of 10^3 (for 16 species) [3]. The underlying idea of ISAT is that an unstructured and adaptive table is constructed to store the reaction mapping (Eq.(6)), and then an *in situ* data retrieval or evaluation of the reaction mapping is conducted according to an error tolerance ϵ_{tol}. The reaction mapping $\mathbf{R}(\phi^0)$ is defined by

$$\mathbf{R}(\boldsymbol{\phi}^0) \equiv \boldsymbol{\phi}(t_0 + \Delta t) \qquad \text{with} \quad \boldsymbol{\phi}^0 \equiv \boldsymbol{\phi}(t_0), \tag{6}$$

which represents the composition vector after a time step Δt at the reaction rate $\mathbf{S}$. The ISAT algorithm has been proven very effective in improving the prediction of minor species with reasonable computational cost in conjuction with detailed chemistry mechanism [4]. Thus, it is adopted, in combination with ARM to calculate the chemical reaction term $\mathbf{S}$ in this work.

The results of this work to be presented as a poster include a detailed comparison of calculations with the available experimental data [1] on mean and conditional mean profiles and distributions of major and minor species, and the examination of the capacity of current model for capturing local extinctions.

References

[1] R. S. Barlow and J. H. Frank. Effects of turbulence on species mass fractions in methane/air jet flames. In *Twenty–seventh Symp. (International) on Combust.*, page 1087, Pittsburgh, 1998. The Combustion Institute.

[2] S. B. Pope. On the relationship between stochastic Lagrangian models of turbulence and second-moment closures. *Phys. Fluids*, 6(2):973, 1994.

[3] S. B. Pope. Computationally efficient implementation of combustion chemistry using *in situ* adaptive tabulation. *Combust. Theo. Modelling*, 1:41, 1997.

[4] V. Saxena and S. B. Pope. PDF calculations of major and minor species in a turbulent piloted–jet flame. In *Twenty–seventh Symp. (International) on Combust.*, page 1081, Pittsburgh, 1998. The Combustion Institute.

[5] S. Subramaniam and S. B. Pope. A mixing model for turbulent reactive flows based on euclidean minimum spanning trees. *Combust. Flame*, 115:487, 1998.

[6] C. J. Sung, C. K. Law, and J.-Y. Chen. An augmented reduced mechanism for methane oxidation with comprehensive global parametric validation. In *Twenty–seventh Symp. (International) on Combust.*, page 295, Pittsburgh, 1998. The Combustion Institute.

[7] P. R. Van Slooten, Jayesh, and S. B. Pope. Advances in PDF modeling for inhomogeneous turbulent flows. *Phys. Fluid*, 10(1):246, 1998.

[8] D. C. Wilcox. *Turbulence Modeling for CFD.* (DCW Industries, Inc.), La Cañada, Ca., 1993.

Numerical simulation of Sandia Piloted CH_4/Air Jet Flame Using the Monte Carlo Joint-Scalar PDF Method

Atsushi Yuasa[1)], Jyh-Yuan Chen[2)] and Osamu Ukai[1)]

1)Advanced Technology Research Center, Mitsubishi Heavy Industries, Ltd.,
8-1, Sachiura 1-chome, Kanazawa-ku, Yokohama 236-0003, Japan
E-mail: yuasa@atrc.mhi.co.jp, ukai@atrc.mhi.co.jp

2)Department of Mechanical Engineering, University of California at Berkeley,
Berkeley, CA 94720-1740, U.S.A.
E-mail: jychen@euler.berkeley.edu

Numerical simulation of Sandia piloted CH_4/air jet flame (FlameD) is performed using the Monte Carlo joint-scalar PDF method combined with a turbulent flow solver provided by the commercial code STAR-CD. The adopted turbulence model is k-ε model with a constant $C_{\varepsilon 2} = 1.7$ in the ε equation modified from its standard value 1.92 in order to reduce the effect of turbulent diffusion. The present simulation is time-dependent with a fixed time step $\Delta t = 1.0 \times 10^{-5}$ [sec] in which a turbulent flow field and scalar fields are interactively solved through density at every time step. The exact inlet boundary conditions (BCs) specified in Dr. Barlow's experiment[1] are used in this simulation.

In the joint-scalar PDF solver, scalar fields are solved by the Lagrangian scheme[2] using 50 particles per cell with each of 3 different molecular mixing models (Curl's model, modified Curl's model and IEM model). As an efficient numerical scheme for calculation of chemical reactions which is the most time-consuming part in the Monte Carlo PDF simulation, the unstructured look-up table method[3] is newly developed in which the least square approximation is introduced for the fitting of the surface formed by the change of each species composition due to reactions. Since data to be stored in a table are only several coefficients of a fitting function (10 in the present study), the size of an unstructured table is considerably reduced compared to that of a structured table in the original method developed by Chen *et. al.*[4] in which all composition data are stored at each grid point in the discretized multi-dimensional composition space. In addition, the applicability of the original method only to binary inlet streams like a fuel and an oxidizer is extended to multiple inlet streams with $N_{\mathrm{inlet}}(>2)$ different BCs such as FlameD. This extension enables to generate a table strictly based on the real inlet BCs of FlameD without replacing them with equivalent ones. While the thermochemical state in the system can be completely determined by only 1 parameter, mixture fraction of 2 inlet streams, in the original method, $(N_{\mathrm{inlet}} - 1)$ parameters are needed to specify the ratio of contribution from each inlet BC in the extended method. The unstructured table of about 17.5[MB] (the size of the corresponding structured table is about 258[MB]) is generated based on 6 scalars (2 contribution ratios of a CH_4/air jet and a pilot and 4 mass fractions of CH_4, CO, O_2 and H) using the following 4-step reduced chemistry for methane combustion proposed by Chen[3].

$$O_2 + 4H = 2H_2O \tag{R1}$$

$$4H_2 + O_2 = 4H + 2H_2O \tag{R2}$$

$$O_2 + 4CO + 2H_2O = 4H + 4CO_2 \tag{R3}$$

$$4CH_4 + 3O_2 + 4H = 8H_2 + 4CO + 2H_2O \tag{R4}$$

Figures 1(a) and 1(b) show the change of the mass fraction of H due to the above reduced chemistry calculated for 3,000 randomly generated chemical compositions using the direct integration method and the look-up table methods. The accuracy of calculation of chemical reactions using both types of look-up tables is pretty good compared to that by the direct integration. Moreover, calculation using the unstructured table is sufficiently accurate and almost comparable with that using the structured table.

Figures 2 and 3 show time-averaged axial and radial (at $x/D = 15$) profiles of several scalars over 1,000 time steps, respectively. Note that no special treatments in the near field are used to burn the flame stably in the present simulation. Both the axial and the radial mixture fractions using all mixing models are in good agreement with experimental data. However, the temperature in the middle field in the axial profile is

underpredicted and peak temperatures are overpredicted in both profiles. In addition, the mass fraction of CO in both profiles are approximately 2 times larger than experimental data. The similar tendency is observed in the profiles of the mass fraction of H_2. Nevertheless, mass fractions of other major species are well predicted with reasonable accuracy (they are not shown here). These discrepancies between numerical results and experimental data mainly come from larger mixing frequencies due to smaller turbulent velocity fluctuations in the simulation. The enhancement of mixing drives scalars of each particle to a better mixed state and results in higher temperature and mass fractions of CO and H_2.

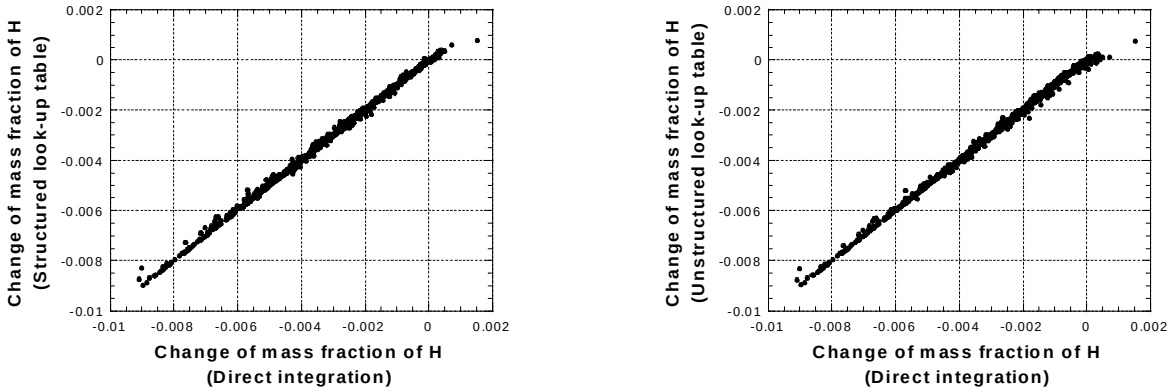

(a)Direct integration vs. structured look-up table (b)Direct integration vs. unstructured look-up table

Figure 1: Comparison of accuracy of calculated changes of the mass fraction of H

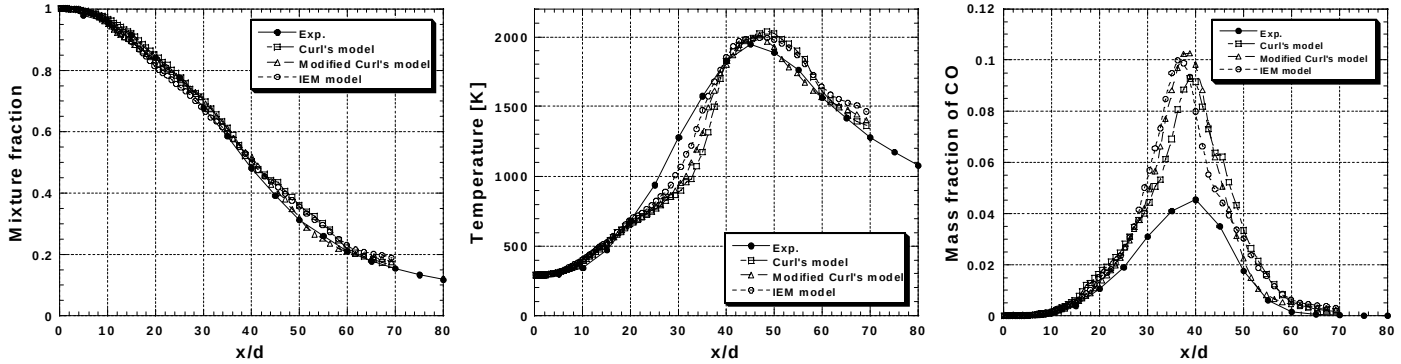

(a)Mixture fraction (b)Temperature (c)Mass fraction of CO

Figure 2: Axial profiles of scalars

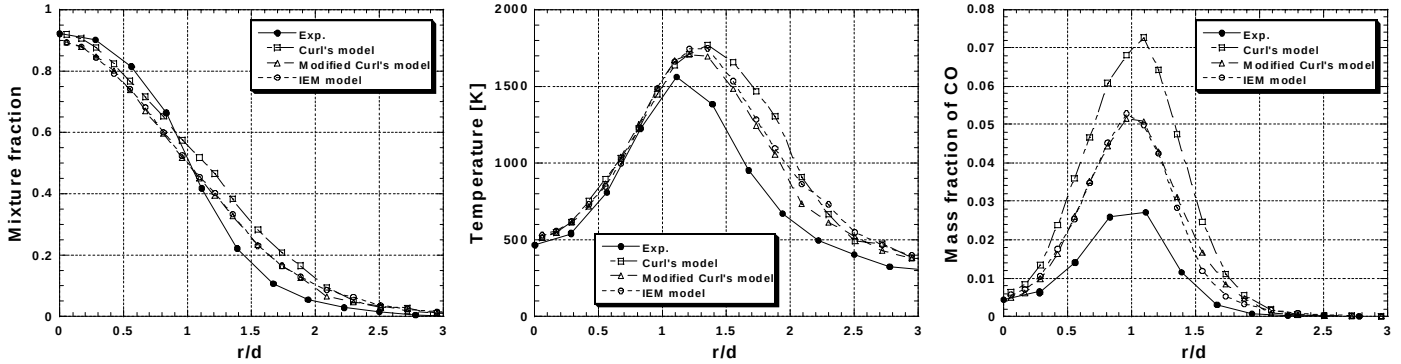

(a)Mixture fraction (b)Temperature (c)Mass fraction of CO

Figure 3: Radial profiles of scalars at $x/D = 15$

References

[1] http://www.ca.sandia.gov/tdf/Workshop.html

[2] S. B. Pope, Pdf Methods for Turbulent Reactive Flows, *Prog. Energy Combust. Sci.*, **11**, pp.119-192, 1985.

[3] Private communications with J.-Y. Chen, unpublished.

[4] J.-Y. Chen, W. Kollmann and R. W. Dibble, Pdf Modeling of Turbulent Nonpremixed Methane Jet Flames, *Combust. Sci. and Tech.*, **64**, pp. 315-346, 1989.

SECTION 4

Additional Contributions

Fourth International Workshop on Measurement and Computation of Turbulent Nonpremixed Flames

Additional Contributions

This section includes information that was presented at TNF4 either as an invited overview talk or in vugraph form during the discussions.

- Turbulent Counterflow Non-premixed Combustion: An Annotated Bibliography
  E. Mastorakos.

- Parametric Calculations of Piloted Flames
  J.-Y. Chen
  a) Comparison of CO and H_2 Results in Steady Opposed Jet Flames
  b) Sensitivity of Computed CO with Respect to Detailed Mechanism
  c) Sensitivity of CO Prediction on Mixing Model

- PDF/EMST/ISAT Calculations of Flames D and F
  Jun Xu and S. B. Pope

  These calculations were not available in time for inclusion in the TNF4 comparison plots generated by Barlow and Hinz. However, separate comparisons with measured results were presented in vugraph form in Darmstadt and are included here.

  These calculations were performed with the mixing model constant C_ϕ=2.0. The numerical accuracy of the calculations has been thoroughly assessed, and is sufficient to test the model performance in the regions of the flames that exhibit local extinction and re-ignition. The numerical errors in mean and rms profiles are around 10% for $x/R_j \leq 30$, less than 20% at x/R_j=60, but are larger at $x/R_j \geq 90$ and for Reynolds stresses. Statistics conditional on mixture fraction show considerably less numerical error. More accurate and efficient numerical algorithms are currently being developed which are expected to yield numerically accurate calculations for the full extent of the flame at reasonable computational cost.

Turbulent Counterflow Non-premixed Combustion: An Annotated Bibliography

E. Mastorakos
Institute of Chemical Engineering and High Temperature Chemical Processes, PO Box 1414, 26500 Patras, Greece. E-mail: mastorak@iceht.forth.gr

1. Introduction to turbulent counterflow flames

Research in turbulent counterflow flames has followed extensive work on laminar counterflow non-premixed and premixed combustion. Interest in laminar counterflow flames has been high due to the reduction in the spatial dimension associated with stagnation-point flows, which facilitates analyses and simulations. The uniformity of the stretch rate on the flame also helps to quantify flame behaviour as extinction is approached. The same advantages are carried over to their turbulent counterparts. In contrast to other turbulent flames, in which the turbulence is usually produced by shear in the flow, turbulence in the counterflow burners is produced by perforated plates before the jets imping on each other. In this way, the experimentalist has a separate control of the bulk strain rate (i.e. the residence time) and the turbulence. The whole range of non-premixed, partially-premixed, or premixed flames can be stabilised by varying the composition of the two jets, and a wide range of Damkohler numbers can be studied (from low-stretch flames to extinction, flamelet and non-flamelet regimes) in a single experimental arrangement.

There are some fundamental characteristics of diffusion flames in opposed jets which make them very suitable as a "benchmark" experiment for models of turbulent non-premixed combustion. As mentioned above, the turbulence, the scalars and the velocity gradients are inhomogeneous only in the axial direction, which imply a uniform Damkohler number along the flame sheet and so extinction is abrupt and global. Hence the stability limit can serve as a test for a combustion model in the same way that the extinction strain rate characterizes laminar counterflow flames and is used for the validation of chemical mechanisms. Good optical access is another advantage. Finally, the counterflow geometry may be identified as a "model" for flow elements in many realistic combustion configurations: most industrial burners involve stabilization, which is usually based on recirculation that introduces stagnation points in the flow.

2. Previous work and recommendations for future research

In the Bibliography list that follows, experimental and theoretical work is categorized to facilitate the entry of the interested researcher to the relevant literature. Some comments are also given on the content of each paper; however, a proper review is not attempted due to lack of space. Premixed flames in opposed jets and stabilised by solid plates are included due to the similarity of the experimental arrangements and turbulence phenomena involved. Methane has been used almost exclusively.

There are perhaps a dozen groups worldwide working (or having worked) on premixed stagnating flames. The corresponding number for non-premixed combustion (fuel *vs*. air) is perhaps four (in UC San Diego, Imperial College, Tokyo-Denki University, and Keio University), which shows that turbulent non-premixed counterflow flames is still a very young and unexplored subject. It may be argued that inert mixing and premixed combustion has been studied to a reasonable extent, but only a handful of publications exist for turbulent counterflow non-premixed flames. Existing work has dealt with extinction and first theoretical analyses. Unlike the case for premixed flames, the author does not know of any archival publications on velocity and species mass fractions measurements, and it seems that no modelling with finite-rate chemistry or for partially-premixed flames has been reported yet. However, some measurements are presented in Refs. [2, 49, 50] and a very useful theoretical description in Refs. [1, 53].

Future measurements should be performed for more complete flame characterization and should include LDV in inert and reactive flows, two-point velocity measurements to obtain eddy lengthscale alterations at stagnation, measurements of mixture fraction and its dissipation rate in reacting flows, imaging, and species concentrations measurements by advanced laser techniques. A comparison of various non-premixed combustion models should also be made. Finally, the prediction of the extinction limit should become one of the ultimate objectives of model validation. This will provide a critical test for turbulent combustion closures and chemistry descriptions alike.

3. Literature on inert and reacting stagnation flows

Reference	Contents / Comments
General reviews	
1	Theoretical analyses on stagnation-point premixed and non-premixed flames and turbulence modelling. Review of advantages of counterflow flames and entries in laminar counterflow flame literature.
2	Includes literature review of laminar and turbulent. First data on turbulent opposed-jet diffusion flames. Small jet separations are necessary for non-premixed flames, unlike for premixed. Partially-premixed flames measured as well. Discussion on flamelet and non-flamelet structure of the various flames.
Inert flows: turbulence production due to straining and mixing between the jets	
3-8	Review of jet structure impinging on solid plates, modifications to k-ε for stagnation-point flows, Reynolds stress models, extensive reference lists.
9	Recent LDV measurements for stagnation flows on walls, velocity pdfs.
10, 11	Eddy shape distortion due to mean flow strain. Rapid distortion theory.
12	First LDV velocity measurements in laminar opposed jet flows.
2, 13	LDV in inert opposed jets, cold-wire measurements of mixture fraction, pdfs, salient features of mixing ("young turbulence" mixing, flapping model).
14	LDV, opposed jets at relatively larger separations than in Refs. [2,13].
15	Conditional scalar dissipation measurements with parallel cold-wires, joint χ-ξ pdfs.
16	k-ε and gradient flux model analysis gives insight into mixing, estimates of χ.
17, 18	Reynolds stress analysis of opposed jet velocity field, turbulence and mixing.
19	Conditional χ measurements, further development of flapping model.
Premixed flames stabilised by stagnation plates and by counterflow	
20-28	Flames stabilised by solid plates. LDV measurements, turbulent flame speed correlations, conditional measurements, spatial scalar structure, comparison of stagnation flames with vee- and bunsen-type flames, extinction, imaging.
29	Different flame shapes in wall stagnation flows.
30-31	Flames on walls. BML analysis, k-ε model, dilution effects, two-dimensional CFD predictions.
32-40	Twin flames. First burner designs, extinction, LDV measurements, progress variable measurements, Rayleigh scattering, flamelet orientation, effects of co-flow, turbulent Tsuji-burner.
2, 41	Single premixed flames (reactant jet impinging on air jet), flames against hot products, ultra-lean premixed flames with vitiated air. Absence of sudden extinction. Close jet separations.
42-48	Twin and single flame theory and modelling. BML analysis, analysis of flames in streams with unequal enthalpies, two-dimensional CFD with transported pdf, flame surface density modelling, Reynolds stress closure with flamelet model. All theoretical/numerical works have also predicted adequately the inert flow field.
Non-premixed flames (fuel jet impinging on identical oxidant jet)	
2, 49	First burner designs. Includes LDV and sampling probe measurements, partially-premixed (fuel+air *vs.* air) flames, hydrogen flame extinction. Flames far from and close to extinction have been measured.
16, 50	Extinction conditions including partially-premixed, correlations, limited temperature measurements.
51	Turbulent Tsuji-burner, extinction limits.
52	Different turbulence levels in the two jets, diluted flames, tomography, extinction limits.
41	Non-premixed flames with oxidant diluted by hot combustion products, extinction.
1, 53	Theoretical analysis, k-ε, equilibrium chemistry with presumed pdf. Tuned model for the scalar dissipation in agreement with "young turbulence" idea from inert opposed-jet experimental data.
Other turbulent counterflow flames	
54	Acoustically-forced non-premixed flames.
55	Droplet combustion.

References

1. K.N.C. Bray, M. Champion & P.A. Libby (1994) Flames in stagnating turbulence. In Turbulent Reactive Flows, P.A. Libby and F.A. Williams (Eds.), Academic Press.
2. E. Mastorakos (1993) Turbulent combustion in opposed jet flows. PhD Thesis, University of London.
3. R. Viskanta (1993) Heat transfer to impinging isothermal gas and flame jets. *Exp. Ther. and Fluid Sci.* **6**, 111.
4. W.C. Strahle, R.K. Sigman & W.L. Meyer (1987) Stagnating turbulent flows. *AIAA Journal* **25**, 1071.
5. D.B. Taulbee & L. Tran (1988) Stagnation streamline turbulence. *AIAA Journal* **26**, 1011.
6. M. Champion & P.A. Libby (1990) Stagnation streamline turbulence revisited. *AIAA Journal* **28**, 1525.
7. M. Champion & P.A. Libby (1991) Asymptotic analysis of stagnating turbulent flows. *AIAA Journal* **29**, 17.
8. M. Champion & P.A. Libby (1994) Reynolds stress description of opposed and impinging turbulent jets. II. Axisymmetric jets impinging on nearby walls. *Phys. Fluids* **6**, 1805.
9. T. Ueda, H. Imaizumi, M. Mizomoto, I.G. Shepherd (1997) Velocity statistics along the stagnation line of an axi-symmetric stagnating turbulent flow. *Exp. Fluids* **22**, 473.
10. M. J. Lee (1989) Distortion of homogeneous turbulence by axisymmetric strain and dilatation. *Phys. Fluids A* **1**, 1541.
11. C.Y. Wei & J.J. Miau (1993) Characteristics of stretched vortical structures in two-dimensional stagnation flow. *AIAA Journal* **31**, 2075.
12. J.C. Rolon, D. Veynante, J.P. Martin & F. Durst (1991) Counter jet stagnation flows. *Exp. Fluids* **11**, 313.
13. E. Mastorakos, A.M.K.P. Taylor & J.H. Whitelaw (1994) Mixing in turbulent opposed jet flows. Turbulent Shear Flows 9, Durst, F. et al. (Eds.), Springer–Verlag, p. 149.
14. L.W. Kostiuk, K.N.C. Bray & R.K. Cheng (1993) Experimental study of premixed turbulent combustion in opposed streams. Part I - Nonreacting flow field. *Combust. Flame* **92**, 377.
15. K. Sardi, A.M.K.P. Taylor & J.H. Whitelaw (1998) Condional scalar dissipation statistics in a turbulent counterflow. *J. Fluid Mech.* **361**, 1.
16. E. Mastorakos, A.M.K.P. Taylor & J.H. Whitelaw (1992) Scalar dissipation rate at the extinction of turbulent counterflow non–premixed flames. *Combust. Flame* **91**, 55.
17. M. Champion & P.A. Libby (1993) Reynolds stress description of opposed and impinging turbulent jets. Part I. Closely spaced opposed jets. *Phys. Fluids A* **5**, 203.
18. L.W. Kostiuk & P.A. Libby (1993) Comparison between theory and experiment for turbulence in opposed streams. *Phys. Fluids A* **5**, 2301.
19. K. Sardi, A.M.K.P Taylor & J.H. Whitelaw (1998) A mixing model for joint scalar statistics. *Combust. Sci. and Tech.* **136**, 95.
20. P. Cho, C.K. Law, J.R. Hertzberg & R.K. Cheng (1986) Structure and propagation of turbulent premixed flames stabilized in a stagnation flow. *21st Symposium (Int.) on Combustion*, p. 1493.
21. P. Cho, C.K. Law, R.K. Cheng & I.G. Shepherd (1988) Velocity and scalar fields of turbulent premixed flames in stagnation flow. *22nd Symposium (Int.) on Combustion*, p. 739.
22. Y. Liu & B. Lenze (1988) The influence of turbulence on the burning velocity of premixed CH4-H2 flames with different laminar burning velocities. *22nd Symposium (Int.) on Combustion*, p. 747.
23. I.G. Shepherd, R.K. Cheng & P.J. Goix (1990) The spatial scalar structure of premixed turbulent stagnation point flames. *23rd Symposium (Int.) on Combustion*, p. 781.
24. R.K. Cheng, I.G. Shepherd & I. Gokalp (1989) A comparison of the velocity and scalar spectra in premixed turbulent flames. *Combust. Flame* **78**, 1989.
25. Y. Liu, B. Lenze & W. Leuckel (1991) Investigation on the combustion-turbulence interaction in premixed stagnation flames of H2-CH4 mixtures. Turbulent Shear Flows 7, Durst et al. (Eds.), p. 357.
26. Y. Yahagi, T. Ueda & M. Mizomoto (1992) Extinction mechanism of lean metahne/air turbulent premixed flame in a stagnation point flow. *24th Symposium (Int.) on Combustion*, p. 537.
27. D. Escudié & E. Haddar (1993) Experimental study of a premixed turbulent stagnating flame. *Combust. Flame* **95**, 433.
28. S.C. Li, P.A. Libby & F.A. Williams (1994) Experimental investigation of a premixed flame in an impinging turbulent stream. *25th Symposium (Int.) on Combustion*, p. 1207.
29. Y. Zhang & K.N.C. Bray (1999) Characterization of impinging jet flames. *Combust. Flame* **116**, 671.
30. K.N.C. Bray, M. Champion & P.A. Libby (1992) Premixed flames in stagnating turbulence Part III-The k-ε theory for reactants impinging on walls. *Combust. Flame* **91**, 165.
31. H. Lahjaily, M. Champion, D. Karmed & P. Bruel (1998) Introduction of dilution in the BML model: application to a stagnating turbulent flame. *Combust. Sci. and Tech.* **135**, 153.
32. L.W. Kostiuk (1991) Premixed turbulent combustion in counterflowing streams. PhD Thesis, University of Cambridge.
33. C. Mounaim-Rousselle (1993) Combustion turbulente premelangée dans un écoulement a jets opposés. PhD Thesis, Université d'Orléans (in french).

34. L.W. Kostiuk, K.N.C. Bray & T.C. Chew (1989) Premixed turbulent combustion in counterflowing streams. *Combust. Sci. and Tech.* **64**, 233.
35. L.W. Kostiuk, K.N.C. Bray & R.K. Cheng (1993) Experimental study of premixed turbulent combustion in opposed streams. Part II-Reacting flow field and extinction. *Combust. Flame* **92**, 396.
37. Ch. Mounaim-Rousselle & I. Gokalp (1994) Strain effects on the structure of counterflowing turbulent premixed flames. *25th Symposium (Int.) on Combustion*, p. 1199.
38. E. Bourguinon, L.W. Kostiuk, Y. Michou & I. Gokalp (1996) Experimentally measured burning rates of premixed turbulent flames. *26th Symposium (Int.) on Combustion*, p. 447.
39. A. Yoshida, H. Kakinuma & Y. Kotani (1996) Extinction of turbulent premixed flames by small-scale turbulence at Kolmogorov microscale. *26th Symposium (Int.) on Combustion*, p. 397.
40. L.W. Kostiuk, I.G. Shepherd & K.N.C. Bray (1999) Experimental study of premixed turbulent combustion in opposed streams. Part III-Spatial structure of flames. *Combust. Flame* **118**, 129.
41. E. Mastorakos, A.M.K.P. Taylor & J.H. Whitelaw (1995) Extinction of turbulent counterflow flames with reactants diluted by hot products. *Combust. Flame* **102**, 101.
42. K.N.C. Bray, M. Champion & P.A. Libby (1991) Premixed flames in stagnating turbulence: Part I. The general formulation for counterflowing streams and gradient models for turbulent transport. *Combust. Flame* **84**, 391.
43. K.N.C. Bray, M. Champion & P.A. Libby (1998) Premixed flames in stagnating turbulence: Part II. The mean velocities and Pressure and the Damkohler number. *Combust. Flame* **112**, 635.
44. K.N.C. Bray, M. Champion & P.A. Libby (1996) Extinction of premixed flames in turbulent counterflowing streams with unequal enthalpies. *Combust. Flame* **107**, 53.
45. W.P. Jones & Y. Prasetyo (1996) Probability density function modeling of premixed turbulent opposed jet flames. *26th Symposium (Int.) on Combustion*, p. 275.
46. A.S. Wu & K.N.C. Bray (1997) A coherent flame model of premixed turbulent combustion in a counterflow geometry. *Combust. Flame* **109**, 43.
47. E. Lee, C.R. Choi & K.Y. Huh (1998) Application of the coherent flamelet model to counterflow turbulent premixed combustion and extinction. *Combust. Sci. and Tech.* **138**, 1.
48. R.P. Lindstedt & E.M. Vaos (1999) Modeling of premixed turbulent flames with second moment methods. *Combust. Flame* **116**, 461.
49. E. Mastorakos, A.M.K.P. Taylor & J.H. Whitelaw (1996) Velocity and scalar fields of turbulent counterflow diffusion flames. Internal Report, Thermofluids Section, Imperial College.
50. E. Mastorakos, A.M.K.P. Taylor & J.H. Whitelaw (1992) Extinction and temperature characteristics of turbulent counterflow diffusion flames with partial premixing. *Combust. Flame* **91**, 40.
51. H. Tsuji, A. Yoshida & N. Endo (1994) Effect of turbulence on extinction of counterflow diffusion flame. *25th Symposium (Int.) on Combustion*, p. 1191.
52. A. Kitajima, T. Ueda, A. Matsuo & M. Mizomoto (1996) Experimental investigation of the flame structure and extinction of turbulent counterflow non-premixed flames. *26th Symposium (Int.) on Combustion*, p. 137.
53. F. Mauri & P.A. Libby (1995) Nonpremixed flames in stagnating turbulence Part I-The k-ε theory with equilibrium chemistry for the methane-air system. *Combust. Flame* **102**, 341.
54. K. Sardi (1998) PhD Thesis, University of London.
55. Y. Hardalupas & M. Orain (1999) Internal Report, Thermofluids Section, Imperial College.

Comparison of CO and H_2 Results in Steady Opposed Jet Flames:

J.-Y. Chen, University of California, Berkeley

Tsuji type opposed jet flames have been computed using reduced mechanisms based on the skeletal workshop mechanism, the GRI-1.22 and GRI-2.11 mechanisms. The fuel side mixture if 25% CH_4 and 75% air, as for the piloted jet flame series. The 4-step-Peters denotes results obtained using the original Peters' 4-step reduced chemistry. We have refined this 4-step mechanism by allowing reverse reactions with full steady state expression. As seen in the comparisons, the differences in the results obtained with these two reduced mechanisms are small. There were two reduced mechanisms developed by us based on GRI-1.22. The results are denoted by 10-step and 12-step in the figures. In comparison with the 10-step reduced chemistry, the 12-step mechanism contains two extra species, HO_2 and H_2O_2. These two species appear to be important for low pressure flames below ambient pressure and at low temperatures. For vigorously burning flames, these two mechanisms gave essentially the same results. We have developed two additional reduced mechanisms based on GRI-2.11. The reduced mechanism denoted by '12-step with NOx ' is essentially the same as the 10-step mechanism but with two additional species NO and NH_3. Similarly, the reduced mechanism denoted by '14-step with NOx ' is essentially the same as the 12-step mechanism based on GRI-1.22. The comparison of CO predictions show good agreement among reduced mechanisms and the detailed GRI-2.11. However, the predictions of H_2 by both 4-step mechanisms are much lower than those by the GRI-2.11 and the associated reduced mechanisms.

Flame D,E,F; 25%CH4+75%Air Tsuji Opposed Flame Equal Diff.

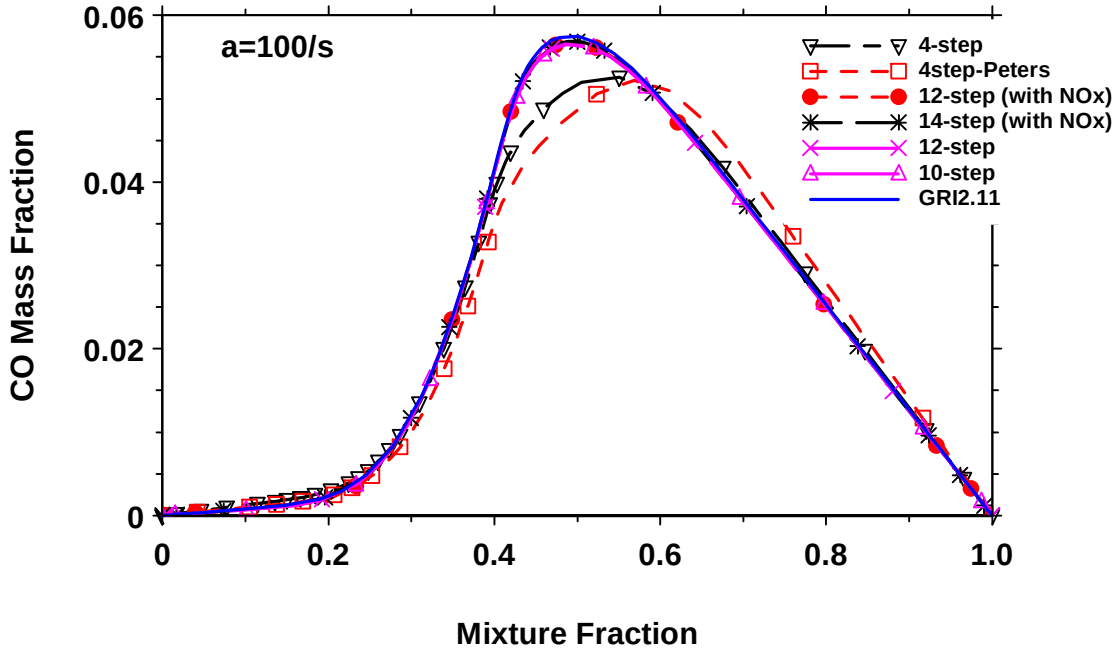

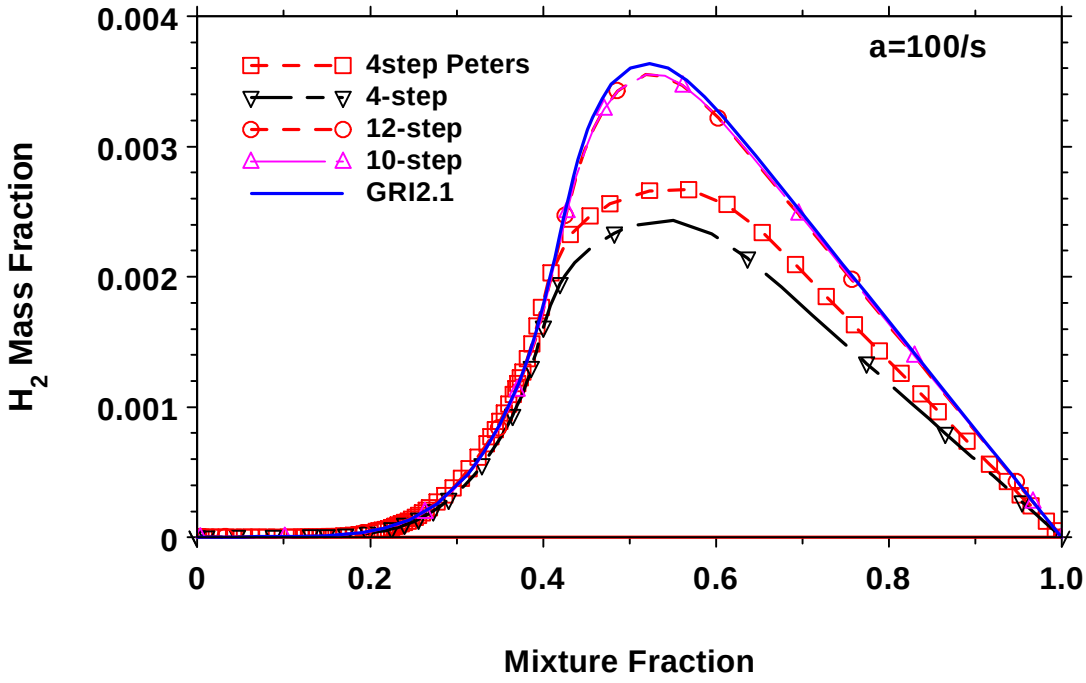

Flame D,E,F; 25%CH4+75%Air Tsuji Opposed Flame Equal Diff.

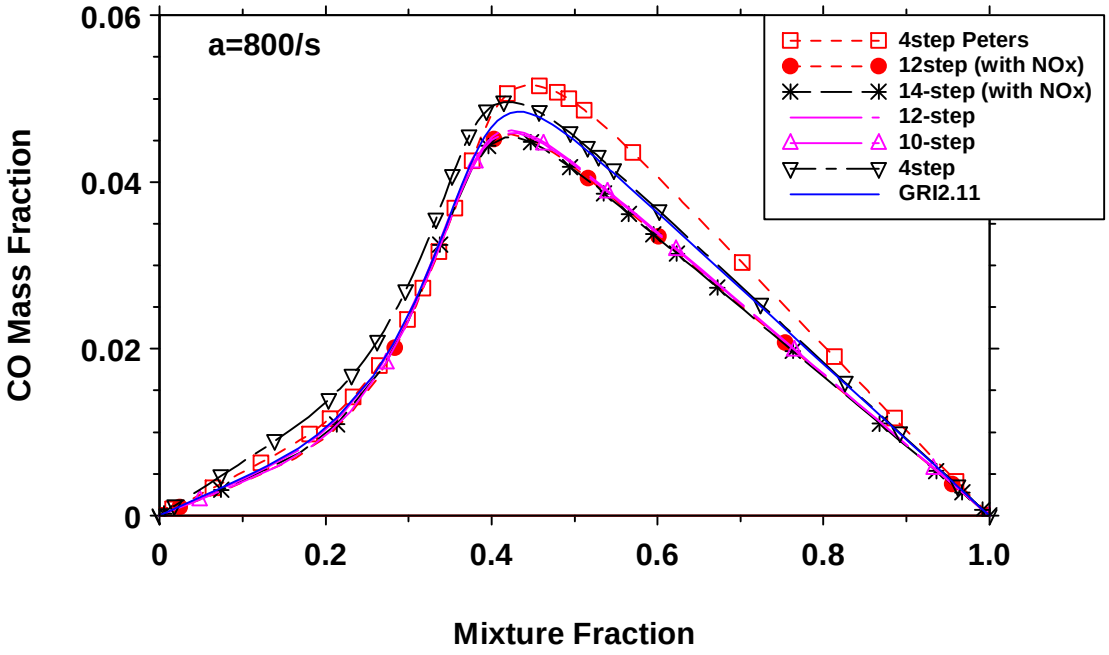

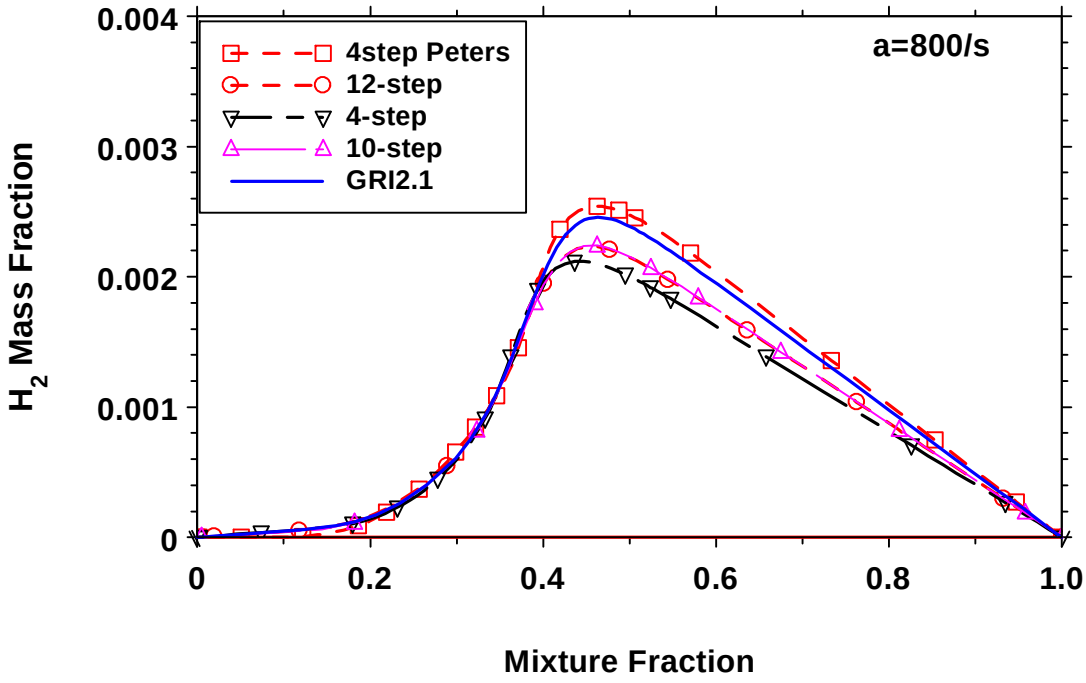

Sensitivity of Computed CO with Respective to Detailed Mechanism

J.-Y. Chen, University of California, Berkeley

One of the uncertainties in comparing various model results comes from the disagreement in detailed mechanisms. We have performed well-mixed reactor calculations with a parabolic marching code for Flame D to illustrate this point using five different mechanisms. The skeletal workshop mechanism (denoted by 'skel-ws') and the mechanism used previously by Correa and Pope (denoted by 'Correa-Pope CH4), contain only C-1 chemistry. The Miller and Bowman mechanism was compiled for modeling NO_x and it was not probably optimized for nonpremixed flames. Both the GRI1.2 and the Warnatz' mechanisms contain C-1 and C-2 chemistry, and they were compiled for both premixed and nonpremixed flames. However, the Warnatz' mechanism presented in the TNF 3rd Workshop was limited to high temperatures. Difficulties were encountered for low temperatures, and the chemical sources were artificially set to zero for temperatures below 1,000K. The first Figure below compares predicted CO mass fractions conditioned on mixture fraction at x/D=15 and x/D=30. As seen in the figure, the CO predictions are in excellent agreement for mixtures with mixture fractions less than 0.4 (the stoichiometric value is ~0.36). Large discrepancies are noted among the computed results for fuel rich mixtures, indicating the uncertainty of chemical kinetics under fuel rich conditions. Among the mechanisms, the mechanism used by Correa and Pope gives highest CO levels in the fuel rich parts. Despite of the lack of C-2 chemistry, the CO levels predicted by the skeletal workshop mechanism are in reasonable agreement with those using GRI1.2. During the TNF3 workshop, Prof. Warnatz acknowledged that the rate for $CO+OH=CO_2+H$ in his detailed mechanism is too large, and a more recent version of the mechanism would produce results close to those from GRI1.2. In the transient flamelet results presented by Pitcsh and Peters, the CO predictions also show a large variation by using different mechanisms. Before the uncertainty in prediction CO for fuel rich mixtures is reduced, it is not feasible to use CO as a criterion for assessing the merits of different turbulence-chemistry interaction models.

Comparison of Chemical Mechanisms
Flame D: Reynolds Stress Model with Well-Mixed Reactor

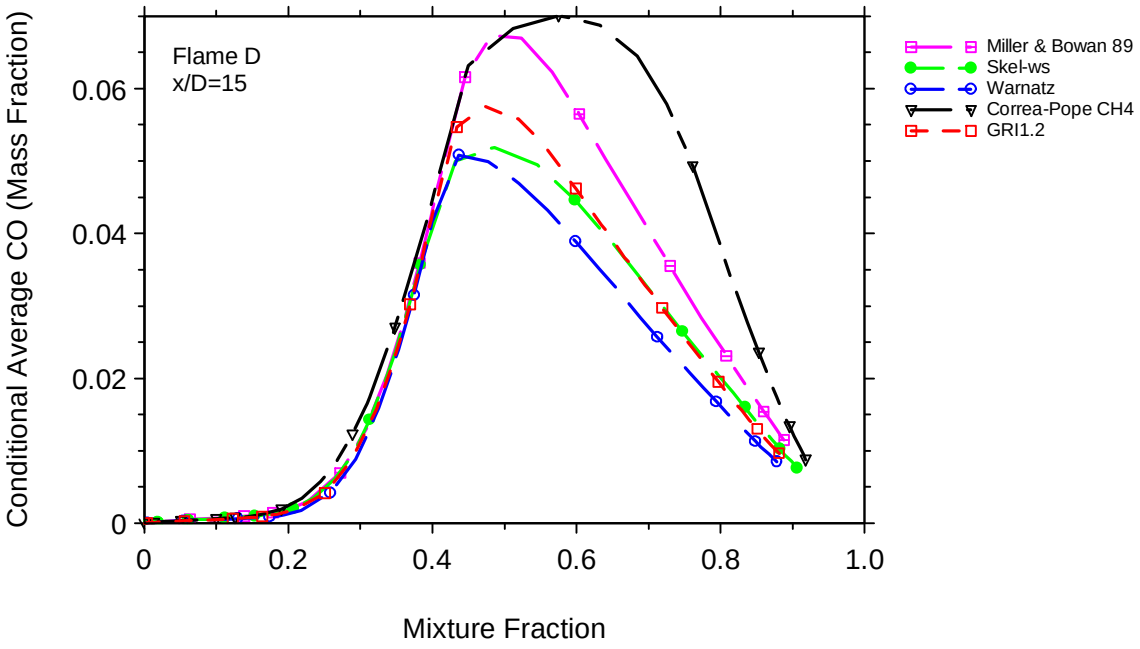

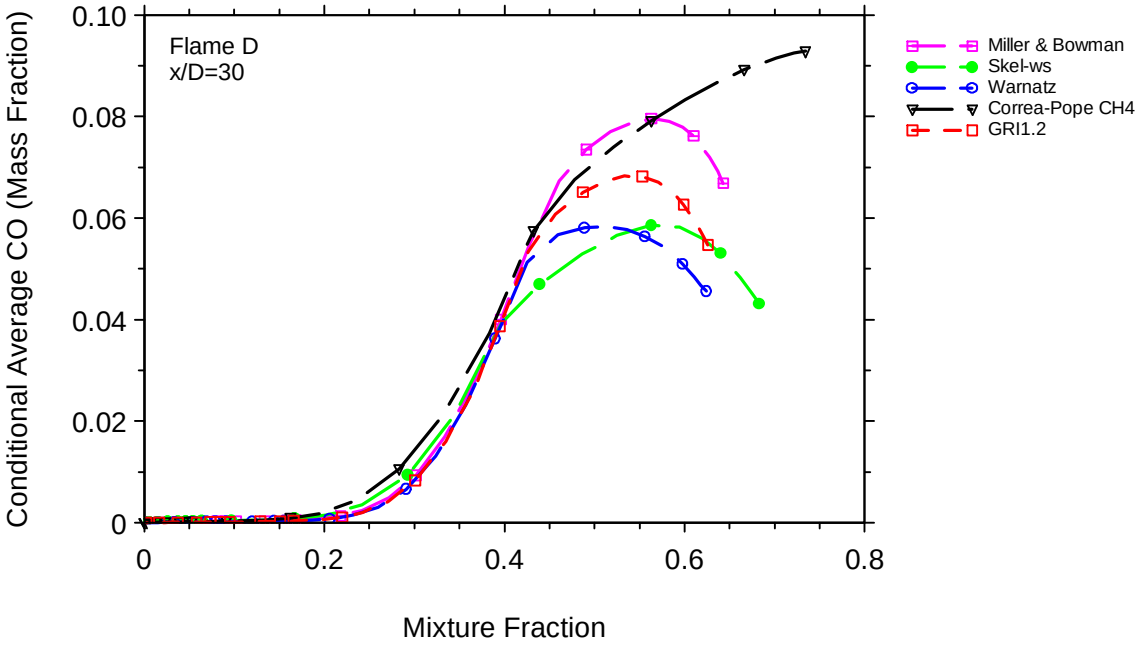

Comparison of Chemical Mechanisms
Flame D: Reynolds Stress Model with Well-Mixed Reactor

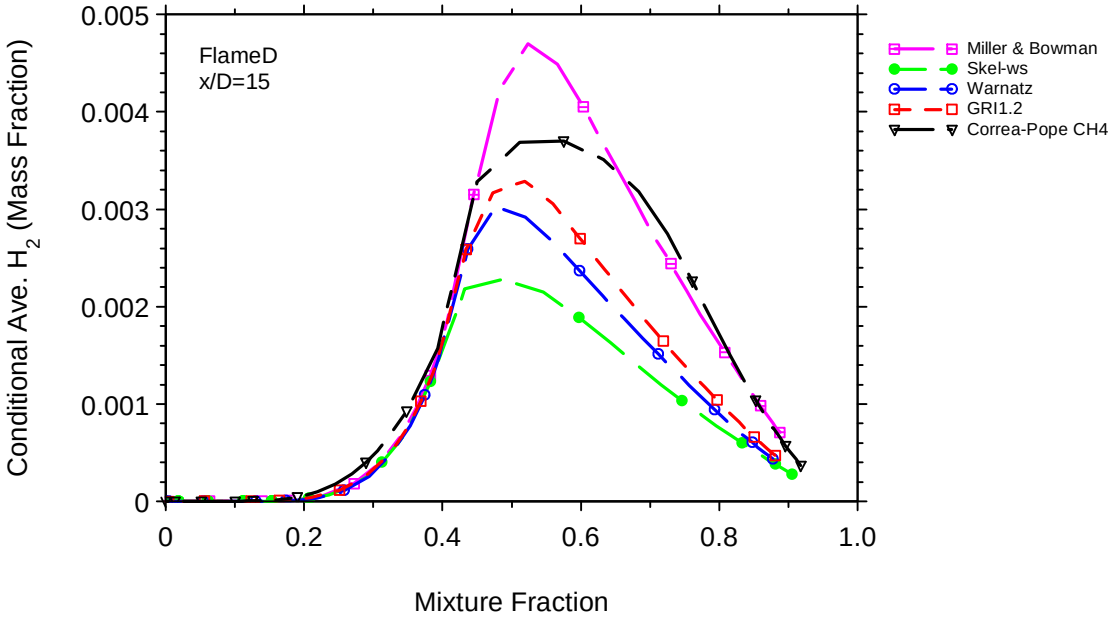

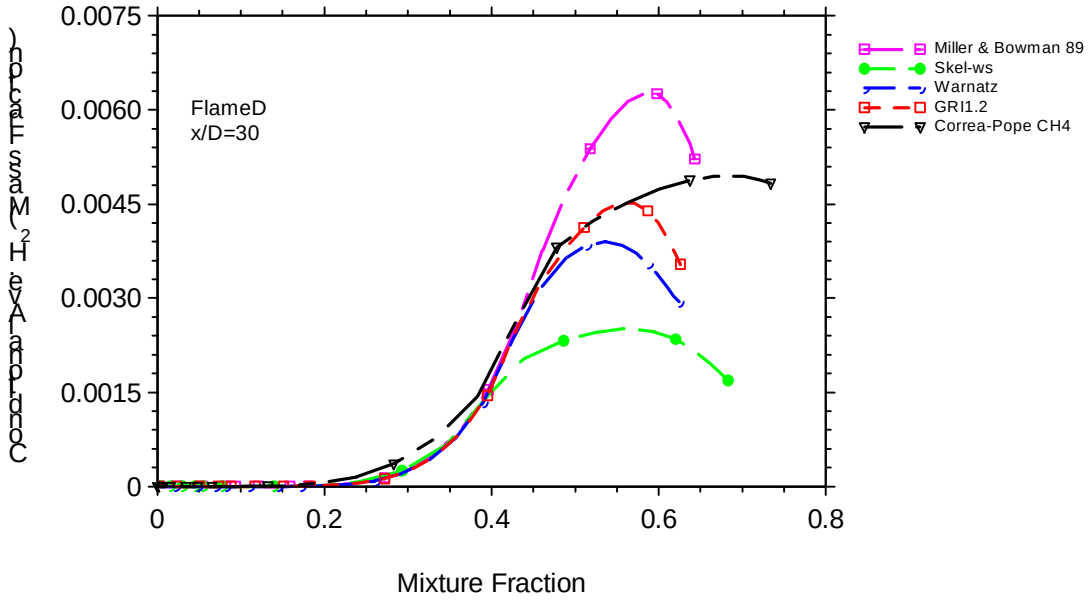

Comparison of Chemical Mechanisms
Flame D: Reynolds Stress Model with Well-Mixed Reactor

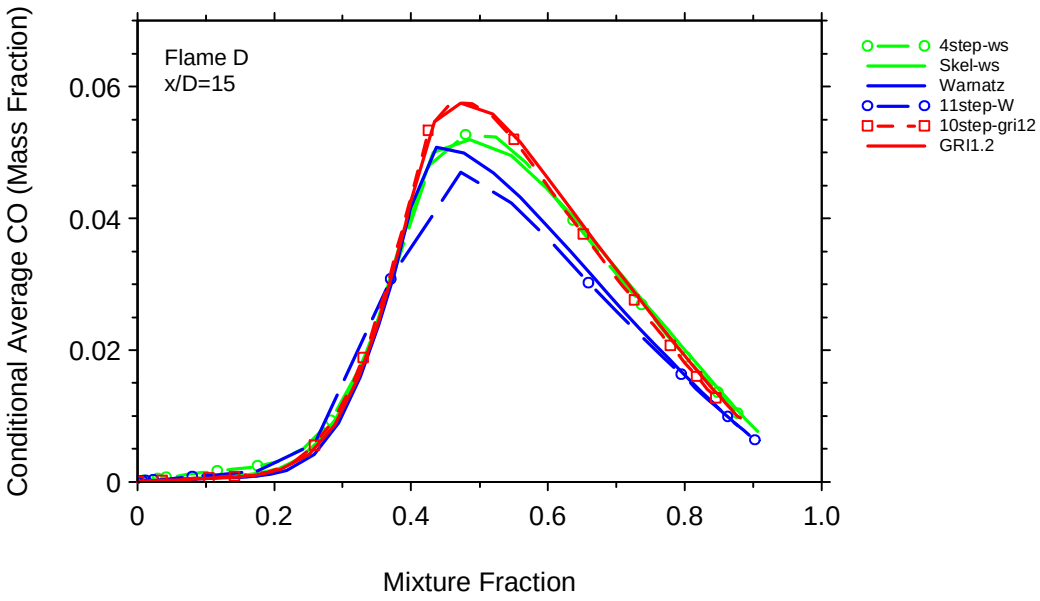

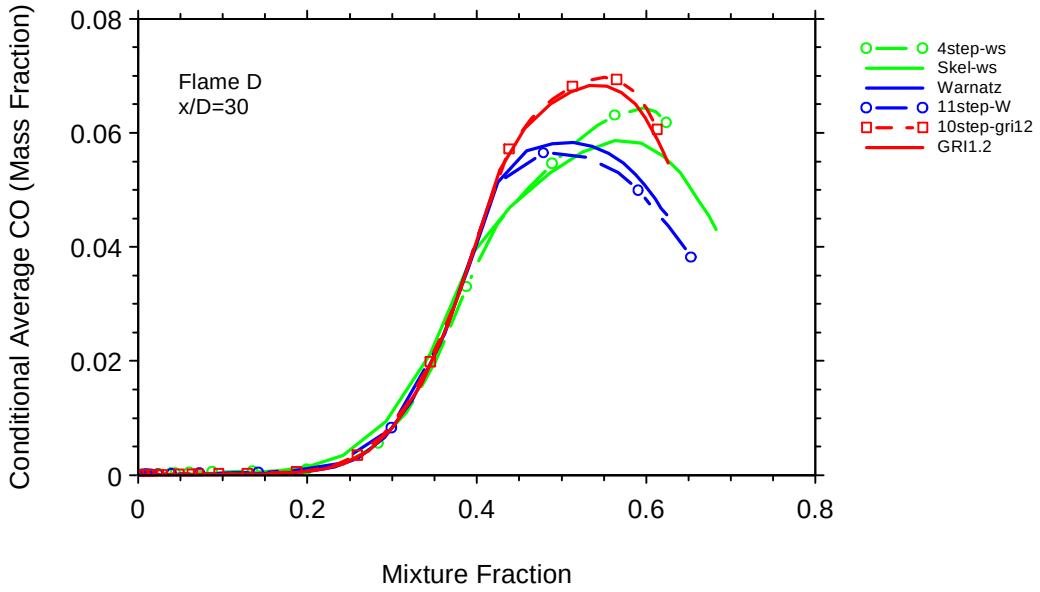

Comparison of Chemical Mechanisms
Flame D: Reynolds Stress Model with Well-Mixed Reactor

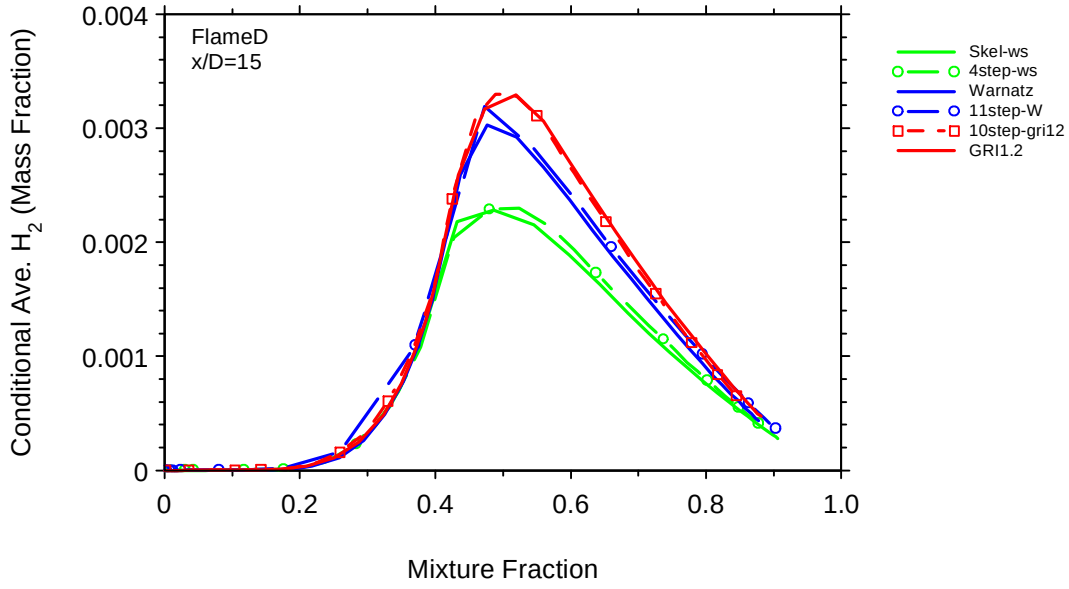

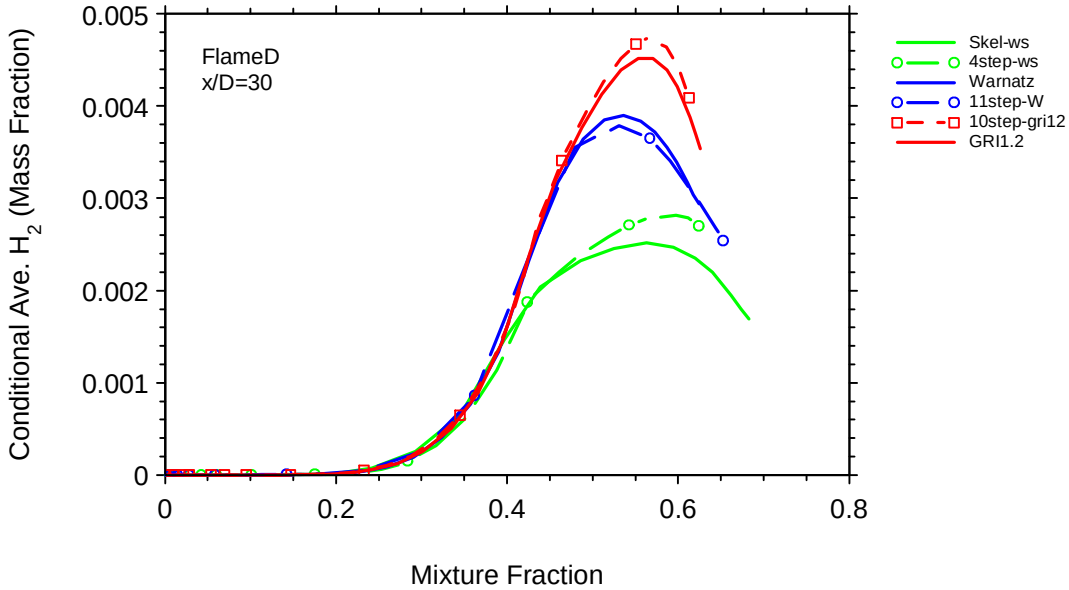

Sensitivity of CO Prediction on Mixing Model

J.-Y. Chen, University of California, Berkeley

The sensitivity of CO predictions on the mixing model is explored using the joint scalar pdf approach (PDF) with a 4-step reduced chemistry. This 4-step reduced chemistry was an improved version of the original Peters' 4-step mechanism by including complete steady-state expressions and reverse steps. The flow field and modeling details can be found in TNF4 case studies of Flame D,E, and F. Six mixing models were included in the comparision:

(1) Modified Curl (designated by TNF as as one of the test mixing models)
(2) IEM (Interaction by Exchange with the Mean, designated by TNF as one of the test mixing models)
(3) Modified Curl with Differential Diffusion[1]
(4) IEM with Differential Diffusion[1]
(5) Linear Eddy Model (LEM)[1,2]
(6) 1-D Mixing Model ~ transient flamelet model

Mixing model (6) was implemented by aligning Monte Carlo particles within each cell according to their mixture values. A one-dimensional diffusion equation is solved for the all species. The physical spacing between the particles is uniform and related to the scalar dissipation rate such that the variance is properly predicted. Model (6) may be equivalent to the transient flamelet model but more expensive as each cell carries its own transient flamelet. Model (6) is also considered similar to Model (5) without stirring events. Details of implementation of Models (3)-(5) can be found in Ref. 1. The comparisons seen below indicate that the CO predictions are highest when the 1D-mixing model is used. The degree of stirring (or randomness generated by the stochastic simulations) appears to stir up CO on fuel rich side, and consequently, the predicted CO levels are lowered and closer to the pure mixing limit (i.e., a straight line). The computed sensitivity of CO prediction on the mixing model increases with jet exit velocity. This may be due partly to differences in the degree of localized extinction obtained with each mixing model.

1.J.-Y. Chen, W.-C. Chang, "Modeling Differential Diffusion Effects in Turbulent Nonreacting/Reacting Jets with Stochastic Mixing Models," Combust. Sci. and Tech. **133**: 343-375, 1998.

2. Kerstein, A. R. (1990). Linear-Eddy Modeling of Turbulent Transport. Part 3: Mixing and Differential Molecular Diffusion in Round Jets. *J. Fluid Mech*., **216**, 411.

Flame D: Piloted 25%CH4+75%Air - Air Turbulent Jet Flame

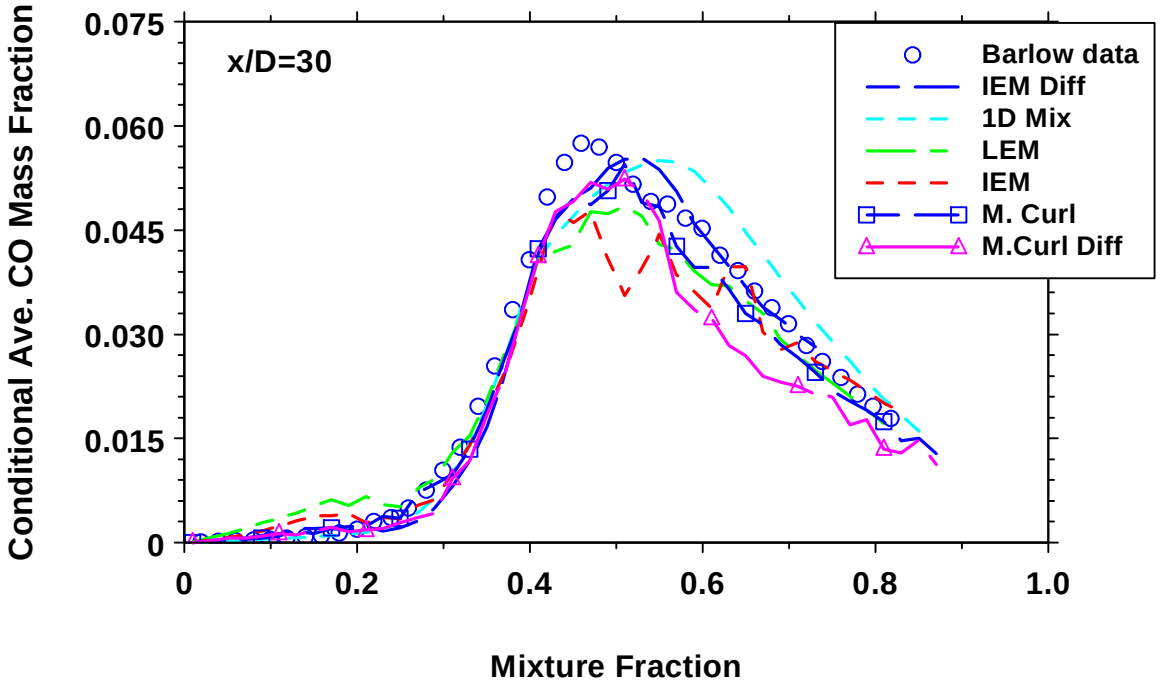

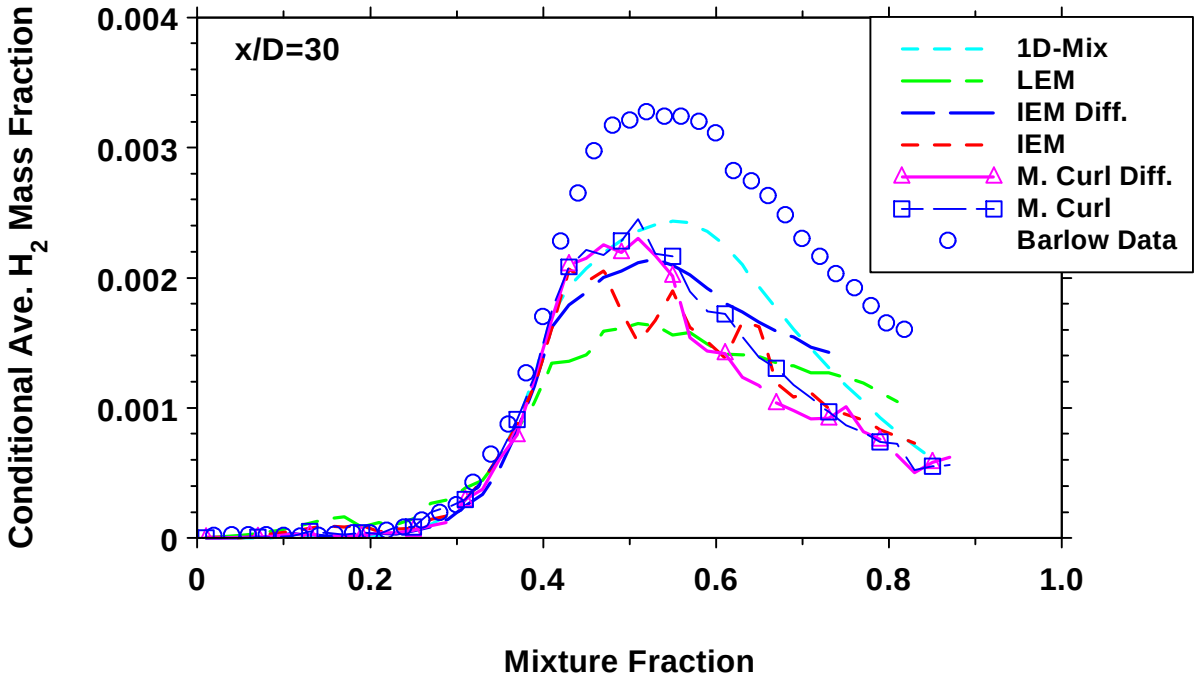

Flame E: Scalar PDF RSM 4Step Reduced Chemistry

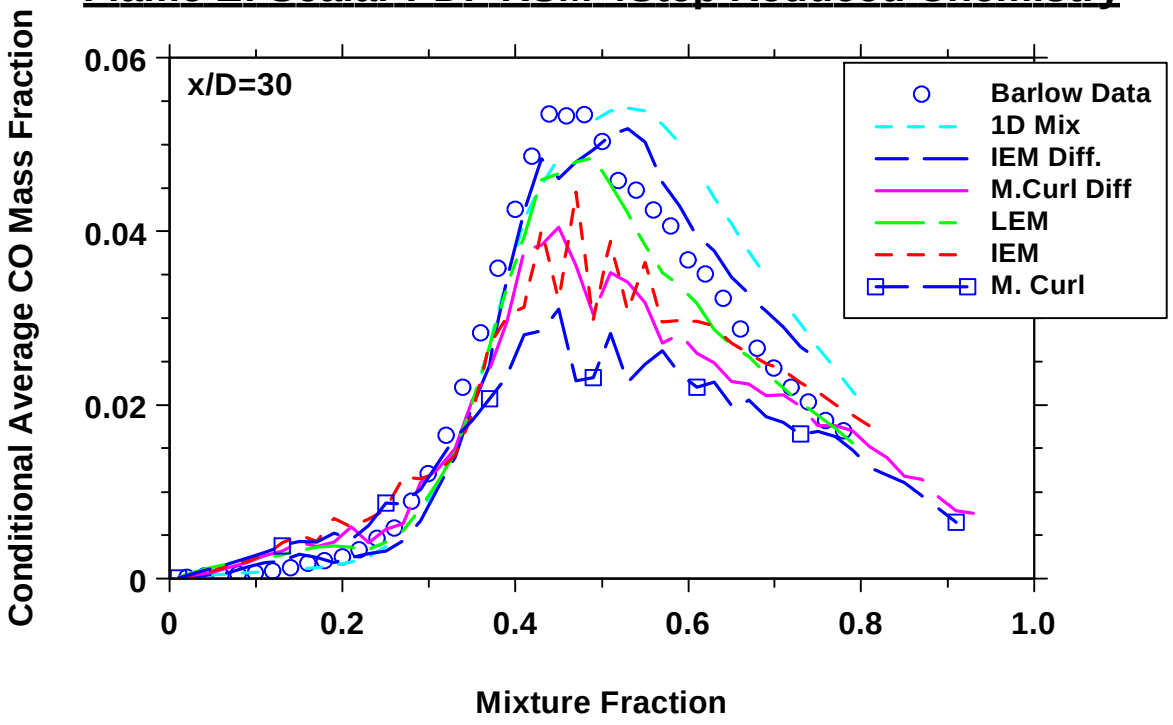

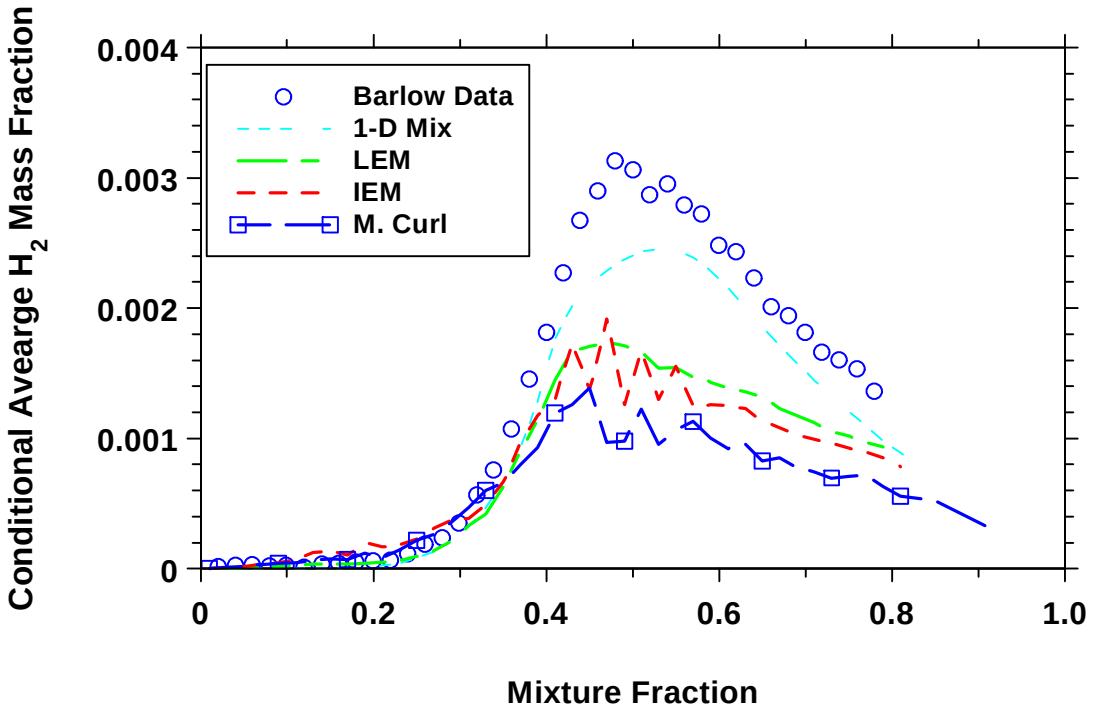

Flame F: Scalar PDF RSM 4Step Reduced Chemistry

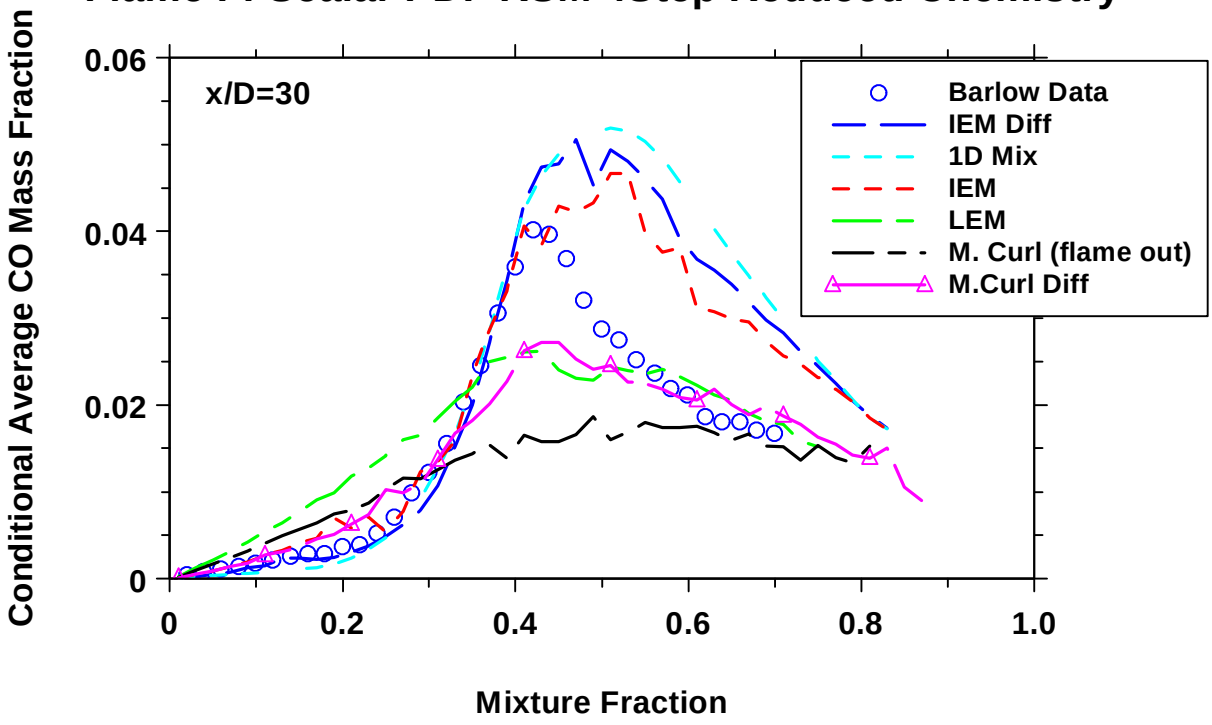

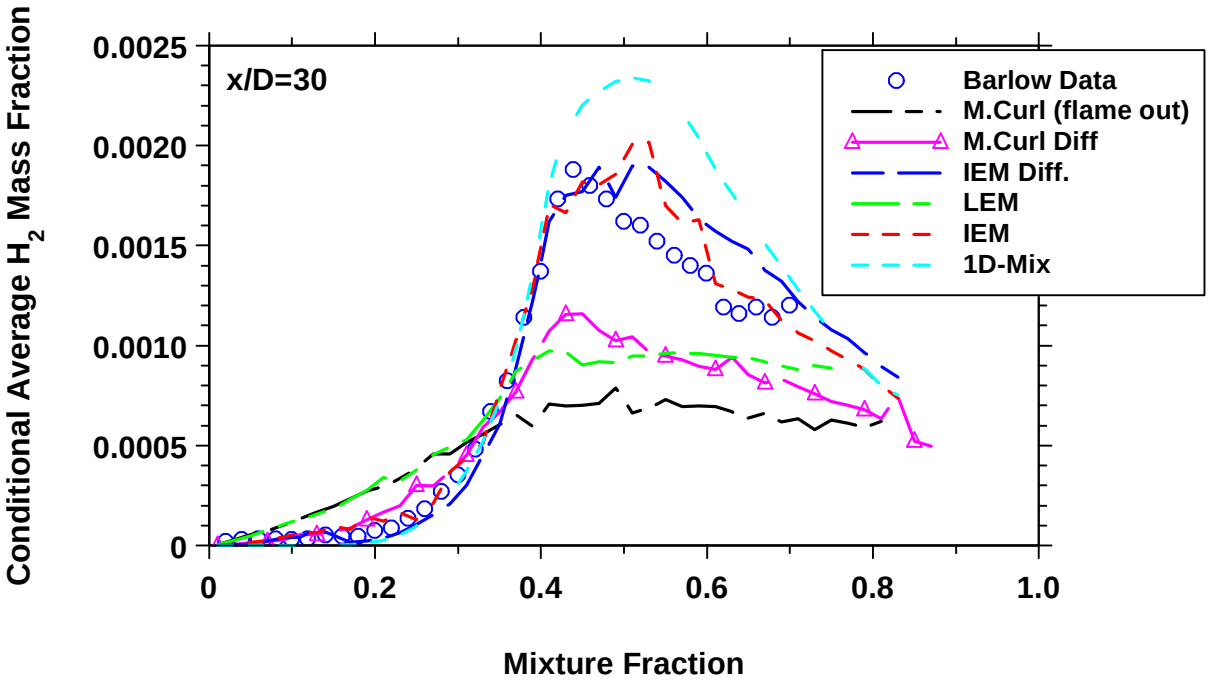

PDF/ISAT Calculations of Flame D and F

- Models:
  - Joint velocity-composition-frequency PDF model
    - velocity: simplified Langevin model;
    - mixing: EMST (Subranmaniam and Pope, 1998) without differential diffusion effects;
    - frequency: stochastic model (Xu and Pope, 1999);
  - ISAT (Pope, 1997): error tolerance 5×10^{-5};
  - Chemistry mechanism: augmented reduced mechanism (ARM, Sung et al., 1998), without radiation;
  - ***No artificial ignition is needed.***
- Numerics:
  - Grids: 61x61; Domain: 120x25 R_{jet};
  - Particles: 100/cell;
  - Starting location of computation: x/D=0;
  - Machine: Intel cluster (5 processors); CPU time: ~100 hours.
  - B.C.'s: same as TNF web for *both* flames.

Conditional means of Flame D

Temperature

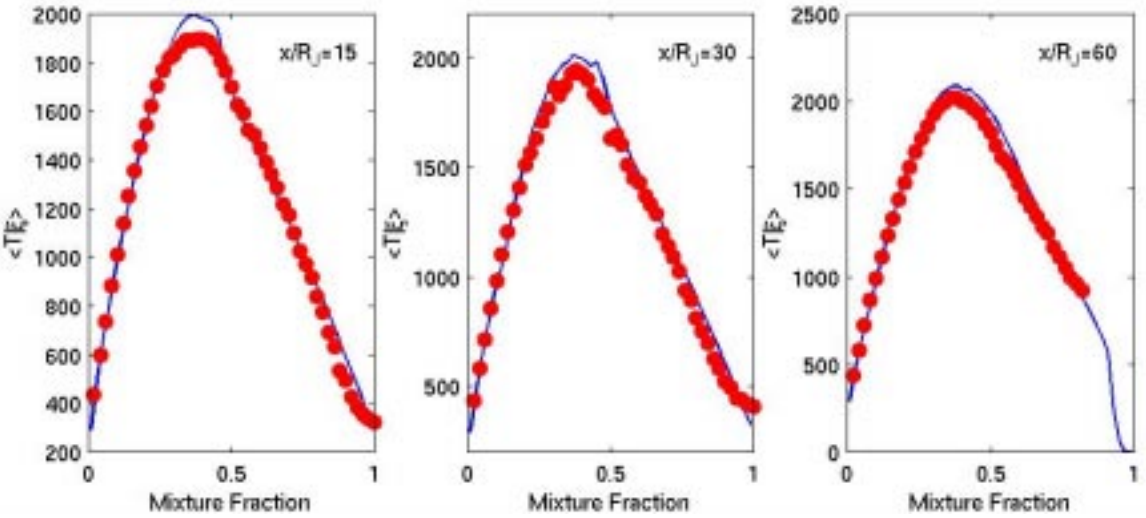

Dots:exp. By Barlow et al. (1998);

Line:PDF

CO_2

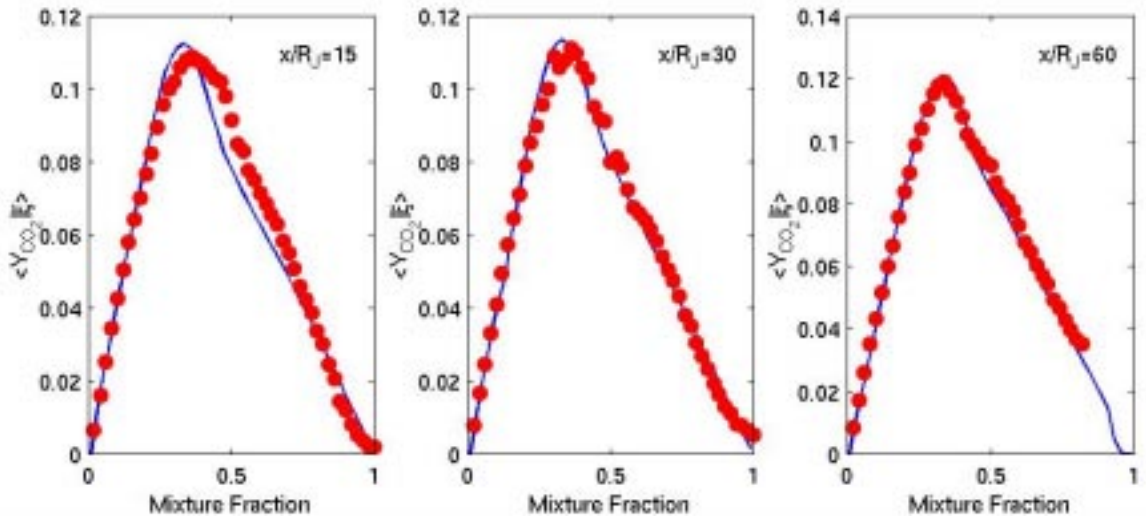

O_2

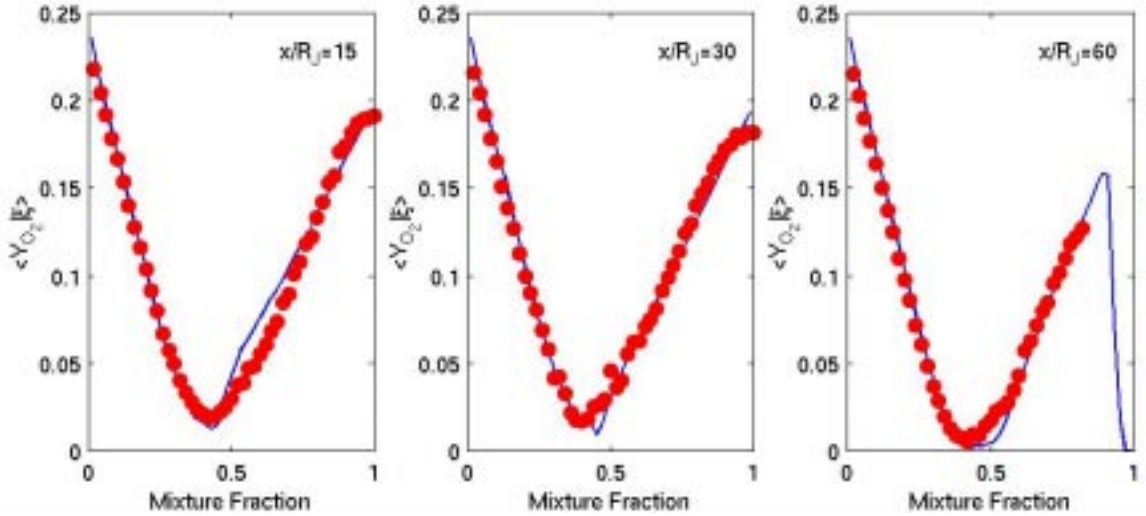

Conditional means of Flame D

H_2O

CO

OH

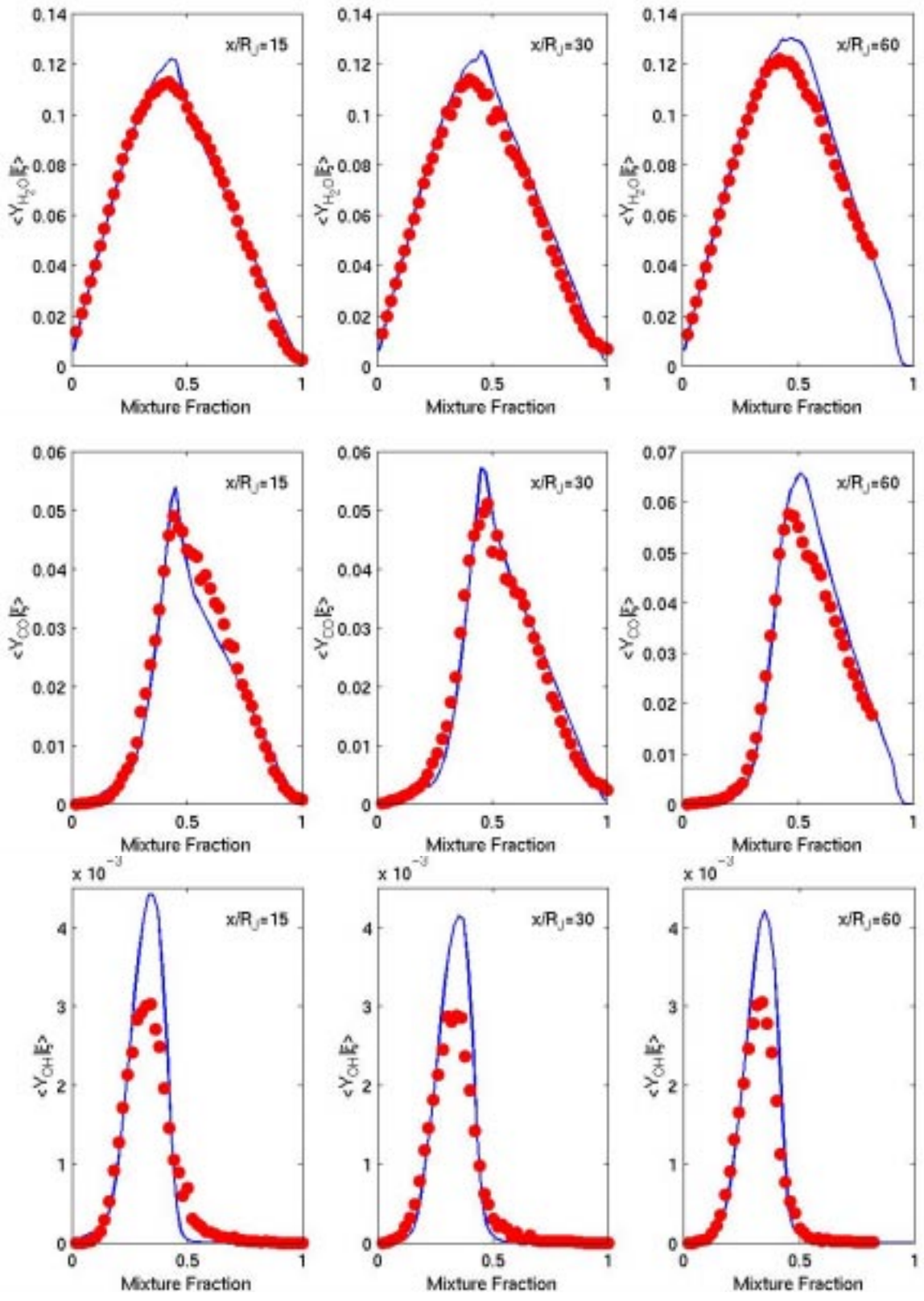

Dots:exp.;

Line:PDF

Conditional PDF of Flame D and F

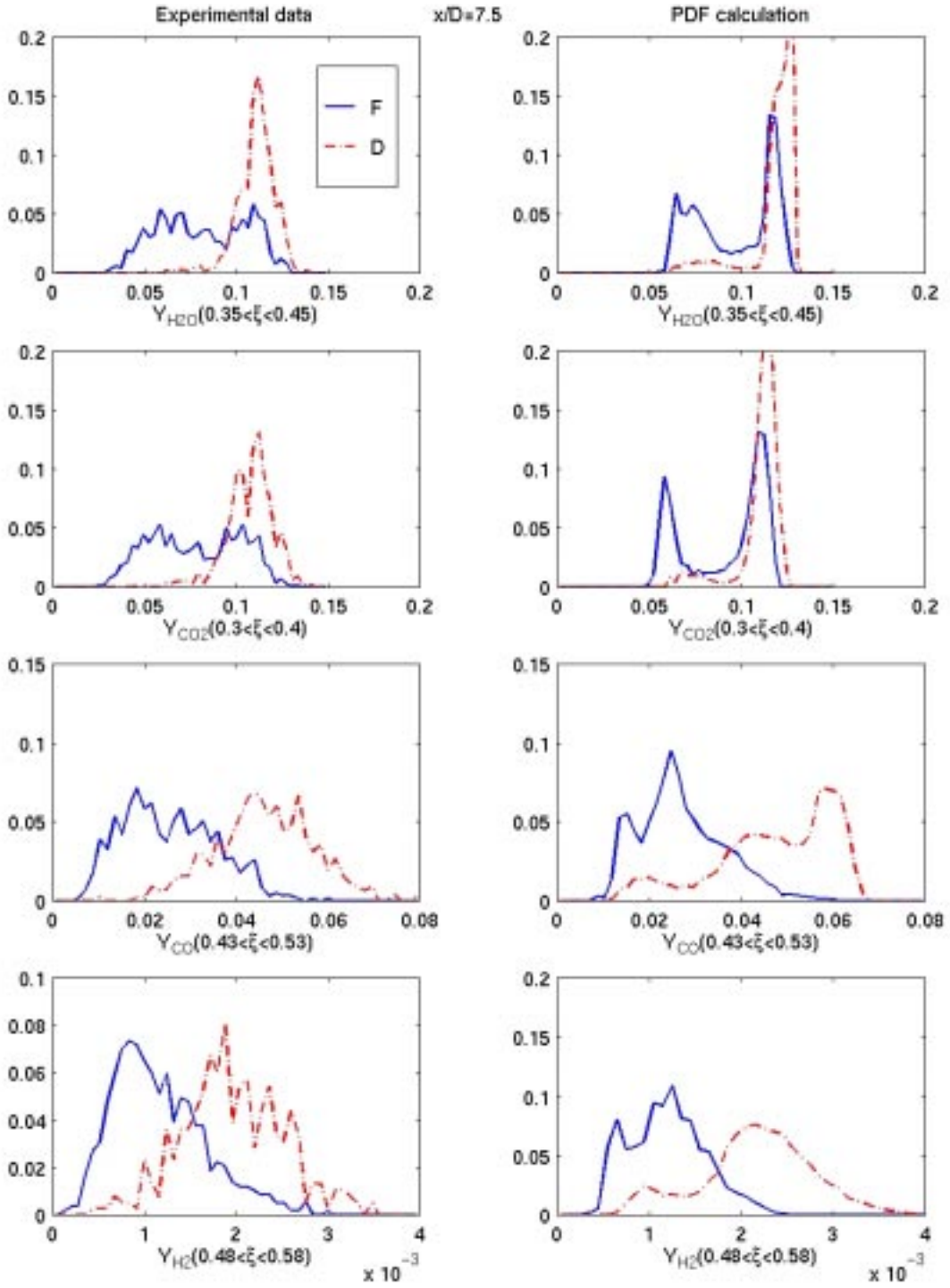

Conditional PDF of Flame D and F

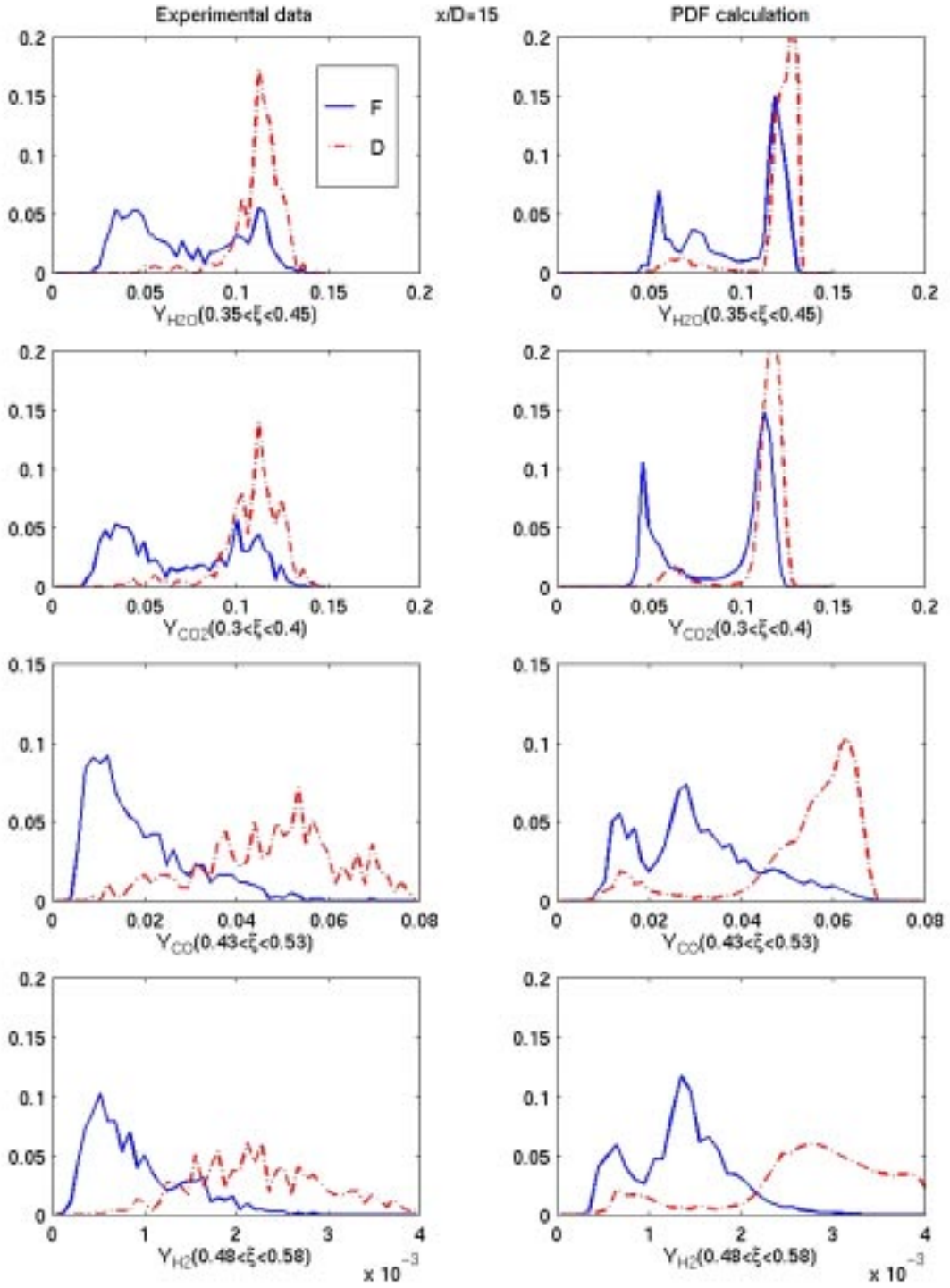

Conditional PDF of Flame D and F

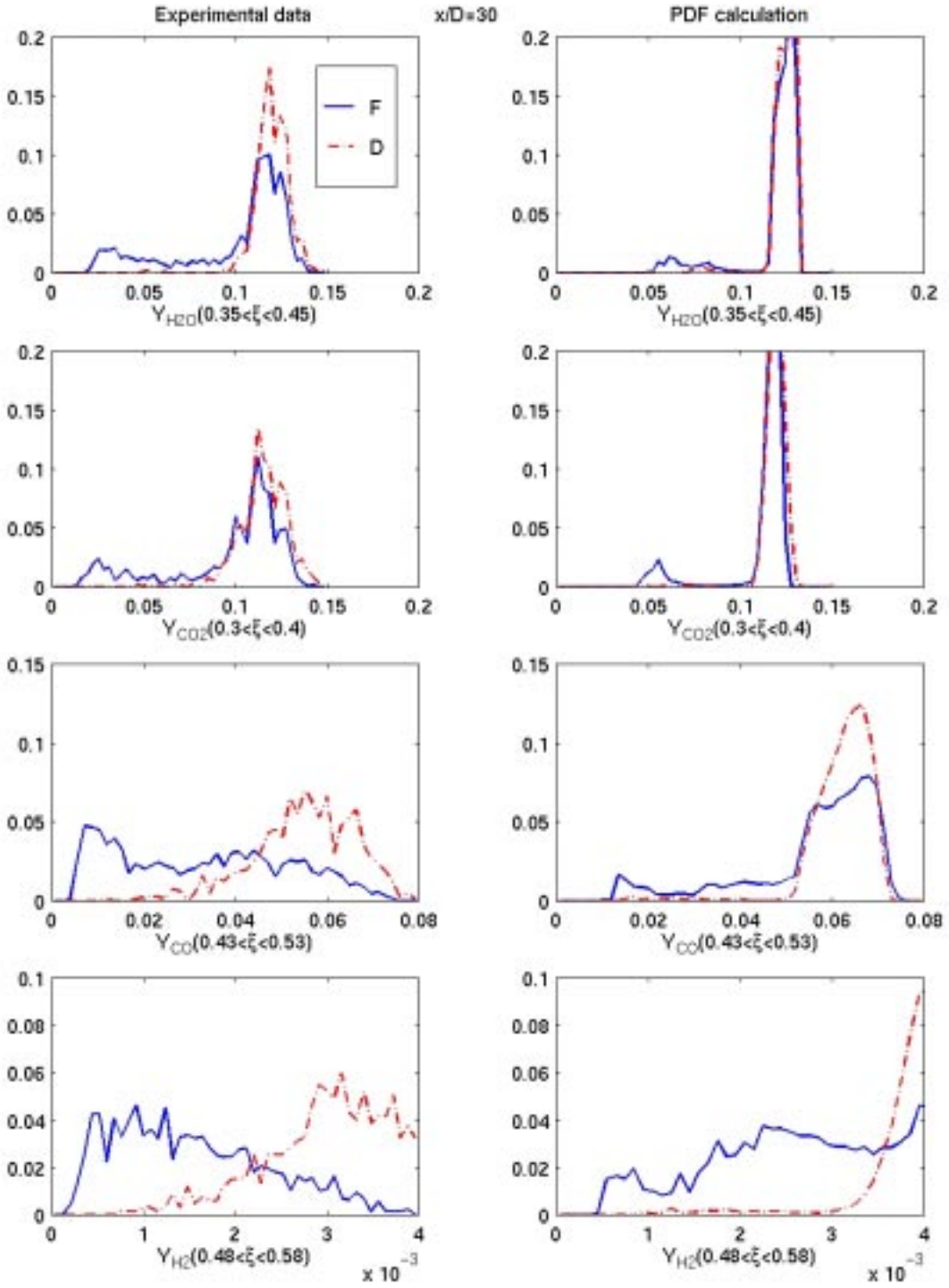

Mean profiles of Flame D and F

Mixture fraction

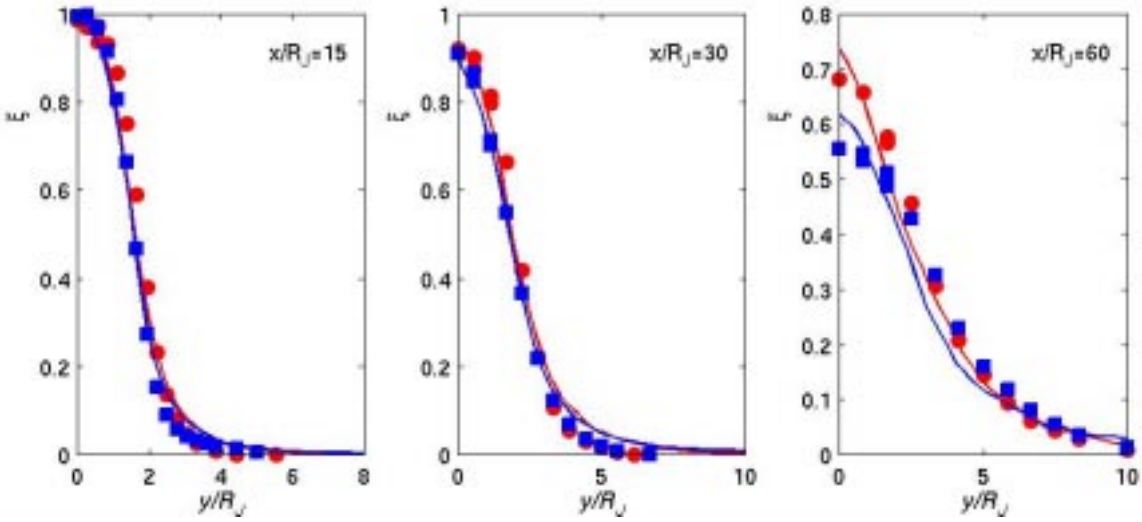

Red: D;

Blue:F

Rms of mixture fraction

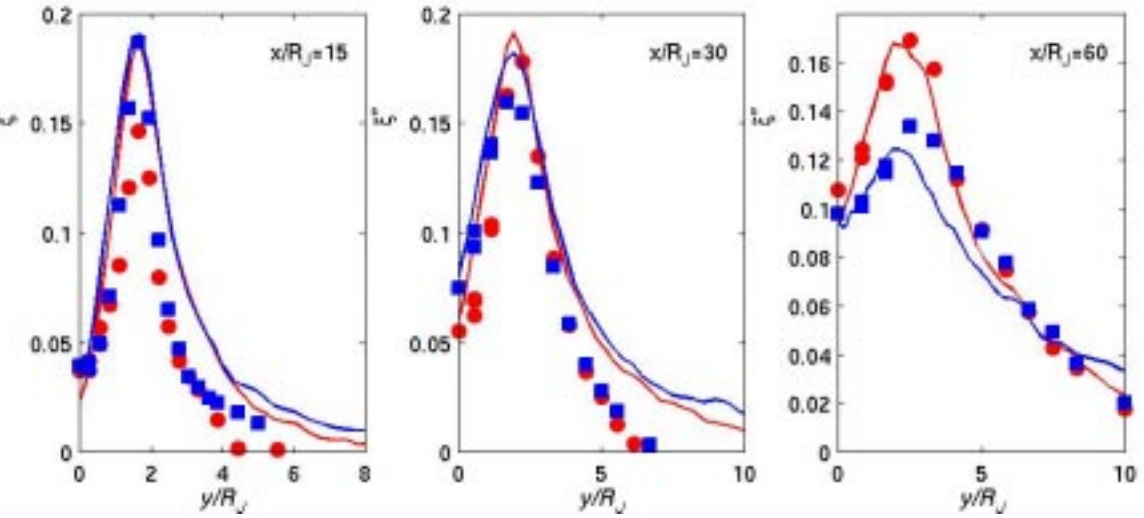

Temperature

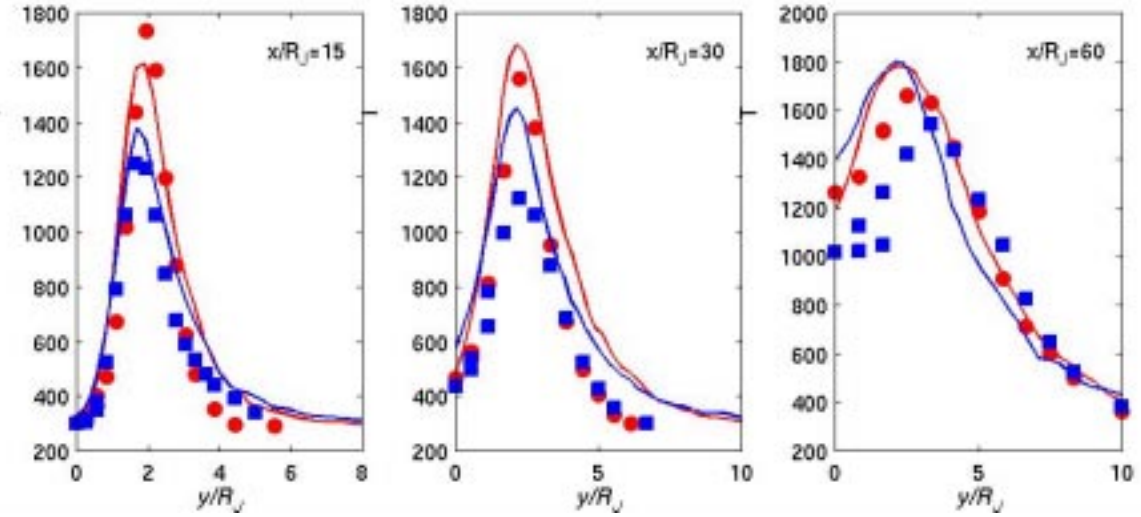

Mean profiles of Flame D

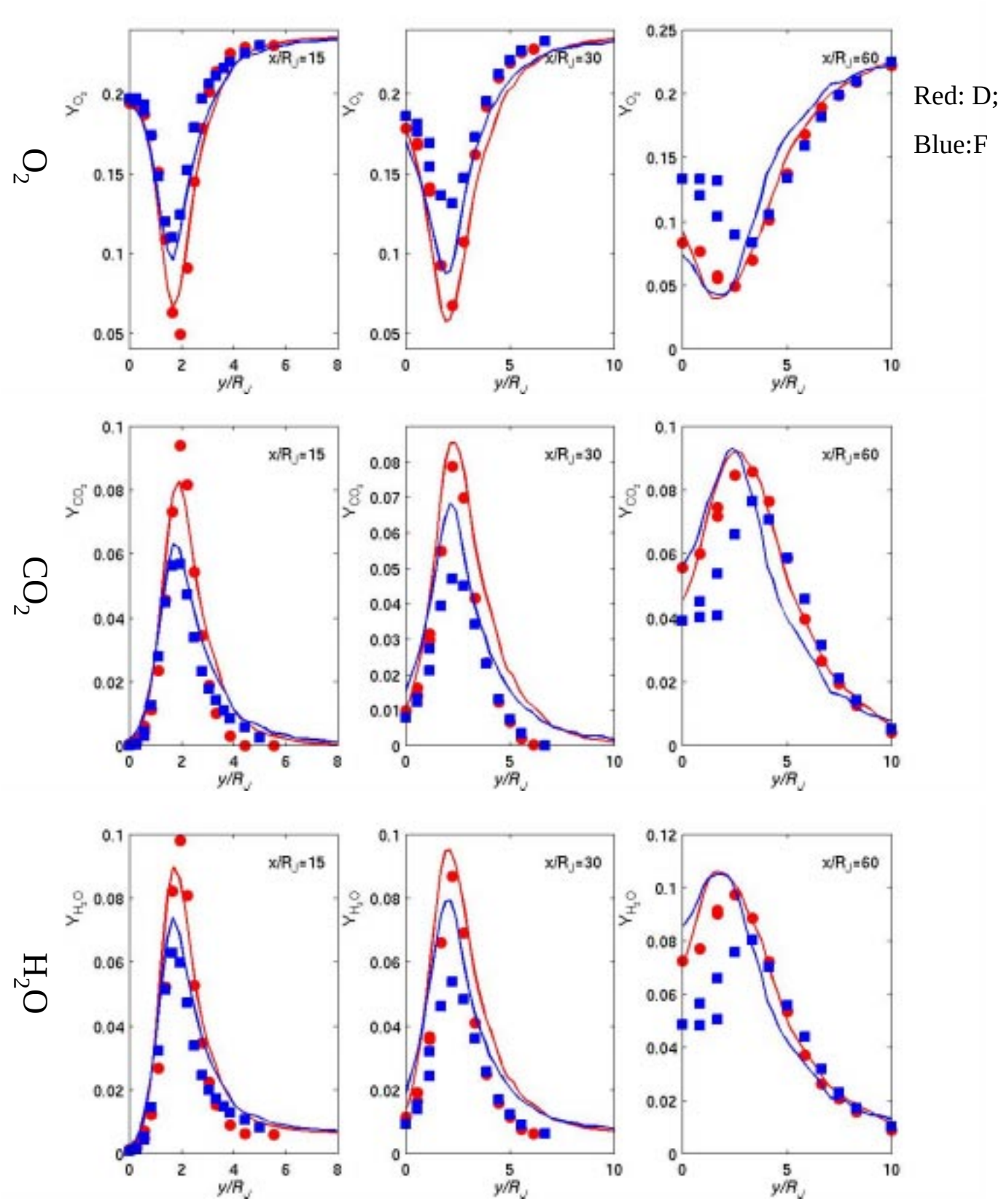

Mean profiles of Flame D and F

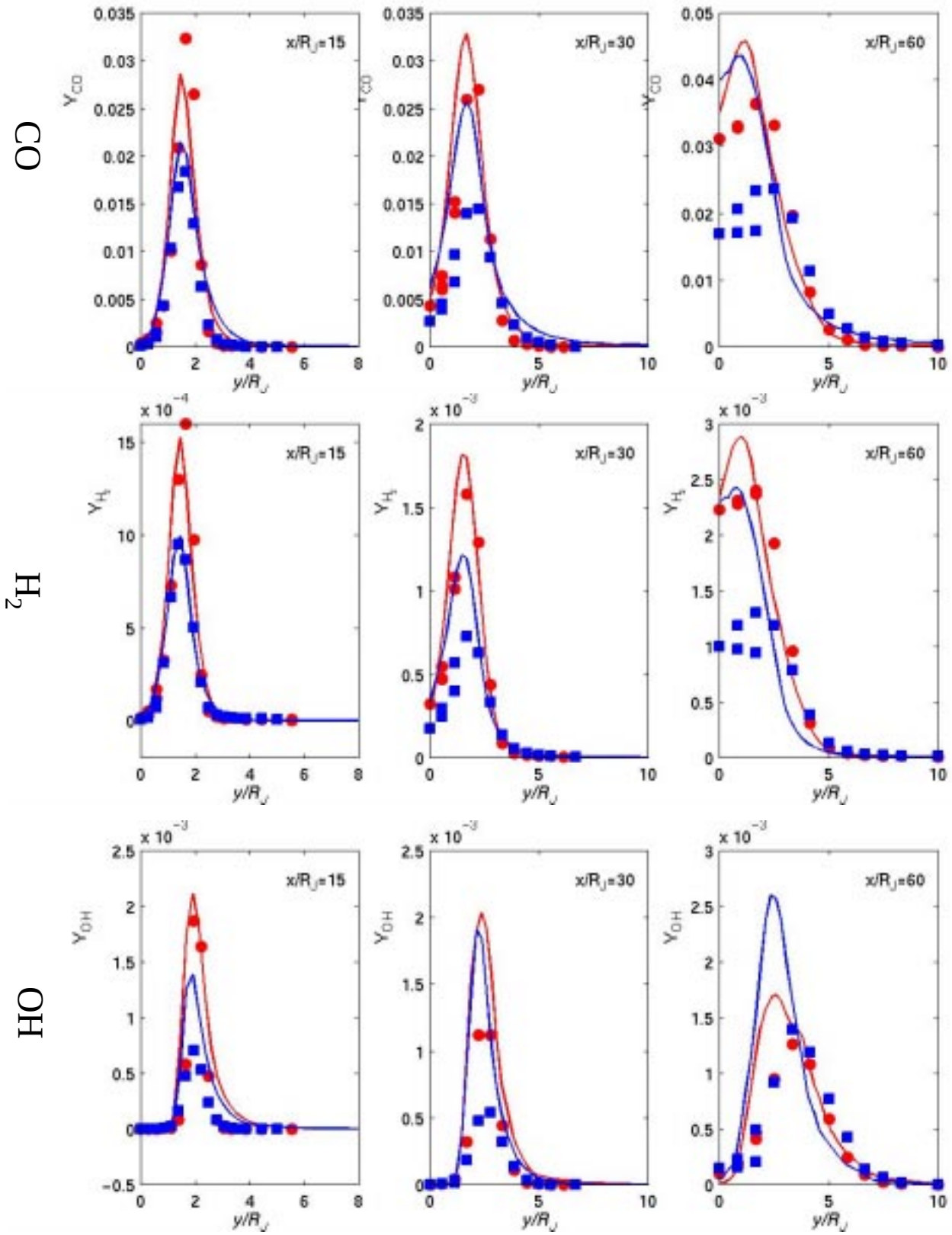

Conclusions

- EMST mixing model is localized in the composition space. With the use of this mixing model, artificial ignition scheme is avoided in PDF calculations;
- Conditional means of Flame D agree to experimental data very well. The advantage of current turbulence chemistry interaction model is apparent. It also appears that ARM represents most species adequately;
- Conditional PDF's of calculations show the same characteristics as the experiment. Especially, for Flame F, bimodal shape implies that local extinction is well captured;
- The mean profiles of Flame D are in very good agreement with experiment;
- For Flame F, mean and rms of mixture fraction are well predicted, but mean temperature at x/R=30 and 60 is over predicted, and the comparison of mass fraction is also deteriorated.